



Power generation from hot waste gases using thermoelectrics

(PowGETEG)

A large, abstract graphic occupies the bottom half of the page. It features flowing, wavy lines in shades of blue and white, creating a sense of motion and energy. In the upper left area, there are faint, semi-transparent circular patterns resembling stylized suns or energy sources.

EUR 30538 EN

Power generation from hot waste gases using thermoelectrics (PowGETEG)

European Commission

Directorate-General for Research and Innovation

Directorate D – Clean Planet

Unit D.3 — Low Emission Future Industries

Contact Andrea Gentili

E-mail RTD-STEEL-COAL@ec.europa.eu

RTD-PUBLICATIONS@ec.europa.eu

European Commission

B-1049 Brussels

Manuscript completed in 2020.

This document has been prepared for the European Commission however it reflects the views only of the authors, and the Commission cannot be held responsible for any use which may be made of the information contained therein.

More information on the European Union is available on the internet (<http://europa.eu>).

Luxembourg: Publications Office of the European Union, 2020

PDF ISBN 978-92-76-27845-0 ISSN 1831-9424 doi:10.2777/21737 KI-NA-30-538-EN-N

© European Union, 2021.

Reuse is authorised provided the source is acknowledged. The reuse policy of European Commission documents is regulated by Decision 2011/833/EU (OJ L 330, 14.12.2011, p. 39).

For any use or reproduction of photos or other material that is not under the EU copyright, permission must be sought directly from the copyright holders.

All pictures, figures and graphs © VDEh-Betriebsforschungsinstitut GmbH, RFSR-CT-2015-00028 PowGETEG

Research Fund for Coal and Steel

Power generation from hot waste gases using thermoelectrics

(*PowGETEG*)

F. Mintus (Coordinator), S. Białek, A. Queck,
VDEh-Betriebsforschungsinstitut GmbH
Sohnstr. 65, 40237 Düsseldorf, Germany

Prof. A. Knox
University of Glasgow
University Avenue, GB-G12 8QQ Glasgow, UK

R. Spillner
Gentherm GmbH
Rudolf Diesel Strasse 12, 85235, Odelzhausen, Germany

H. P. Domels, T. Frese
thyssenkrupp Steel Europe AG
Kaiser Wilhelm Strasse 100, 47166 Duisburg, Germany

J. Esarte NAITEC.
Centro tecnológico en automoción y mecatrónica
C/Tajonar, 20, 31006 Pamplona, Navarra, Spain

Grant Agreement RFSR-CT-2015-00028

1/07/2015-30/06/2019

Final Report

Table of contents

	<i>Page</i>
<u>Final Summary</u>	7
<u>Scientific and technical description of the results</u>	17
1. Objectives of the project	17
2. Description of activities and discussion	17
2.1 WP 1: Process and waste heat assessment	17
2.1.1 Task 1.1: Process and waste heat evaluation (all)	17
2.1.2 Task 1.2: Measurements (tkSE, BFI)	19
2.1.3 Task 1.3: Data evaluation (tkSE, BFI)	23
2.1.4 Task 1.4: Process selection (all)	25
2.2 WP 2: Design of TE demonstrator and its bench scale unit	25
2.2.1 Task 2.1: Requirements definition (all)	25
2.2.2 Task 2.2: Concept development (all)	26
2.2.2.1 Design of the TE cartridge (GNTH)	26
2.2.2.2 Design of the power conversion system (GUN)	26
2.2.2.3 Design of the connection between the TE system and the waste gas pipe (all)	27
2.2.2.4 Design of alternative heat exchanger concepts (CEM)	29
2.2.3 Task 2.3: Bench scale unit design and assembly (GNTH)	30
2.2.4 Task 2.4: Power conversion development and system automation (GUN)	31
2.2.5 Task 2.5: Design and function review (all)	35
2.2.6 Task 2.6: Demonstrator design (all)	37
2.2.6.1 Final layout of the TE cartridges (GNTH)	37
2.2.6.2 Adaption of a GEN3 cartridge for utilization with the heat pipe heat exchanger (GNTH)	39
2.2.6.3 Final layout of the bypass (tkSE, BFI)	39
2.2.6.4 Final layout of the heat pipe heat exchanger (CEM)	40
2.2.7 Task 2.7: Design integration (GNTH)	43
2.3 WP 3: Heat exchanger design for safety and sustained performance (antifouling)	43
2.3.1 Task 3.1: Design of TE cartridge safe-guarding design (CEM)	44
2.3.2 Task 3.2: Fatigue tests (CEM)	47
2.3.3 Task 3.3: Understanding the mechanism of build-up on heat transfer related surfaces (BFI, tkSE)	47
2.3.4 Task 3.5: Design of a system to prevent the formation of deposits (CEM)	52
2.3.5 Task 3.6: Dummy manufacturing and testing (tkSE, CEM)	56
2.4 WP 4: Design & construction of the test-bed; Testing of the bench scale unit	58
2.4.1 Task 4.1: Test-bed design and construction (BFI, GUN)	58
2.4.2 Task 4.2: Executing experiments (BFI, GUN)	61
2.4.3 Task 4.3: Data Mining and data analysis (BFI, GUN)	62

2.4.4	Task 4.4: Test-bed deconstruction (BFI)	65
2.5	WP 5: Industrial testing of the demonstrator	65
2.5.1	Task 5.1: Demonstrator Documentation (all)	66
2.5.2	Task 5.2: Demonstrator construction (all)	66
2.5.3	Task 5.3: Installation and commissioning (tkSE, BFI, GNTH)	71
2.5.4	Task 5.4: Operational long-term testing (BFI, tkSE)	72
2.5.5	Task 5.5: De-installation of the demonstrator (tkSE, BFI)	74
2.5.6	Task 5.6: Data analysis (CEM, GUN, BFI, GNTH)	74
2.5.7	Task 5.7: Economic and technical evaluation, including analysis of improvement possibilities (all)	75
2.5.8	Task 5.8: Economic and technical comparison with other waste heat power generation systems (BFI, GNTH)	79
2.5.9	Task 5.9 Development of application concepts for other industries (BFI)	81
2.6	WP 6: Coordination and Dissemination	81
2.6.1	Task 6.1: Project management (all)	82
2.6.2	Task 6.2: Dissemination (all)	82
3.	Conclusions	83
	<u>List of figures</u>	85
	<u>List of tables</u>	87
	<u>List of Symbols, Indices, Acronyms and Abbreviations</u>	89
	<u>List of references</u>	91
	<u>Appendices</u>	93
4.	Deliverables of WP 1	93
4.1	Deliverable 1.1: Evaluation document of tkSE processes and their waste heat, qualitative & quantitative (Task 1.1, tkSE)	93
4.2	Deliverable 1.2: Measurements evaluation document, describing all relevant waste gas properties and their fluctuations (Task 1.2, BFI)	93
4.3	Deliverable 1.3: Summary document for the use of waste heat source selection (summarizing the results of D 1.1, D 1.2 and derived parameters (Task 1.3, BFI)	95
4.4	Milestone 1: Gaseous waste heat source selected (all)	96
5.	Deliverables of WP 2	97
5.1	Deliverable 2.1: Requirements to bench scale unit and demonstrator defined (Task 2.1, BFI)	97
5.2	Deliverable 2.2 Design concepts finished (Task 2.2, GNTH)	98
5.3	Milestone 2a: System for power conversion complete and ready for WP 4 testing (GUN)	99
5.4	Milestone 2b: Bench scale unit assembled (GNTH)	100
5.5	Deliverable 2.5: Demonstrator design adaptations defined (Task 2.5, GNTH)	101

5.6	Milestone 4: Demonstrator design is reviewed and adjusted (Task 2.5, all)	102
5.7	Deliverable 2.6: Demonstrator design document (Task 2.6, GNTH)	102
6.	Deliverables of WP 3	106
6.1	Deliverable 3.1: Design document of TE safe-guarding system (Task 3.1, CEM)	106
6.2	Deliverable 3.2: Construction requirements (considering the assembly and its connection to the gas duct) sheet finished (Task 3.2, CEM)	106
6.3	Deliverable 3.3: Build-up quantified (Task 3.3, BFI)	107
6.4	Deliverable 3.4: Evaluation document about the deposition phenomenon and its effect on the heat transfer (Task 3.4, BFI)	107
6.5	Deliverable 3.5: Developed concept for preservation of high heat transfer and performance results (Task 3.5, CEM)	111
6.6	Milestone 3: Solutions for sustained performance tested (CEM)	112
7.	Deliverables of WP 4	112
7.1	Deliverable 4.1: Test-bed design document (Task 4.1, BFI)	112
7.2	Milestone 4.1: Bench scale unit & power conversion system integrated in test-bed (BFI)	113
7.3	Deliverable 4.2: Data set ready for analysis (Task 4.2, BFI)	113
7.4	Deliverable 4.3: Model for TE power production available (Task 4.3, BFI)	116
8.	Deliverables of WP 5	117
8.1	Deliverable 5.1: Demonstrator documentation including manual ready (Task 5.1, GNTH)	117
8.2	Deliverable 5.2: Demonstrator constructed (Task 5.2, GNTH)	122
8.3	Milestone 5: Demonstrator tests have started (BFI)	122
8.4	Deliverable 5.4: Data set of demonstrator tests available (Task 5.4, BFI)	123
8.5	Deliverable 5.6.1: Recommendations for TEG optimizing ready (Task 5.6, GUN)	124
8.6	Deliverable 5.6.2: Models ready for techno-economical evaluation (Task 5.6, CEM)	124
9.	Deliverables of WP 6	127
9.1	Deliverable 6: PowGETEG website online (Task 6.1, BFI)	127
9.2	Milestone 6: Publishable results from bench scale testing	128

Final Summary

Thermoelectric generators (TEG) have the ability to directly convert waste heat into electricity. They consist of arrays of N and P type semiconductors which exhibit a strong relationship between a current and heat flow through the material. This is due to the Seebeck and the Peltier effect. The Seebeck effect shows itself as the generation of electrical power if opposite ends of the semiconductor are subjected to hot and cold temperatures respectively, the Peltier effect is the opposite. If an electrical current is passed through a semiconductor material, then one end gets hot and the other end gets cold. **Figure 1** shows the scheme of N and P type arrays of a TEG (left), scheme of a TE module consisting of several N and P type arrays (middle) and an image of a common Bi_2Te_3 TE module (right).

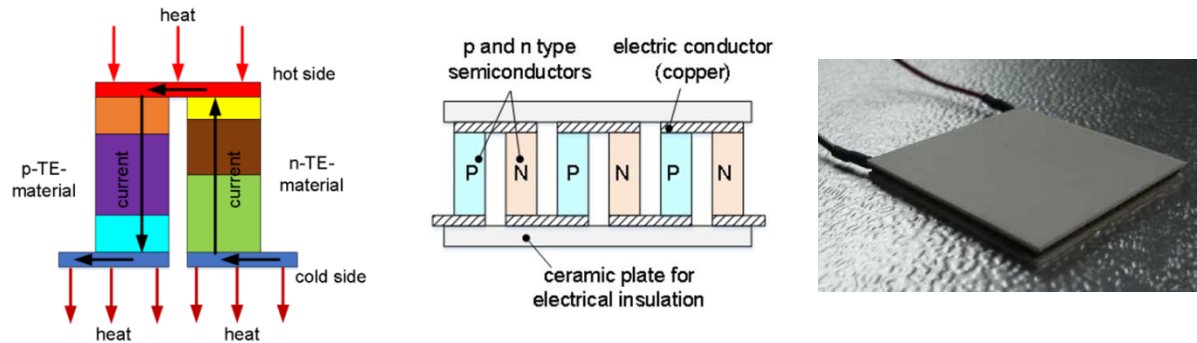


Figure 1: Scheme of N and P type arrays (left), scheme of a TEG consisting of several N and P type arrays (middle) and image of a common Bi_2Te_3 TE module (right)

Despite their low conversion efficiency (usually approx. 5 %), TEG have well known advantages in comparison to other heat to electricity conversion technologies (e.g. ORC): no moving parts, simple configuration, long-run unattended operation for thousands of hours, nearly maintenance free, scalable, and no release of pollutants during operation. Main fields of research are currently the development of more efficient TE materials, the mass production of TE materials as well as large scale production of TE modules. Another crucial research field, which was the main topic of this project, is the integration of TE systems into industrial production processes for waste heat utilization as well as the performance optimization of such TE systems.

TEG are already used in special applications, e.g. in air and space industry. However, the use of this technology in a large-scale industrial application has not been sufficiently investigated until now. Thus, the PowGETEG project dealt with determination of possibilities of thermoelectric power generation using industrial gaseous waste heat at temperatures above 550°C. Main objectives were:

- Development of new solutions for control, power conversion (WP 2), heat exchange as well as for overheating and fouling protection (WP 3).
- Bench-scale tests with a 200 W_{el} unit (WP 4).
- Design and construction of a demonstrator with an output of approx. 800 W_{el} (WP 2) as well as a long-term test (WP 5) at a preliminary selected waste heat source of thyssenkrupp (tkSE) steel plant (WP 1).
- Determination of techno-economical possibilities of large scale TE power production based on testing campaign results. (WP 5).

WP 1: Process and waste heat assessment

To identify a suitable waste heat source at tkSE steel work for the long-term test of the TEG demonstrator (WP 5) the waste heat streams of several plants were evaluated. Main selection criterions were:

- Waste gas temperature well above 550°C.
- Good accessibility.
- Enough amount of space for the installation of a demonstrator.

Evaluated plants were:

- Hot dip galvanizing lines 1 and 2 (HDGL 1 and 2).
- Compact strip production (CSP).
- Hot rolling mill (HRM).

A first data evaluation narrowed the selection of possible waste heat sources down to the HDGL 1 (behind the recuperator) and the CSP. Since the waste gas temperature (530 – 560°C) of the HDGL 1 is at the lower useful limit (550°C) the CSP was identified as the most promising waste heat source, due to its waste gas temperature of 600 – 800°C and the good accessibility. **Figure 2** shows the waste gas pipe of the CSP, where the demonstrator was installed for the operational long-term test.



Figure 2: CSP, exhaust gas system (good accessibility and enough amount of space for demonstrator installation)

Following measurements and detailed process data evaluation resulted in a waste heat potential of the CSP in the range of 1.7 - 3.6 MW. Long-term pressure and temperature measurements showed an average waste gas temperature about 600 – 800°C. The pressure drop through the demonstrator installation should not exceed 4 mbar. Based on waste gas and dust measurements no major problems through corrosion or build-up formation were expected.

WP 2: TEG demonstrator design

Next step in the project was the design of the TE demonstrator. Main components of the developed demonstrator were two types of TEG Cartridges, a Power converter and a new MPPT (Maximum power point tracking) algorithm, a bypass system for the connection of the TE system to the CSP waste gas pipe and an alternative approach based on a heat pipe heat exchanger.

In respect of economic reasons, the cartridge design was based on former concepts from GNTH.

Figure 3 shows the scheme of the selected cartridge design. The inner tube yields fins for improved heat exchange. The outer tube comprises the coolant water jacket which lets water circulate around the cartridge. The inner tube fins remove heat from the waste gas flowing through the centre opening and conduct the heat to the TE pellets which are placed between inner tube and outer tube. The cartridges were connected to the waste heat source via flanges

For the entire demonstrator two different kind of cartridges were foreseen, which differ in their diameter and length and thus also in their performance. The smaller cartridge with an inner tube diameter of 90 mm was named GEN3 and the bigger cartridge (inner tube diameter 160 mm) was named GEN4. The design point for the TEG cartridges was a waste gas mass flow of 130 kg/h and a waste gas temperature of 800°C. The expected power output of a GEN4 cartridge at the design point is in the range of 340 W at an efficiency of approx. 5.6 %. The power output of the GEN3 cartridge is lower (240 W at 800 °C waste gas temperature) but at a higher efficiency of 6.9 %.

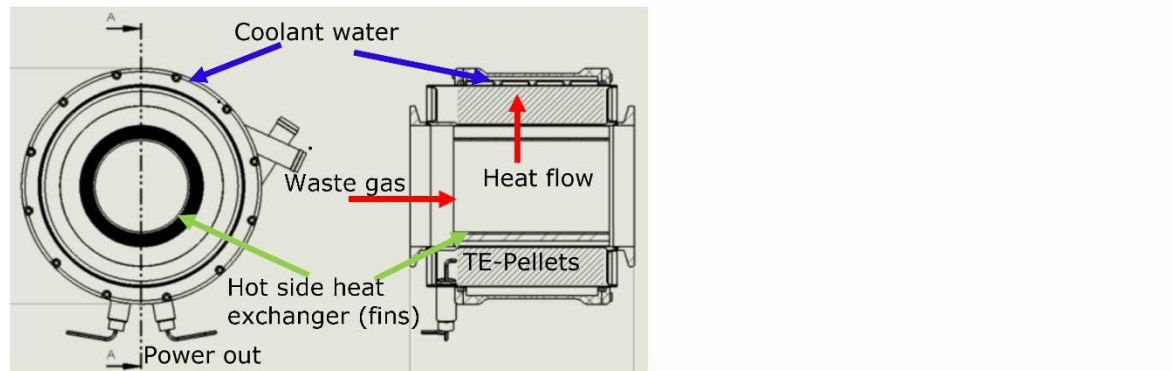


Figure 3: Scheme of the proposed cartridge design

Another point of the demonstrator design was the construction and testing of a MPPT power converter, to extract the maximum power from the TE system. The function of the developed

Power converter is to track the maximum power available from the thermoelectric generator(s) connected at its input.

The converter developed for this application was a MPPT converter designed specifically for TE power generating modules. One was used for each TE cartridge and it operated the cartridge at its optimal operating point and efficiently transfers electrical power to the connected output battery. The converter also included battery charging management software to ensure the battery is not over-charged.

The goal of MPPT algorithms is to set the TE system to operate at its optimum power output according to the temperature conditions. The developed Power converter used a special newly developed MPPT algorithm (a modified FOC algorithm) that tracks fast thermal transients and recognises steady states to increase the thermal-to-electrical efficiency of the system.

The Power converter can communicate to other devices through I2C. This allowed the converter to provide measurements of input and output voltage and current.

To monitor the operational testing of the demonstrator at tkSE it was decided to develop an Online Monitoring system, which enables all partners to view and download live data via a web interface. Monitoring and logging parameters included temperatures, flow rates, electronic parameters and electrical efficiencies.

The hardware of the monitoring and logging system consisted of an electrical interface to connect the various sensors from the demonstrator; a data processing unit for data collection; MPPT systems (see above); web server to publish the data on a website for online access; database storage. A 4G internet connection was included with a Raspberry Pi. This allowed access to the Raspberry Pi web interface globally to allow any project partner to view and download data.

Due to the TE cartridge design the consortium decided not to install the demonstrator directly in the waste gas pipe of the CSP but to install a bypass pipe to the waste gas pipe in which the demonstrator was installed. The design of such a bypass system was not foreseen in the proposal. However, the use of a bypass for the demonstrator test was identified as the best solution, so that the bypass design was included into WP 2.

Several design options were weighed and calculated with CFD simulations. The final design, which was implemented, is shown schematically in **Figure 4**. Due to cost reasons the number of TE cartridges was limited to one GEN3 cartridge (connected to the heat pipe heat exchanger, see below) and two GEN4 cartridges (placed in series). Thus, the expected power output of the demonstrator was limited to 700 – 800 W (approx. 350 W of GEN4 at 800°C, approx. 250 W of the 2nd GEN4 at lower waste gas temperature of 700°C due to the expected decrease of the temperature through the first GEN4 cartridge, approx. 200 W of GEN3 with the heat pipe approach) which was slightly less than expected in the proposal (1,000 W).

The bypass system works as follows: The waste gas is removed from the CSP waste gas pipe after the main heat exchanger. A special connection plate at an inspection chamber of the heat exchanger was used to link the bypass system to the CSP waste gas pipe. Two safety valves were installed to protect the demonstrator from damages e. g. through overheating. To ensure the waste gas flow through the bypass a fan was integrated after the cartridges. This allowed the investigation of the cartridges at different conditions.

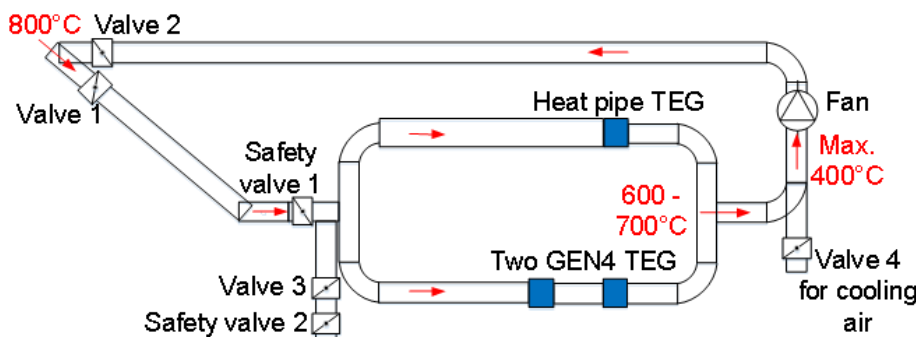


Figure 4: Scheme of the final bypass design

One of the main bottlenecks for applying TEG directly to an exhaust gas pipe is the pressure drop TE cartridges introduce into waste gas pipes. This is an issue, since the waste gas flow of a lot of heating furnaces is driven just by the stack. To deal with this issue an additional approach was designed, constructed and tested. This consists on transferring the exhaust gas temperature to the

TE cartridge via heat pipes. That means that the TE cartridge is placed outside and the hot side of the heat pipe is placed inside of the waste gas pipe. To increase the heat transfer from the waste gas to the heat pipe a heat exchanger was connected to the heat pipe. By doing it, it was expected to be able to transfer the heat required causing minimum pressure loss (less than 4 mbar). Several design options were calculated by CFD. **Figure 5** shows a scheme of the final design of the indirect heat transfer solution. The heat pipe heat exchanger was used within the demonstrator for the GEN3 cartridge.

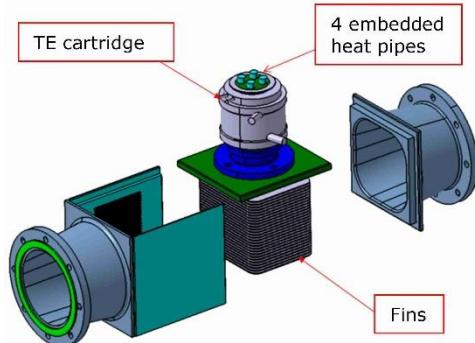


Figure 5: Scheme of the alternative approach based on a heat pipe heat exchanger

WP 3: Heat exchanger design for safety and sustained performance (antifouling)

Due to potential temperature fluctuations into exhaust systems, it is worth introducing temperature absorbers if using TEG to prevent them from overheating damage. Even if the temperature profile at the selected heat source (CSP) of this project was quite even the development of a safeguarding system is highly important for other applications of such TE systems in other industries and plants. At this regard, a system based on phase change materials (PCM) was studied and developed. For a working temperature of approx. 700°C, salts are the best suitable material, particularly "carbonates" which perform well at temperatures in the range of 650 - 800°C.

Finally, Lithium carbonate (Li_2CO_3) has been selected as a material which meets requirements regarding a proper melting point and high enthalpy. Further investigations showed no degradation of the PCM after performing several cycles and that it is capable of absorbing thermal peaks (in this case of 800°C) for different times depending on the weight of the material. Thus, it can be stated that Li_2CO_3 shows a good behavior to be used for overheating protection of high temperature TEG. Next step of WP 3 was the identification of high temperature resistant coatings that prevent the formation of deposits in the heat exchanger system, in order to maintain its efficiency. These coatings consist of industrial high temperature resistant coatings modified with anti-adherent additives in order to increase its anti-adherent properties. A theoretical study of coating and additive characteristics narrowed the selection of coatings and additives. In a first step the selected materials were investigated under high temperature conditions (750°C) in a lab scale oven for 8 h. Coatings and additives were applied on substrates made of the type of materials that can be used for the construction of the heat exchanger. Main results were:

1. Five industrial high temperature resistant coatings have been investigated: Cerastil E-1001, Silixan T330-40/IPA, X-clean EC 2048, Silixan S400-35/PE and Thermobarp 800.
2. Four additives have been used to improve the anti-adherence properties of the industrial high temperature resistant coatings and to avoid or reduce the formation of deposits on their surface: Molybdenum Disilicide, Boron Nitride, Alpha-Silicon Nitride, and Aluminum Nitride.
3. In the first approach, Cerastil E-1001, X-Clean EC 2048 and Silixan T330 were considered. Cerastil E-1001 was discarded due to its hydrophilic behavior. Then, X-Clean EC 2048 and Silixan T330 were modified with the four additives. Silixan T330 showed better adherence to the substrates than X-Clean, therefore Silixan T330 was selected to be tested in industrial conditions.
4. In the second approach, Silixan S400-35/PE and Thermobarp 800 were considered and additivated with the four anti-adherent additives. Both presented good adherence and not detachment was observed. Therefore, they were selected as samples to be evaluated in industrial environment, too.

In a next step Silixan T330, Silixan S400-35/PE and Thermobarp 800 were tested under industrial conditions in the waste gas pipe of the CSP at tkSE. Results were:

- Silixan T330 showed a weight loss. This means that a degradation of the substrate or the coating may have occurred.
- S400-35/PE and Thermobarp 800 showed no deposition, good thermal behavior, and no degradation

Overall the results show, that the waste gas of the CSP shows just a minor dust load and that no deposits are expected for the long-term demonstrator test. Nevertheless, some of the heat pipe heat exchanger fins were treated with Thermobarp to test them over a longer period during the demonstrator test at tkSE. The operating tests showed that the coating was worn very much after only a short application time. In summary, it can be stated that coatings are neither necessary nor suitable in this application.

WP 4: Design and construction of lab test facility

In front of the operational long-term tests of the demonstrator, experiments with a GEN3 cartridge were carried out at a testing facility of the BFI. Therefor a test bed was constructed in which a GEN3 cartridge was integrated. Waste heat source was the waste gas from blast furnace gas, which was burned in a combustion chamber and sucked into the waste gas pipe in which the TEG cartridge was located. Experiments included different

- Waste gas temperatures (400 – 800°C).
- Waste gas flows (33 – 155 kg/h).
- Cooling water flows (300 – 1,000 l/h).

During the experiments data of waste gas flow, waste gas temperature, waste gas composition, pressure drop, cooling water flow and cooling water temperature were recorded every second.

Performance data of the TE cartridge (power, current and voltage) were recorded by the developed I-V Tracer and Power Converter (see WP 2).

The experiments showed that the waste gas temperature influences significantly the TEG performance. At high waste gas temperatures, the maximum usable current of the Power converter (which is in the range of approx. 27.5 A) was reached at a voltage level of 9.5 V. Maximum measured electrical power was approx. 260 W at a waste gas temperature of 800°C. The maximum measured power at 700°C was approx. 175 W.

Figure 6 shows a comparison of some experimental data with performance data from Gentherm (GNTH, the producer of the TE cartridges), which were won by experiments with hot air in the laboratory of GNTH. The comparison of power output shows a good agreement between experimental and GNTH data. In the waste gas temperature range of the CSP of 700 – 800°C a power output of 175 W up to 260 W can be expected from such a GEN3 cartridge.

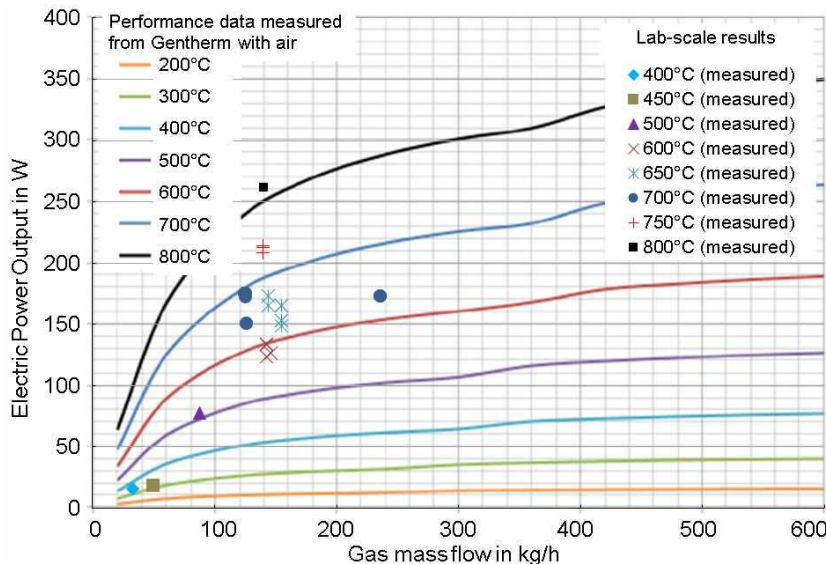


Figure 6: Comparison of data from Gentherm with experimental data: power as a function of waste gas temperature and waste gas flow

Overall results of the test bed experiments were:

- The measured power output is in good agreement with data from Gentherm. An average output of approx. 700 - 800 W_{el} can be expected for the entire demonstrator, consisting of one GEN3 and two GEN4 cartridges.

- The I-V Tracer and Power Converter operated well in combination with the cartridge. The average electrical efficiency was approx. 94 %.
- The influence of the cooling water flow on the power output was minimal.

WP 5: Industrial testing of demonstrator

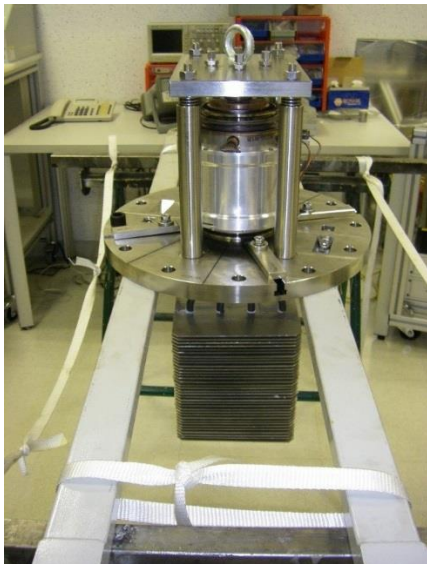
Based on the demonstrator design (WP 2 and 3) and the lab tests the components of the demonstrator were constructed and sent to tkSE. **Figure 7** shows images of the demonstrator components.



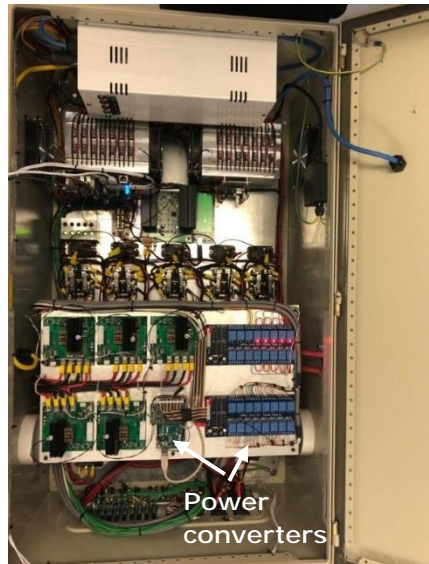
GEN4 cartridge



Adapted GEN3 cartridge, refit for conductive heat transfer with a heat pipe core.



Heat pipe heat exchanger already connected to the adapted GEN3



Monitoring system inclusive Power converter

Figure 7: Finished components of the demonstrator

The construction of the demonstrator followed the concept in Figure 4. This task proved to be a challenge. The requirements regarding safety, autonomous operation and physical effects such as strain required a much higher effort than initially expected. **Figure 8** gives a planning overview of the test facility with all instrumentation.

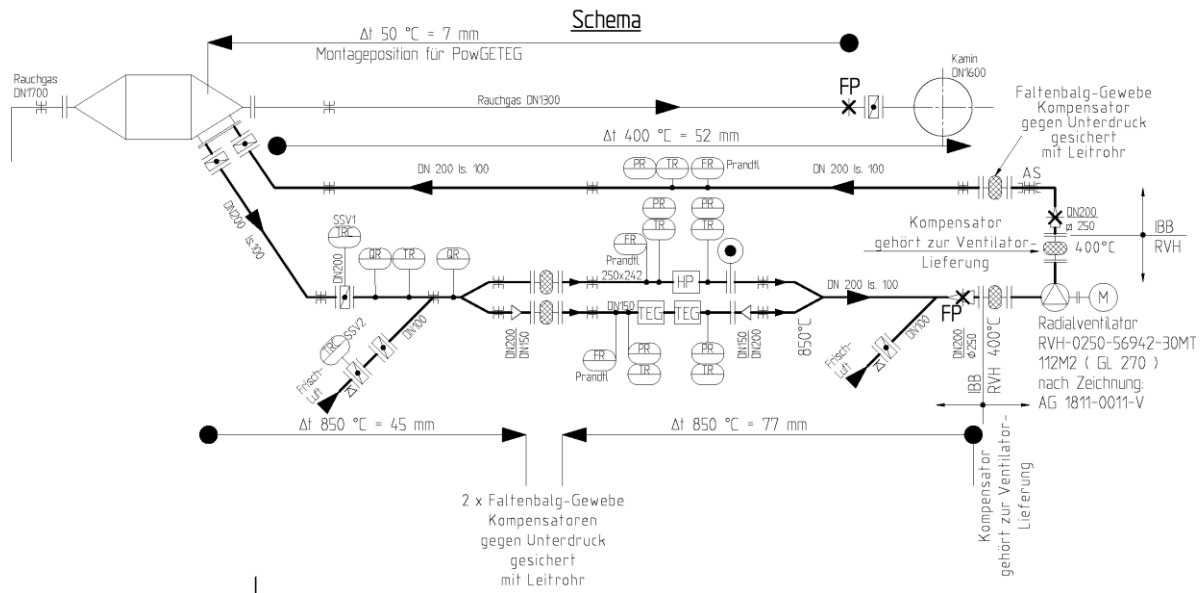


Figure 8: Drawing of the test facility with extensive measurements

The installed measurement technology included sensors for the temperature of flue gas and water, of pressure, flow and a gas analysis. The measuring points included four measurements of the water temperature, six of the gas temperatures, three times the water volume flow, seven pressure measurements, the determination of the O₂, CO₂ and CO content and of course the voltage generated at the TEG. In addition, there were temperature measurements for the safety equipment.

Despite various attempts, the monitoring system was not able to record all measured values, especially the recording of the signals from the temperature sensors was not correct. In addition, problems with the mobile phone provider arose during the creation of the project website and the connection could often not be established reliably. This led to the decision, to collect all measurement data via different systems. Consequence was that the MPPT algorithm could not be used and thus the power output of the TEG was not maximal. Furthermore, the measurement data were not available online for the project members but were collected and evaluated daily.

This approach led finally to success. A photo of the final industrial testing setup can be seen in **Figure 9**.



Figure 9: Top-view of the industrial testing

In the bottom part of the figure the two paths of the flue gas can be seen, one for the two cascading GEN4-TEG-cartridges, another one for the heat pipe-TEG. The upper pipe is used to take the flue gas back to the chimney.

The demonstrator was tested for several weeks. During this time, variations of temperature levels and mass-flow took place. In **Figure 10** the generated power by the cascading TEG during 24 h is shown.

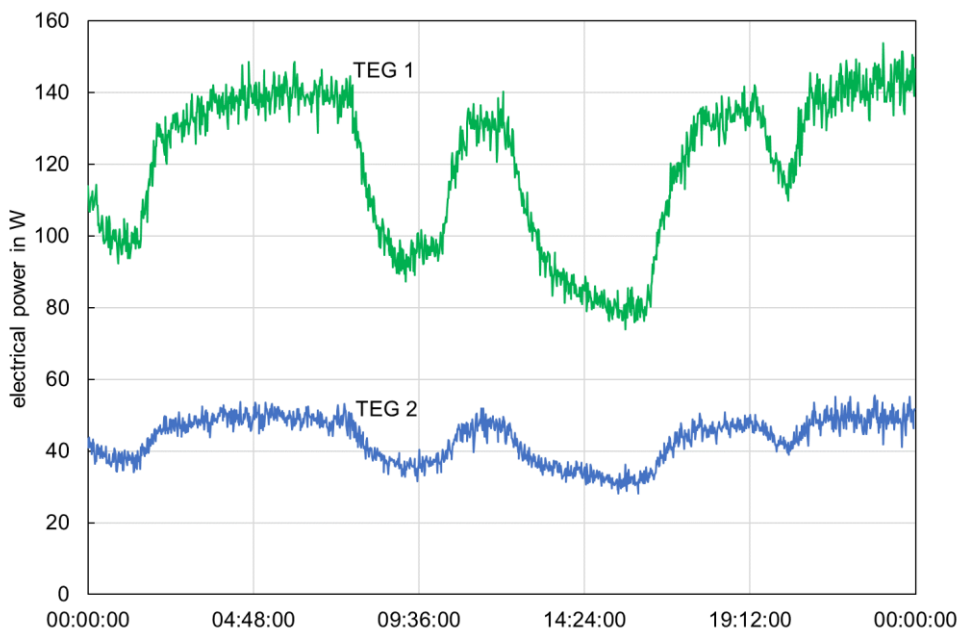


Figure 10: Power generation of cascading TEG

The cascading TEGs show the expected behavior, due to the heat loss for the operation of the first TEG the second TEG has a much lower power output. The maximum generated power was higher than 140 W for on TEG and reached a peak value of 200 W for the sum of both TEG. A change in the flue gas temperature leads to corresponding effects in both TEG.

The durability of the structure could be demonstrated over a period of several weeks of continuous and autonomous operation. The construction of the heat exchanger of the heat pipe proved to be a problem. After three weeks of operation, the heat pipe TEG was removed and checked due to very low performance measurements. Figure 11 shows a detailed view of the fins of the heat exchanger with severe damage, metal chips were found between the fins.



Figure 11: Damaged connectors between fins and heat pipe

The connections between the fins and the heat pipes were damaged, for which neither the process temperature nor the components of the atmosphere were responsible. Until the end of the project, the cause of this wear could not be determined in detail. Everything indicates that there has been some kind of chemical reaction among the materials. This could have several causes, one of which is the creation of a kind of galvanic battery between the copper spile and the stainless-steel fins. Besides, it looks like a type of coating has been generated on the stainless-steel fin's surface. The wear has considerably reduced the physical contact between the copper spile and the heat pipe what resulted in a poor thermal contact and consequently in less heat transport by the heat pipes. All other materials showed no signs of corrosion after the operating time.

The evaluation of the economic viability is highly dependent on the costs of TE systems and on the electricity rate the companies are subject to. Cost estimation for TE technology showed that costs of systems for utilisation of low temperature waste heat (up to 300°C) currently are in the range of 6,000 – 10,000 €/kW_{el}. Since high temperature TEG are less common and just produced in very small quantities the cost for such waste heat recovery systems can be estimated with 10,000 €/kW_{el} minimum. Nevertheless, it is expected that the production costs can be significantly

reduced by a couple of measures in the near future e.g. by advanced TE materials, new concepts for mass production of TE materials as well as economical TEG manufacturing and automated fabrication techniques for mass production of complete TE systems. The electricity rate for the industry in Europe is subject to significant fluctuations, since the companies are subject to different amounts of fees and taxes, especially depending on the country they are located, their electricity intensity as well as the industrial sector.

Result of the economic evaluation was that the investment in TEG applications seems not to be profitable for large-scale electricity consumers which are subject to low electricity rates. For smaller companies with higher electricity rates TEG could be interesting. By reaching the target prize of 2,000 – 4,000 €/kW in the future a considerable profitability of such systems could be reached, so that they could be of interest even for large companies.

Compared to other techniques (like ORC and SRC) the payback period of TE technology is currently clearly the highest, but with decreasing costs (see above) the use of TEG for waste heat recovery can certainly pay off and could be an alternative to other systems. Under these conditions TE systems currently may have better chance for producing electric power from

- smaller waste heat sources (lower temperatures or waste heat flows), which are not usable for ORC and SRC,
- discontinuous waste heat or
- waste heat sources, which are not accessible by ORC and SRC, e.g. due to shortage of space.

WP 6: Coordination and dissemination

One face to face project meeting with all partners present took place every semester. Regular telephone conferences of all partners and continuous information exchange via telephone and email have been established. The minutes of meetings and telephone conferences were distributed to all partners by the BFI.

Three Annual reports (2015, 2017, 2018) and a Mid-term report were created and approved. A project- website was created (www.bfi-blogs.de/powgeteg/) in 2017 and continuously updated. Due to the delay of the bypass construction (WP 5) an extension of the project duration to 30th June 2019 was requested by the partners in August 2018 and approved by the Commission in October 2018.

The project was presented at:

1. 15th European Conference on Thermoelectrics (ECT'17) on 26th September 2017 in Pardova, Italy, by GUN. Focus of the presentation "MPPT Electronic System for Power Generation from Hot Waste Gases Using a 250 W TEG" was on the results of the Power converter experiments at the test-bed.
2. Cleantech 4 on 28th/29th December 2018 in Bergamo, Italy, by BFI. The presentation "POWER GENERATION FROM HIGH TEMPERATURE WASTE HEAT USING THERMOELECTRIC GENERATORS" was about the done work in the project and the current results. Further a paper about the project was published in the proceedings of the conference.
3. ESTAD 2019 in Düsseldorf, Germany, by BFI. The presentation "Recovery of High Temperature Waste Gas Heat by Thermoelectric Generators" was about the entire project. A paper was published in the proceedings of the conference.

Conclusions

A TEG system was developed for the use of high temperature waste gas heat. During the development of the system new solutions for control (Monitoring system), power conversion (Power converter and MPPT algorithm), heat exchange (heat pipe heat exchanger) and TEG protection (antifouling coating and overheating protection by PCM) were designed and investigated. A small-scale demonstrator was investigated in the lab. Test data showed an electrical output of 175 - 260 W at a waste heat temperature of 700 – 800 °C. The newly developed Power converter and MPPT algorithm operated well in combination with the TEG. Based on the small scale tests the entire demonstrator design was adjusted, finished and the demonstrator was constructed.

Operational long-term testing of the whole system at the CSP at tkSE showed:

The generated power output was lower than expected after the lab trials. Especially the heat pipe TEG could not show its assumed potential. The design of the heat exchanger connection to the heat pipe was a weak point. The industrial suitability of the heat pipe is not apparent at this stage. The economic evaluation showed that TEG applications seem not to be profitable for large-scale electricity consumers which are subject to low electricity rates. The expected payback periods

cannot be fulfilled (lower than 3 years) at the currently high TEG costs (6,000 – 10,000 €/kW). For smaller companies with higher electricity rates and tolerating higher payback periods (up to 5 years) TEG could be of interest. An NPV calculation (which considers the whole lifetime of the TEG) showed that even at the currently high investment costs of 10,000 €/kW a good profitability over the lifetime of the plant can be achieved with increasing electricity rates.

Compared to other techniques (like ORC and SRC) the payback period of TE technology is currently clearly the highest. In the future the production costs of TEG have to be significantly reduced to the target price of 2,000 €/kW by a couple of measures e.g.:

- Advanced TE materials.
- New concepts for mass production of TE materials as well as economical TEG manufacturing.
- Automated fabrication techniques for mass production of complete TE systems.

Under these conditions TE systems currently may have better chance for producing electric power from smaller waste heat sources (lower temperatures or waste heat flows), which are not usable for ORC and SRC and for smaller applications like power supply of sensors at movable plants/processes.

Scientific and technical description of the results

1. Objectives of the project

Thermoelectric generators (TEG) can directly convert waste heat into electricity. They are already used in special applications, e.g. for power supply of sensors in remote areas or in air and space industry. However, the use of thermoelectric power generation from waste heat in a large-scale industrial application has not been sufficiently investigated until now. Thus, the PowGETEG project dealt with determination of possibilities of thermoelectric power generation using industrial gaseous waste heat at temperatures above 550°C. Main objectives were:

- Development of new solutions for control, power conversion (WP 2), heat exchange as well as for overheating and fouling protection (WP 3).
- Bench-scale tests with a 200 W_{el} unit. Therefor a test bed at which industrial conditions can be approached was designed and installed (WP 4).
- Design and construction of a demonstrator with an output of approx. 800 W_{el} based on results from the bench-scale tests and simulations. The demonstrator was long-term tested (WP 5) at a preliminary selected waste heat source of tkSE steel plant (WP 1).
- Determination of techno-economical possibilities of large scale TE power production based on testing campaign results. This included making conclusions on the possibility to use the technology in non-iron and steel industries (WP 5).

2. Description of activities and discussion

2.1 WP 1: Process and waste heat assessment

Objectives of WP 1 were:

- Study of a selection of iron and steel processes at tkSE and their flue gases possibly suitable for power production by using waste heat.
- Measurements to provide lacking information (e. g. about temperature and pressure fluctuations) of the waste heat source.
- Selection of a waste heat source where the demonstrator will be tested.

2.1.1 Task 1.1: Process and waste heat evaluation (all)

This task was devoted to the preliminary selection and analysis of eligible waste heat sources for the demonstrator test at tkSE steel plant. For that an evaluation document of process and waste gas data as well as additional required plant information, which were necessary to specify the boundary conditions of the TE system, was prepared by all partners. The document can be found in the appendix, **Deliverable 1.1**. Based on this document it was possible to identify a couple of plants, which could be suitable as the waste heat source for the demonstrator test at the end of the project (see WP 5).

After a first evaluation of different processes following plants were considered by tkSE to be used as proper waste heat sources:

- Hot dip galvanizing line 1 (HDGL 1), Radiant Tubes.
- HDGL 1, behind the recuperator.
- Hot dip galvanizing line 2 (HDGL 2).
- Hot rolling mill (HRM).
- Compact strip production (CSP).

Hot dip galvanising line

Figure 12 shows the scheme of the HDGL. In the entry section of the HDGL the strip is unrolled, and consecutive lengths are welded together to form an endless strip. An entry-looper provides a buffer stock at the entry to stop the strip for welding, without affecting the production process. A cleaning section is essential, if strip material must fulfil special surface requirements. After that the strip is preheated in the preheating furnace by hot waste gases from the direct fired preheater or Non-Oxidizing Furnace (NOF) which flow counter current to the strip. The NOF incorporates open fired gas burners to heat up the strip to the necessary process temperature. Combustion takes place in sub-stoichiometric levels of oxygen so that there is no oxidation of the strip surface.

Following the NOF, the strip passes into the radiant tube furnace (RTF). In the RTF it is heated up to the necessary annealing temperature by gas fired radiation tubes. After annealing the strip must

be cooled. The cooling starts in a slow cool furnace in which air-cooled tubes are used to cool the strip. Finally, cooled inert gas is blown on the strip in the jet cool furnace to ensure that the strip has a temperature equal to that of the zinc pot (460°C). After cooling the strip enters the zinc pot via a submerged snout, which guarantees that an oxygen free atmosphere is maintained up to the point where the zinc coating is applied. After galvanizing is complete the strip must be cooled down to 50°C to obtain a good result at the temper mill. The first cooling phase is carried out by blowing air onto the strip, followed by a water quench and hot air drying. Once the strip is cooled it is tempered, a chromate coating is applied, and the strip is dried.

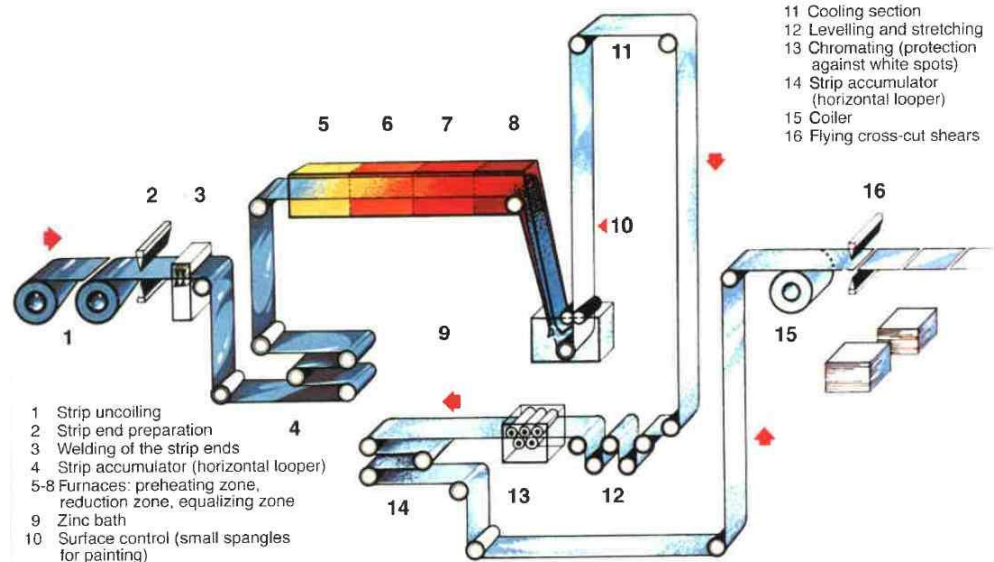


Figure 12: Scheme of a HDGL [2]

Hot rolling mill

A rolling mill comprises all the equipment and components needed for producing the hot or cold-rolled products within a certain product mix. A hot rolling mill is generally divided into the furnace zone (for supplying the heat required prior to deformation), rolling train and dressing and finishing department. **Figure 13** shows the scheme of the HRM. First the slabs are preheated to the required rolling temperature in the rolling mill furnace, which is a continuously-charged walking beam furnace. After that the slabs are running through a descaling facility. Bevor the slabs enter the roughing stand, they are centred by shiftable lateral guides. During transport to the finishing mill, width, thickness, thickness profile and temperature of the transfer bars are measured. In the next step, the crop shear cuts the ends. The descaler removes the secondary scale from the transfer bars by water. The finishing train forms the transfer bar to its intended thickness and width. The strip cooling is used to comply with customer-specific properties of the strip. Finally, the strip is coiled in the downcoiler.

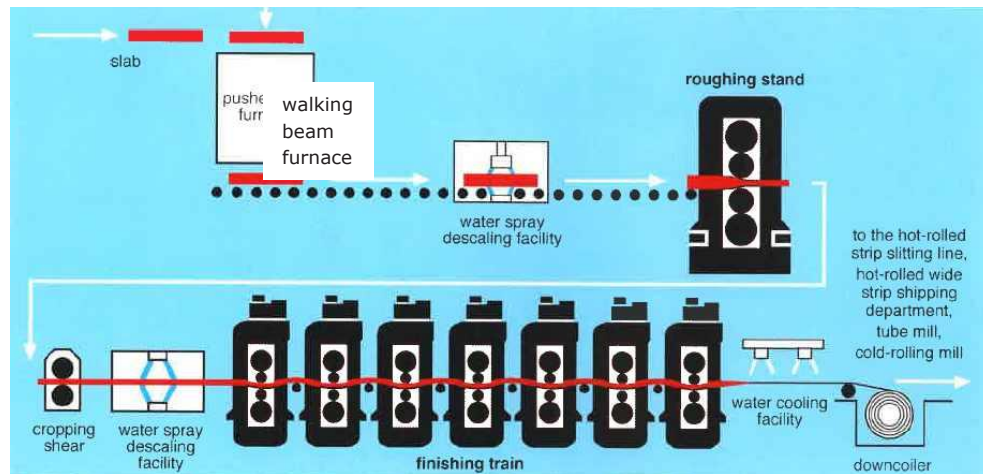


Figure 13: Scheme of a HRM [2]

Compact strip production

In the CSP, liquid steel is initially cast into thin slabs of 48 to 63 mm thickness and up to 1,600 mm width. After that the slabs are rolled into strips of 1.0 to 12.7 mm thickness. The direct combination of casting and rolling results in high flexibility with regard to delivery times and represents a resource-saving production route. In addition, the plant's modern roll stands permit the production of very thin hot band, previously only attainable by an additional rolling operation in a cold rolling mill. This is made possible by integrated heating/homogenizing furnaces securing a uniform hot band temperature and by modern rolling stands. The heating/homogenizing furnace is divided into 3 zones: Heating zone, Setting zone and Store zone. The furnaces are fired with blast oxygen furnace (BOF) gas. In the Heating and Setting zone the material is heated up to a temperature of 1,080 – 1,230°C (depends on the product quality), while in the Store zone the temperature is held. The scheme of the CSP at tkSE site is shown in **Figure 14**.

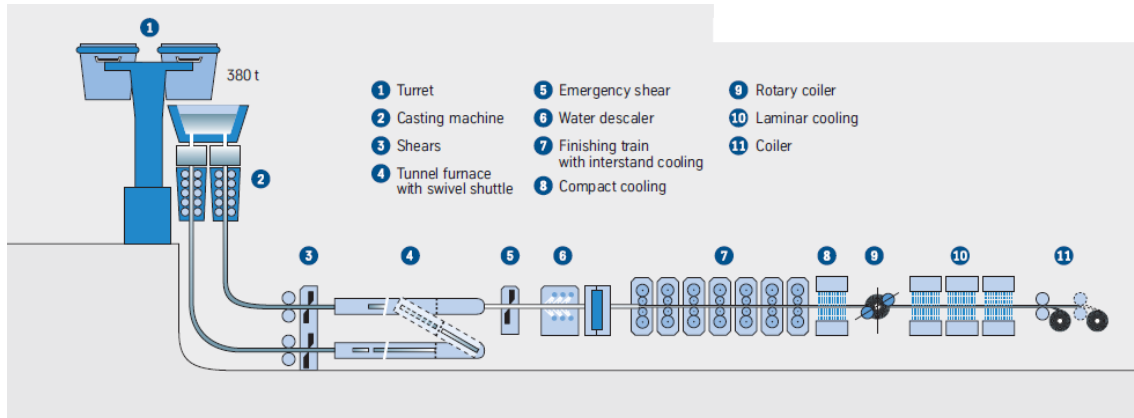


Figure 14: Scheme of the CSP at tkSE

2.1.2 Task 1.2: Measurements (tkSE, BFI)

Aim of this task were measurements, where data cannot be put available by tkSE but were required to design the TE system and to select a proper waste heat source.

tkSE collected available process data of the above-mentioned plants. For that an evaluation document including the required process data of the considered plants was created. With this information about the fuel gas, waste gas and cooling water were collected from the process control systems and missing data/information were identified. The document is attached in the appendix, **Deliverable 1.2**.

The main criterion to select a proper waste heat source was the waste gas temperature, which should be well above 550°C. A comparison of the five plants showed, that the waste gas temperature of the HRM is much too low (360 – 460°C) and was not considered anymore. The waste gas temperature of the HDGL 1, Radiant Tube, is too low, too (450 - 500°C). The waste gas temperatures of the HDGL 1 after the recuperator (530 – 560°C), the HDGL 2 (500 – 900°C) and the CSP (600 - 780°C) are at the lower limit of the required temperature or well above 550°C.

Other important criterions for the plant selection were the accessibility and the amount of space, to install the demonstrator and the necessary measuring equipment in/at the waste gas pipe. **Figure 15**, **Figure 16** and Figure 2 show the waste gas piping of the three plants. While there is enough space at the HDGL 1 and the CSP, the accessibility at the HDGL 2 is very bad and there is not enough space for the demonstrator installation. The waste gas pipe length between the recuperator and the stack of the HDGL 2 is just approximately 1.5 m. A control valve is installed in this short sector of the pipe, which makes it impossible to install the demonstrator in the pipe. Since the waste gas is mixed with air in the stack by a fan and thus cooled down below 550°C, an installation of the demonstrator in the stack of the HDGL 2 seemed not possible, too.



Figure 15: HDGL 1, recuperator for combustion air preheating (good accessibility and enough amount of space for demonstrator installation)



Figure 16: HDGL 2, recuperator for combustion air preheating (bad accessibility and not enough amount of space for demonstrator installation)

In summary a first data evaluation narrowed down the selection of possible waste heat sources to the HDGL 1 (behind the recuperator) and the CSP. Since the waste gas temperature ($530 - 560^{\circ}\text{C}$) of the HDGL 1 is at the lower useful limit (550°C) the CSP was identified as the most promising waste heat source. **Deliverable 1.3 (part 1)** in the appendix summarizes the results of the waste heat source pre-selection.

To collect more detailed information about the waste gas flow at the CSP measurements of the waste gas volume flow and temperature, the dust content and dust composition in the stacks of the CSP were planned and executed by tkSE and BFI.

Figure 17 shows the scheme of the waste gas system of one furnace zone of the CSP. The waste gas systems of the three zones (Heating zone, Setting zone and Store zone) are equal. The waste gas, coming from the furnace, passes a heat exchanger for combustion air preheating. If the temperature of the waste gas is higher than 950°C in front of the heat exchanger, cooling air is injected to protect the heat exchanger from overheating. Approx. 8 m after the heat exchanger a valve is installed for pressure and flow control. The measuring positions for the long-term measurements are marked with the numbers 1 – 3.

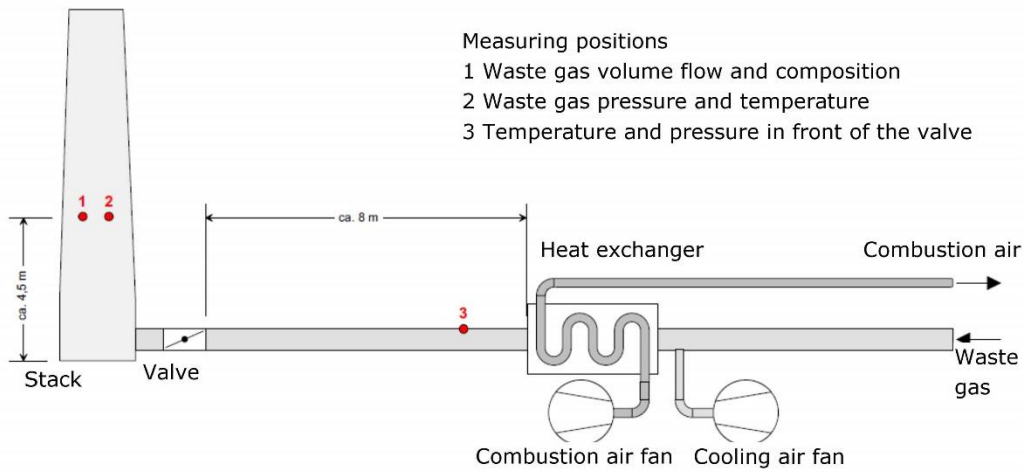


Figure 17: Scheme of the waste gas system of one zone of the CSP

It was decided, that measurements in the waste gas system of all three zones of the CSP are necessary, since the three zones are fired differently. Thus, different waste heat potentials of the three zones were expected.

Figure 18 shows the waste gas temperature at the three zones from 26th October to 23rd November 2015. The waste gas temperature is highest in the Heating zone with a value of about 800°C and fluctuations between 400 and 800°C. In the Store zone the waste gas temperature is lowest with a level between 350 and 600°C. To determine the waste heat flow the waste gas flow and the waste gas composition were measured, too.

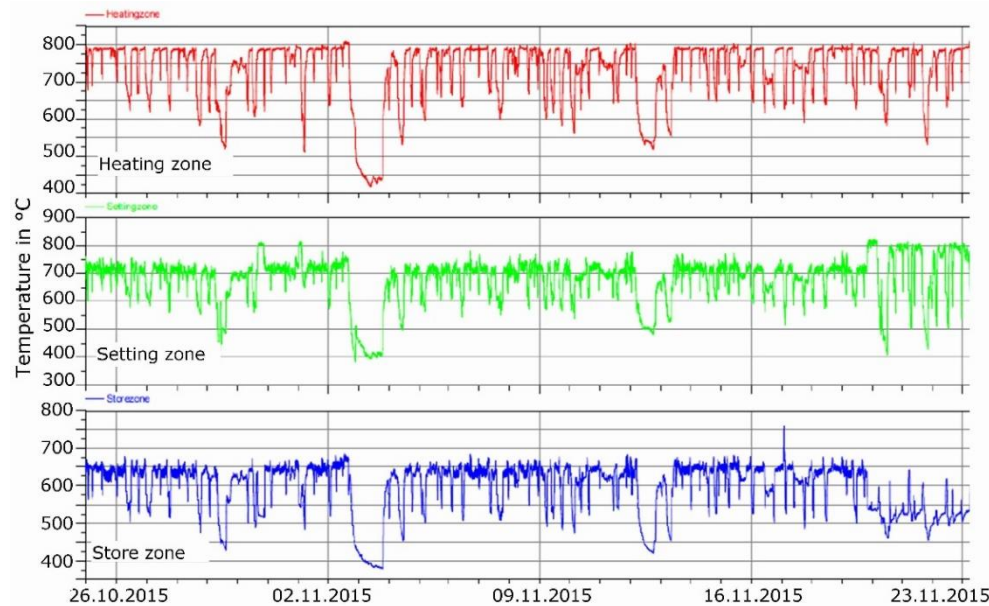


Figure 18: CSP, waste gas temperatures of all 3 zones of the furnace (data from the control system, measuring position No. 3, see **Figure 17**)

First step of the measuring campaign were traversing measurements in the stacks of the three zones of the CSP. These measurements were necessary to identify the correct position of the flow rate sensor in the waste gas stream during the long-term measurements. After evaluation of the collected data the long-term measurement of waste gas temperature, pressure, composition and volume flow was installed by tkSE and BFI, see **Figure 19**.



Figure 19: Installed pressure, temperature and waste gas flow measurement in a stack of the CSP

Figure 20 shows measured waste gas temperatures and pressures in front and behind the control valve as a result of the installed long-term measurement. The temperature measurements are in good agreement with the values extracted from the plant control system (see Figure 18). The pressure drop is very low with the highest pressure drop of approx. 400 Pa in the waste gas pipe of the Store zone.

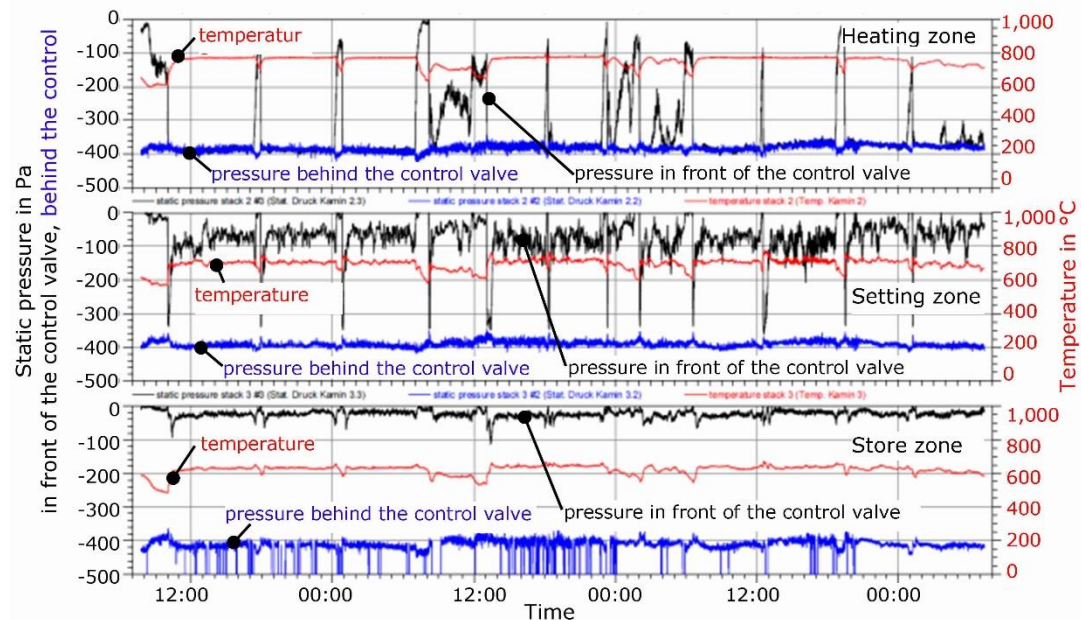


Figure 20: CSP, waste gas temperatures and pressures of all 3 zones of the furnace

To determine corrosive components in the waste gas, tkSE retrieved a sample of the waste gas at the CSP. The sample was taken with a heated removal lance, which was inserted into the appropriate stack via a flange system. During sampling, the exhaust gas from the stack flew through the heated lance and a heated filter with a volume flow of approximately 2 - 3 liters per minute. Afterwards, the exhaust gas passed a series of wash bottles. The bottles contained a selective absorption media. The final analysis took place in the laboratory by using an ion chromatograph.



Figure 21: Picture of the exhaust gas sample extraction at a stack of the CSP

To determine the composition of the dust deposits from the inside of the waste gas pipe were extracted. From these deposits, samples were taken and analyzed in the laboratory by using an optical emission spectrometry.

2.1.3 Task 1.3: Data evaluation (tkSE, BFI)

Main objective of this task was the evaluation of data, both data from tkSE plant control system and data from measurements (see Task 1.2), that determine the operation and design of the demonstrator.

Figure 22 shows a 24 h standard analysis of BOF gas used in the CSP from December 17th, 2015.

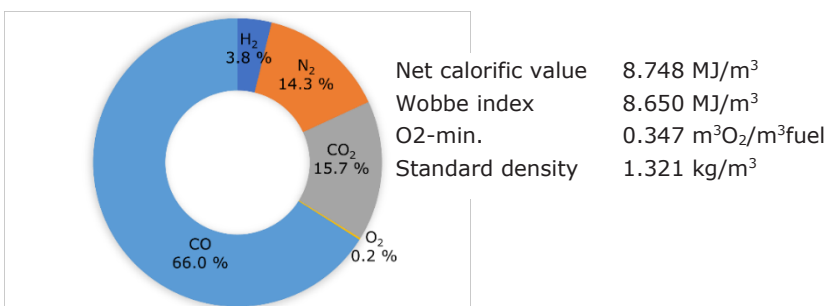


Figure 22: 24 h standard analysis of BOF gas used in the CSP from December 17th, 2015

Table 1 summarizes the major waste gas composition from the BOF gas combustion at the CSP.

Table 1: Waste gas composition at the CSP from BOF gas combustion

Waste gas from BOF gas combustion		
CO ₂	29.19	Vol.-%
H ₂ O	1.36	Vol.-%
O ₂	3.72	Vol.-%
N ₂	65.74	Vol.-%

The results of the long-term measurement at the 3 zones of the CSP showed following results:

- Maximum waste gas temperatures 610°C (Store zone) – 790°C (Heating zone)
- Waste gas flow 8,000 – 15,000 m³/h
- Pressure drop over the control valve max. 4 mbar (Store zone)

Calculations of a 4-week average from operational data of combustion fuel flow and waste gas temperature showed following waste heat potential of the CSP:

- Store zone: 1.7 MW, average waste gas temperature ~ 600°C
- Setting zone: 2.1 MW, average waste gas temperature ~ 680°C
- Heating zone: 3.6 MW, average waste gas temperature ~ 730°C

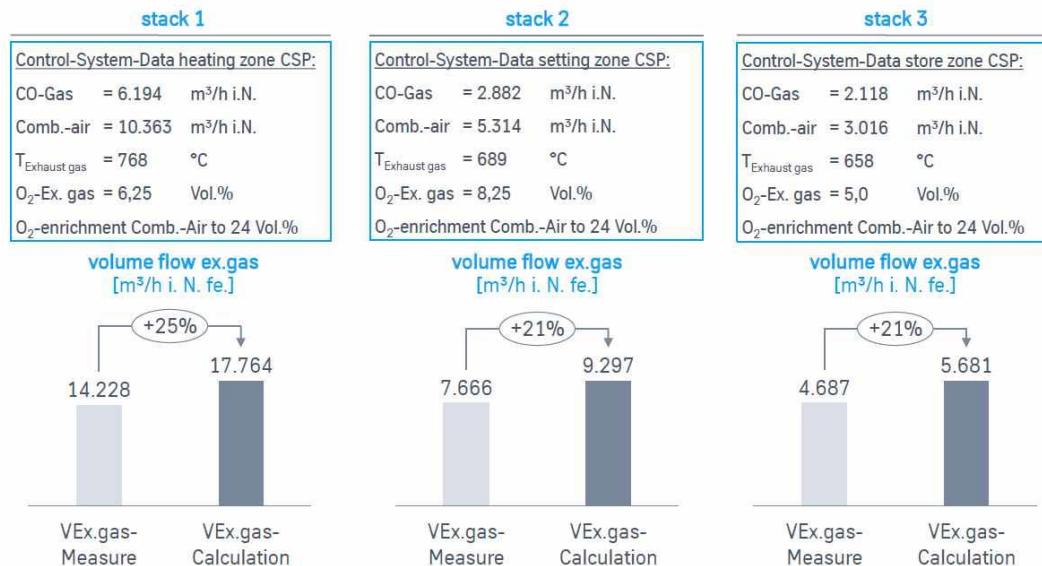
The results indicate that all 3 zones / waste gas systems of the CSP are suitable for the demonstrator tests (WP 5).

A comparison of the traversing measurements from 17th December with the calculated waste gas flow based on the fuel gas combustion shows a difference of about 20 – 25 %, see **Figure 23**. Reasons for the differences are:

- The 3 zones of the furnace of the CSP are not strictly separated. Thus, it is possible that waste gas from one zone enters the next zone.
- The traversing measurements provide data for a short period of several minutes and cannot be compared exactly with the average data of the plant control system.

Evaluation of the exhaust gas measurements from the 17th.Dez.2015

CSP: exhaust gas stack 1-3 oven 2



The differenz between the measurement results and the theoretical calculation has some reasons!

Figure 23: CSP, evaluation of the waste gas measurement from December 17th, 2015

The results from the measurement of additional components in the waste gas especially Cl, F and SO₂ are shown in Table 2. The measured values are quite low in the range of 0.3 – 2 mg/m³ (standard condition), so that no corrosion problems for the heat exchanger are expected.

Table 2: Results of the measurement of additional components in the waste gas

Component	Value	Unit
Cl	0.37	mg/m ³ (standard condition)
F	0.3	mg/m ³ (standard condition)
SO ₂	2.0	mg/m ³ (standard condition)

The measurement of dust composition showed that the main component is Fe. Further the dust contains a lot of other components, mainly metals. Since the dust content of the waste gas is < 10 mg/ m³ (standard condition) no major problems with deposit formation for the demonstrator test were expected. However, the mechanism of deposit formation and build-ups were investigated in Tasks 3.3 and 3.4. The detailed dust composition of the waste gas is summarized in the appendix, **Deliverable 1.3**, part 2. Main results of the evaluation of collected and measured data at the CSP are collected in **Deliverable 1.3**, part 3 in the appendix.

Altogether the evaluation of collected and measured data from the CSP showed:

- The average waste gas temperature of the three zones is in the range of the required temperature (min. 550 – max. 850°C) of the TE modules.
- The waste heat flow is in the range of 1.7 – 3.6 MW and thus high enough for the demonstrator with a target output of approx. 800 W_{el}. To produce electricity of 800 W_{el} a waste heat flow of approx. 16 – 40 kW_{th} is necessary, depending on the efficiency of the TE modules, which is normally between 2 and 5 %
- The allowed pressure drop through the installation of the demonstrator in the waste gas pipe is very low (< 4 mbar). This must be considered in the demonstrator design

The above described results show that all 3 zones / waste gas systems of the CSP are suitable for the demonstrator tests.

2.1.4 Task 1.4: Process selection (all)

Objective of this task was the selection of the best suitable waste heat source for the demonstrator test at tkSE steel plant.

As described above the favoured plant was the CSP. Thus, the measurements were concentrated on this plant. The waste gas temperature of the 3 zones differs between 600°C (Store zone) and nearly 800°C (Heating zone). The waste gas temperature of the Store zone is near to the lowest required temperature. Thus, this zone was rejected for the demonstrator tests. After an inspection of the localities at the waste gas systems of the Setting and Heating zone by tkSE and BFI, the Heating zone of furnace 1 was selected (MS 1) as the best suitable plant for the demonstrator test. Main criterions were:

- The waste gas temperature is well in the usable range of the TE cartridges.
- Good accessibility.
- Enough amount of space for demonstrator installation.
- The area is roofed, so that the measuring equipment and data acquisition system are well protected from environmental impacts.

2.2 WP 2: Design of TE demonstrator and its bench scale unit

Objectives of WP 2 were:

- Define performance requirements for each of the system components of a 200 W_{el} bench scale unit and an 800 W_{el} demonstrator.
- Development of (1) a concept and (2) a design of both the bench scale unit and demonstrator based on the results of process selection from WP 1 including e.g. TE packaging, heat exchanger, power output and power conversion, optimal arrangement of the TE facility in the waste heat stream, ability to withstand stresses, etc.
- Continuous design improvement based on the results of tests, simulations and design analyses in WP 2 – 4.
- Assembly and delivery of a TEG bench scale unit to be tested in the test-bed in WP 4.
- Delivery of the large-scale demonstrator's final design for WP 5.

2.2.1 Task 2.1: Requirements definition (all)

Aim of this task was the collection of requirements for the bench scale unit and the demonstrator, based on the selected waste heat source.

During project duration two main test series were foreseen:

1. Tests of a bench-scale unit, which produces 200 W_{el}, at the testing facility of the BFI (WP 4)
2. Operational long-term tests of a demonstrator, which produces approx. 800 W_{el}, at the CSP waste gas system at tkSE site (WP 5).

The bench scale tests were dedicated to investigate some specific aspects of the TE system and its components under defined boundary conditions. Based on these tests the design of the entire demonstrator was adapted. The final demonstrator long-term test aimed the investigation of long-term behaviour and performance of a system consisting of several TE cartridges, heat exchanger, power converter and measuring devices. **Table 3** gives an overview of the identified main objectives of above-mentioned tests.

Table 3: Main objectives of planned tests

Test	Objectives
Tests of a bench-scale unit, which produces 200 W _{el}	Determination of the warm-up and cool-down behaviour of the bench-scale unit. Determination of the electrical output and efficiency at different waste heat flows and conditions (waste heat temperature, waste gas volume flow and velocity, ...). Determination of the behaviour and efficiency at discontinuous conditions. Determination of effects of the TE application on waste gas pressure and temperature.
Operational long-term tests of a demonstrator, which produces 700 - 800 W _{el} at the selected waste heat source	Determination of the long-term performance of the entire demonstrator, consisting of TE cartridges, heat exchanger, power converter and measuring devices (Efficiency drop during the testing period, discontinuous behaviour). Determination of effects of the TE application on waste gas pressure and temperature. Determination of the growing of build-ups on the surface of the waste heat exchanger

To prepare these tests suitable instrumentation of the bench scale unit and the demonstrator was defined by GUN and BFI. The instrumentation of both the bench scale unit and the demonstrator

comprised waste gas measurements (temperature, composition, volume flow, pressure), cooling water measurements (temperature and mass flow), and measurements of the electrical output of the TE cartridges (voltage, current, power). For the bench scale test a data logging for each second was aimed to determine exactly the performance of the bench scale unit, even for discontinuous conditions. The data logging rate for the demonstrator tests could be reduced to every 5 or 10 seconds, since highly discontinuous conditions were not expected, due to the results of the measurements at the CSP in WP 1. For the long-term test it was mandatory that daily or (in the best case) online checks of the measured data must be possible, to detect errors/failures of the demonstrator or measuring equipment as soon as possible. For that the development of an Online Monitoring system was foreseen. Further the demonstrator setup and the measuring equipment would have to be checked regularly (minimum weekly) by tkSE and/or BFI staff. If necessary, the measuring equipment has to be recalibrated during the long-term testing. The detailed equipment requirements for both the bench-scale unit and the demonstrator are summarized in **Deliverable 2.1**, part 1 in the appendix.

In the next step boundary conditions and limits for the TE application were defined by all partners. Main limits for the TE system were a maximum waste gas flow 300 kg/h and a maximum allowed waste gas temperature of 850°C. The cooling of the TE cartridges had to be ensured, since the TE cartridges would be damaged without cooling. Another point to be considered in the demonstrator design was the maximum allowed pressure drop of less than 4 mbar (see also Task 1.3). Further it was clear that the demonstrator design must be adjusted to the waste gas pipe dimensions, or, if this is not possible (e. g. due to available and economic TE cartridge designs) that the installation of a bypass system and a fan for the demonstrator tests could be necessary. Another point to be considered was the tolerable waste gas temperature drop, due to the demonstrator installation in the CSP waste gas pipe. This depends on the stack effect and the dew point of the waste gas. But, since the output of the demonstrator was foreseen with max. 800 W_{el} and the waste heat flow of the CSP is in the range of 1.7 to 3.6 MW (with a temperature > 550°C, see WP 1) it was excluded that the waste gas temperature could fall below the dew-point. All defined boundary conditions are summarized in **Deliverable 2.1**, part 2 in the appendix.

2.2.2 Task 2.2: Concept development (all)

This task was dedicated to the design of a first overall concept of the TE system. This included concepts for the TE cartridge, outline of the Power converter design, concepts for the connection of the TE system to the waste gas pipe of the CSP and an alternative concept for the heat exchanger.

2.2.2.1 Design of the TE cartridge (GNTH)

In respect of economic reasons, the TE cartridge design was based on former concepts from GNTH. Several TE cartridge design options were weighed in which the hot side heat exchanger was either on the outside or on the inside. It was found that a design with an inside heat exchanger would be easier to integrate into the CSP waste gas pipe system. **Figure 3** shows the scheme of the selected cartridge design. The inner tube (diameter 90 – 160 mm, see also Task 2.6) yields fins for improved heat exchange. The outer tube comprises the coolant water jacket which lets water circulate around the cartridge. The inner tube fins remove heat from the waste gas flowing through the centre opening. Between inner and outer tube, a number of thermoelectric pellets (p and n doted) are placed. The heat flux through the pellets yields a Seebeck-voltage. The pellets are electrically connected to add their individual voltages to the power output. The cartridge can be connected to the waste heat source via flanges. The heat is rejected to the cooling water of the outer tube. For cooling a water flow in the range of 10 - 20 l/min and below 90°C is required. For the entire demonstrator two different kind of cartridges were foreseen, which differ in their diameter and length and thus, also in their performance. The smaller cartridge with an inner tube diameter of 90 mm was named GEN3 and the bigger cartridge (inner tube diameter 160 mm) was named GEN4. A more detailed description of the cartridges can be found under Task 2.6.

2.2.2.2 Design of the power conversion system (GUN)

The function of the developed Power converter is to track the maximum power available from the thermoelectric generator(s) connected at its input. This includes also the implementation. Since the design of the Power converter is directly linked with the development of MPPT algorithms the developed power converter is described under Task 2.4.

2.2.2.3 Design of the connection between the TE system and the waste gas pipe (all)

The consortium decided not to install the demonstrator directly in the waste gas pipe of the CSP but to install a bypass pipe to the waste gas pipe in which the demonstrator could be installed. The design of such a bypass system was not foreseen in the proposal. However, the use of a bypass for the demonstrator test was identified as the best solution, so that the bypass design was included into Tasks 2.2 and 2.6. Reasons for this decision were:

- In respect of economic reasons, the cartridge design was based on former concepts from GNTH. The target cartridge design with an inner diameter of 90 – 160 mm was not suitable for an installation directly in the CSP waste gas pipe (inner diameter 1.3 m).
- The allowed pressure drop in the waste gas pipe is just max. 3 - 4 mbar. To avoid process interruptions of the CSP through a forbidden pressure drop in the waste gas pipe during the demonstrator tests the best solution was the installation of a bypass for the demonstrator test.
- The use of a bypass allowed an installation and de-installation of the demonstrator independently from standstills of the CSP. The time planning for in-situ work at the demonstrator was more flexible.
- By using the inspection chamber as the connection to the waste gas pipe new access openings for the demonstrator installation at the waste gas pipe were not necessary. Thus, the static of the waste gas pipe had not to be reviewed.
- The utilization of an appropriate fan in the bypass allowed the investigation of the condition like it is found in the original waste gas pipe. Further, in terms of TE utilization in other plants and industries, it was possible to investigate a wide range of other process conditions (waste gas volume flow, waste gas velocity). These investigations gave valuable information for the latter technical and economic evaluation of such TE systems.

It was foreseen to connect the bypass an inspection chamber at the recuperator of the waste gas pipe. **Figure 24** shows the inspection chamber of the recuperator.

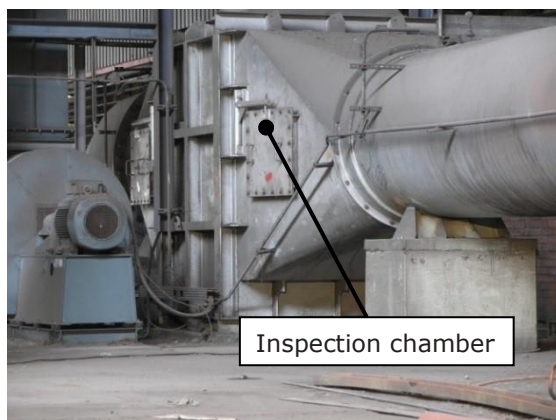


Figure 24: Waste gas pipe of the CSP, connection of the bypass pipe for the demonstrator test

In a first approach three options for the bypass design were considered:

1. Ladder design 1: The branches to the TE cartridges are connected to a distributor in the form of a pipe. The waste gas inlet into the distributor is in the middle, **Figure 25 top left**.
2. Ladder design 2: The branches to the TE cartridges are connected to a distributor in the form of a pipe. The waste gas inlet into the distributor is at the beginning, **Figure 25 top right**.
3. Revolver design: The branches to the TE cartridges are connected to a cone shaped distributor, **Figure 25 bottom**.

All three options included shut-off valves to disconnect the TE system from the waste gas flow, if necessary (e. g. for protection reasons or alteration of the set-up). Further a fan was foreseen to provide exact waste gas volume flows and velocities in the bypass system.

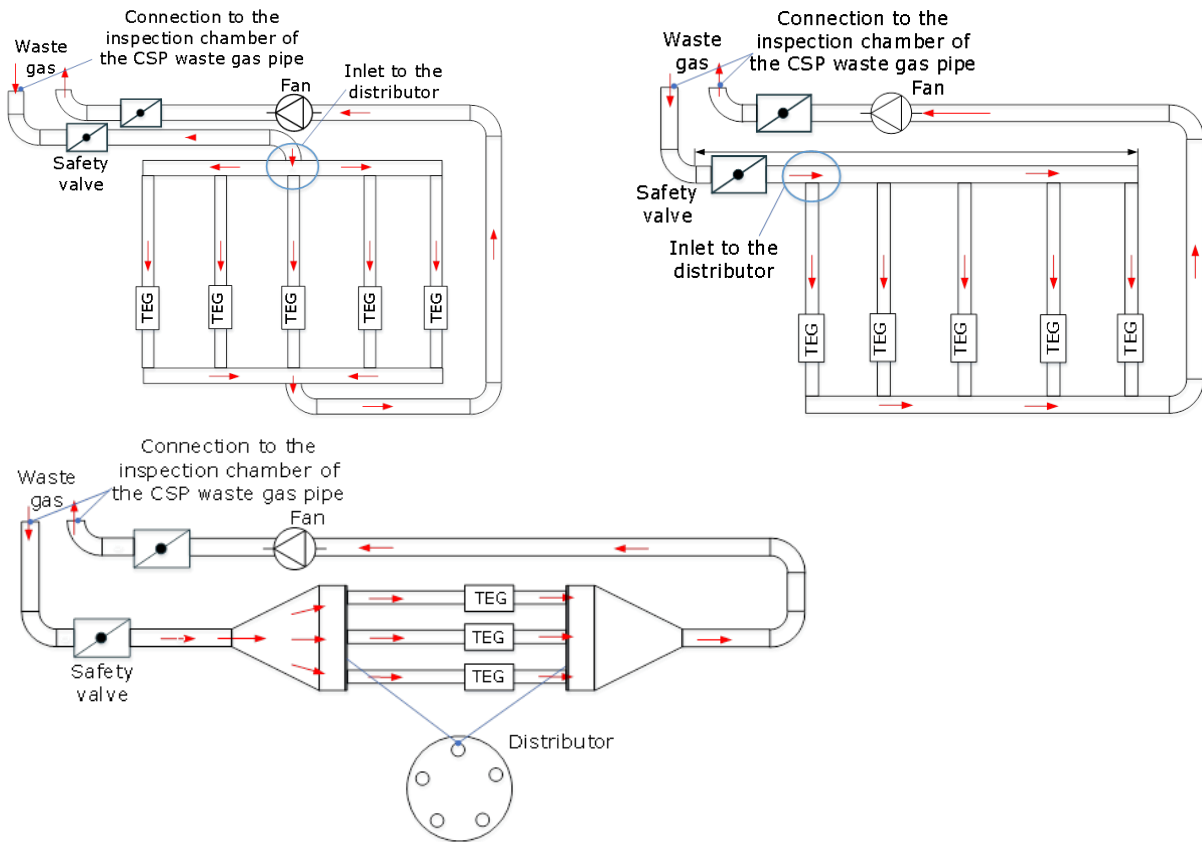


Figure 25: Schemes of bypass options: ladder design 1 (top left), ladder design 2 (top right), revolver design (bottom)

To identify the best suitable bypass configuration CFD simulations of the waste gas flow were carried out by BFI. **Figure 26** shows exemplary calculated gas streamlines of the revolver design.



Figure 26: Example of calculated waste gas streamlines (revolver design)

Overall results of the simulations were:

- The ladder design 1 showed the highest pressure loss (342 Pa) from inlet to outlet, followed by ladder design 2 (303 Pa). The revolver design showed the lowest pressure loss (280 Pa).
- The streamlines showed flow detachments at the inlets of the branches within the ladder designs. For the revolver design a free jet with recirculation at the inlet of the distributor and turbulences at the exit were clearly visible.
- The velocity distribution for both ladder designs showed inhomogeneous flow patterns. For the ladder design 2 it was furthermore shown, that a main ratio of the flow is in branch 1. For the ladder design 1 especially branches 3 and 4 showed an inhomogeneous flow which originates from the flow detachment. The flow rates for the individual branches of the revolver design were quite even distributed.

Thus, the revolver design was considered as the best bypass option and was designed in detail. After finishing the detailed design, the order of the bypass construction was placed by tkSE by a tendering process, due to the expected cost of the bypass. Despite the long duration of the tendering process (5 months) no company made an offer until September 2018. In September 2018 tkSE received an offer of 350,000 € for the bypass construction. This was the only offer tkSE

received. Since 350,000 € for the bypass construction were out of the proposed and granted costs of tkSE topics, the bypass design had to be massively changed to reduce the costs. Thus, following main changes in the bypass design were proposed:

- Replacement of the cone shaped distributor by a pipe with two branches.
- Reduction from 5 to 2 branches. One branch for the heat pipe approach (see chapter 2.2.2.4 and Task 2.6) and one branch for the integration of two GEN4 cartridges. The two branches will have different diameters. The different diameters are a result of different necessary waste gas flows for the Heat pipe heat exchanger (650 kg/h) and the directly into the bypass installed GEN4 cartridges (130 kg/h). The temperature of the waste gas will be the same, so that the results of the directly installed GEN4 cartridges will be comparable with the Heat pipe heat exchanger approach.
- Replacement of the high temperature resistant fan by a normal fan. For that cooling air is sucked into the bypass behind the TE cartridges to cool down the waste gas to 400 °C.
- Reduction of the overall size of the bypass system from 13 m to approx. 9 m.

Figure 4 shows the scheme of the newly designed bypass. Technical drawings of the new design can be found under **Deliverable 2.6** in the annex.

Consequences of the change in the bypass design were:

- Less complex construction with less need of material and much easier to install.
- Presumably no new base plate necessary due to the reduced weight.
- Power output of the demonstrator in the range of 700 – 800 W (approx. 350 W of GEN4 at 800°C, approx. 250 W of the 2nd GEN4 at lower waste gas temperature of 700°C due to the expected decrease of the temperature through the first GEN4 cartridge, approx. 200 W of GEN3 with the heat pipe approach) which is slightly less than expected in the proposal (1,000 W). However, the influence on the final assessment should be minimal since the plus of information through the usage of more TEG cartridges than 3 will be low. Rather the performance information of the two in series connected GEN4 cartridges will give more valuable information about possibilities to use several cartridges for one waste gas stream.
- Reduction of the necessary waste gas flow from approx. 1,150 kg/h to approx. 800 kg/h.
- Possibility to investigate the impact on power production of in series connected cartridges.

2.2.2.4 Design of alternative heat exchanger concepts (CEM)

One of the main bottlenecks for applying TEG directly to an exhaust gas pipe is the pressure drop TE cartridges introduce into waste gas pipes. This is an issue, since the waste gas flow of a lot of heating furnaces is driven just by the stack. To deal with this issue an additional approach was designed, constructed and tested. This consists on transferring the exhaust gas temperature to the TE cartridge via heat pipes. That means that the TE cartridge is placed outside and the hot side of the heat pipe is placed inside of the waste gas pipe. To increase the heat transfer from the waste gas to the heat pipe a heat exchanger will be connected to the heat pipe. By doing it, it was expected to be able to transfer the heat required causing minimum pressure loss (less than 4 mbar). **Figure 27** shows a scheme of the indirect heat transfer solution.

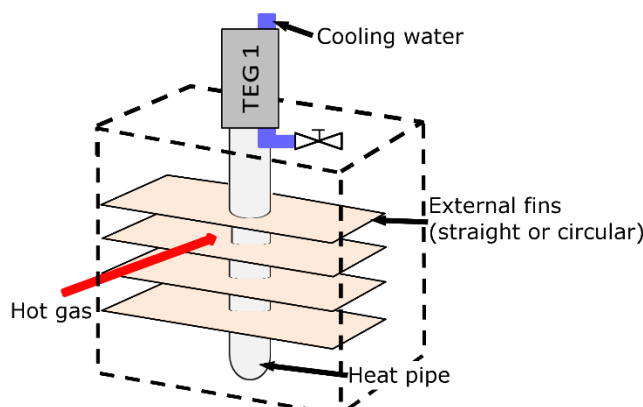


Figure 27: Scheme of proposed solution for indirect heat-transfer to the TE cartridge via heat pipes

To design the heat exchanger geometry following specifications were set:

- Approx. 200 W of electric power of the TE cartridge → approx. 6 kW heat transfer rate
- Pressure drop in the waste gas pipe < 4 mbar

Main design parameters were:

- Number and diameter of heat pipes

- Number of fins, fin radius and thickness, gap between the fins
- Finned heat pipe length

The bypass tube's length upstream from the heat exchanger assembly must be long enough as to assure a completely developed flow at the heat exchanger location (around 2 m). Likewise, the bypass pipe's length downstream from the heat exchanger should be around 1 m to avoid any back flow that could affect the heat exchange.

Under these considerations, a first draft of the heat exchanger and bypass assembly was designed. The detailed design is described under Task 2.6.

Apart from the above written, the heat exchanger used in both approaches (direct and indirect) must fulfill two main requirements: to minimize the dust deposition on the heat exchanger fins and to dump any exhaust gas temperature fluctuation. For such purposes, a high temperature resistance and antifouling coating and a static temperature absorber were defined (see WP 3). A summary of the design concepts is given in **Deliverable 2.2** in the appendix.

2.2.3 Task 2.3: Bench scale unit design and assembly (GNTH)

Aim of this task was the design and assembly of a bench scale unit with an electrical power output of approx. 200 W. After construction the bench scale unit was tested at the BFI testing facility.

A GEN3 cartridge (see Task 2.2) was used as the bench scale unit generator. To investigate its performance, it was outfitted with additional sensors as depicted in **Figure 28**. Temperature measurements in front and after the TE cartridge were foreseen to evaluate the influence of the cartridge on the waste heat temperature and to be able to calculate the efficiency of the cartridge. Further the temperature of the cartridge was measured to prevent an overheating of the it and to evaluate the performance of the heat exchanger at the hot side of the cartridge. The temperature of the cooling water was measured in front and after the cartridge. Another important measure was the pressure respectively the pressure loss of the waste gas due to the heat exchanger of the cartridge, which was determined by pressure measurements in front and after cartridge. For power and performance measurements it was intended to connect the cartridge to the newly developed Power converter, see Task 2.4 and 2.6.

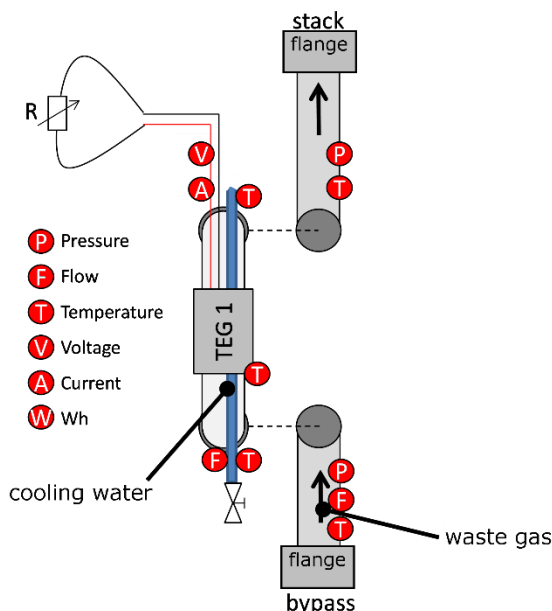


Figure 28: Scheme of the location of necessary measuring points for the tests

The cartridge must be installed in the bypass with a minimum distances 10 times of the bypass diameter after the last bend or cross-sectional variation of the pipe.

The connection of the cartridge with the bypass pipe was done by a flange system, as shown in **Figure 29**. The flanges are not screwed but braced with the shown clamp. Advantage of this design is that the cartridge was easy to install and to de-install.



flange

clamp

Figure 29: Flange system for the connection of the cartridge with the bypass pipe

Finally, a cartridge for the bench scale unit was assembled and carried to the BFI testing facility, see **Milestone 2b** in the appendix.

2.2.4 Task 2.4: Power conversion development and system automation (GUN)

This task was devoted to the development, construction and testing of a MPPT Power converter, to extract the maximum power from the TE system. This includes the design of a test rig and a power converter as well as the development of MPPT algorithms.

In order to properly deliver this task a hot gas test system was constructed. This allows an array of common sample TEGs to be tested under the conditions likely to be experienced in the current deployment. Specifically, thermal energy transfer is to the TEG via hot gases (convection) rather than by conduction. The developed MPPT was then connected to the TEG array and the operating point is modified from the “default” of the 50 % point of the open circuit voltage to investigate the impact on the output power and overall heat flux transferred from the hot gases due to the parasitic Peltier effect. In the final demonstrator it was anticipated that several of the thermoelectric cartridges are required, operated thermally and electrically in parallel. For this reason, a parallel TEG array was included in the design of lab scale tests, thereby requiring the use of a distributed MPP converter architecture connected to a common energy output channel.

Hot gas test system

The hot gas system shown in **Figure 30** and **Figure 31** was built with the purpose of replicating the constant heat TEG application at the tkSE steel plant. The system operates on the following principle: the heat source for the TE modules is realized using an inlet fan set to a specific rotational speed blowing the ambient air through hollow electrical heaters into the system. The hot air heats the heat exchanger that holds the TE modules and afterwards it is dispersed into the ambient, replicating the flue arrangement in the steel plant. The fan is an axial flow PWM (pulse width modulation) controlled device that has a low stall pressure, mimicking the low tolerance of back pressure in the flue gas path.

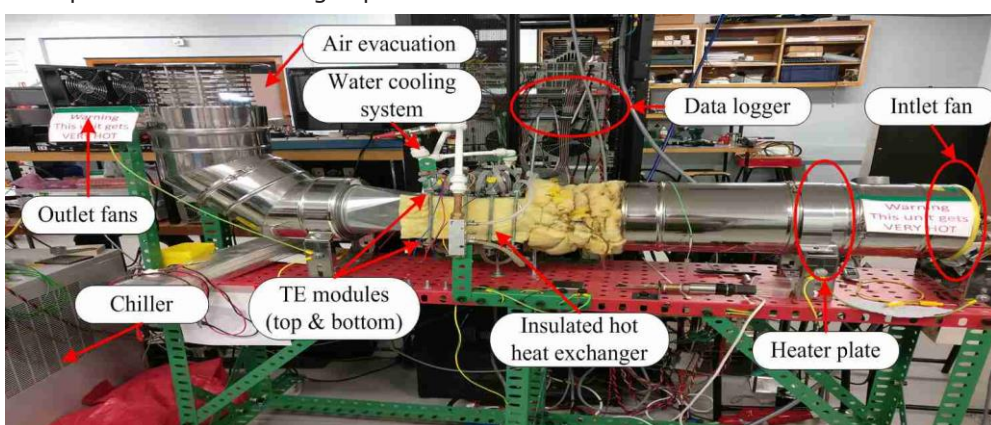


Figure 30: Hot gas system

The air is first blown into the plenum (area between inlet fan and heater plate) to achieve a uniform pressure and then passed through 27 hollow metallized alumina igniters (rated at 300 W/1,050°C) into the mixing region as shown in Figure 31. The igniters are supplied from a 415 V / 3-phase star-connected supply with 9 igniters connected per phase. The hot air exits the system through a standard chimney. Each TE module has a cold side heat exchanger composed of a water block with labyrinth. The temperature of the water entering the system is controlled at a desired temperature by a chiller unit capable of removing up to 4.3 kW of heat.

Each TE module has a cold side heat exchanger composed of a water block with labyrinth. The temperature of the water entering the system is controlled at a desired temperature by a chiller unit capable of removing up to 4.3 kW of heat.

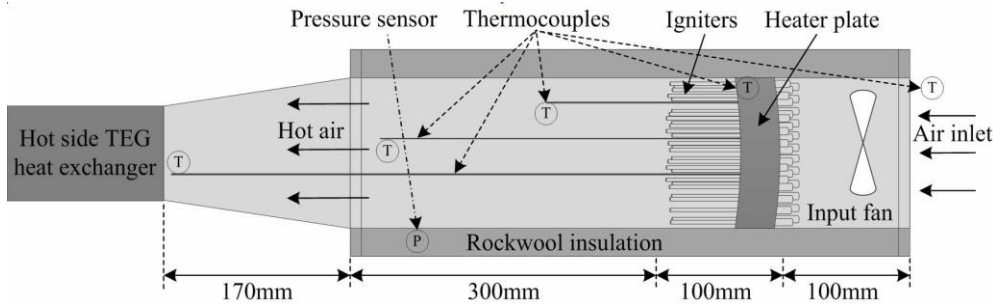


Figure 31: Scheme of the air flow in the hot gas system

An Agilent 34980A data acquisition and control (DAQ) unit was interfaced with a custom electronic controller and used to control and monitor the system. The unit controls the inlet and outlet fans control duty cycles, a voltage reference for a three Crydon phase angle controllers to vary the supply to the heaters and switching of each of the six channels of TE modules between I-V trace and MPP modes. Moreover, the unit monitors the power ratings of each array of modules, the load on each phase of the heater supply, the battery voltage and various temperatures throughout the system. A 240 Ah lead acid battery was used as a sink for six Thermoelectric Conversion Systems KM2 MPPT converters, thus allowing for constant loading on the TE devices at various power points (demonstrating the parasitic Peltier effect) and energy collected to be analysed.

There is a total of 12 thermocouples placed around the system as follows: one next to the inlet fan to measure the ambient temperature, four in the heater section at different positions, 4 for the temperature of the hot heat exchanger, one for the hot air exiting the heat exchanger, two for the inlet and outlet of the coolant water. The thermocouples are connected to the DAQ unit.

Choice of MPPT algorithm

The goal of MPPT algorithms is to set the TE system to operate at its optimum power output according to the temperature conditions. The MPPT algorithms that are implemented in TE systems were originally designed for PVs which required fast control (order of milliseconds) to comply with the rapidly changing irradiation conditions. These control methods were changed according to the maximum power transfer theorem condition and integrated into TE systems. Examples of MPPT algorithms for PV system are:

- The P&O (Perturb & Observe) is perhaps the most used hill-climbing method due to its simplicity and high efficiency.
- The Incremental Conductance is another hill-climbing algorithm often used instead of P&O with very similar efficiencies, but slightly more complex to implement. Both methods require voltage and current measurements and significant computational power to perform the MPP search.
- The fractional open-circuit voltage V_{oc} method is less frequently used for PVs because their MPPs differ among the various solar panel technologies. In case of TEGs it is known from the maximum power transfer theorem that no matter the material the module is constructed from, it will operate at the MPP if the load voltage is at half of the open-circuit voltage. For this reason, the fractional V_{oc} method is a very good choice for TE systems, and it requires only one voltage measurement (and no current measurement) that significantly reduces the computational demand.

However, in a PV system temperature is not considered whereas temperature in the majority of TEG applications presents significantly slower dynamics (order of minutes) and is an essential requirement for system operation. Moreover, the presently used control methods do not take into account the electro-thermal interactions present in TE systems, mainly the parasitic Peltier effect which varies with the current magnitude and affects the temperature of both the TEG element and the heat exchangers. The Peltier effect is the opposite of the Seebeck effect. The greater the current flowing due to Seebeck power generation, the greater the current-induced Peltier effect that increases heat flux through the TEG. If the thermal dynamics of both the Peltier and Seebeck effects are considered simultaneously, the power generated by the TE systems can be increased and at the same time the system efficiency can also be improved. The implications for MPPT algorithms for TE power generation systems are thus profound: to find the "true" maximum power point of a TE power generation system the algorithm must be able to simultaneously accommodate the coupled microseconds electrical response and many-minutes thermal response – some ten orders of magnitude difference in time constants. Further, the "best" value for the input impedance of the power converter varies with heat flux and in most practical systems the heat flux itself is unlikely to remain constant, e.g., an automotive exhaust gas stream, during the period required for the system to reach equilibrium.

A fractional V_{oc} algorithm is designed to repeatedly measure the open-circuit voltage and set the voltage according to that indicated by the Maximum Power Transfer Theorem as being the optimal operating condition for the TEG - i.e., $0.5 \times$ the open-circuit voltage (the case for PV systems). This condition leads to current flowing through the module and the Peltier effect to slowly cause a temperature difference reduction across the device. The effect of the temperature gradient decrease is also observed in the open-circuit voltage, meaning that the value of the next V_{oc} sample will not equal the previous one. The MPPT algorithm continues setting the load voltage to be half of the instantaneous V_{oc} , but this value changes until the system reaches thermal equilibrium. The instantaneous open-circuit voltage corresponding to this point is always less than the first open circuit voltage measurement if no current was flowing in the TEG. "Hill-climbing" MPPT methods such as P & O or Incremental Conductance that are derived from PV systems would behave similarly but oscillate around the true maximum power point.

Overall, the fractional V_{oc} is the most easily implemented control method, cheap because it does not need a complicated control system and has low computational demand. For most TE systems the rate of temperature change is slow, therefore this method can be most suitable even if used with a low frequency V_{oc} reading. Thus, the fractional V_{oc} was selected as basis for the MPPT algorithm developed within this project. The newly developed MPPT algorithm was named "Modified FOC".

Power conversion

The function of the developed Power converter is to track the maximum power available from the thermoelectric generator(s) connected at its input. Maximum power is tracked every 500 ms with high accuracy. Electrical energy converted by the converter is stored in a 12 V lead-acid battery. Battery charging control algorithm is included in the converter which shuts down if the battery voltage exceeds a pre-defined threshold. The MPPT capability of the converters is assessed by comparing the operating point set by the converter and the MPP obtained during a TEG electrical characterisation

The power converter to be used with the GEN3 and GEN4 cartridges is a Synchronous Boost converter. The converter used with the hot gas rig described here is a Synchronous Buck-Boost converter. Both are standard and well-known topologies. Images and more details of the developed Power converter are given in **Milestone 2a** in the appendix.

Laboratory tests of the Power converter and MPPT algorithm

16 TEG devices were used for testing, two banks of four on each of the top and bottom sides of the heat exchanger (**Figure 32**). Devices of a common colour as shown in the figure were connected in parallel, each connected to one of the MPPT/I-V channels. Devices 1 through 4 and 9 through 12 were type GM250-241-10-12, each connected in parallel pairs whereas the other modules were of type GM250-241-10-16, in a parallel group of 4. **Figure 33** shows the scheme of the overall test configuration including the hot gas system and the power conversion system.

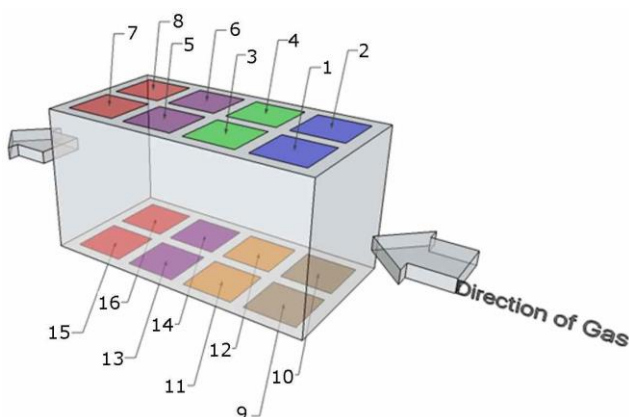


Figure 32: Scheme of the TEG arrangement in the test configuration

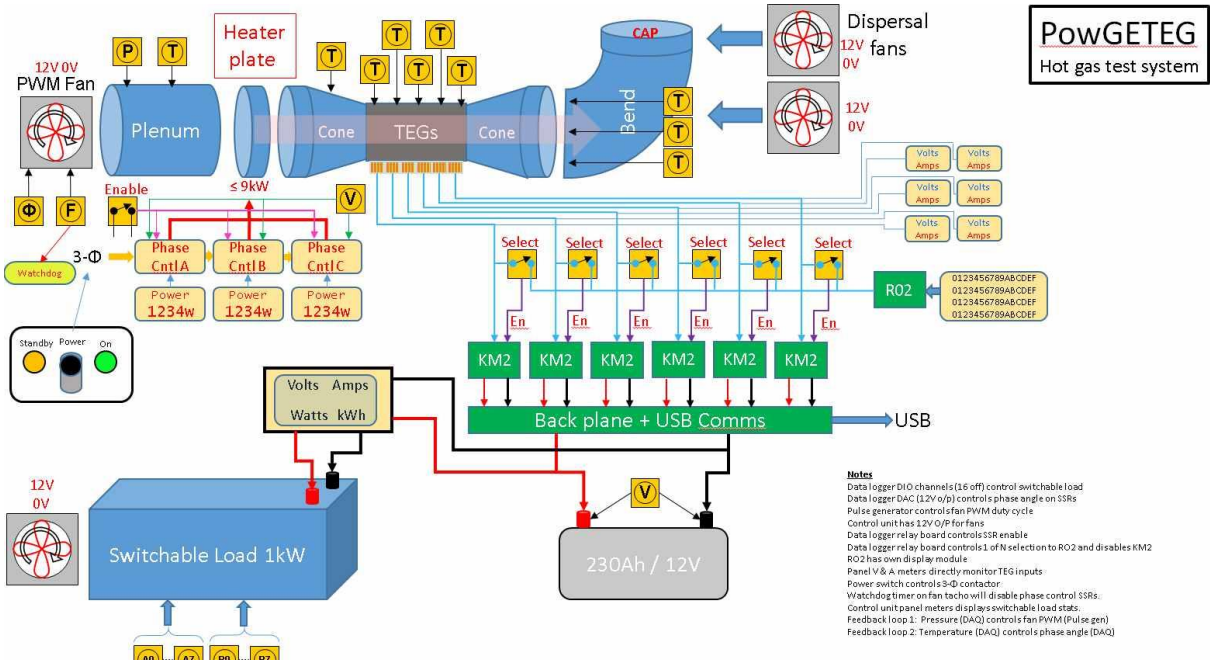


Figure 33: Scheme of the overall test configuration

The experimental results obtained from this system are shown in the following curves (Figure 34) – all TEGs are simultaneously heated and therefore the full interaction across the whole system of separate thermal conductance of each TEG contributes to the results obtained.

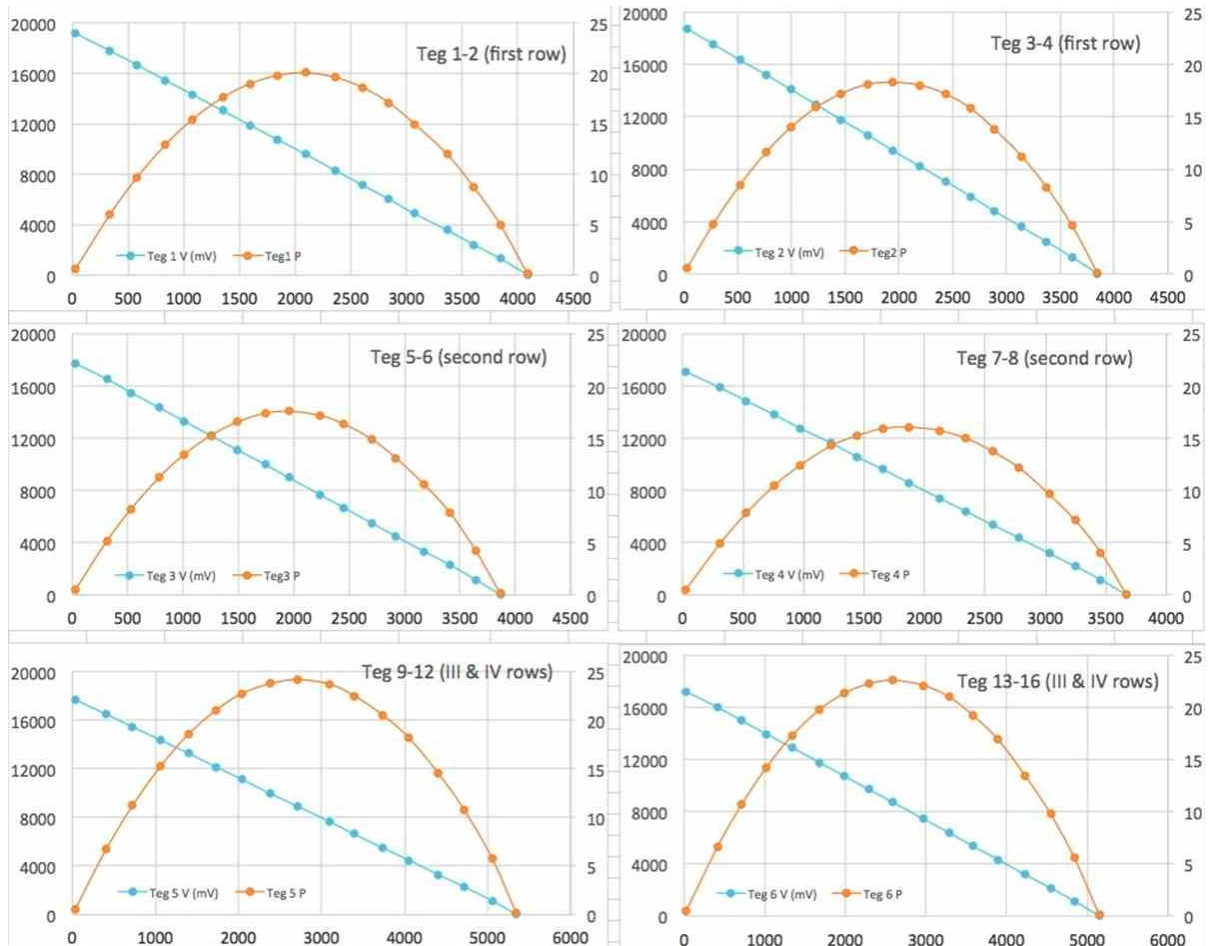


Figure 34: Experimental results from the hot gas system

The summary of the performance enhancement is provided in Figure 35 and Figure 36 and Table 4. The GUN-developed algorithm is described as the “Modified FOC” (Fractional Open Circuit Voltage) and out-performs all other presently available algorithms. The performance of the Power converter is also summarised. The use of this algorithm also results in a reduced heat flux passing through the module to the cold side, reducing system cooling requirements. During testing, in excess of 100 W of electrical power is continuously delivered to the 240 Ah battery: all losses in

the Power converters and cabling between the TEGs and the MPP converters are additional to Figure 36, which shows high efficiency of up to 98 % of the Power converter.

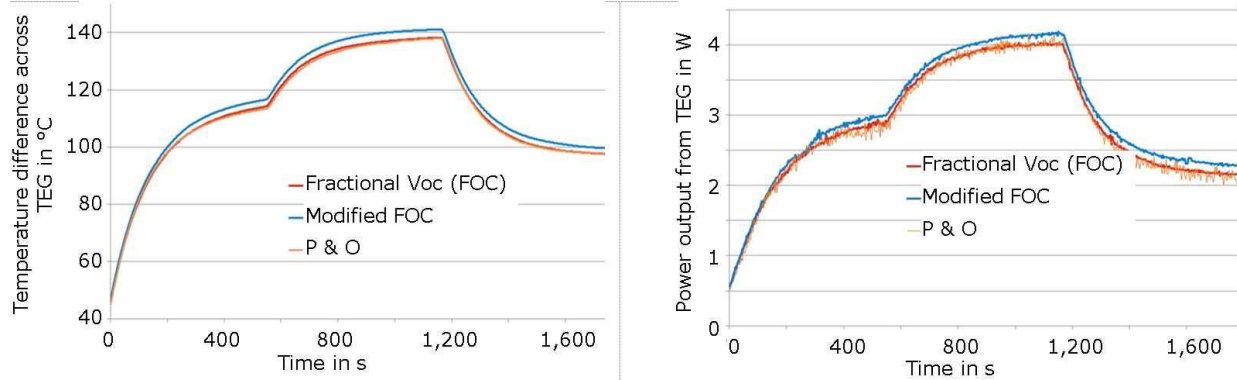


Figure 35: Comparison of MPPT algorithms: Temperature difference (left) and power output (right)

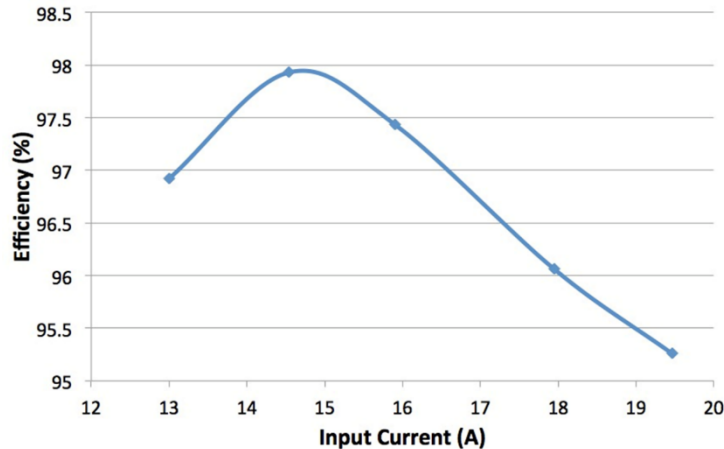


Figure 36: Performance of boost converter under test: Electrical Efficiency

Table 4: Summary of increased system performance from new MPPT algorithm

	Unit	FOC (50 % V_{oc})	P & O	Modified FOC
Total energy obtained	kJ	5.11	5.07	5.3
Percentage increase from FOC (50 % V_{oc})	%	-	- 0.70	3.7
MPPT efficiency (100 % if $V_L=V_{oc}/2$)	%	99.90	99.30	103.7

Altogether the done work proved that the condition of the Maximum Power Transfer theorem is not sufficient to reach the optimum operating point of a TEG system. Instead, by considering the thermal interactions in the TEG by reducing the Peltier effect the total power generation can be improved. This means that by selecting a different voltage operating point for the MPPT converter the thermal equilibrium of the system can be changed and a greater temperature gradient across the TEG element (and a lower difference across the heat exchangers) provided, which in turn equates to a power increase above that predicted by the Maximum Power Transfer theorem. So far, a +3.7% increase of the efficiency through the newly developed MPP Power converter was achieved, see Table 4. **Milestone 2a** (see appendix) was reached.

2.2.5 Task 2.5: Design and function review (all)

Aim of this task was to improve the demonstrator design, based on the results of the bench scale unit experiments at the BFI testing facility (see WP 4). Following conclusions from the bench scale unit experiments were drawn:

- A GEN3 cartridge was used for the test-bed experiments. Maximum measured power was approx. 260 W at a waste gas temperature of 800°C. The maximum measured power at 700°C was approx. 175 W. It was planned to use one GEN3 cartridges (in combination with the heat pipe heat exchanger, see Tasks 2.2 and 2.6) and two bigger GEN4 cartridges for the demonstrator. The expected power output of the GEN4 cartridges is 340 W at 800°C waste gas temperature and 250 W at 700°C. Thus, a power output of the demonstrator in the range of 800 W_{el} can be expected.
- At high waste gas temperatures and flows the maximum usable electrical power is generated by the cartridges at a current of approx. 25 A. The voltage generated by the cartridge was stepped up to the battery voltage by the Power Converter. A maximum short-circuit current of 52 A was

measured using a current-voltage characteristic analyzer during the test-bed experiments. Both the Power Converter and the I-V tracer withstand the electrical conditions produced by the GEN3 cartridge. Nevertheless, this must be considered for the further improvements of the Power Converter with a view to maximizing electrical efficiency and hence power generation.

- The measured pressure drop was higher than the values determined by GNTH (with air), which cannot be explained only by the difference of density (approx. 10 %) and viscosity (approx. 10 %) between air and waste gas. Since the GEN3 cartridge of the demonstrator will be used in combination with the heat pipe heat exchanger this will be not a problem for the demonstrator. Based on data of GNTH the pressure drop of the GEN4 cartridges is expected to be lower (approx. 1 mbar). Nevertheless, higher pressure losses by the two GEN4 cartridges could be possible and must be considered for the selection of an appropriate fan within the bypass.
- To get an even waste gas flow to each cartridge, diaphragms in the branches of the bypass should be foreseen, so that the waste gas flow can be adapted. Since the cartridges are fixed by flanges with clamps it is possible to integrate the diaphragms between the flanges behind the cartridge.
- The cartridges of the demonstrator should be installed in that way that the cooling water supply is located at the top of the cartridge to ensure the cooling of the whole circumference of the cartridge with a minimal cooling water flow.

Design of an online data logging system for the demonstrator test at tkSE (GUN, BFI, GNTH)

In view of the bench scale tests it was further decided to develop an Online Monitoring system, which enabled all partners to view and download live data via a web interface during the long-term test of the demonstrator at tkSE site. In the following main characteristics of the Monitoring system design are given. The construction of the Monitoring system was done by GUN. Images of the final system are shown under Task 5.2. More details of the Monitoring system are given under

Deliverable 2.5 in the appendix.

- The proposed system enabled monitoring and logging of the installed TE system at tkSE. The system was designed for use of max. 4 "in-line" cartridges and one cartridge with its thermal energy provided via the heat pipe arrangement. Target power met or exceed the putative 800 – 1,000 W level originally set for the project. Monitoring and logging parameters included temperatures, flow rates, electronic parameters and electrical efficiencies. Further, the monitoring and logging system must operate independently of the tkSE plant and require no operator input unless a fault develops. The system must be 'fail-safe' meaning that should any faults develop, they are handled in a safe manner ensuring plant integrity and safety is not compromised. The Monitoring system and tkSE plant safety systems were also be interconnected so that a fault on either triggers protective action in the other.
- In terms of functionality, the monitoring and logging system must provide up-to-the-minute readings from the installed demonstrator system and to ensure reliable and robust data collection, the monitoring and logging system was calibrated prior to data collection.
- The hardware of the monitoring and logging system consisted of an electrical interface to connect the various sensors from the demonstrator; a data processing unit for data collection; MPPT systems developed by GUN; web server to publish the data; database storage; 4G internet connection for access to data produced by the system over-the-air.
- The electrical interface consisted of three subsections: sensors (thermocouples/flow metering/pressure/gas composition); control systems including shut-off valve states and voltage outputs that give the immediate state of the system to the tkSE operator; switchable loads that act to absorb power from the TE system in event of a system failure.
- The MPPT power electronics were connected through a set of relays to each of the TEG arrays. Under the control of the data processing unit, the input and output power, voltage and current generated by each TEG array will be transmitted and logged. The 'input' power values give the user the instantaneous TEG data, and the 'output' power values gives the performance of the MPPT. Together, the efficiency of the MPPT and TEG could be calculated. Further, the power electronics also included an advanced I-V tracing system, which worked as follows: At a predefined time interval, the MPPT system is disconnected using the relay system, and the I-V tracer is connected and the complete I-V trace of the TEG is obtained and transmitted to the data processing system. Upon completion of the I-V trace, the MPPT is reconnected and the power generation operating continues. The data processing system disconnects each TEG in the array in turn, and within 100 ms the I-V trace is performed and the MPPT is reconnected. This operation had negligible effect on the temperature of the TEGs.

- The data processing unit consisted of a Raspberry Pi running Linux-based operating system. The operating system was responsible for automation of the data collection from the electrical interfaces using a scripting language, Python. The Raspberry Pi also integrated the database function based on the SQLite framework and webserver. The website for online access was built in PHP following the Model-View-Controller concept. This allowed for maximum flexibility cross platform while ensuring data integrity. The data generated by the system was stored locally on the Raspberry Pi before being uploaded to Cloud Storage at weekly intervals. Further, the website included a calendar function that enables the user to view and download any dataset from the system start.
- A 4G internet connection was included with the Raspberry Pi. This allowed access to the Raspberry Pi web interface globally to allow any project partner to view and download data.

Further development of the Power Converter (GUN)

- The tests carried out at the BFI facilities provided satisfactory results in terms of general functionality of the second prototype of Power converter and the I-V tracer necessary to evaluate its electrical and MPPT performance. Further work was required to improve electrical power conversion efficiency and to optimise the MPPT algorithm for constant heat application, e.g., at tkSE.
- More work was required to interface the power converter and the I-V tracer to operate seamlessly with the monitoring system (see above) to ensure reliable communication of data and operational parameters through I2C. It was also necessary to improve the electronics system to ensure safe and reliable operation for a prolonged operation time, unattended.

Deliverable 2.5 in the appendix gives an overview of the design adaptions. After implementing them into the final demonstrator layout **Milestone 4** was reached.

2.2.6 Task 2.6: Demonstrator design (all)

Aim was the detailed layout of demonstrator components based on the concepts created in Task 2.2. In the following the final layout of following demonstrator components is described: TE cartridges, heat pipe heat exchanger and the bypass. The Power converter was already described in detail under Task 2.4. The construction of the overall demonstrator, to be tested at tkSE, is described in Task 5.2.

2.2.6.1 Final layout of the TE cartridges (GNTH)

Two different TE cartridges were used for the demonstrator: One GEN3 cartridge and two GEN4 cartridges. The GEN3 cartridge was used in combination with the heat pipe heat exchanger (see also Task 2.2, Task 5.2 and the next chapter). The cartridges differ in their size and power. Further one GEN3 cartridge was provided for the test-bed experiments (see WP 4).

Two GEN4 thermoelectric generators were built, assembled and tested in the GNTH laboratory. Their tubular design with its 6" flanges and standard coolant connections allows for easy on-site installation. Earlier designs had the hot side heat exchanger on the outside, impeding with integration as many I/O components could not withstand the high temperatures and corrosive agents without additional shielding. With the hot side heat exchanger on the inside, no additional insulation from the heat source was needed. The inner tube is fitted with a fin based low backpressure heat exchanger (HEX) and a centre cone to direct the hot gases to the fins.

Figure 37 provides a comparison of the cartridge's function using hot air for a GEN4 cartridge. The left figure shows the increase of the electrical output of a cartridge with increasing temperature. The increase is not straight proportional but is rising more and more with higher air temperature. The hot air mass flow influences the electrical output mainly in the range up to 400 kg/h. At lower mass flow rates up to 300 kg/h the pressure drop increases nearly linear (right figure). At higher mass flow rate the growth rate of the pressure drop is increasing.

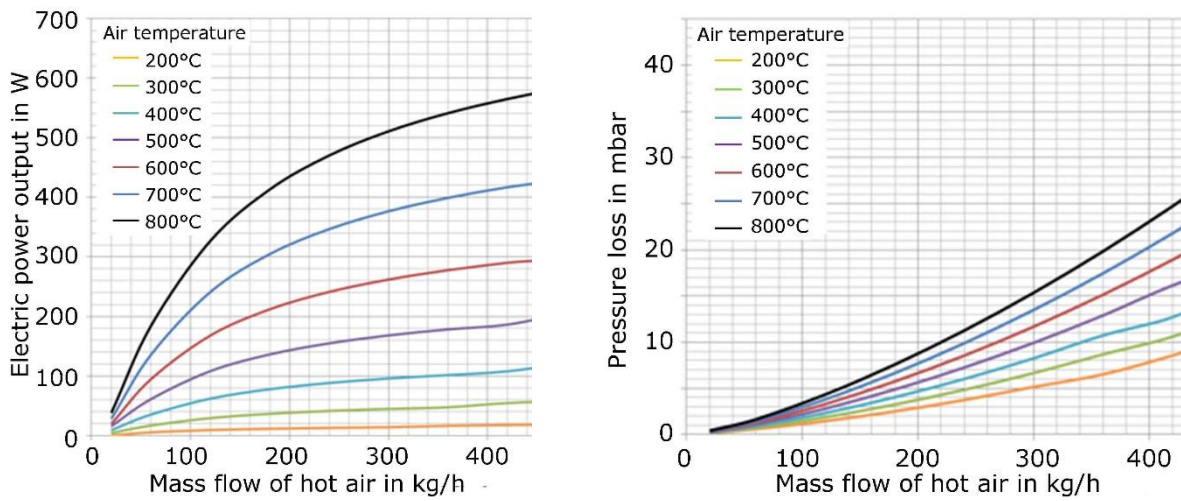


Figure 37: Testing results of a GEN4 cartridge at different air temperatures, left: electric output in dependency of the hot air mass flow; right: pressure drop of the air flow through cartridge heat exchanger in dependency of the hot air mass flow

In order to be able to determine the efficiency (η) of the TE cartridge, the following equation has been considered under the simplifying assumption that there are no heat losses of the TE system:

$$\eta = \frac{P_e}{\dot{Q}_H} \text{ with}$$

P_e : electrical output in W

\dot{Q}_H : heat transfer to the cartridge in W.

The expected electrical output of a GEN4 cartridge within the proposed range of application and the resulting efficiency are shown in **Table 5**. A considerable increase of the efficiency mainly with increasing air temperature can be seen. The design point of the cartridges was a waste gas mass flow of 130 kg/h and a waste gas temperature of 800°C. Thus, the expected output of GEN4 cartridges is in the range of 340 W at an efficiency of approx. 5.6 %. Performance data of a GEN3 cartridge show a lower electrical output – 240 W at 800 °C waste gas temperature – but a higher efficiency of 6.9 %.

Table 5: Expected performance of GEN3 and GEN 4 cartridges

Air temperature in °C	Air mass flow rate in kg/h	Heat transfer to the cartridge in W	Electrical output in W	Efficiency in %
GEN4				
700	100	4,750	210	4.4
	130	5,200	250	4.8
	200	5,900	320	5.4
800	100	5,500	280	5.1
	130	6,100	340	5.6
	200	7,000	415	5.9
GEN3				
700	100	2,850	165	5.8
	130	3,000	180	6.0
	200	3,200	205	6.4
800	100	3,300	220	6.7
	130	3,500	240	6.9
	200	3,750	275	7.3

Table 6 shows some more data of the two types of cartridges. Drawings of the cartridges are part of **Deliverable 2.6** in the appendix.

Table 6: Data of the TE cartridges

	GEN3	GEN4
Inner diameter	90 mm	149 mm
Length	164 mm	238 mm
Expected pressure drop	20 mbar	4 mbar

2.2.6.2 Adaption of a GEN3 cartridge for utilization with the heat pipe heat exchanger (GNTH)

The design of a GEN3 cartridge needed to be adapted to allow fitting of a conductive heat transfer via heat pipes (see also Task 2.2 and 5.2). However, it was found that a GEN3 cartridge could not be reworked without risking permanent damages to the generator. Thus, a new generator was required to be built from ground up.

To allow fitting of the heat pipe heat exchanger, the inner tube of a GEN 3 was witted with fin-less steel tube. Suggestions on how to interface the inner tube with the heat pipes without exerting high thermal stress in operation were provided. Main point that needs addressing is the thermal expansion of the inner tube, while mechanical contact is required for good thermal conduction. Exceeding forces can permanently hamper heat transfer or damage the generator. One approach is the use of an elastic or phase changing material as an intermediate layer. This however raises high requirements for the interface material. It would need to withstand high temperatures, retain volume, elasticity or fluidity over the course of several cycles, cause no corrosion, diffusion, alloying or other interactions with the inner tube and have a good thermal conductivity. Another approach is the use of a segmented core (to allow for thermal expansion) with high temperature resisting thermal paste (for improved thermal contact) or graphite foil. This seemed most promising and was finally implemented. Details about the interface between the TE cartridge and the heat pipe heat exchanger are explained in Task 5.2. Images of the adapted GEN3 cartridge can be found in the annex under **Deliverable 5.2**.

2.2.6.3 Final layout of the bypass (tkSE, BFI)

As described in Task 2.2 the layout of the bypass was adapted to reduce the cost. Technical drawings of the final bypass design are given under **Deliverable 2.6** in the appendix. The scheme of the bypass can be seen in Figure 4. The function of the bypass is as follows:

The bypass was connected to the CSP waste gas pipe at the heat exchanger of the waste gas system. Therefore, a special connection plate at an inspection chamber of the heat exchanger was used. The waste gas was removed and refed to the waste gas pipe via this plate. In both the waste gas input and output valves were installed (valves 1 and 2) to close the pipes, so that it was possible to work at the demonstrator during the normal operation of the CSP. Two safety valves (SSV1 and SSV2) were installed to protect the demonstrator from damages e. g. through overheating. In front of the TEG and of the fan branches to suck in cooling air were integrated to protect the TE cartridges and the fan from overheating and to change the waste gas temperature e. g. for investigation of different process conditions.

3 TE cartridges in two branches were installed: one branch with two GEN4 cartridges placed in series and one branch for the heat pipe approach with the adapted GEN3 cartridge. The branches had different diameters: DN 150 for the GEN4 cartridges and a rectangular shape with lengths of approx. 0.24 m for the heat pipe approach. To ensure the waste gas flow through the bypass a fan was installed after the cartridges. This allowed the investigation of the cartridges at different waste gas flows.

Up to the fan the pipe material was high temperature resistant steel. The pipes were insulated to minimize heat losses of the waste gas and for safety reasons. After the fan the waste gas temperature was much lower, due to the cooling air supply in front of the fan. Thus, temperature resistant hoses could be used instead of insulated steel pipes due to cost reasons.

Following measuring positions were foreseen for the demonstrator testing:

- Temperatures: Waste gas and cooling water in front and after the TE cartridges.
- Flow: Waste gas and cooling water flow.
- Pressure: Waste gas pressure in front and after the TE cartridges.
- Gas composition: Waste gas composition (CO_2 , CO, O₂).
- Electrical output: each TE cartridge.

To protect the TE cartridges and the fan from overheating a safety concept of the demonstrator was formulated. Four malfunctions were identified:

- Cooling of the TE cartridges stops.
- Waste gas temperature > max. allowed temperature of the TE cartridges.
- Fan stops.
- Waste gas temperature in front of the fan > max. allowed temperature of the fan.

To protect the cartridges and the fan from damages a safety concept as shown in **Figure 38** was implemented. The scheme of the bypass is shown in Figure 4. A more detailed scheme of the safety loop is part of **Deliverable 2.6** in the appendix.

In all four cases safety valve SSV 2 will open to cool the waste gas stream. In the cases "cooling of TE cartridges stops", "fan stops" and "Waste gas temperature > max. fan temperature" SSV 1 closes additionally, so that no more waste gas flows through the bypass. In these cases, the cooling or fan have to be checked and repaired, if necessary, before the demonstrator test can continue. In the case of "waste gas temperature > max." it is sufficient to cool the waste gas stream with ambient air until the waste gas temperature decreases below the max. temperature.

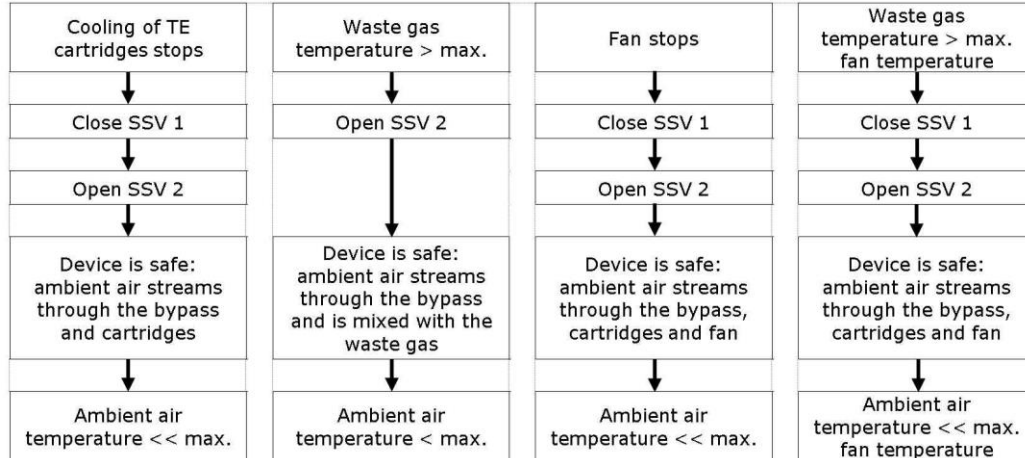


Figure 38: Flow diagram of the safety concept

2.2.6.4 Final layout of the heat pipe heat exchanger (CEM)

During WP 2, it was observed that the axial approach, **Figure 39**, can introduce a pressure drop higher than that allowed by the industrial installation (< 4mbar). To solve this issue an additional TEG approach was considered. The new one is based on the use of heat pipes to transport heat from the exhaust gases to the cartridge which will be placed outside of the waste gas pipe. It required the design of an optimum heat exchanger (HEX) that transfers heat from the exhaust gases to the heat pipes. The system must fulfil following fluid and electrical constraints.

	Expected power generation of GEN3 cartridge	approx. 200 W
	Pressure drop	≤ 4 mbar
	Gas temperature	700 - 800°C
	Heat load	≈ 6 kW

Figure 39: Axial thermoelectric generator approach and constraints.

Prior starting with the HEX design, a search for high temperature heat pipes was done till finally a provider was found. Finally, selected heat pipes were high temperature heat pipes, made of steel and with potassium as the liquid.

The first approach was based in the use of several heat pipes, each one with its own tube and set of circular fins. This strategy optimizes the heat exchange between the heat pipe and its fins, but it is more expensive in terms of final volume needed. Furthermore, its implementation would be more expensive. The first stage of this work has studied this strategy in order to get the optimal fin design. All the knowledge acquired in this stage was used in the next strategy solution.

The second strategy has been the design of a rectangular heat sink set up with several rectangular fins with the purpose to fit several heat pipes in the sink. This strategy is optimal in terms of volume needed for the solution and it is cost efficient compared with the first strategy.

Circular finned tube design

The first strategy studied along this work was the construction of a finned tube for each heat pipe.

For simulations a hollow stainless-steel tube with several circular fins design was supposed. The heat pipe was placed inside the tube considering perfect contact between the pipe and the tube, in order to decrease the power computation needed to complete the simulations. This heat pipe was designed to interact with a TE cartridge in order to make the thermal to electric energy conversion. The circular fins had the objective of maximizing the heat exchange surface between the exhaust gases and the heat pipe. As commented above, the head losses had to be less than 4 mbar value because of the constraints of the system.

With this information, a set of design parameters was defined in order to generate a Design of Experiments (DoE) optimization strategy. This first set of parameters was composed by:

- Number of circular fins along the tube.
- Fin radius, thickness and gap between fins.
- Finned tube length.
- Tube inner and outer radius.

With the purpose of limiting the total number of experiments, only three independent variables were defined for the DoE: Thickness of the fins, gap between fins and fin radius. The dependent variables of the DoE were: Number of fins, tube length, tube inner radius (or heat pipe outer radius) and tube outer radius.

Table 7 shows the values rank of each independent variable.

Table 7: Values rank of each independent variable

Variables/Values	Maximum	Minimum
Fin radius in mm	60	30
Fin thickness in mm	5	2
Gap between fins in mm	3	6

With this information a set of experiments was gathered. Each experiment had to be solved using Computational Fluid Dynamics (CFD) specialized software. In this case the ANSYS FLUENT software was used. The simulations gave valuable information about the performance of each design studied. For example, it is possible to get a contour plot of total temperature along the fins or a contour plot of velocity magnitude along the pipe as pictured in **Figure 40**.

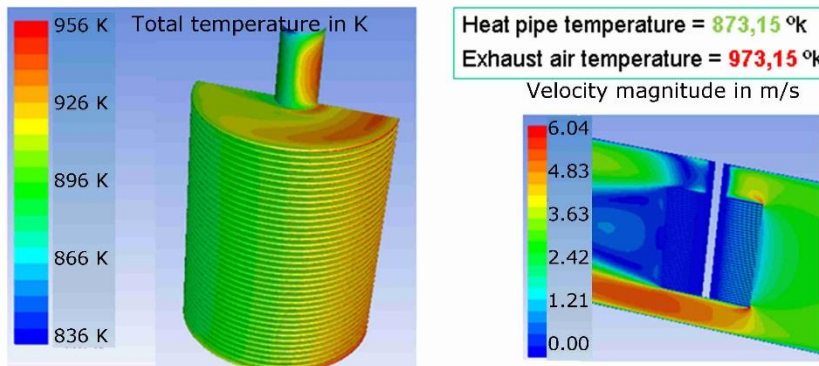


Figure 40: Example of CFD results

The simulation of the entire set of experiments resulted in following conclusions:

- Fin radius was the most statistically significant variable.
- Heat exchange rate increased with bigger radius and thinner fins.
- Head loss increased with bigger radius and smaller gap between fins.
- Maximum heat transfer calculated was 805 W with 0.0194 mbar of head loss.

The best experiment had the following parameters:

- Fin thickness: 2 mm
- Gap between fins: 4 mm
- Fin radius: 60 mm

Rectangular heat exchanger design

The best experiment with the finned tube gave only 805 Watts of thermal energy per tube and heat pipe. Taking in account that the conversion efficiency between thermal and electrical energy is about 3 – 8 %, it is needed more than five finned tube elements to get 200 - 250 W_{el}. Therefore, it was compulsory to think into another design to increase the available heat exchange surface. The solution was using a rectangular heat sink perforated with several heat pipes, **Figure 41**.



Figure 41: Rectangular fins design. The heat pipes will be placed in perforations through the fins.

Using the knowledge acquired in the previous work, the best configuration of the fins was defined with: thickness of 2 mm and gap between fins of 4 mm.

Several ways to perforate the fins in order to place the heat pipes were simulated, with the goal to maximize the heat exchange power between the exhaust gases and the heat pipes, **Figure 42**.

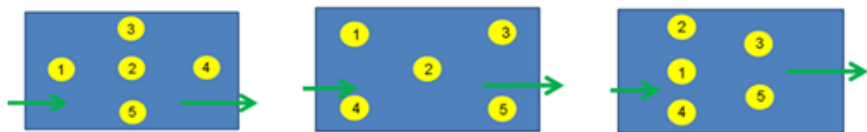


Figure 42: Configurations for the heat pipes. Top view of the geometry. Green arrows show gases flow direction. Left) Diamond Centre; Middle) Alternate parallel rows; Right) Triangle

The best performance achieved in the set of experiments defined had 30 rectangular fins of 200 x 150 mm with a thickness of 2 mm and 4 mm gap between fins. 4 heat pipes were used with 12 mm external diameter and 8 mm internal diameter. **Figure 43** shows the optimal configuration (only two heat pipes are shown because YZ symmetry has been applied).

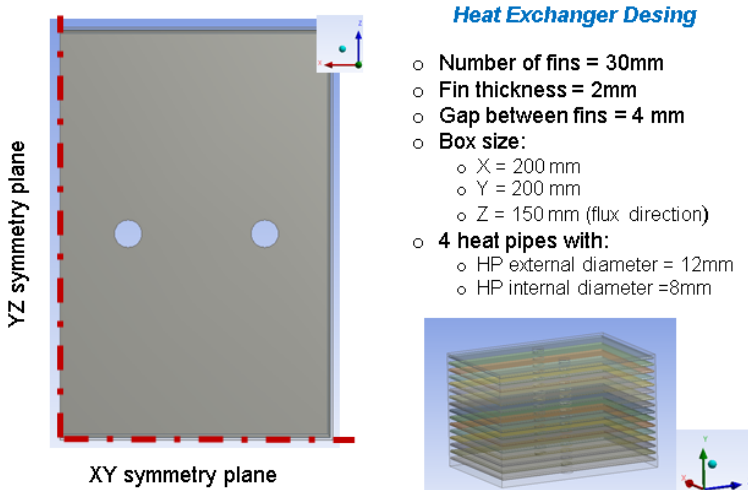


Figure 43: Optimal experiment with rectangular heat sink configuration

Results for different working points showed that a volume flow above 1,400 m³/h is needed to get a heat power exchange of 4,000 W. With a thermal to electrical conversion efficiency around 5 - 6 % it is possible to achieve 200 - 250 W of electrical power. In the worst scenario, with a volume flow above 2,000 m³/h the head losses are still far below 3 mbar. In **Figure 44** (left) a contour plot for the fin's temperature is shown. Also, some thermal simulations were done in order to get an optimal distribution of the heat pipes in the TEG module as shown in **Figure 44** (right).

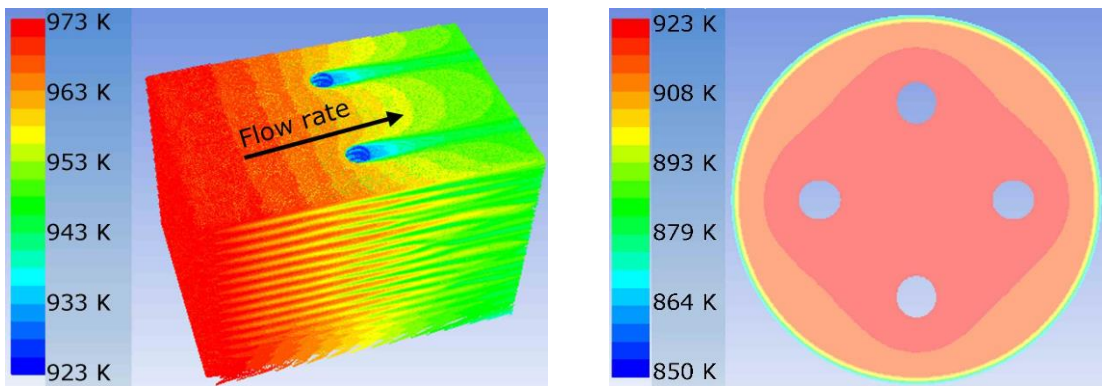


Figure 44: Left: Contour plot of fins temperature in Kelvin degrees. Only two heat pipes are shown because YZ symmetry has been applied.
Right: Thermal contour plot in a cross section of the TEG module with the four heat pipes assembled.

Finally, the theoretical work presented above was evolved into a practical design ready to be constructed, assembled (Task 5.2) and tested in a real application environment. The four heat pipes used in the former design could be assembled in the bypass and connected to the TE cartridge as it is schematically shown in Figure 5. Technical drawings of the heat pipe HEX are given in **Deliverable 2.6** and **Deliverable 5.2** in the appendix.

Conclusion

1. An optimal heat sink design was found with the purpose to define an indirect heat transfer strategy between the exhaust gases flowing in the chimney and the TE device.
2. Using 4 heat pipes fitted with minimum 30 rectangular stainless-steel fins are able to transfer more than 4,000 W_{th} with a mass flow of 630 kg/h at 700°C gas temperature.
3. The configuration introduces approx. 1 mbar of additional head losses in the system.

Table 8 summarizes main data of the heat pipe HEX.

Table 8: Heat exchanger characteristics

Number of fins	30
Fin thickness	2 mm
Gap between fins	4 mm
Number of high temperature heat pipes	4
Liquid	Potassium
Heat exchanger dimensions	200 x 200 x 150mm
Pressure drop	1 mbar

2.2.7 Task 2.7: Design integration (GNTH)

This task was about the coordination of the different measures for the demonstrator design in WP 2 and regular updates of all partners to communicate changes / adjustments and efficiently integrate the changes into the overall design. To facilitate proper integration and compatibility drawings of relevant parts and connections were shared between the partners. Simulation and calculation results of operational parameters such as power point, pressure loss and estimated flow rates were provided to all partners. A deeper trade-off took place between GNTH and GUN regarding the TE system, the Power Converter design and the MPPT. To plan the test-bed experiments BFI, GUN and GNTH were in continuous contact and shared information about dimensions, connections and performance data of the used benchmark cartridge and the Power Converter to be able to integrate them into the test-bed. To ensure the correct dimensioning of the bypass system at the CSP plant and the test-bed at the BFI testing facility technical drawings of the TE cartridge and the alternative heat exchanger were provided to tkSE and BFI.

2.3 WP 3: Heat exchanger design for safety and sustained performance (antifouling)

Objectives of WP 3 were:

- Design, construction and testing of a heat storage system capable of absorbing temperature peaks that the TE can't withstand.
- Fatigue tests based on the assembly and clamping configuration designs.

- Develop a solution that prevents the aggregation of solid particles over the heat exchanger surface. Theoretical analysis, antifouling system definition (active or passive "coating" system) and tests.
- Manufacture and test the final heat exchanger. This prototype does not consider the integration of TEG modules as the objective here is to assess the heat exchanger performance.

2.3.1 Task 3.1: Design of TE cartridge safe-guarding design (CEM)

Aim of this task was the development of a system for overheating protection of the TE modules. Due to potential temperature fluctuations into exhaust systems, it is worth introducing temperature absorbers if using TEG to prevent them from overheating damage. Even if the temperature profile at the selected heat source (CSP) of this project is quite even the development of a safe guarding system is highly important for other applications of such TE systems in other industries and plants. At this regard, a system based on phase change materials (PCM) was studied and developed.

First step was to define the most appropriate PCM material from those existing in the market. To do it, a document, including all the specifications the material had to fulfil was written. Main criterions were: working temperature, thermal capacity and thermal conductivity. A list of all specifications can be found in **Deliverable 3.1** in the appendix.

For a working temperature of approx. 700°C, salts are the suitable material, particularly "carbonates" which perform well at temperatures in the range of 650 - 800°C. In **Table 9** the melting points of different salts are summarized.

Table 9: Melting points of different possible salts as PCM

Salt system	Melting point in °C
Li ₂ CO ₃	723
Na ₂ CO ₃	854
K ₂ CO ₃	891
Li ₂ CO ₃ - Na ₂ CO ₃ (52 – 48 mol %)	501
Li ₂ CO ₃ - K ₂ CO ₃ (62 – 38 mol %)	498
Na ₂ CO ₃ - K ₂ CO ₃ (56 – 44 mol %)	710
Li ₂ CO ₃ - Na ₂ CO ₃ - K ₂ CO ₃ (43.5 – 31.5 – 25.0 mol %)	397
K ₂ CO ₃ - MgCO ₃ (57 – 43 mol %)	460

Among those in the market, Li₂CO₃ and Na₂CO₃-K₂CO₃ have been selected due to their compliance with several restrictions, see **Table 10**.

Table 10: Comparison of different properties of Li₂CO₃ and Na₂CO₃-K₂CO₃

Li ₂ CO ₃	Na ₂ CO ₃ -K ₂ CO ₃
✓ Pure material	✗ Mixture of materials
✓ Thermal stability	✗ Sub-cooling problems (additives to reduce it)
✓ High thermal storage density	✓ High thermal storage density
✓ Compatible with metallic containers	✓ Compatible with metallic containers
✗ Toxic	✗ Toxic

From these two materials, Li₂CO₃ was finally selected for further performance tests, dynamic charge and discharge tests) since no sub-cooling effect is presented in comparison to Na₂CO₃-K₂CO₃.

To measure the melting point temperature and the fusion enthalpy of the material a DSC (Differential Scanning Calorimetry) equipment was used. DSC is a thermo-analytical technique in which the difference in the amount of heat required to increase the temperature of a sample and reference is measured as a function of temperature. The result of a DSC experiment is a curve of heat flux versus temperature or versus time. This curve can be used to calculate enthalpies of transitions. The technique is widely used in polymer characterization.

The test with Li₂CO₃ has been carried out in a nitrogen atmosphere with a heating rate of 10°C/min, from 500°C to 750°C. The sample has a melting point of 717.14°C and its enthalpy is 487.2 J/g, as shown in **Figure 45**. **Figure 46** plots the crystallization temperature which results to be lower than the melting one, revealing the sub-cooling phenomena.

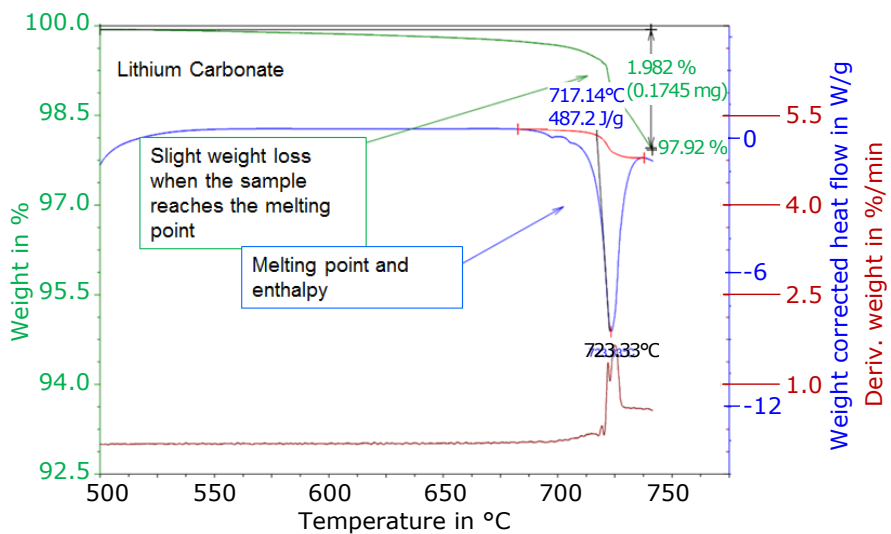


Figure 45: Heating curve obtained in the DSC/TGA (Thermogravimetric analysis) test

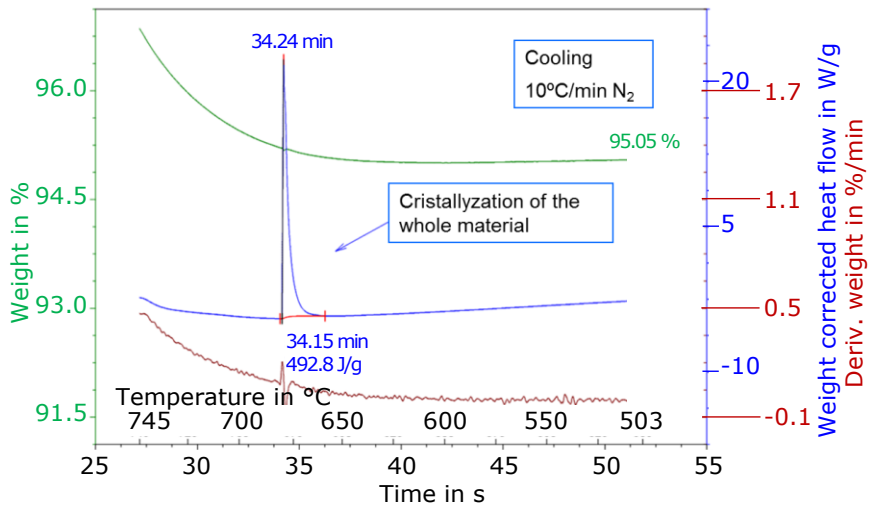


Figure 46: Cooling curve obtained in the DSC/TGA test

In a second heating cycle (**Figure 47**) the sample suffers a weight loss of 4.46%, which suggests degradation of the material. In the bibliography, the decomposition of Lithium carbonate happens at 1,310°C, but in this case, this effect has happened at lower temperatures, close to the melting point. As this effect does not correspond to the material data sheet, it was necessary to verify whether this degradation could affect to the efficiency of the PCM after several thermal cycles.

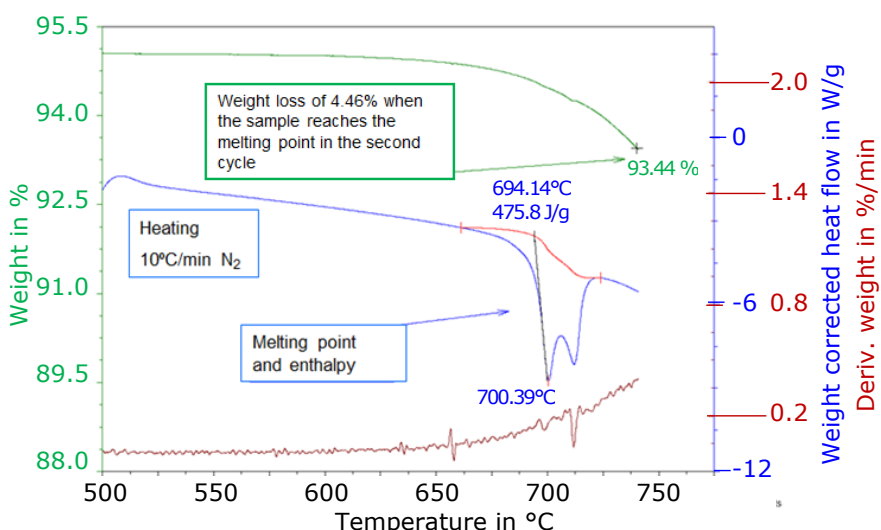


Figure 47: Second heating curve obtained in the DSC/TGA test

If the material does not completely crystallize or during the fusion process suffers some degradation, it will gradually lose its heat absorption capacity. Thus, further tests were carried out regarding the validation of the thermal properties of the selected PCM. For that several containers in AISI 304 stainless steel have been manufactured. 50 g of PCM have been introduced into the

container. Different maximum temperatures have been tested, from 750°C to 950°C to determine the minimum working temperature.

As can be seen in **Figure 48**, the material has the same behavior with final temperatures between 800 and 950°C. In these cases, the time of the energy absorption is the same, between 6 - 7 min. Nevertheless, at 750°C, the energy absorption time is higher, approximately 22 min, because the PCM is close to its melting point.

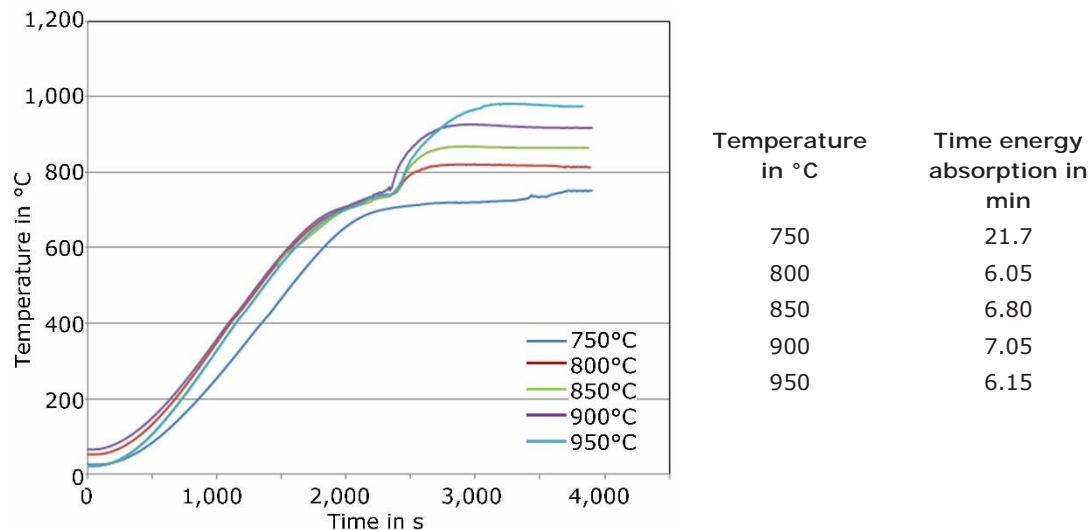


Figure 48: Curves obtained and energy absorption time at several maximum temperatures

After this study, the final temperature was set at 800°C. This value has been chosen as a standard value from the possible peaks of temperature that the thermoelectric device could suffer in the application. The cycles have been carried out at 800°C in order to analyze whether the PCM suffers some degradation. All the cycles have the same behavior which indicates that the material does not suffer a meaningful degradation, as can be seen in **Figure 49**. The PCM is capable of absorbing thermal peaks (in this case of 800°C) for 6 - 7 min before its complete melting.

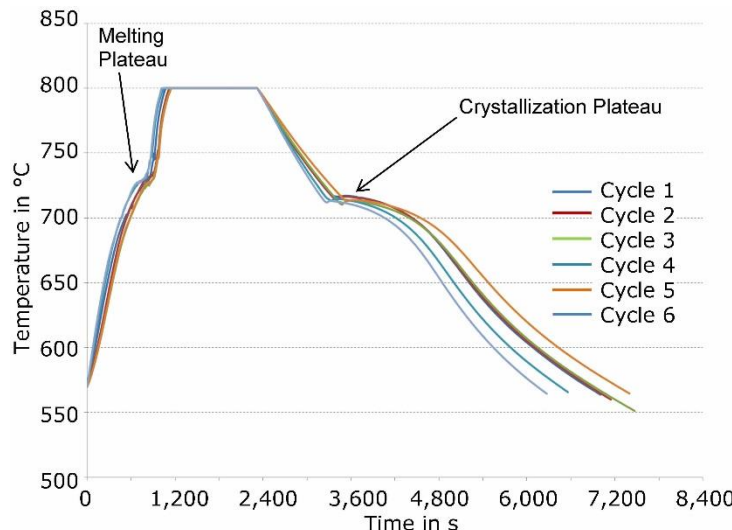


Figure 49: Behaviour of the PCM (50g of Li₂CO₃) in the thermal cycles

After carrying out the thermal cycle test, the container has been weighed again to check if there has been loss of mass. In this case, the mass after the test is 49.8 g. The loss of mass is practically zero, compared to the 4.46% loss observed in the thermal analysis in DSC/TGA.

The test has been repeated using a bigger container, to verify the results with a greater mass of PCM. The mass of PCM used, in this case, has been 160.8 g. Result was that the material has the same behavior. The duration of the plateau was 17 min, compared to the 6-7 min observed in the small container. In this case, the mass after the test is 159.3 g. The loss of mass is 0.9%, compared to the 4.46% loss observed in the thermal analysis in DSC/TGA.

After subjecting the material to thermal cycles, simulating real conditions, there is a total repeatability, with a minimal loss of mass. These differences with the results obtained in the DSC/TGA test suggesting a degradation of the PCM, may be due to a surface phenomenon. In the thermal cycles,

this degradation is hardly appreciable. The sample begins to melt at the same temperature in all the cycles and the duration of the plateau is identical.

Conclusion

Due to the design of the TE cartridges the firstly supposed overheating protection of the TEG by a PCM material cannot be integrated into the demonstrator. Nevertheless, different PCM materials for overheating protection have been investigated for their possible use in other TEG applications. Lithium carbonate (Li_2CO_3) has been selected as a material which meets following requirements: a proper melting point (723°C) and high enthalpy (487 J/g). These values have been confirmed with a DSC/TGA analysis. Further investigations showed no degradation of the PCM after performing several cycles and that it is capable of absorbing thermal peaks (in this case of 800°C) for different times depending on the weight of the material. If a temperature absorber is required, the salt should be confined inside a stainless-steel container highly resistant to corrosion, since the salt is toxic. The degradation temperature (weight loss) of the selected salt is $1,300^\circ\text{C}$, which is far away from proposed the $700 - 800^\circ\text{C}$ operating temperature. Therefore, there is no risk once confined to the container.

2.3.2 Task 3.2: Fatigue tests (CEM)

Aim of this task was to investigate the influence of vibrations on the TE system.

Contrary the contemplated approach in the proposal the TE system was not installed directly into the waste gas pipe but a bypass system was designed and constructed in which the TE system was integrated. Reasons are explained in WP 2. Two TE cartridges were connected via flanges to the bypass (see Task 5.2). The 3rd cartridge was connected to the heat pipe heat exchanger (see Task 5.2). The heat pipe heat exchanger was connected to the bypass via a flange which was fixed with screws. See also **Deliverable 3.2** in the appendix.

The bypass included two compensators and was stabilized by pillars. Due to the compensators the thermal induced mechanical stress and stress caused by vibrations to the demonstrator was minimized. Thus, no fatigue tests were necessary.

2.3.3 Task 3.3: Understanding the mechanism of build-up on heat transfer related surfaces (BFI, tkSE)

In order to determine the specifications of the particles transported within the off gas a dust measurement has been conducted. The analysis of the particles and the resulting density are presented in **Table 11**.

Table 11: Specification of the dust particles

iron	66	wt.-%		nickel	0.06	wt.-%
silicium	1.3	wt.-%		magnesium	0.05	wt.-%
aluminium	0.71	wt.-%		zinc	0.05	wt.-%
calcium	0.57	wt.-%		tin	0.05	wt.-%
manganese	0.38	wt.-%		potassium	0.04	wt.-%
sodium	0.33	wt.-%		phosphor	0.04	wt.-%
chromium	0.17	wt.-%		lead	0.02	wt.-%
copper	0.1	wt.-%		titane	0.02	wt.-%
density	6.021	kg/m ³				

The dust-particle load of the off gas has been determined with $1,48 \text{ mg/m}^3$.

The first operational testing of the demonstrator lasted 3 weeks. After this period no buildup could be detected on the surfaces. Instead of depositions several damages of the coating and connectors were observed (see Figure 62, Figure 80 and Figure 11). The cause of this wear could not be identified. Due to the lack of operational and experimental data the build-up mechanisms have been thoroughly studied within Task 3.4 on a theoretical basis.

Task 3.4: Determination of the relation between build-up and heat flow to module hot side (BFI)
To evaluate the impact of dust on the heat exchanger fins of the heat-pipe TEG a parametric CFD study has been conducted. The geometry of the CFD model is depicted in Figure 50.

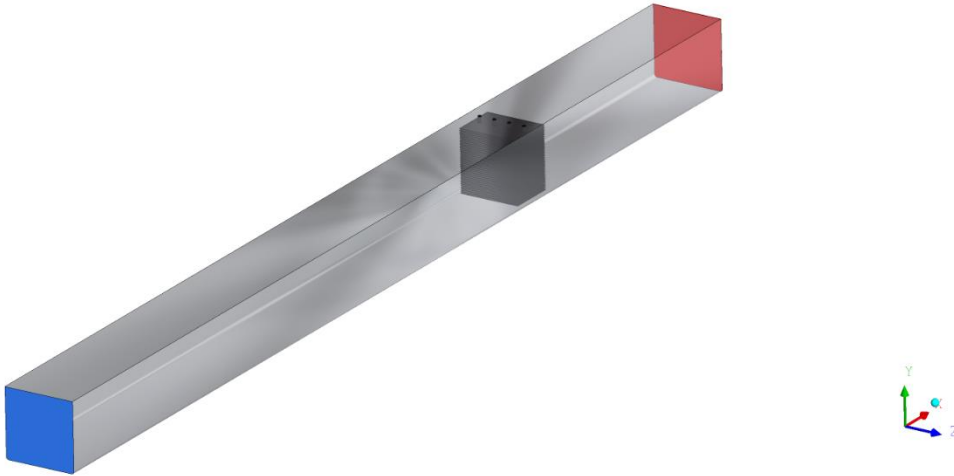


Figure 50: Isometric view of the physical model with gas inlet (blue), outlet (red) and heat exchanger fins with heat pipes (dark grey)

Elaborated flow rates and dust loads were implemented in a discrete phase model with 1-way interaction. The particles are modelled as inert particles and the following laws are applied:

- Particles are affected by the continuous gas flow (drag/lift)
- No interaction between particles
- The continuous gas phase is not affected by the particles
- Deposition of particles (accretion) does not affect geometry
- Particle trap conditions on heat exchanger surfaces
- Particle reflect conditions on pipe walls

From dust analysis the main components are metallic residues (66 mass-% iron) with an estimated density of 6.021 kg/m³. As no further data was available, the particle size was estimated with 20 µm and a uniform distribution across the inlet surface is assumed. For the gas phase an off-gas is considered with a temperature of 800 °C (composition is given in **Table 12**).

Table 12: Gas composition

Waste gas from BOF gas combustion		
CO ₂	29.19	Vol.-%
H ₂ O	1.36	Vol.-%
O ₂	3.72	Vol.-%
N ₂	65.74	Vol.-%

The target flow rate is given with 630 kg/h, with partial loads to be investigated at 300, 400 and 500 kg/h. Typical dust loads are below 10 mg/m³, however different higher dust loads as well as a measured dust load (Case 4) are simulated. The boundary conditions for the conducted simulations are given in Table 13.

Table 13: Boundary conditions for particle simulations

Variant	Mass flow Off-gas	Dust load Case 1	Dust load Case 2	Dust load Case 3	Dust load Case 4
	in kg/s	in mg/s	in mg/s	in mg/s	in mg/s
I	0.083	0.569	1.708	2.846	0.008
II	0.111	0.759	2.277	3.795	0.112
III	0.139	0.948	2.846	4.744	0.140
IV	0.175	1.196	3.587	5.978	0.177

The trajectories of 100 sample particles is shown in **Figure 51** for maximum velocity and dust load (Variant II case 3). Approximately 33 % of the calculated particles is trapped on the heat exchanger.

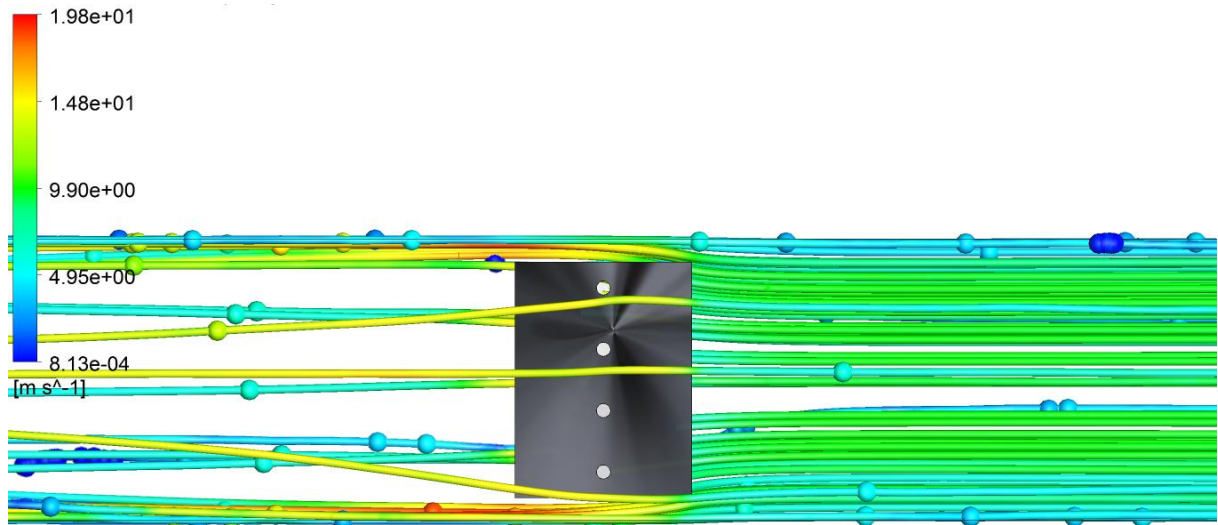


Figure 51: Sample particle tracks for variant II case 3 colored by particle velocity

The results of the particle simulation in terms of accretion is calculated as the sum of mass deposition on the surfaces of the heat exchanger (total surface: 2.14 m^2). As there are no elaborated laws for particle capture, the calculated rates are upper limits. The results of the simulation are shown in **Table 14**.

Table 14: Total accretion of particles on the heat exchanger surface

Variant	Case	Accretion in $\text{kg}/(\text{s m}^2)$	Variant	Case	Accretion in $\text{kg}/(\text{s m}^2)$
I	3	3.38E-07	II	3	4.77E-07
	4	1.00E-08		4	1.41E-08
III	1	1.36E-07	IV	1	3.62E-07
	2	4.08E-07		2	5.02E-07
	3	6.80E-07		3	8.36E-07
	4	2.01E-08		4	2.48E-08

For a given flow rate of the gas, the accretion rate of particles is quasi linear with the dust load, therefore only cases 3 and 4 have been simulated for variants II and I. Trend for particle accretion versus gas velocity for the simulated dust loads is shown in **Figure 52**. Maximum of $0.84 \text{ mg}/(\text{s m}^2)$ is reached for V IV case 3 and minimum at $0.01 \text{ mg}/(\text{s m}^2)$ is observed for V I case 4.

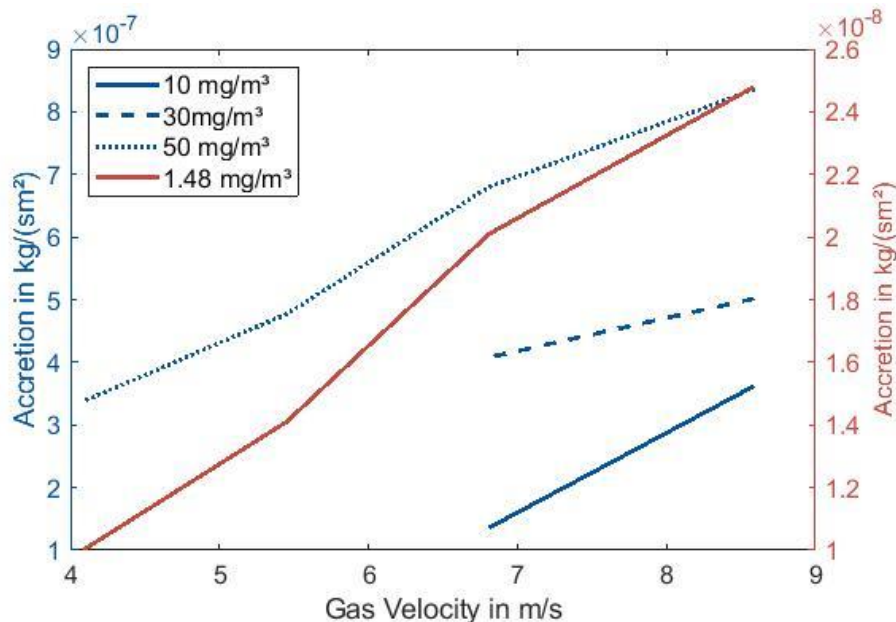


Figure 52: Accretion of particles on the heat exchanger versus gas velocity.

The impacts and accretion rates on the surface of the heat exchanger surfaces are shown for a maximum dust load for the selected flow rates in Figure 53 (isometric view) and Figure 54 (top view). The simulation results show, that due to gravity the accretion rate is higher on the lower region of the fins. Due to turbulence interaction and small vortices a fraction of the particles is

deposited between the fins. The mean value for deposition on the bottom and top side of the fins is 42 % of total particle deposition, where the fraction increases slightly with higher velocity of the gas. On average 51 % of the particle deposition is on the front side of the fins with decreasing fraction towards higher gas velocities. The average deposition fraction on the heat pipes is 7 % with an increase towards lower gas velocities.

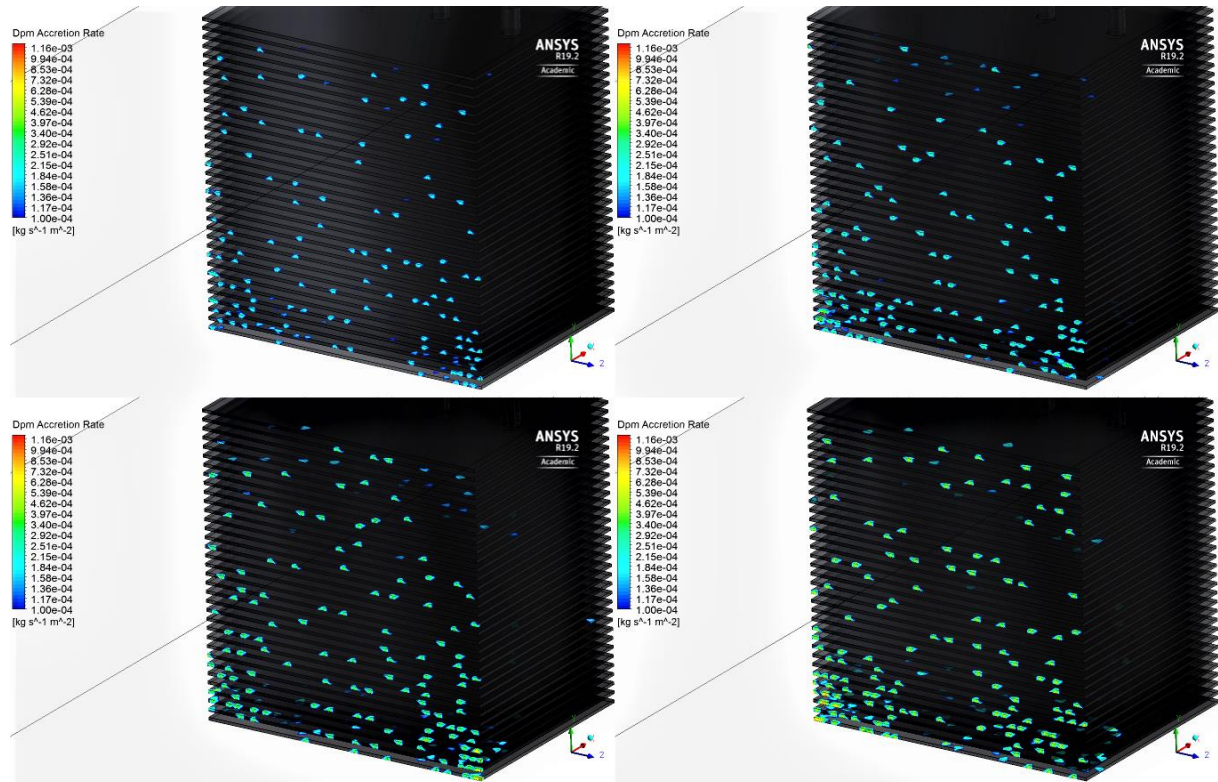


Figure 53: Isometric view of the accretion rate at the heat exchanger fins for the cases I/3 (top left), II/3 (top right), III/3 (bottom left) and IV/3 (bottom right)

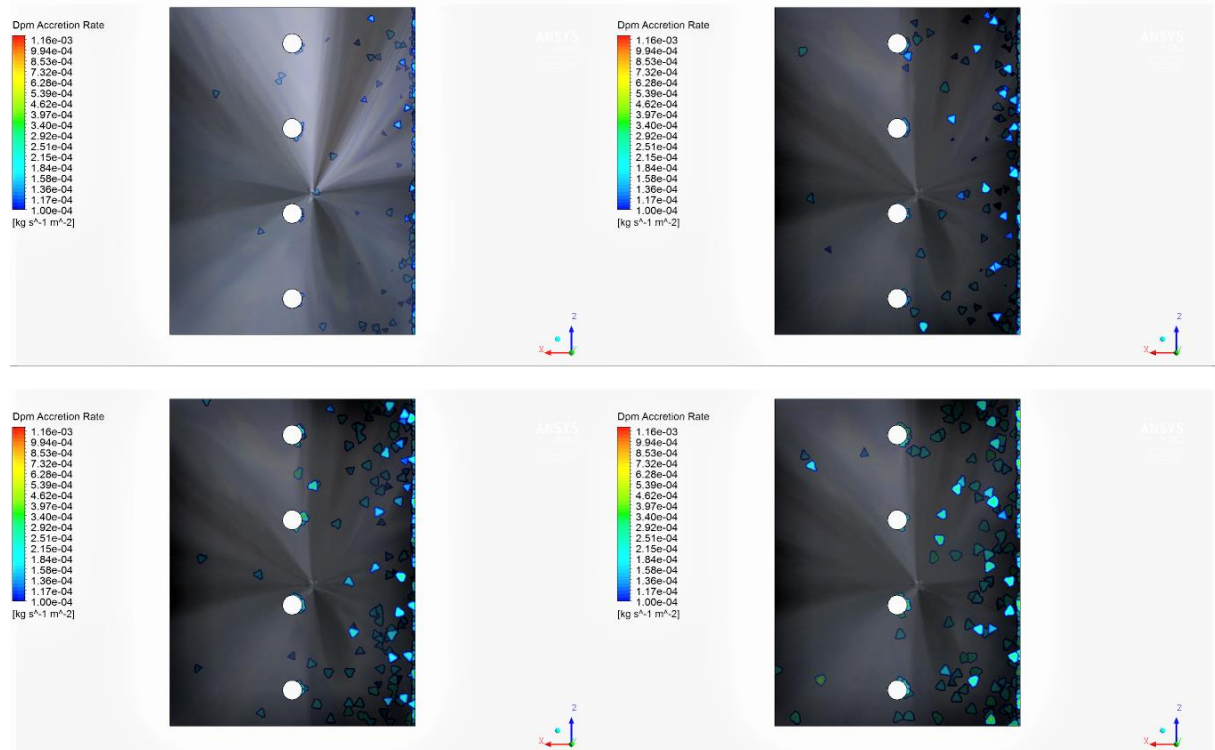
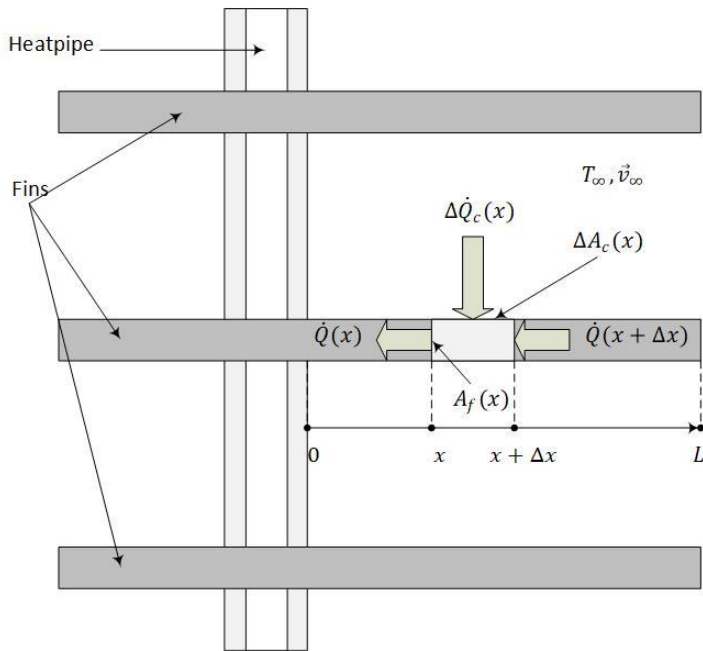


Figure 54: Top view of the accretion rate at the heat exchanger fins for the cases I/3 (top left), II/3 (top right), III/3 (bottom left) and IV/3 (bottom right)

Impact on heat transfer

The heat transfer to the hot side of the module consists of two main mechanisms, the convective heat transfer to the fins and the heat conduction within the fins towards the heatpipes. The energy balance for an element is depicted in **Figure 55**.



The balance for the depicted element is given by

$$\dot{Q}(x) = \dot{Q}(x + \Delta x) + \Delta \dot{Q}_c(x)$$

Where the conduction is given by

$$\dot{Q}(x) = -\lambda_f A_f(x) \frac{dT}{dx}$$

And the convective transfer is given by

$$\dot{Q}_c = \Delta A_c(x) \alpha_m (T_f(x) - T_\infty(x))$$

Figure 55: Main heat transfer mechanisms inside the fins

To simplify the calculation, the heat transfer coefficient is considered as a mean value over the total fin surface. The Nusselt number for the estimation of the mean heat transfer coefficient is given for the laminar regime ($Re < 5 \times 10^5$) of a parallel flow above a flat plate as

$$Nu_m = 0,664 Re^{1/2} Pr^{1/3}$$

The characteristics of the heat exchanger fins are shown in **Table 15**. The small Biot numbers indicate, that the heat transfer to the heatpipes is mainly affected by the convective heat transfer.

Table 15: Heat transfer characteristics of the heat exchanger fins

Property	Variant I	Variant II	Variant III	Variant IV	Unit
Dynamic viscosity		4.31E-05			Pa*s
Thermal conductivity		7.19E-02			W/Km
Specific heat capacity		1206.39			J/kgK
Prandtl Number		7.23E-01			
Density		0.37			kg/m³
Gas velocity	4.09	5.45	6.81	8.59	m/s
Reynolds number	5,306	7,074	8,843	11,142	
Nusselt number	43.41	50.12	56.04	62.90	
Heat transfer coefficient	20.80	24.02	26.85	30.14	W/m²K
Thermal conductivity (steel)		50			W/Km
Biot number	8.32E-04	9.61E-04	1.07E-03	1.21E-03	

The simulation results have shown, that most of the fouling occurs on the front faces of the fins (51 %) and the horizontal surfaces of the fins (42 %). With a total surface of 0,014 m² and an accretion rate of 1,9 mg/(m² s) for Variant IV case 4 (target flow rate, measured dust load) this yields a buildup of 0,03 mg/s on the front faces of the fins. With a density of the dust of 6.021 kg/m³ a maximum buildup of 4,4*1e- 3 mm³/s is possible. On the horizontal surfaces with a total area of 2,1 m² and an accretion rate of 0,02 mg/(m² s) a maximum buildup of 3,6*1e- 3 mm³/s is possible. With an assumed dust load of 50 mg/m³ (Variant IV case 4) buildups of 0,12 mm³/s on the horizontal surfaces and 0,15 mm³/s on the front faces may occur.

The CFD simulations consider worst case scenarios, as in the current applications a fraction of the particles will not stick to the surfaces on impact. With the heat transfer characteristics given above the impact on the convective heat transfer must be considered. The buildup will result in a

diminishing cross section between the fins and thus the pressure drop across the fins will increase resulting in a lower flowrate and velocity. However, the CFD results show, that - assuming a homogenic distribution of buildup across the surfaces - a maximum buildup of 0,06 mm on the horizontal surfaces is possible for an operation of 1 year with the measured dust load (1,48 mg/m³). The pressure drop is defined as

$$\Delta p = \lambda \frac{l}{d_h} \frac{\rho}{2} v^2 \Leftrightarrow v = \sqrt{2 \frac{\Delta p \cdot d_h}{\lambda \cdot l \cdot \rho}}$$

Assuming constant pressure drop and flow coefficient the resulting velocity v_2 after buildup is approximated as

$$v_2 = v_1 \sqrt{\frac{d_{h,2}}{d_{h,1}}}$$

Given the assumptions and characteristics above, this would yield a loss of approximately 0,7 % of the convective heat transfer to the fins.

Conclusion

The CFD results have shown, that the particle buildup is quasi linear proportional to the flow rate. On average 42 % of the particle deposition occurs on the horizontal surfaces and 51 % at the front faces of the fins. The remain depositions occur on the heatpipe surfaces. The particle modelling assumes immediate deposition on impact on the surfaces of the heat exchanger, which will not be the case in current operation. The CFD results therefor show a worst-case scenario and the current deposition will be a fraction of the calculated values.

For the given boundary conditions and the design of the heat exchanger the buildup of particles will have an impact on the convective heat transfer. The diminishing cross section will induce an increased pressure drop and thus the flowrate will decrease. For a runtime of 365 days the data was extrapolated to yield a decrease in the heat transfer coefficient of approximately 1 %. The current particle deposition will be less than the results of the CFD calculations have shown and the effect of the cumulated depositions on the fluid regime has not been considered. Further operational long-time testing will give a thorough insight. At this point it is assumed, that the impact of the dust load of the fluid regime will be neglectable for the buildup related heat transfer.

2.3.4 Task 3.5: Design of a system to prevent the formation of deposits (CEM)

Objective of this task was the study, selection and modification of high temperature resistant coatings that prevent the formation of deposits in heat exchanger systems, in order to maintain its efficiency. These coatings consist of industrial high temperature resistant coatings modified with anti-adherent additives in order to increase its anti-adherent properties. The selection criteria adopted for the coating's selection were:

- Thermal stability up to 750 – 800°C.
- Ease of handling and application.
- Widely industrially available.
- Non-hazardous.

Table 16: Selected coatings and their characteristics.

Product name	Producer	Description	Active agent	Anti-adherent?	Main solvent	Thermal stability	Application	Curing	Colour
Cerastil E-1001	Panacol	High temperature anti-stick and anti-slag coating	Carbon black	Yes	Water	> 2.000 °C	Spray, roller, brush	Room temperature	Dark grey
Silixan T 330-40/IPA	Silixan	Clear tarnish protection coating for stainless steel	Inorganic-organic polymer on silica base	No	Isopropanole	> 800 °C	Spray, brush, dip or aerosol	Room temperature or 100-500 °C	Transparent
Silixan S400-35/PE	Silixan	Aluminium in an inorganic-organic matrix	Aluminium	No	Petroleum ether	> 800 °C	Spray, brush, dip or aerosol	Room temperature	Silver grey
X-clean EC 2048	Nano-X	One-component coating material for high-temperature working ceramic rollers	Boron nitride / aluminium in an inorganic-organic silane based matrix.	Yes	Isopropanole	> 800 °C	Spray, brush	Room temperature	Silver grey
Thermobarp 800	Barpimo	High temperature resistant paint based on modified resins	Unknown	No	Xylene, ethylbenzene	800 °C	Airless gun, aerographic gun	Room temperature	Black

In order to assure the safety of the technicians and workers, the use of less dangerous materials was preferred. Hazard statements of the above products showed that Silixan S400-35/PE and Thermobarp 800 have important health hazards which make their use undesirable (e. g. flammable, could cause serious damage to the eyes or organs). The use of these materials would require the application of more demanding safety precautions. Thus, in the first approach these products have not been included in the study, although they have been reconsidered in a second study. Therefore, the products selected and studied for the development of the anti-adherent high temperature resistant coating in the first study have been Cerastil E-1001, from Panacol. Silixan T330-40/IPA, from Silixan and X-clean EC 2048, from Nano-x.

The wettability and adhesion behaviour of the coatings were characterized by room temperature contact angle measurement and surface energy measurement techniques. The performance of the coatings was evaluated before and after its introduction at high temperature (750°C) for a fixed time (8 hours). Following change directions of contact angle and surface energy are desired:

- The increase of contact angle is desired (greater hydrophobicity).
- The decrease of surface energy is desired (greater repulsion to water).

Selected coatings have been applied on substrates made of stainless steel and room temperature contact angle and surface energy have been measured. **Figure 56** shows pictures of the influence of the investigated coatings on the contact angle between the surface and a water drop. It can be seen, that the contact angle varies between nearly 90° (x-clean) and lower 10° for Cerastil. Main results: Cerastil E-1001: hydrophilic, Silixan: no big changes. X-clean: increases contact angle.

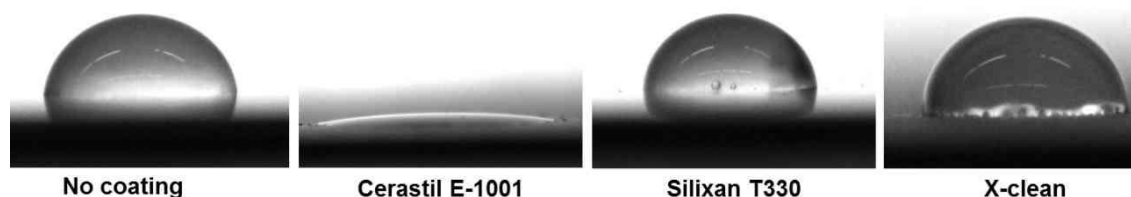


Figure 56: Picture of the influence of different coatings on the contact angle

Results of the investigation regarding the surface energy of the different coatings were:

- Silixan: reduces surface energy, higher repellency to water.
- X-clean: no big changes in surface energy.
- Cerastil E-1001: the surface energy has not been measured as it is highly hydrophilic.

In view of the results (contact angle and surface energy), none of the coatings completely met the requirements of contact angle increase and energy surface reduction. Therefore, Silixan and X-clean (since their performance was better than Cerastil) were modified with Nano-additives in order to assess how much contact angle and surface energy change.

Regarding the anti-adherent additives, the criteria is:

- Anti-adherent or hydrophobic behaviour.
- Thermal stability up to 750 – 800°C.
- Ease of handling and application.
- Non-hazardous.

- Widely industrially available.

Under such criteria, the additives selected were as shown in **Table 17**.

Table 17: Additives characteristics

Product Name	Producer	Chemical formula	Chemical name	Description of product	Particle size distribution (D_{50})	Hazard statements
Molybdenum Disilicide - Grade C	H.C. Stark	MoSi ₂	Molybdenum Disilicide	Greyish powder	2.0-3.0 microns	None
Boron Nitride - Grade A 01	H.C. Stark	BN	Boron Nitride	White powders / Hexagonal	0.4-0.7 microns	None
Alpha-silicon nitride - Grade M11	H.C. Stark	$\alpha\text{-Si}_3\text{N}_4$	Silicon Nitride	High alpha phase Si ₃ N ₄	0,5-0,7 microns	None
Aluminum nitride - Grade B	H.C. Stark	AlN	Aluminum Nitride	Fine particle size, deagglomerated, high purity. Hexagonal.	2.0-4,5 microns	None

The coatings were applied on substrates made of stainless steel and copper, the type of materials that can be used for the construction of the heat exchanger. Three substrates have been selected:

- Copper.
- Rusting Steel.
- Stainless Steel, AISI 304, most common, AISI 310S, specific for high temperatures.

For the preparation of the coatings, mechanical stirring has been used. For the application of the coating in flat substrates, a bar coater was used.

Substrates heat resistance

Different selected substrates were introduced in an oven at 750°C for 8 h in order to evaluate their heat resistance. Copper samples and rusting steel do not show resistance to this heating treatment. Stainless steel, AISI 304, apparently resists to stove tests, although a darkening of the sample and a detaching of small particles were observed. This is the reason why stainless steel, AISI 310, specific stainless steel for high temperatures, was also included as a possible substrate. In **Table 18** a summary of the stove results at 750°C for 8 h of the different substrates is collected.

Table 18: Substrates heating resistance

Substrate	Stove results (8h @ 750°C)	
Copper	Deformation and darkening	✗
Rusting Steel	Deformation and detachment	✗
Stainless Steel AISI 304	Darkening of the sample and a detaching of small particles	⚠
Stainless Steel AISI 310	Darkening	✓

Although Stainless Steel AISI 310 shows the best behavior, stainless Steel AISI 304 was selected as substrates to be used in the laboratory trials, since it is an accessible and affordable material.

First approach: Additivation of coatings Silixan T330 and XClean EC2048

According to the results of the experiments regarding contact angle and surface energy Silixan T330 and X-clean EC 2048 were selected to be additized.

Initially, Silixan T330 was additized with the four selected anti adherent additives (MoSiO₂, Si₃N₄, BN and AlN) in 3 different percentages: 1, 5 and 10% in weight.

In **Figure 57** the additized coated samples are presented before and after stove test at 750°C for 8 h. As it can be observed, the adherence before and after stove test was ok, except from the samples coated with Si₃N₄ that was partially detaching of the coating.

Complementary to the additivation of Silixan T330, additivation of X-clean EC2048 was carried out. As previously, it was additized with the four selected anti adherent additives (MoSiO₂, Si₃N₄, BN and AlN) in 3 different percentages: 1, 3 and 5% in weight. In **Figure 58** the additized coated samples are presented before and after stove test. As it can be seen, X-clean presents worse adherence to the substrates than Silixan. Laboratory validation tests (surface energy and contact

angle) had not been performed due to this adherence behavior of X-clean and this is the reason why Silixan T330 was selected to be tested in industrial conditions (Task 3.6).

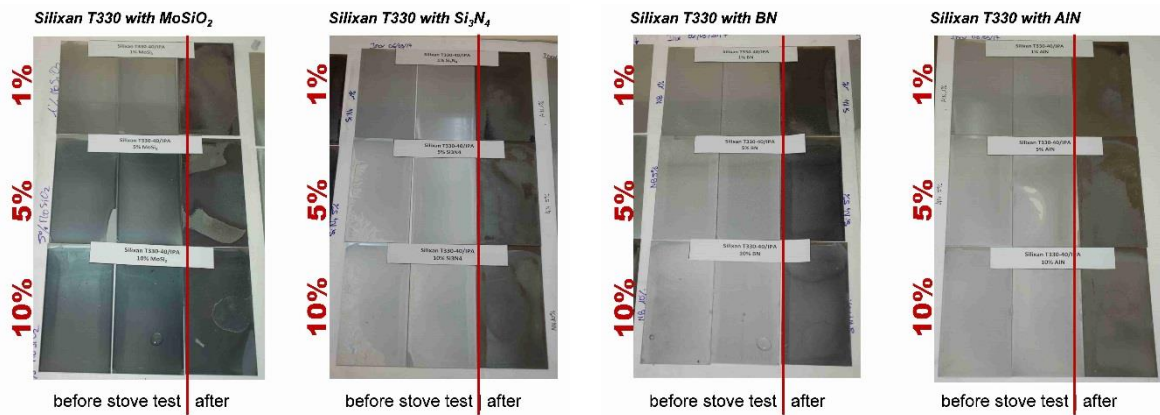


Figure 57: Silixan T330 additivated samples

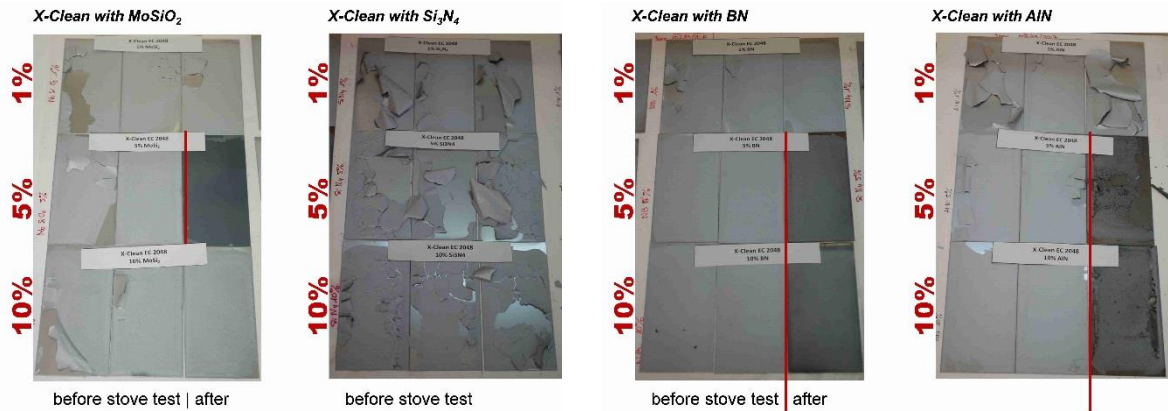


Figure 58: X-clean EC2048 additivated samples

Second approach: Additivation of coatings Silixan S400-35/PE and Thermobarp 800

In a second approach, Silixan S400-35/PE and Thermobarp 800, previously excluded for its toxicity were tested, due to the test results of Silixan T330 under industrial conditions (see Task 3.6).

The non additivated coatings were applied on stainless steel AISI 304 and submitted to a thermal treatment. In **Figure 59** the images of the samples before and after the heating treatment are presented. After heating treatment Thermobarp 800 was coated successfully and passed the test whereas Silixan S400 coating was detached in some areas. Although this partial detachment in Silixan S400 samples, it was decided to continue with the additivation of both coatings.

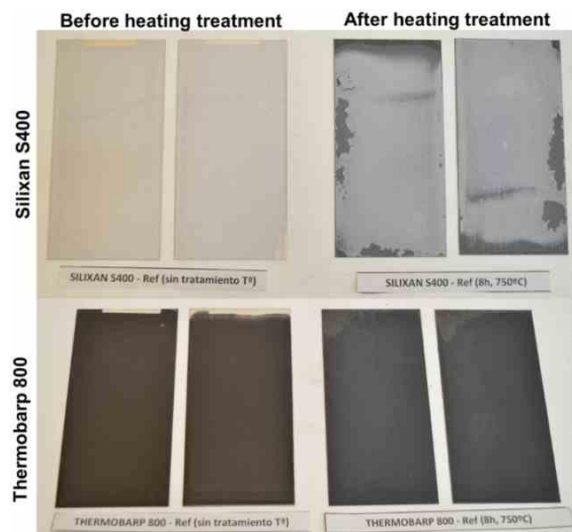


Figure 59: Silixan S400 and Thermobarp 800 before and after heating treatment test

Additivation of coatings: Thermobarp 800 and Silixan S400

Thermobarp 800 and Silixan S400 were additivated with 1 and 3% of BN, applied on stainless Steel AISI 304 and introduced in the stove for heating treatment. In **Figure 60** the images of the samples of Thermobarp 800 before and after heating treatment are presented. Both presented good adherence and no detachment was observed. Therefore, they were selected as samples to be evaluated in industrial environment, see Task 3.6.

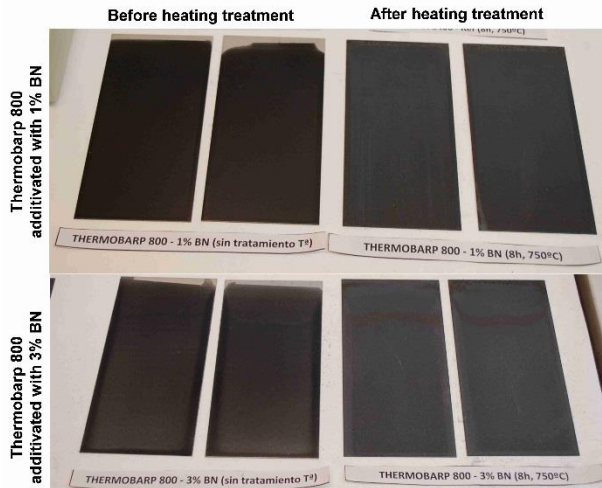


Figure 60: Additivated Thermobarp 800 samples before and after heating treatment test

In parallel, surface energy measurements of Thermobarp 800 were carried out. Before the heating treatment, the surface energy of the samples was between 31 and 33 mN/m, however after heating treatment it increased up to 72 mN/m. This is the reason why it was not possible to measure contact angle due to the hydrophilicity of the coating that absorbs the water drop. Anyway, the coating was validated in industrial environment (see Task 3.6) in order to study the real anti adherent behavior at high temperatures that will be the final use of the coatings.

2.3.5 Task 3.6: Dummy manufacturing and testing (tkSE, CEM)

In order to evaluate the behavior of the coatings in industrial environment against dust deposition, samples were placed inside the industrial pipes of the CSP where the demonstrator will be installed. In **Figure 61**, a schematic view of the pipe is presented. In green the location of the coated samples is indicated.

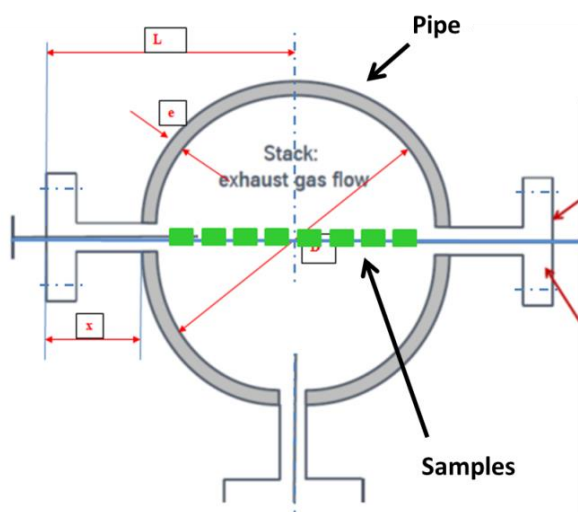


Figure 61: Industrial validation. Location of coated samples in the industrial pipes

Samples weight differences between the beginning and the end of the test were used to evaluate the deposition of dust and other impurities.

Based on the results obtained in the laboratory additivated Silixan T330 samples were selected to be tested in industrial conditions using stainless steel AISI 304 as substrate. For that purpose, the following samples were introduced in the industrial pipes of tkSE facilities for 14 days being measured before and after this time:

- 4 reference samples without coating.

- 4 coated reference samples with Silixan T330 coating without additive.
- 4 samples coated with Silixan T330 additivated with 10% of MoSiO₂.
- 4 samples coated with Silixan T330 additivated with 10% of Si₃N₄.
- 3 samples coated with Silixan T330 additivated with 10% of BN.
- 3 samples coated with Silixan T330 additivated with 10% of AN.

Most of the additivated coated samples showed a weight loss after being placed in the pipes for the mentioned time. This means that a degradation of the substrate or the coating may have been occurred. The results are summarized in **Table 19**.

Table 19: Validation test results of additivated Silixan T330

Sample	Initial weight in g	Final weight in g	Difference in g
Reference samples	72.9636	73.3369	0.3733
	73.0448	73.2568	0.212
	72.9285	73.4782	0.5497
	72.9879	73.6403	0.6524
Coated reference samples	73.3712	73.4006	0.0294
	73.2940	73.0820	-0.2120
	73.1093	Lost during removing	
	73.0770	73.3839	0.3762
Samples additivated with 10 % of MoSiO ₂	73.1333	73.3577	0.2244
	73.3896	73.7213	0.3317
	73.2545	72.9878	-0.2667
	73.3854	73.2920	-0.0934
Samples additivated with 10 % of Si ₃ N ₄	73.5317	73.4775	-0.0542
	72.9524	73.1953	0.2429
	73.5674	73.2789	-0.2885
	73.4347	73.2407	-0.1940
Samples additivated with 10 % of BN	73.1335	73.0306	-0.1029
	73.4076	73.5263	0.1187
	73.4848	73.0586	-0.4262
Samples additivated with 10 % of AN	73.4007	72.9185	-0.4192
	73.4215	Lost during removing	
	73.5698	73.1717	-0.3981

Therefore, new coatings (Silixan S400-35/PE and Thermobarp 800) additivated with BN at 3% in weight were prepared and tested at tkSE facilities. To assure the heat resistance of the substrates in the industrial environment validation, stainless steel AISI 310 was used in the preparation of these samples. The samples were placed inside the CSP waste gas pipe for 14 days:

- 3 reference samples without coating.
- 3 coated reference samples with unmodified Thermobarp 800 coating.
- 3 coated reference samples with unmodified Silixan S400 coating.
- 3 samples coated with Thermobarp additivated with 3% of BN.
- 3 samples coated with Silixan S400 additivated with 3% BN.

Test results showed that no deposition was observed, see **Table 20**, the thermal behaviour was good and no degradation of the coating due to the high temperature.

Table 20: Deposition evaluation of the coating test at tkSE

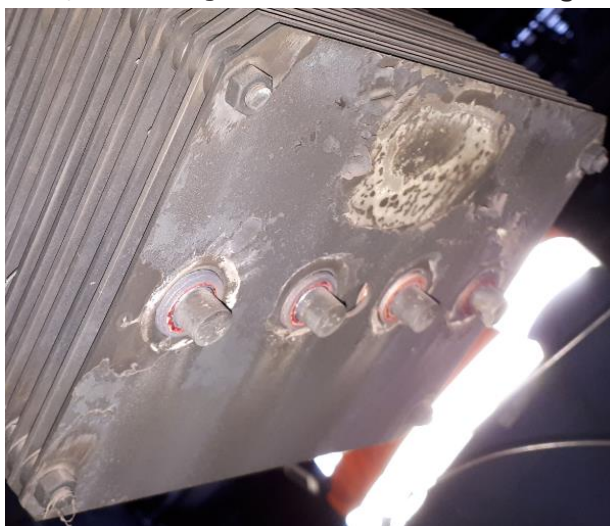
Sample	Initial weight in g	Final weight in g	Difference in g	Average difference in g
Thermobarp	168.8823	168.9308	0.0485	0,0628
	175.2404	175.2990	0.0586	
	171.5863	171.6675	0.0812	
Thermobarp with 3% of BN	175.1549	175.2133	0.0584	0,0546
	168.5595	168.6244	0.0649	
	171.3268	171.3674	0.0406	
Silixan S400	170.7254	170.8299	0.1045	0,0950
	172.7423	172.8292	0.0869	
	173.0205	173.1140	0.0935	

Sample	Initial weight in g	Final weight in g	Difference in g	Average difference in g
Silixan S400 a with 3% BN	175.6210	175.6812	0.0602	0,0629
	172.8310	172.9211	0.0901	
	172.9882	173.0267	0.0385	
Uncoated sample	171.5201	171.7166	0.1965	0,1110
	172.2598	172.3107	0.0509	
	169.1792	169.2647	0.0855	

The results showed, that the dust load of the CSP waste gas is just minor and that no deposits are expected for the long-term demonstrator test. Thus, it was decided that it is not necessary to coat the heat exchangers of the TEG cartridges and the fins of the heat pipe heat exchanger.

Nevertheless, one of the heat pipe heat exchanger fins was treated with the Thermobarp coating (which showed the best performance during the tests in industrial environment) to test its thermal resistance over a longer period (see WP 5).

After three weeks of operation in the industrial environment with different temperatures and flow rates, the coating at the fin was examined. **Figure 62** shows a photo of the bottom fin.



Flow direction



Figure 62: Coating after several weeks of demonstrator operation

The coating shows considerable wear. In the edge areas and around the heat pipes the coating has detached from the fin. The greater detachment of the coating visible in the picture above is probably due to condensation. In the flow shadow of the heat pipes there are optical differences of the surface. In summary, it can be stated that coatings are neither necessary nor suitable in this application.

2.4 WP 4: Design & construction of the test-bed; Testing of the bench scale unit

Objectives of WP 4 were:

- Design and construction of a test-bed to study the bench scale unit of the TE generator
- Integration of power conversion and system control/automation together with other measuring equipment that allow a complete characterization of TE systems
- Executing experiments
- Validation of available Simulink models that allow the coupling of the energy input, Seebeck effect, Peltier Effect, Joule heating and energy dumped to the cooling system

2.4.1 Task 4.1: Test-bed design and construction (BFI, GUN)

The task was devoted to the construction of a test-bed at the BFI testing facility to be able to investigate the benchmark cartridge under near-service conditions.

In front of the operational long-term tests of the demonstrator, experiments with a GEN3 cartridge were carried out at a testing facility of the BFI. Based on the test results the design of the demonstrator (WP 2) was adapted.

The BFI testing facility at a steel mill in Duisburg, Germany, was selected as the location for these tests. The testing facility is mainly used for burner tests and includes a combustion chamber (inner

cross section 2 x 2 m, length approx. 6.5 m, available fuel gases: coke oven gas (CO gas), blast furnace gas (BF gas) and natural gas). It was foreseen to use the combustion chamber during the bench scale unit tests for the waste gas production.

The CSP, as the selected waste heat source at tkSE for the demonstrator long-term test, is fired by BOF gas. Since there is no BOF gas available at the BFI testing facility, calculations of the waste gas composition of the available gases (BF and CO gas) and a comparison with the waste gas composition from BOF gas combustion were necessary. **Table 21** shows the results of the waste gas composition calculation. The waste gas data from BF gas combustion are in good agreement (deviation approx. 1 %) with waste gas data of the CSP. In contrast, the waste gas composition from CO gas combustion differs in a wide range (deviation between 4 and 17 %) from waste gas data of the CSP. Thus, it was concluded that the use of BF gas is sufficient for the bench scale tests.

Table 21: Calculation of waste gas compositions

BOF gas at the CSP			Waste gas from BOF gas combustion				
CO	66.0	Vol.-%	CO ₂	29.19	Vol.-%		
H ₂	3.8	Vol.-%	H ₂ O	1.36	Vol.-%		
CH ₄	0.0	Vol.-%	O ₂	3.72	Vol.-%		
C ₂ H ₄	0.0	Vol.-%	N ₂	65.74	Vol.-%		
C ₂ H ₆	0.0	Vol.-%	standard density	1.487	kg/m ³ standard		
CO ₂	15.7	Vol.-%	density at 700°C	0.417	kg/m ³		
O ₂	0.2	Vol.-%	average Cp at 700°C	1.086	kJ/(kg K)		
N ₂	14.3	Vol.-%	kinematic viscosity	1,060	10 ⁻⁷ m ² /s		
			Prandtl-Number	0.735	-		
BF gas at BFI testing facility			Waste gas from BF gas combustion				
CO	25.2	Vol.-%	CO ₂	27.82	Vol.-%		
H ₂	4.7	Vol.-%	H ₂ O	2.65	Vol.-%		
CH ₄	0.0	Vol.-%	O ₂	2.53	Vol.-%		
C ₂ H ₄	0.0	Vol.-%	N ₂	67.01	Vol.-%	Comparison with BOF waste gas	
C ₂ H ₆	0.0	Vol.-%	standard density	1.469	kg/m ³ standard	-1.21	%
CO ₂	24.2	Vol.-%	density at 700°C	0.412	kg/m ³	-1.20	%
O ₂	0.0	Vol.-%	average Cp at 700°C	1.094	kJ/(kg K)	0.74	%
N ₂	45.9	Vol.-%	kinematic viscosity	1,072	10 ⁻⁷ m ² /s	1.08	%
			Prandtl-Number	0.737	-	0.26	%
CO gas at BFI testing facility			Waste gas from CO gas combustion				
CO	6.9	Vol.-%	CO ₂	5.75	Vol.-%		
H ₂	62.2	Vol.-%	H ₂ O	18.88	Vol.-%		
CH ₄	21.4	Vol.-%	O ₂	4.29	Vol.-%		
C ₂ H ₄	1.1	Vol.-%	N ₂	71.08	Vol.-%	Comparison with BOF waste gas	
C ₂ H ₆	0.5	Vol.-%	standard density	1.238	kg/m ³ standard	-16.75	%
CO ₂	1.6	Vol.-%	density at 700°C	0.347	kg/m ³	-16.79	%
O ₂	0.0	Vol.-%	average Cp at 700°C	1.203	kJ/(kg K)	10.77	%
N ₂	6.3	Vol.-%	kinematic viscosity	1,243	10 ⁻⁷ m ² /s	17.25	%
			Prandtl-Number	0.766	-	4.09	%

A waste gas pipe in which the bench scale unit was installed was connected to the combustion chamber. By cooling pipes in the combustion chamber and adjustment of the burner capacity the investigation of different scenarios was possible. The scheme of the test-bed at the BFI testing facility is shown in the appendix, **Deliverable 4.1**. The waste gas, produced in the combustion chamber by a BF gas burner, is sucked into the DN 150 waste gas pipe by the fan at the end of the

waste gas system. The waste gas can be cooled in a double wall pipe section, if necessary. The following safety relief valve was controlled by the waste gas temperature measurement in front of the valve (TIHS), to protect the TE cartridge from overheating. The length of the inlet path between the safety relief valve and the TE cartridge was tenfold of the inner pipe diameter to get a non-disturbed flow in front of the cartridge. The allowed max. temperature of the flow measurement after the cartridge was 200°C. Thus, to cool down the waste gas to the allowed temperature two cooling coils were installed inside the waste gas pipe between the TEG cartridge and the volume flow measurement. The bypass to the volume flow measurement was installed for safety reasons, to protect the flow measurement from overheating and water condensation during the start-up process of the test-bed. The test-bed was connected to the main waste gas pipe of the combustion chamber which was located beneath of the combustion chamber. An additional air supply in the waste gas pipe was used for control reasons of the fan. Behind the fan the waste gas pipe was connected to the chimney of the combustion chamber.

Following measurements were integrated: Waste gas composition (WG composition), waste gas temperature in front and after the TE cartridge (T_{WG}), waste gas pressure in front and after the cartridge (p_{WG}), waste gas volume flow (F_{WG}), cooling water temperature in front and after the cartridge (T_{CW}) and cooling water flow (F_{CW}).

Figure 63 shows images of the test-bed during the construction.



Figure 63: Construction of the test-bed at the BFI testing facility

After finishing the experimental set-up (BFI and GUN) the measuring equipment and data logging system were installed and connected. The I-V Tracer and Power Converter (see Task 2.4) to maximise/optimise the TEG performance were integrated into the test-bed. Images of the final experimental set-up are attached in the appendix, **Milestone 4.1**.

Figure 64 displays schematically the test setup of the I-V Tracer. The I-V Tracer and at-load Tester device is an independent electronic load specifically designed to test TEGs and to operate them at load. The tracer can instantaneously inspect the electrical performance of the device connected to its input terminals or continuously operate it at-load. The power obtained from the TEG is dissipated internally to the tracer unit.

The tracer can also emulate a MPPT converter thus allowing the test of a TEG system at load to verify overall thermal and electrical performance. It can also be used as a constant current or constant voltage electronic load. The tracer used in the PowGETEG project was rated for 150 W continuous power dissipation and 250 W during I-V trace measurements.

A 4-wire voltage sensing method is used to remove the influence of voltage drops on power cables and thus ensure the data provided is as accurate as possible since this is being used to characterise the performance of the TEG in-situ and is the way by which project results can be evaluated.

The converter developed in this project is a MPPT converter (see task 2.4) designed specifically for TE power generating modules. The converter includes battery charging management software to ensure the battery is not over-charged. To do this if activated (i.e. if the battery terminal voltage reaches a pre-set level) the converter “throttles back” the power drawn from the cartridge, decreasing the current drawn and therefore reducing the parasitic Peltier effect in the TEG, which reduces the thermal conductivity, which increases overall system efficiency.

The design of the Power converter also interfaces TEGs whose voltage can be either lower or higher than that of the output battery (this is necessary because if the TEG is “cold”, the voltage is lower and needs to be boosted. If the TEG is “hot”, the voltage is higher than the battery and needs to be reduced to the battery voltage in a very efficient way.)

The Power converter can communicate to other devices through I2C. They answer to an I2C master using a communication protocol, based on the PMBus protocol. This allows the converter to provide measurements of input and output voltage and current (4 measurements) and from these the Power converter efficiency can also be determined.

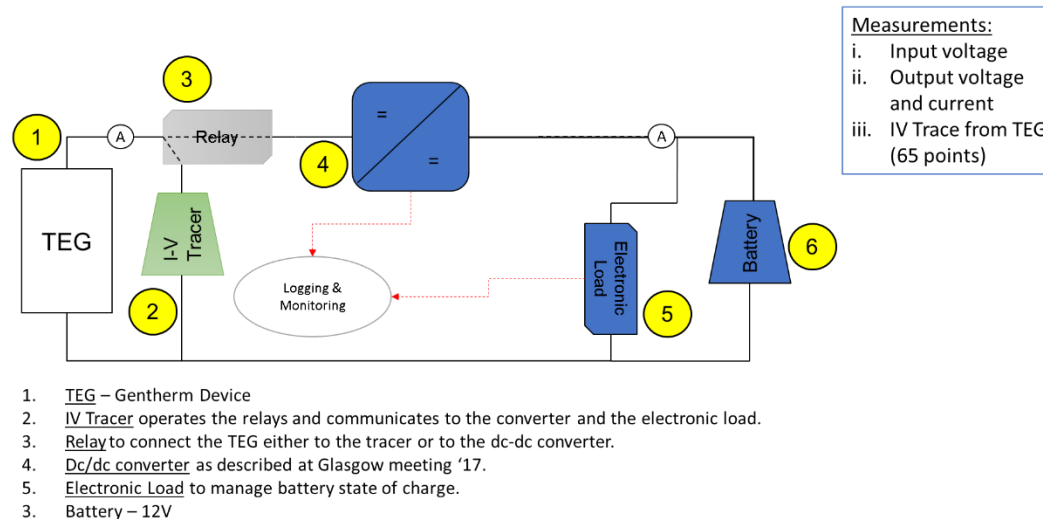


Figure 64: I-V Tracer test setup

2.4.2 Task 4.2: Executing experiments (BFI, GUN)

Objective of this task was the investigation of the benchmark cartridge under different conditions. The experiments were executed at the BFI testing facility on August 15 and 16, 2017, by the BFI and GUN. Main boundary conditions of the experiments were:

- Combustion gas: BF gas.
- Average waste gas data in comparison to the waste gas composition of the CSP at tkSE are shown in **Table 22**:

Table 22: Average waste gas data during the experiments and at the CSP

	test-bed	CSP	
O ₂	2.2	3.7	Vol.-%
CO ₂	27.8	29.2	Vol.-%
H ₂ O	2.7	1.4	Vol.-%
N ₂	67.3	65.7	Vol.-%
Standard density	1.42	1.49	kg/m ³

- TE cartridge: GEN3 cartridge (expected power output of approx. 180 W at a waste gas flow of 130 kg/h and waste gas temperature of 700°C).
- Cartridge cooling: Water.

Several experiments were carried out with different:

- Waste gas temperature (400 – 800°C).
- Waste gas flow (33 – 155 kg/h).
- Cooling water flow (300 – 1,000 l/h).

During the experiments data of waste gas flow, waste gas temperature, waste gas composition, pressure drop, cooling water flow and cooling water temperature were recorded every second. Performance data of the TE cartridge (power, current and voltage) were recorded by the I-V Tracer and Power Converter. The recording of these data was initialized by personnel of GUN when a steady state of waste gas temperature, waste gas flow and cooling water flow was reached.

Initially the TE cartridge was installed with the cooling water supply position in the bottom of the cartridge. After the experiments on August 15 the cartridge was installed in that way that the cooling water supply was on the top of the cartridge. Reason was that the cooling water flow of 600 l/h was too low to cool the whole circumference of the cartridge with the cooling water supply at the bottom of the cartridge. So, the cooling water flow could be minimized on the 2nd day of the experiments.

On August 15 the waste gas after the TE cartridge was cooled (necessary to protect the volume flow measurement from overheating) just in the 2nd of two cooling sections, since the water supply for the first section was broken. On August 16 the first cooling section was repaired and the waste gas after the cartridge was cooled in both pipe sections.

At 11 am on August 16 the waste gas pipe in front of the cartridge was insulated, to be able to increase the waste gas temperature above 700°C without increasing the waste gas volume flow anymore.

2.4.3 Task 4.3: Data Mining and data analysis (BFI, GUN)

This task was about the analysis of the experimental data and the evaluation of experimental results.

During the experiments data of the main parameters (waste gas flow and temperature, cooling water flow and temperature, electrical power, ...) were recorded. A more detailed description of the recorded data sets is attached in the appendix, **Deliverable 4.2**. In a first step periods of steady state were identified in the different data sets. Since the recording density of several values (see chapter 2.4.2) was 1 s average values for the steady state periods were calculated. Based on time and date the performance data of the TE cartridge (which were recorded selective, see chapter 2.4.2) were assigned to the steady state periods. After that the data were analysed and the result evaluation was done.

Table 23 summarizes the average waste gas composition and density during the experiments. Compared to the waste gas data of the CSP (see chapter 2.4.2) it can be seen, that the used waste gas for the experiments was similar. Conclusion is that the experimental results are significant for the demonstrator test at the CSP.

Table 23: Average waste gas data during the experiments

	O ₂ in Vol.-%	CO ₂ in Vol.-%	H ₂ O in Vol.-%	N ₂ in Vol.-%	Standard density in kg/m ³
August 15	2.3	27.4	2.7	67.6	1.41
August 16	2.1	28.2	2.7	67.0	1.42

Table 24 shows in each line average main data during a steady state period. Greyed out and bold values are parameters which were changed between two steady state periods. This makes it easier to see the influence of the parameters on the TEG performance.

An increase of the waste gas temperature increases the difference of the cooling water temperature as well as the waste gas pressure drop across the cartridge and increases, as supposed, the power output of the cartridge. The increase of the waste gas flow shows similar results. An increase of the cooling water mass flow shows decreasing cooling water temperature across the cartridge. Power output of the cartridge and the waste gas temperature are not influenced significantly by the cooling water mass flow.

The maximum power output was approx. 260 W at a waste gas temperature of approx. 800°C and a waste gas mass flow of approx. 140 kg/h. A comparison of these values with the power output at lower waste gas temperatures and flows (to the point of the lowest power output of approx. 15 W at a waste gas temperature of approx. 400°C and a waste gas mass flow of approx. 33 kg/h) shows that the decrease of the power output is not linear with decreasing temperature and waste gas flow. The more waste gas temperature and flow decrease the more the power output of the cartridge diminishes.

At low waste gas flows (up to 88 kg/h, data from 15th August) the measured heat losses in the waste gas are lower than the increase of heat in the cooling water. That cannot be possible and is probably caused by inaccuracies of the waste gas volume flow measurement at such low gas flows. A comparison of the data from 15th August with the data from 16th August shows, that the waste gas cooling after the TE cartridge influenced the measured waste gas temperature difference across the cartridge (difference on August 15 approx. 70 - 85°C with waste gas cooling after the cartridge just in the 2nd pipe section and 100 - 120°C with waste gas cooling in both pipe sections, see chapter 2.4.2). Reason is probably the colder pipe due to the higher cooling and thus a higher heat flow from the waste gas to the pipe walls. This is probably also the reason for the big difference between the determined heat losses in the waste gas and the heat increase in the cooling water.

Table 24: Steady state periods (greyed out and bold values were changed in comparison to the previous period, see Task 4.2)

Waste gas		Coolin g water flow in l/h	Pressur e drop throug h the TEG in mbar	Difference of			Coolin g water heat in W	Waste gas velocity in front of the TEG in m/s	Maximum power in W
mass flow in kg/h	temperatu re in front of TEG in °C			waste gas temperatu re in front and after TEG in °C	coolin g water tempe rature in °C	wast e gas heat in W			
August 15 (waste gas cooling after the cartridge only in one cooling section)									
33.1	405	579	7.5	68.7	1.2	754	780	2.1	15.6
49.5	456	567	12.9	54.3	1.6	908	1,077	3.3	18.8
80.4	500	565	19.2	46.2	2.6	1,273	1,717	5.7	--
88.0	508	1,005	19.1	73.4	2.1	2,212	2,470	6.3	77.5
146.5	599	993	26.8	75.1	2.6	3,874	2,988	11.7	126.8
154.7	652	999	34.6	78.6	3.0	4,347	3,485	13.1	165.0
August 16 (waste gas cooling after the cartridge in both cooling sections)									
142.8	602	991	32.0	129.5	2.6	6,422	3,007	11.4	134.0
144.3	649	998	32.1	122.8	2.9	6,295	3,331	12.1	173.3
235.5	698	992	76.1	114.3	3.4	9,699	3,859	20.9	173.3
139.9 *	751	999	43.6	141.6	3.7	7,210	4,249	13.1	214.2
140.4	799	1,023	46.4	139.6	3.7	7,241	4,370	13.7	261.3
125.8	795	1,001	40.0	144.8	3.9	6,717	4,534	12.3	--
124.5	699	609	36.3	123.2	5.4	5,517	3,840	11.0	175.6
124.9	697	490	36.2	123.2	6.7	5,523	3,799	11.1	175.6
125.0	700	409	36.4	123.1	8.0	5,533	3,818	11.1	175.6
125.1	701	306	36.3	121.9	10.7	5,490	3,824	11.1	172.5
125.7	700	417	36.4	120.9	8.1	5,471	3,944	11.2	151.2
126.3	647	623	34.4	104.9	5.5	4,702	3,508	10.6	151.2
* To increase the waste gas temperature in front of the TE cartridge above 700°C the pipe in front of the cartridge was insulated for the following experiments									

Figure 65 shows I-V and I-P curves of the TE cartridge for several steady state periods. As mentioned above it can be seen that waste gas temperature and flow influence significantly the TEG performance. At high waste gas temperatures and flows the maximum usable current of the Power Converter, which is in the range of approx. 27.5 A, was reached at a voltage level of 9.5 V.

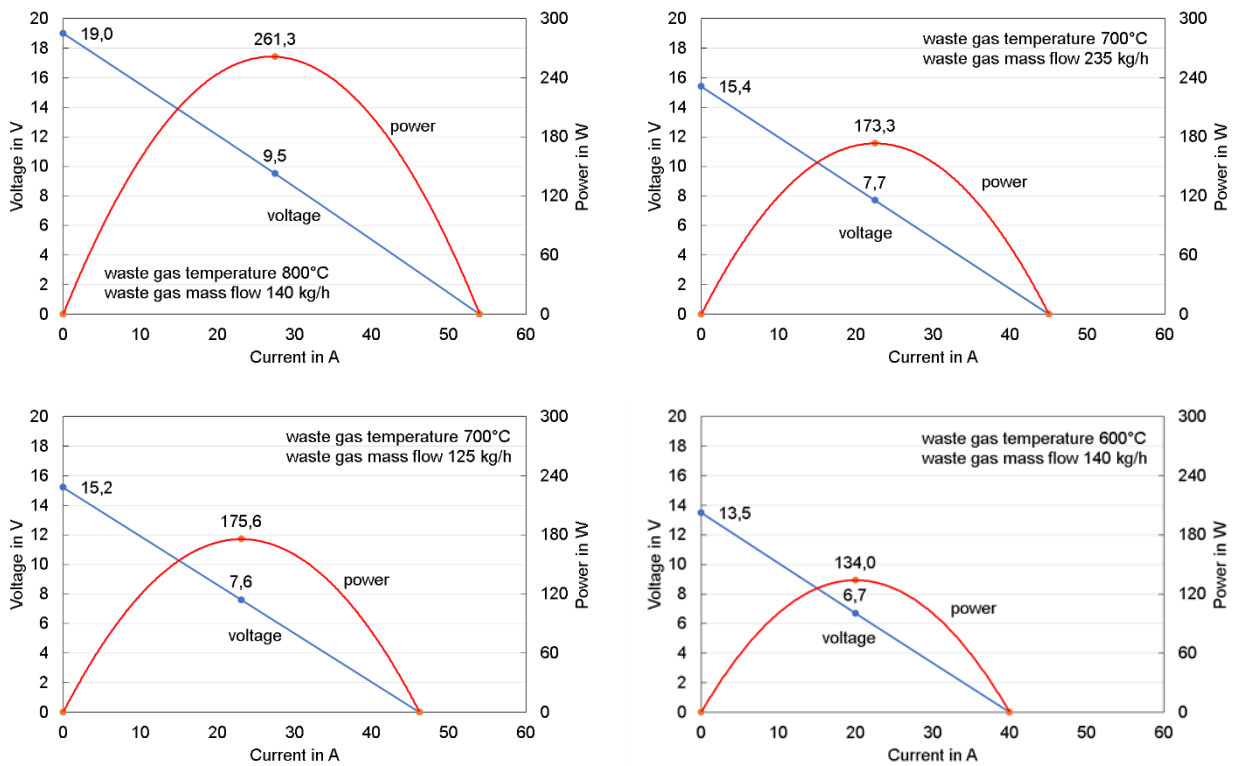


Figure 65: Voltage and power as a function of current at different waste gas temperatures and waste gas flows

Figure 66 displays the dependency of power, voltage and current from the waste gas temperature. **Figure 6** and **Figure 67** show a comparison of the experimental data with data from GNTH. GNTH generated the performance data with hot air in the laboratory. The comparison of power output (**Figure 6**) shows a good agreement between experimental and GNTH data. In the waste gas temperature range of the CSP of 700 – 800°C a power output of 175 W up to 260 W can be expected from such a GEN3 cartridge. The comparison of the pressure drop of the waste gas across the cartridge shows that the experimental pressure drop is higher than the values determined by GNTH (with air). This must be considered for the demonstrator and the fan selection.

The average electrical efficiency of the Power converter was approx. 94 %, which is in the range of the efficiency achieved in lab tests at GUN.

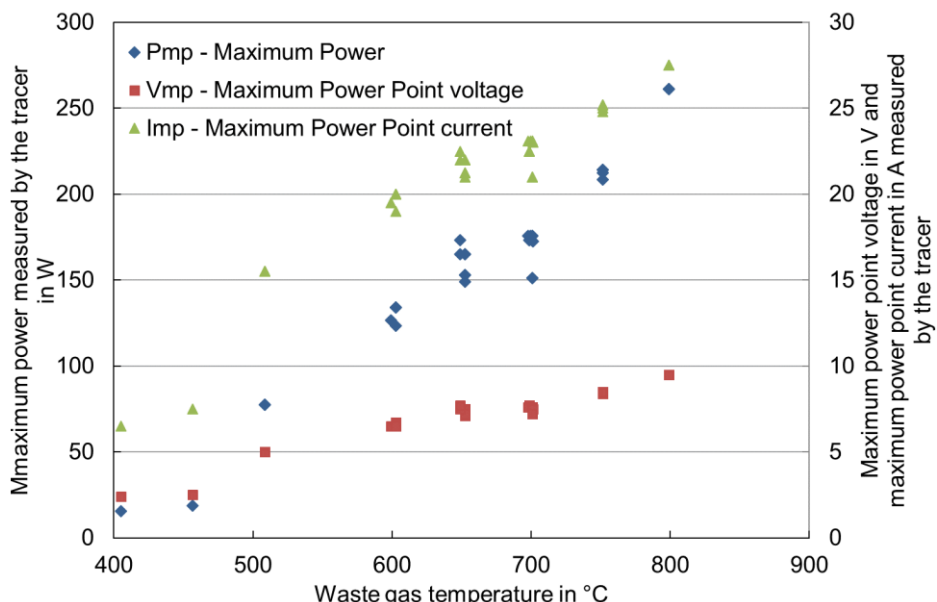


Figure 66: MPP voltage, current and power as a function of waste gas temperature

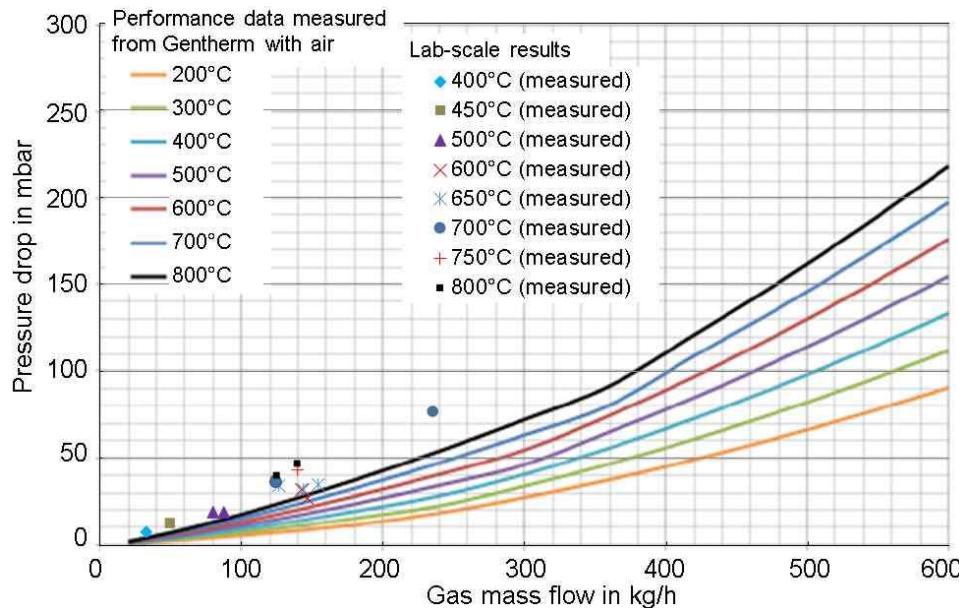


Figure 67: Comparison of data from GNTH with experimental data: pressure drop as a function of waste gas temperature and waste gas flow

Further an already existing Simulink model was verified. The aim of this model is to develop a computer tool to accurately simulate the thermal and electrical dynamics of a real thermoelectric power generating system. The model considers the complex and non-linear interactions of the thermoelectric effects (Seebeck, Peltier), electrical (Joule heating) and heat transfer through the module and heat exchanger materials (1-D Fourier). The way in which the coupling between these parameters is modified during changes in the operating conditions, e.g. temperature or electrical load variations, can also be analysed. The computer model has been experimentally verified and found to predict system performance with good accuracy in both transient and steady-state conditions. Details about the model can be found in the appendix, **Deliverable 4.3**.

Summary of the experimental results was:

- The measured power output is in good agreement with data from GNTH. Maximum measured electrical power was approx. 260 W at a waste gas temperature of 800°C.
- The measured pressure drop was higher than the values determined by GNTH (with air), which must be considered for the fan selection of the demonstrator.
- The I-V Tracer and Power Converter operated well in combination with the cartridge. The average electrical efficiency was approx. 94 %, which is in the range of the efficiency achieved in laboratory tests at GUN.
- The influence of the cooling water flow on the power output was minimal.
- The cartridge should be installed at tkSE in that way that the cooling water supply is located at the top of the cartridge to ensure the cooling of the whole circumference of the cartridge with a minimal cooling water flow.

2.4.4 Task 4.4: Test-bed deconstruction (BFI)

After the experiments the Power Converter and the TE cartridge were removed. The measuring and data logging system were disconnected. The waste gas pipe and the connection of the pipe to the combustion chamber and to the main waste gas pipe of the combustion chamber were deconstructed.

2.5 WP 5: Industrial testing of the demonstrator

Objectives of WP 5 were:

- Construction of a $\sim 800 \text{ W}_{\text{el}}$ demonstrator.
- Long-term testing of the demonstrator at a suitable waste gas source at tkSE site.
- Data analysis and evaluation of the test results.
- Economic and technical evaluation of the TEG system.
- Economic and technical comparison of TEG with other waste heat power generation systems.
- Development of application concepts for other industries.

2.5.1 Task 5.1: Demonstrator Documentation (all)

Objective of this task are manuals with all relevant information that allows a safe operation of the demonstrator.

TE cartridges (GNTH)

A manual for handling of the TE cartridges was generated. It includes:

- Description of the function and the application area together with images and schemes of the cartridges.
- Safety instructions regarding installation and de-installation, operation (cooling, mechanical stress, electrics), flammability, toxicity and disposal.
- Minimum and maximum values for cooling water flow and temperature, and for mechanical stresses are given as well as the electrical resistance of the cartridges. The maximum allowed temperature of the inner tube of the cartridge is 850 °C.

Language of the manual is German, since the staff at tkSE is German. Images of the manual can be found under **Deliverable 5.1** in the appendix.

Power converter and Monitoring system (GUN)

A manual and a technical report of the monitoring system were generated. Contents are:

- Technical report:
 - General description of the monitoring system, Detailed description of the RO3 I-V Tracer, including specifications, connection, operation circuit diagram and thermal performance.
 - Detailed description of the switchable electronic load for battery management, including specifications, connection, operation circuit diagram and thermal performance. Detailed description of the electronic load for TEG protection, including connection and thermal performance.
- Manual:
 - System overview, Liabilities and system support, Supporting hardware requirements (TEG devices, energy storage battery), Mains system overview including data acquisition, power management cabinet, connector panel, gas flow connector, fan contactor, Power input system, Internal measurements, User interface, Administrative access credentials, Mobile connectivity, Local access, Database IDs

Detailed tables of content can be found under **Deliverable 5.1** in the appendix.

Heat pipe heat exchanger (CEM)

Drawings and instructions for the heat pipe heat exchanger were generated by CEM. This includes:

- Detailed technical drawings of the heat pipe heat exchanger, the connection flange, the rectangular pipe in which the heat exchanger has to be placed, and the positioning of heat exchanger in the pipe.
- Item lists of required components of the heat exchanger.
- Further a safety data sheet for the heat pipe fluid potassium was given to BFI and tkSE for correct handling of the heat pipes.

A specific manual for the heat pipe heat exchanger was not necessary, since it has no moving parts or electrical connections. The utilization of the GEN3 cartridge is described in the manual from GNTH regarding the GEN3 and GEN4 cartridges (see above).

Images of the heat pipe heat exchanger documentation are given in **Deliverable 5.1** in the annex.

Commissioning procedure of the demonstrator (BFI, tkSE)

A commissioning procedure for the demonstrator was generated. This includes step by step instructions for starting the components of the demonstrator, necessary valve positions, allowed temperature and flow values as well as activities for inspection. The overall procedure is summarized in the appendix under **Deliverable 5.1**.

2.5.2 Task 5.2: Demonstrator construction (all)

Objective of this task is the overall construction of the demonstrator. This includes the assembly of all designed components (TE cartridges, Power Converter and Monitoring system, heat pipe heat exchanger) as well as the construction of the bypass.

Bypass (tkSE)

The plate which connects the bypass to the waste gas pipe was constructed and finally installed by tkSE during a standstill of the CSP. **Figure 68** shows the finished plate before and after the installation at the inspection chamber of the waste gas heat exchanger of the CSP. The plate consists of two pipe sections: one for the waste gas supply from the CSP waste gas pipe into the bypass and the other to refeed the waste gas from the bypass into the waste gas pipe. Both pipe

sections include a separate valve to close the pipe, so that the later installation of the bypass (see **Deliverable 5.2**) was be done during the normal operation of the CSP.

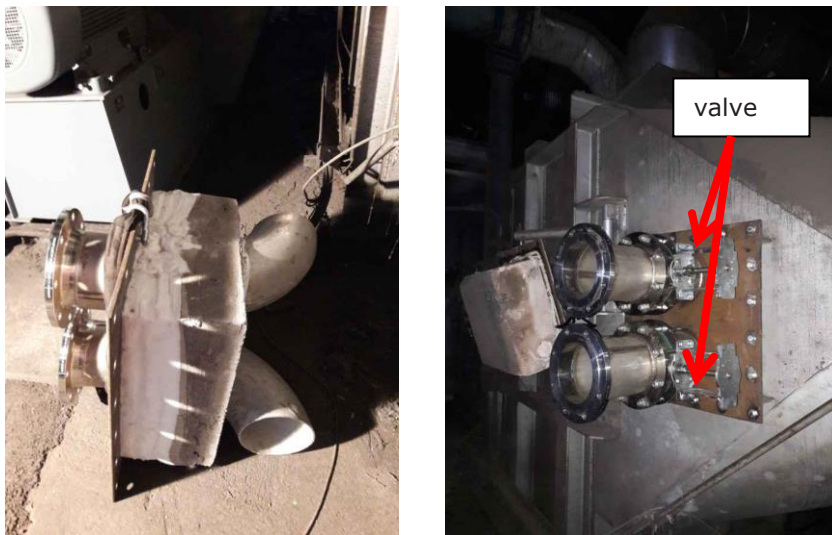


Figure 68: Left: Connection plate for the bypass before installation, right: after installation

TE cartridges (GNTH)

Two GEN4 cartridges and one GEN3 cartridge were finalized. Images of the assembled cartridges are part of **Deliverable 5.2** in the annex. Expected performance data and dimensions of the cartridges are given in Deliverable 2.6.

Power converters and Monitoring system (GUN)

The Monitoring system was designed to provide an autonomous mechanism for obtaining the maximum electrical power from up to 5 TE cartridges up to a 250 W each. The energy generated is stored in a large external 12 V lead acid battery with over charge and discharge management controlled by an internal electronic load. Each TE cartridge input channel is also individually protected from overvoltage. Various temperature, energy and other external sensors are monitored at a configurable time interval, including an I-V trace for each cartridge connected. The information is stored in a database which can be accessed via a web browser.

The system described comprises of a main data acquisition and power management unit (Cabinet), the internal power conversion, data acquisition, system monitoring and supporting hardware and a suite of external sensors as described. The physical dimensions of the cabinet are: size 1,000 x 600 x 450 mm, weight 100 kg. **Figure 69** shows a scheme of the cabinet outside. **Figure 70** gives an overview about the connector panel on the monitoring unit with the location of each connector.

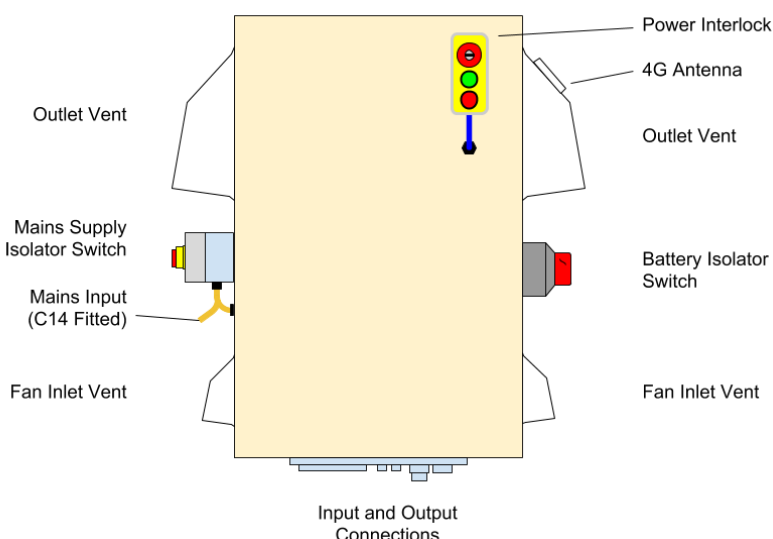


Figure 69: Scheme of the cabinet

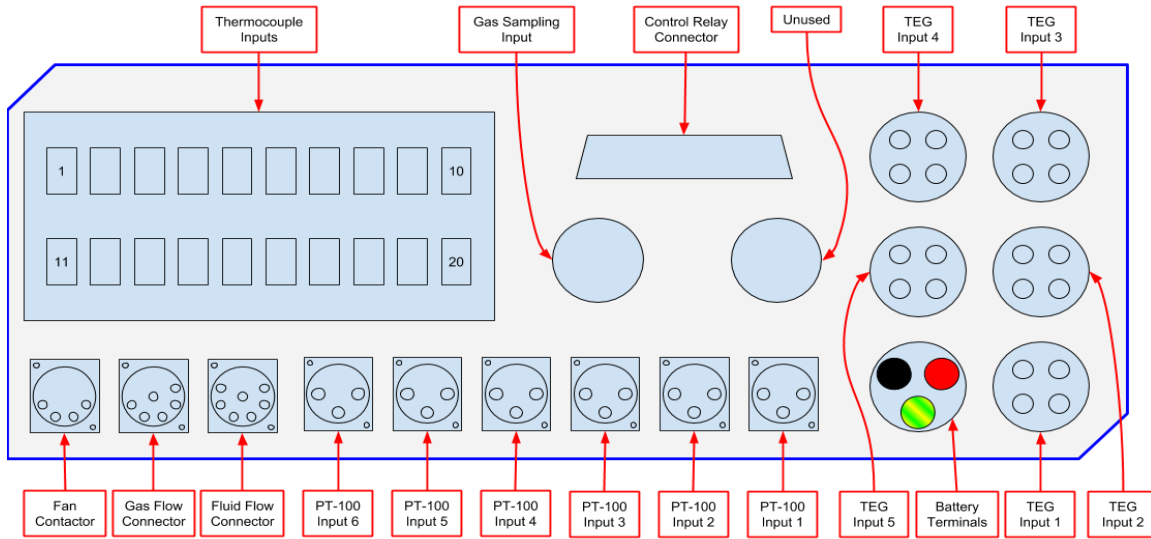


Figure 70: Location of each connector on the connector panel

The power system is designed to precisely monitor the available power from the attached devices in addition to optimally recovering this energy to the attached battery. Each of the TE cartridge inputs are normally connected to their individual MPPT Power Converter. The power is output through the battery isolator switch to the attached battery.

Periodically (every 30 minutes by default), each cartridges controlling relay is operated individually to allow an I-V trace to be obtained. The corresponding relay is closed; Disconnecting the TE cartridges output from the Power converter and connecting the I-V Tracer. A trace is taken and the data obtained is stored, taking up to 5 seconds, before the relay is returned to its original state. This process is repeated for each of the TE cartridges inputs in turn.

Over Voltage Loads are provided to prevent the system presenting an over-voltage from any cartridge to either the I-V Tracer or the MPPT Power converter. These operate autonomously and apply a resistive load to the system. **Figure 71** gives an overview about the described interconnection of the Power converters in the cabinet.

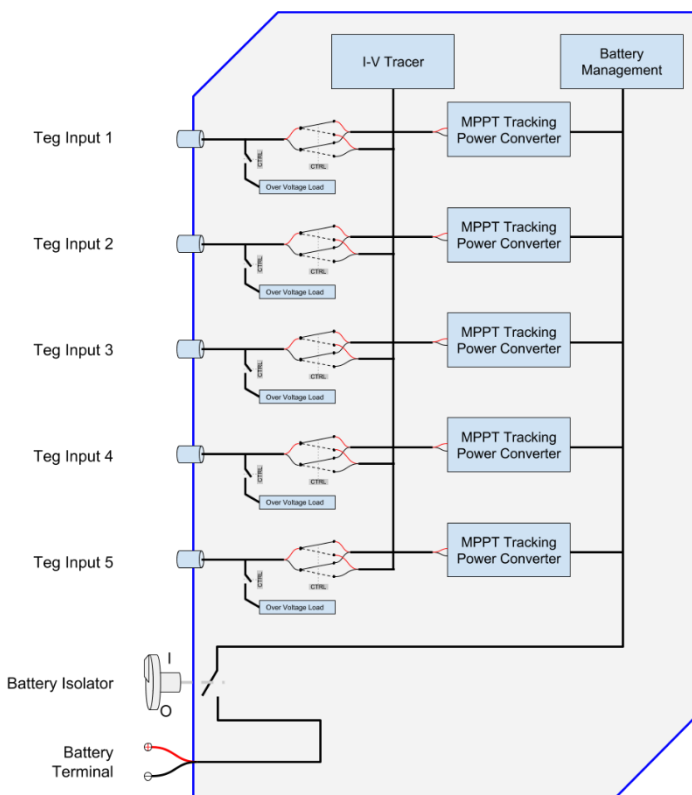


Figure 71: Interconnection of the Power converters in the cabinet

The system uses the built in 4G modem to host the data online. **Figure 72** shows a typical set of data displayed by the monitoring system via the web interface. The most up to date information is

textually displayed alongside graphs showing historical data for various elements of the system. By default, data collected since midnight is displayed, with data filter options displayed at the top of the page. A Download All button allows to save a file containing all data within the currently filtered range. Due to the nature of the 4G connection, loading the site may take several minutes. An error message will be displayed in the event the data is not available.



Time Profile

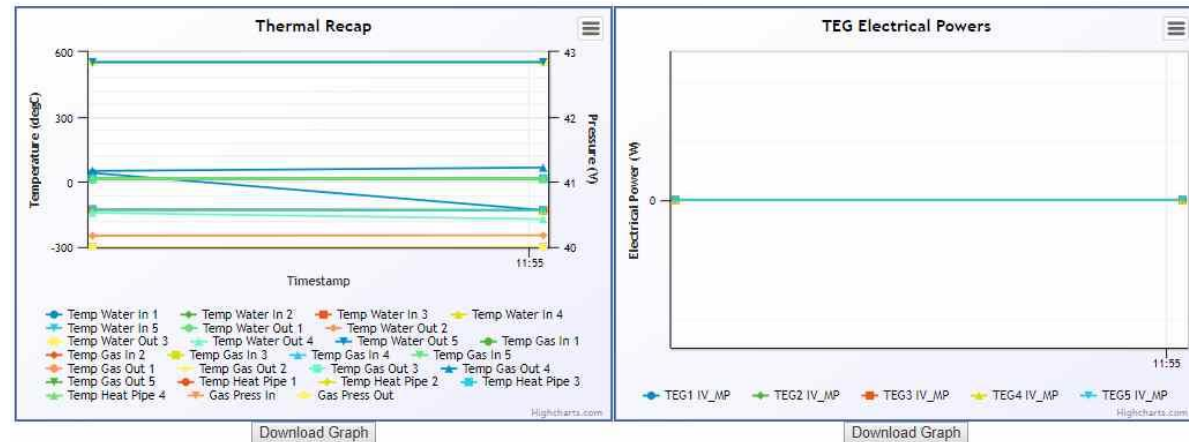


Figure 72: Typical set of data displayed by the Monitoring system

Figure 73 shows some images of the Monitoring system during construction. An image of the finalized Monitoring system including the Power converters is part of **Deliverable 5.2**, see annex.

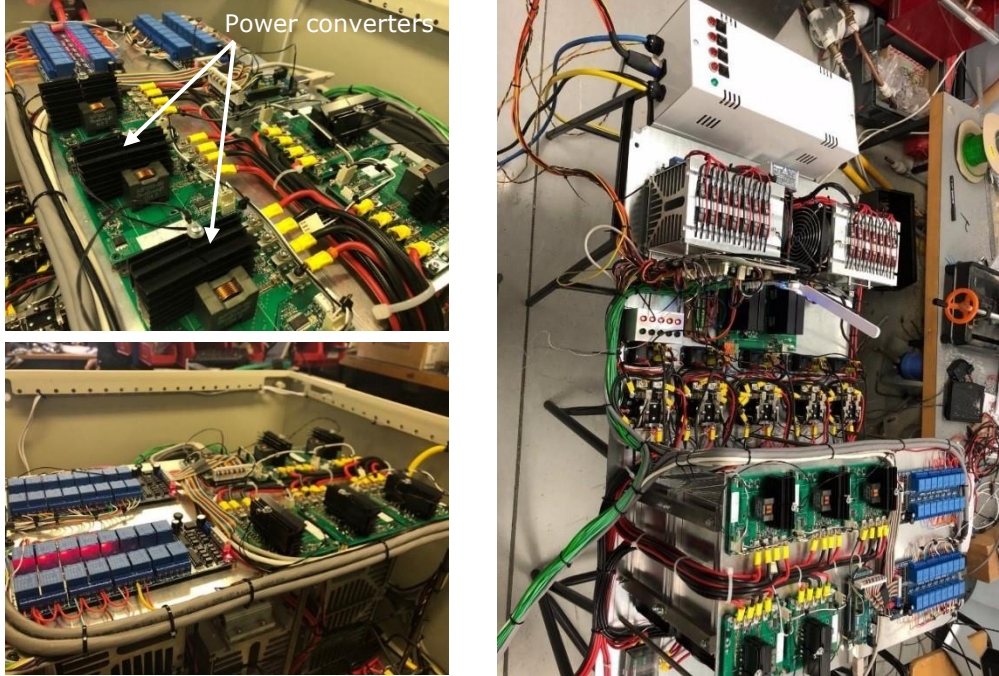


Figure 73: Images of the Monitoring system during construction at GUN

Heat pipe approach (CEM)

The design of the heat pipe heat exchanger was finished in 2017 (see Annual Report 2017). Regarding the simulation results from the design work the heat exchanger was constructed by CEM in early 2018. Main data are summarized in **Table 25**:

Table 25: Main data of the heat pipe heat exchanger

Heat pipes		Heat exchanger	
Number of heat pipes	4	Number of fins	35
Heat pipe fluid	potassium	Fin thickness	2 mm
Material	stainless steel	Gap between fins	4 mm
Heat pipe diameter	12 mm	Heat exchanger dimensions	200 x 200 x 150mm
Heat pipe length	600 mm	Expected pressure drop	1 mbar
		Expected heat transfer at 700 °C	> 4,000 W _{th}
		Necessary waste gas flow	630 kg/h

The heat will be extracted from the waste gas by the heat exchanger, then transported by the heat pipes out of the waste gas pipe. The cold end of the heat pipes is connected to a copper block which transfers the heat to the TE cartridge, which is stuck around the copper block. The heat pipes are bended (see **Figure 74**) so that they match with the copper block, since its diameter (90 mm) and shape differ compared to the heat exchanger.



Figure 74: Bended heat pipes

As it can be observed in **Figure 75**, left, the copper block is longitudinally divided into 4 equal parts (4 cheeses), to allow thermal expansion. Each part contains a heat pipe. Finally, a sheet of graphite (black foil) was placed around the copper block (interface between copper block and the cartridge) to increase the heat transfer from the copper block to the TE cartridge, **Figure 75**, right.

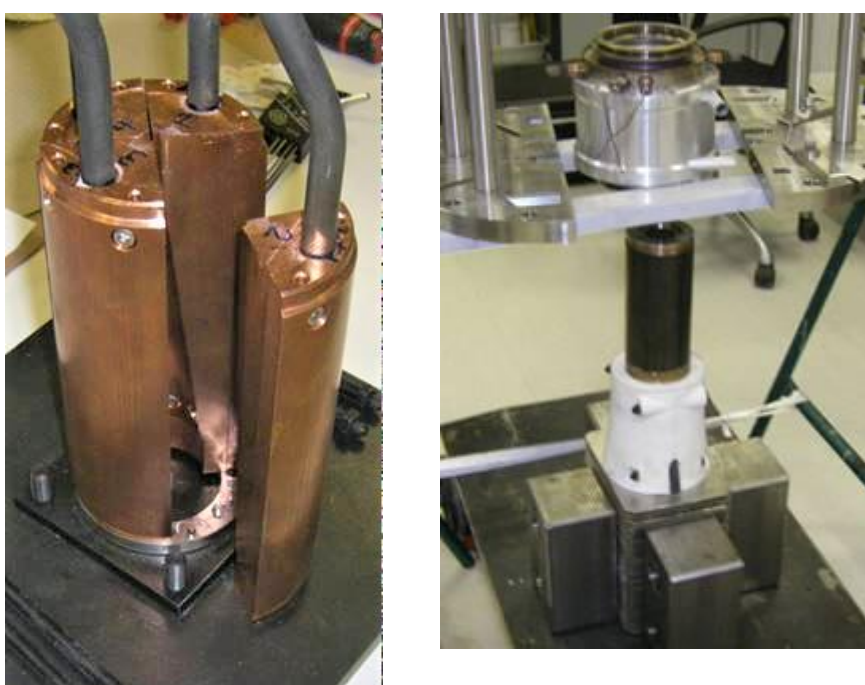


Figure 75: Connection of the heat pipes to the TEG cartridge by a copper block

An image of the finalized heat pipe heat exchanger can be found in **Deliverable 5.2**. in the annex. The drawing of the demonstrator, with piping and measurements, is shown in Figure 8.

Figure 76 shows the completed final demonstrator at tkSE. The construction followed the initial design plan as shown in Figure 4.



Figure 76: Final construction of the demonstrator facility at tkSE

2.5.3 Task 5.3: Installation and commissioning (tkSE, BFI, GNTH)

In accordance with the requirements of safety and operability, a description of the commissioning was prepared. This includes step by step instructions for starting the components of the demonstrator, necessary valve positions, allowed temperature and flow values as well as activities for inspection. The overall procedure is summarized in the appendix under Deliverable 5.1.

The installed measurement technology included sensors for the temperature of flue gas and water, of pressure, flow and a gas analysis. A comprehensive list of the measurements with details regarding type, sensor and range is given in Table 26.

Table 26: List of measurements at PowGETEG test plant

	detector	range
Temperature		
Inlet Gas Flow	thermocouple	0-1000°C
Gas behind TEG 1	thermocouple	0-1000°C
Gas behind TEG 2	thermocouple	0-1000°C
Gas behind TEG 3	thermocouple	0-1000°C
TEG 5 Heat pipe 1	thermocouple	0-1000°C
TEG 5 Heat pipe 2	thermocouple	0-1000°C
TEG 5 Heat pipe 3	thermocouple	0-1000°C
Inlet water	PT 100 / thermocouple	0-100 °C
Outlet TEG 1	PT 100 / thermocouple	0-100 °C
Outlet TEG 2	PT 100 / thermocouple	0-100 °C
Outlet TEG 3	PT 100 / thermocouple	0-100 °C
Electric data		
Current TEG 1	Current output from MPP converter	0- 50 A
Current TEG 2	Current output from MPP converter	0- 50 A
Current TEG 3	Current output from MPP converter	0- 50 A
Flow		
Waterflow TEG1	flowmeter	3-30 l/min
Waterflow TEG2	flowmeter	3-30 l/min
Waterflow TEG3	flowmeter	3-30 l/min
gas flow TEG 1	Prandtl	0-2 mbar
gas flow TEG 2	Prandtl	0-2 mbar

	detector	range
gas flow TEG 3	Prandtl	0-2 mbar
Pressure		
Pipe TEG 1	Pressure sensor	0-50 mbar
Pipe TEG 2	Pressure sensor	0-50 mbar
Pipe TEG 3	Pressure sensor	0-50 mbar
Quality		
CO ₂ Wastegas	Advance Optima Uras 14	0-100 Vol-%
CO Wastegas	Advance Optima Uras 15	0-5000 ppm
O ₂ Wastegas	Advance Optima Uras 16	0-25 Vol-%

In addition, there were temperature measurements for the safety equipment.

2.5.4 Task 5.4: Operational long-term testing (BFI, tkSE)

The demonstrator was fully autonomous operating over a period of several weeks. Figure 77 shows the evaluation of the measured flue gas temperature in front of the TEG for a period of four weeks.



Figure 77: Long-term evaluation of flue-gas temperature

During the trials, the rotational speed of the ventilator was changed, starting from 3000 min^{-1} down to 900 min^{-1} and again set to 3000 min^{-1} . The change of the ventilator speed correlates with the average gas temperature in front of the TEG.

An overview of the generated power at TEG 1 is shown in **Figure 78**.

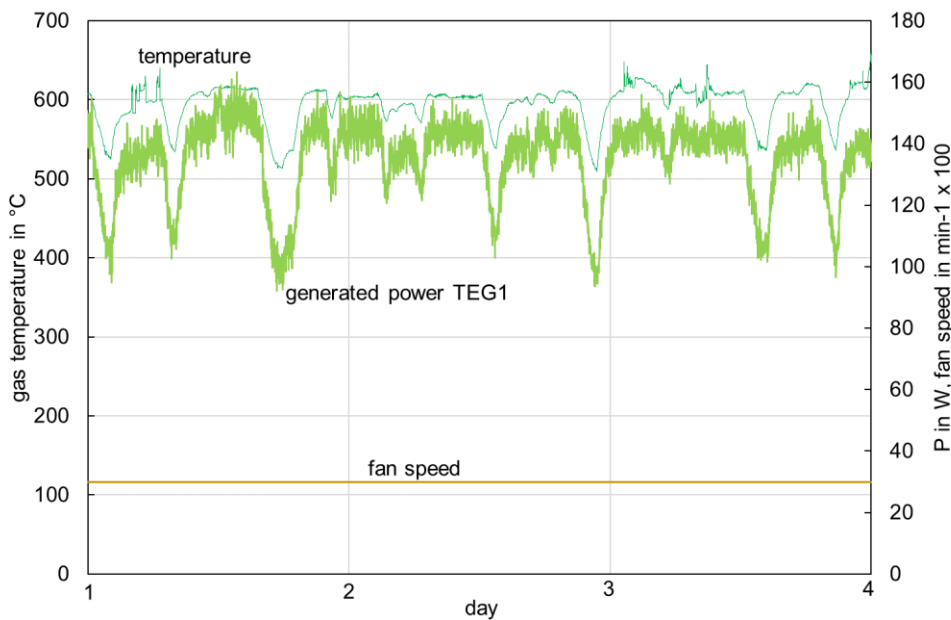


Figure 78: Temperature and Power at TEG 1

In a period of three days with constant mass flow the average gas temperature was around 600°C. Changes in the gas temperature related to changes in the CSP line, the fuel gas was changed between BOF gas and a mixed gas, which resulted in a drop in flue gas temperature. The generated power at maximum flue gas temperature reached more than 140 W. The system is very sensitive to changes in the temperature, a drop of 70 K (from 600 to 530°C, 12%) in the flue gas temperature resulted in a drop of the generated power by 40 W (from 140 to 100, >30%). This shows that TEG systems have to be operated in the optimum temperature range to achieve an reliable power production, see also Figure 34 and Figure 65. Aberrations from the optimum temperature range can result in a significant loss power and thus in a decrease of the economic efficiency of such a system.

Of greater interest was the effect of cascading two identical TEG. Figure 10 shows an example of the measured data.

The cascading TEGs show the expected behaviour, due to the heat loss for the operation of first TEG the second TEG has a much lower power output. Even if the TEG1 generates 140 W, the second TEG only generates below 60 W. A change in the flue gas temperature leads to corresponding effects in both TEG.

A very different and unexpected behaviour was seen in the heat pipe TEG, as **Figure 79** illustrates.

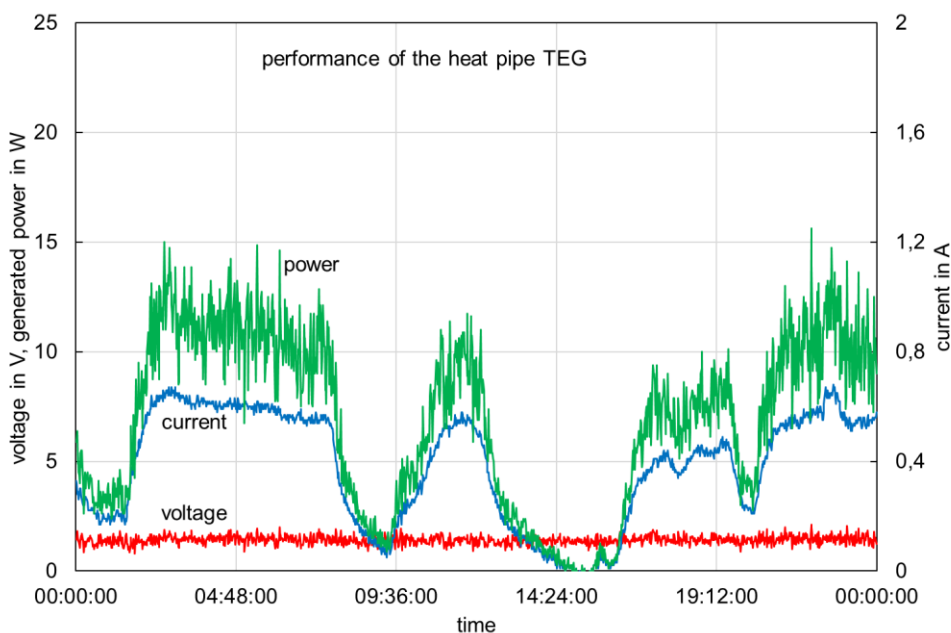


Figure 79: Power generation by the heat pipe TEG

The power generation was very low. Although the validation of the operational circumstances showed, that the level of temperature ($>600^{\circ}\text{C}$) and the mass flow of the flue gas to the heat pipe (575 kg/h) reached nearly the required values, the power output was low. The validation of the measurements showed no problems, a problem with the heat transfer was assumed and the heat pipe TEG was inspected. After the demonstrator test lasting three weeks, additionally the build-up on the heat transfer surfaces was examined. For this purpose the demonstrator was switched off, the heat pipe TEG was disconnected and carefully removed. In **Figure 80** the lifted heat exchanger and a view into the channel are shown.



Figure 80: Left: Lifted heat exchanger with metal chips, Right: View into the channel

Unexpected was the amount of metal chips that could be seen between the single fins of the heat exchanger. A view into the channel showed further metal chips. Obviously, these were not related to deposits from the exhaust gas but consist of the material of the connectors between the fins and heat pipes. In Figure 11 the damaged connectors are shown in detail.

This was surprising because neither the temperature during the tests ($<650^{\circ}\text{C}$) nor the composition of the atmosphere (no corrosive parts) should have damaged the connectors. Although all the fins were still firmly attached to the structure, the current construction is not yet robust enough for industrial use. Until the end of the project, the cause of this wear could not be determined in detail. Everything indicates that there has been some kind of chemical reaction among the materials. This could have several causes, one of which is the creation of a kind of galvanic battery between the copper spile and the stainless-steel fins. Besides, it looks like a type of coating has been generated on the stainless-steel fin's surface. The wear has considerably reduced the physical contact between the copper spile and the heat pipe what resulted in a poor thermal contact and consequently in less heat transport by the heat pipes. All other materials showed no signs of corrosion after the operating time.

The setup proved to be reliable for autonomous operation over several weeks, during steady and unsteady process conditions. The generated power output was lower than expected. The reasons for this are on the one hand the achieved lower temperature level and on the other hand a defect of the heat exchanger in the heat pipe. The overall durability of the demonstrator setup could be proven. Dust load of the gas was not a problem in this application.

2.5.5 Task 5.5: De-installation of the demonstrator (tkSE, BFI)

Due to the long delays in ordering and commissioning and the considerable additional costs involved, it was decided to continue operating the demonstration plant. For this reason, the plant has not yet been dismantled.

2.5.6 Task 5.6: Data analysis (CEM, GUN, BFI, GNTH)

The long-term testing allowed data analysis of measurement data in varying process states. As an example, in Figure 77 the variations of gas temperature and mass flow during a four week period is shown. Figure 81 shows the evaluation of the gas temperatures in the cascading TEG pipe on one day.

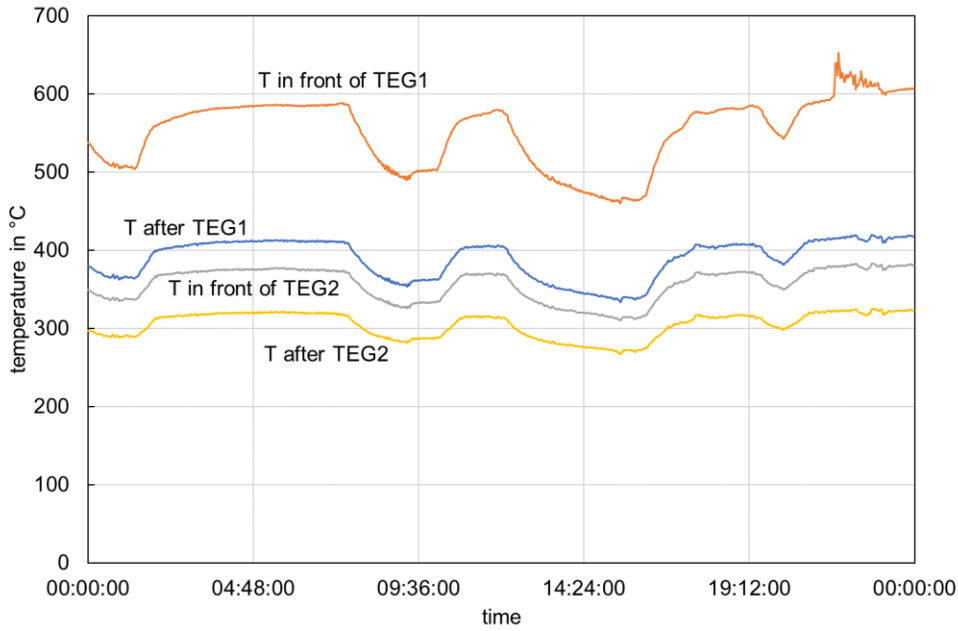


Figure 81: Gas temperatures in the cascading TEG pipe

From top to bottom the temperatures refer to gas before TEG1, after TEG1, before TEG2 and after TEG2. As expected, the temperature of the flue gas drops down due to the heat extraction by the TEG. But, as shown in Figure 10, even at a lower temperature level the TEGs are able to generate power, although due to the temperatures lower 700°C the power generation of test-bed and laboratory trials could not be reached. The GEN4 TEG showed reliability and usage in a wide operating range. The heat pipe TEG could not fulfil the expectations, as shown in **Figure 79** and explained in detail in 2.5.4. Furthermore, due to the problem with the setup of the monitoring system at the CSP-site, optimizations of the TEG-output were not possible during the test period.

2.5.7 Task 5.7: Economic and technical evaluation, including analysis of improvement possibilities (all)

This task was dedicated to the economic evaluation of TE power production using gaseous high temperature waste heat. Different scenarios for assessment of the economic viability of TE power production were considered. The comparison with other heat to power technologies was part of Task 5.8.

The economic viability of power generation systems is significantly influenced by the electricity rate and the production costs of the heat recovery system. Thus, in the following a short description of electricity rates in Europe and production costs of TE systems can be found, on which the economic evaluation is based.

The electricity rate for the industry in Europe is subject to significant fluctuations, since the companies are liable to different amounts of fees and taxes, especially depending on the country they are located, their electricity intensity and consumption as well as the industrial sector. **Figure 82** shows average electricity rates for the industry in European countries in the year 2017. Huge differences of the price can be observed depending on the country and electricity consumption.

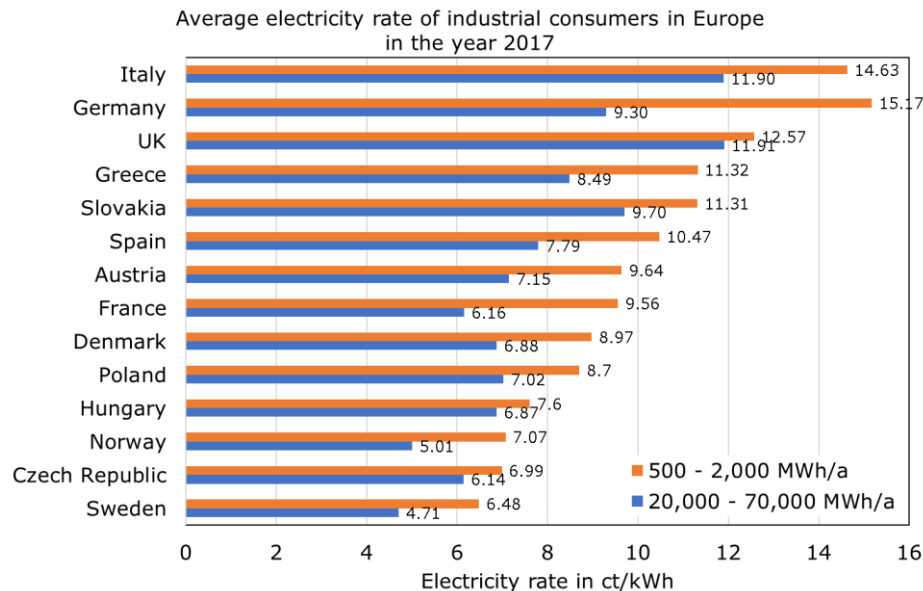


Figure 82: Average electricity rates of the industry in Europe for the year 2017 [1]

Figure 83 breaks down in detail the influence of the amount of consumed electricity on the electricity rate in Germany. Smaller consumers paid approx. 17 ct/kWh in the year 2017 while the rate for large consumers with an electricity consumption up to 150 Mio kWh/a was just approx. 10 ct/kWh. Furthermore, the electricity rate is influenced by the fact that the companies are subject to different amounts of fees and taxes depending on their electricity consumption and the industrial sector. Figure 83 (right) illustrates minimum and maximum electricity rates for companies with an annual electricity consumption of 100 Mio kWh in 2017: the fluctuation margin of the electricity rate was 4 to 16 ct/kWh.

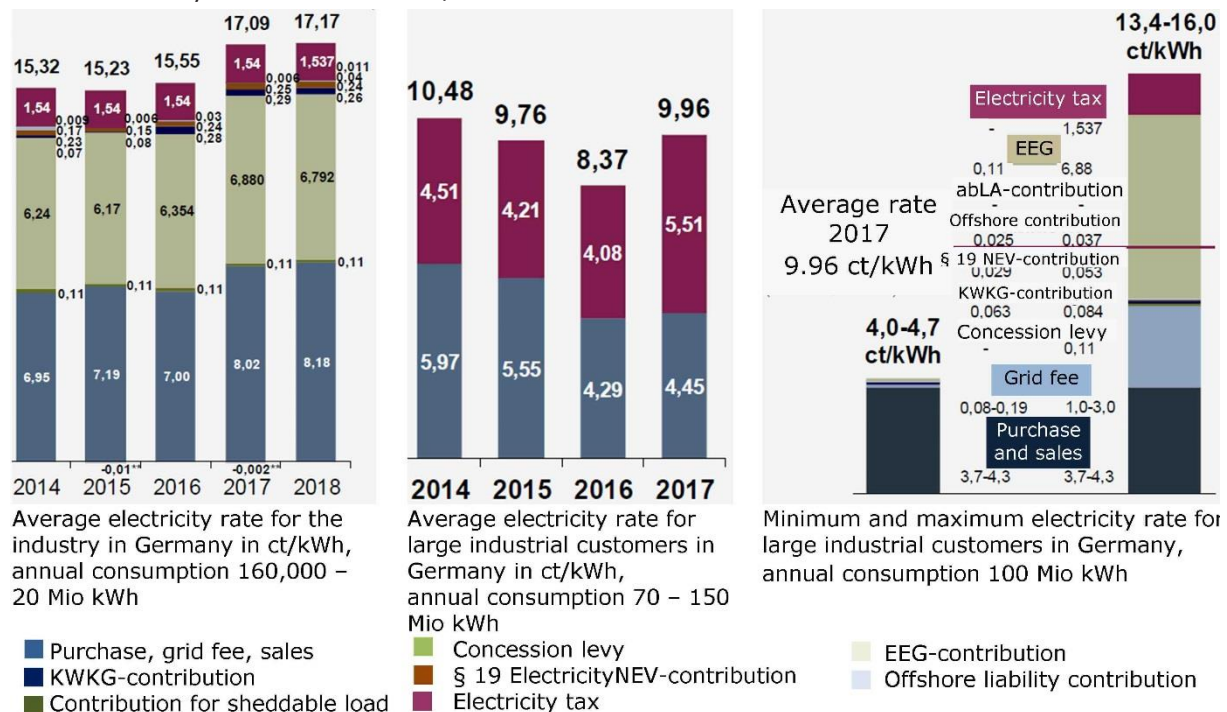


Figure 83: Electricity rates of the industry in Germany [3]

left: annual consumption of 160,000 – 20 Mio kWh

middle: annual consumption of 70 – 150 Mio kWh

right: minimum and maximum electricity rate, annual consumption 100 Mio kWh

Thermoelectric power generation from waste heat in industrial scale is currently under development. Thus, the costs for such systems are currently quite high. Based on the price for common available BiTe-TEG, which is in the range of 3 – 5 €/kW_{el} [4], and that necessary devices like heat exchanger, wiring, DC converter, cooling etc. can double these costs, it can be estimated that the costs of systems for utilisation of low temperature waste heat (up to 300°C) are in the range of 6,000 – 10,000 €/kW_{el}. Since high temperature TEG are less common and just produced in very small quantities the cost for such waste heat recovery systems can be currently estimated with

10,000 €/kW_{el} minimum. Nevertheless, it is expected that the production costs can be significantly reduced by a couple of measures in the near future [5] - [7]:

- Advanced TE materials with higher efficiency and for higher temperatures.
- New concepts for mass production of TE materials, e.g. via induction melting, vibration ball milling, spark and pulse plasma sintering ([8], [9]) gas phase atomization or rapid thermal synthesis methods.
- Economical TEG manufacturing and automated fabrication techniques for mass production of TEG and complete TE systems including necessary devices.
- High performance heat exchangers for convective and radiative heat transfer and high performing connection to the TEG.
- High temperature and corrosion resistant antifouling coatings to extend lifetime of the heat exchangers and to ensure their performance during life time.
- Optimization of TEG structure e.g. by segmentation of different TE materials for the TEG.

Due to these measures it is expected that TE systems can be commercially available at a price ranging from 1,500 - 4,000 €/kW_{el} in the near future [10] - [12].

Based on the above explained boundary conditions the following evaluation of economic viability of TE waste heat recovery was carried out.

Initially a general economic analysis of TE power generation takes place. Three cases were considered:

- a. Annual electricity consumption 160,000 kWh to 20 Mio kWh, average electricity price 17.17 ct/kWh.
- b. Annual electricity consumption 70 to 150 Mio kWh, average electricity price 9.96 ct/kWh.
- c. Annual electricity consumption 100 Mio kWh, average electricity price 4.0 ct/kWh.

For the three cases, the permitted specific investment costs of a plant for waste heat recovery by means of TEG were calculated as a function of the maximum tolerated payback period. In large companies, a payback period of 3 years maximum is usually tolerated, while in smaller companies 5 years are often accepted. Further boundary conditions of the calculation were:

- Plant availability 90 %
- Depreciation period 19 years

The calculations are based on the following equations:

$$\text{Payback period} = \frac{\text{Investment}}{\text{Saved costs} + \frac{\text{Investment}}{\text{depreciation period}}}$$

$$PP = \frac{z \cdot P_{el}}{R \cdot P_{el} \cdot 8.760 \text{ hours/year} \cdot b + \frac{z \cdot P_{el}}{t}}$$

with

PP: tolerated payback period

z: maximum permitted specific investment to meet the tolerated payback period in €/kW

P_{el}: TEG performance in kW

R: electricity rate in €/kWh

b: plant availability (-)

t: depreciation period in years

Figure 84 shows the maximum permitted specific investment costs depending on the maximum tolerated payback period and the electricity rate. It is observed that the permissible investment costs for industrial bulk consumers amount to a maximum of approx. 2.000 €/kW, even at an assumed tolerated payback period of 5 years. As explained above the specific investment costs for industrial applications of TEG can be estimated currently with 6,000 €/kW minimum, even for commercial TEG with a maximum operating temperature of approx. 300°C. With this background it follows that only at relatively high electricity rates of at least 17 ct/kWh the required payback periods can be met.

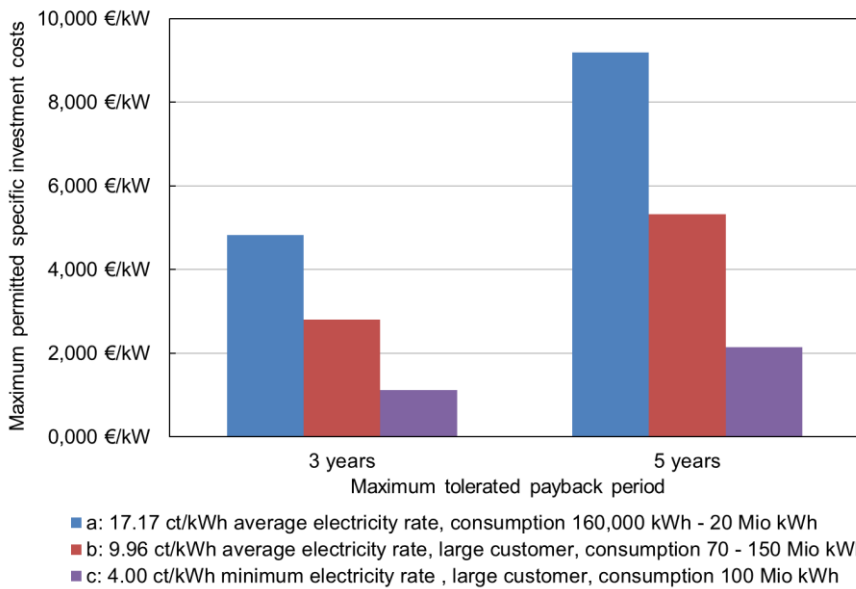


Figure 84: Maximum permitted specific investment costs of a plant for waste heat recovery by means of TEG as a function of the maximum tolerated payback period

Disadvantage of evaluation of feasibility using the payback period is that savings after the payback period are not considered. This is not the case if the net present value (NPV) is used for evaluation, since this method considers the entire lifetime of the plant:

$$NPV = \text{Investment} + \sum_{t=1}^{t=25} \frac{\text{saved costs}}{(1 + \text{rate of interest})^t}$$

If the NPV is positive within the lifetime of the plant, the investment can be considered as economic. If comparing the payback period calculation with the NPV method, it is possible that investments that exceed the maximum tolerable payback period still have an $NPV > 0$ and thus are profitable over their entire lifetime. Investment decisions based on the NPV method are often taken by companies in terms of long-term investment. In the following, three scenarios for a 10 kW_{el} TEG application were calculated with the NPV method, see **Table 27**.

Table 27: Scenarios for NPV calculations

	Scenario 1	Scenario 2	Scenario 3
Electrical power	10 kW	10 kW	10 kW
Plant availability	90 %	90 %	90 %
Electricity rate	4.00 ct/kWh	9.96 ct/kWh	17.17 ct/kWh
Annual increase of electricity rate	0.1 ct/(kWh a)	0.2 ct/(kWh a)	0.3 ct/(kWh a)
Rate of interest	4 %	4 %	4 %
Plant lifetime	20 years	20 years	20 years

The results of the NPV calculations are summarized in **Figure 85**. In all scenarios different investment costs were assumed. According to the above explained costs for TEG, following values were assumed: 3,000 €/kW (possible costs in the future), 6,000 €/kW (estimated minimum costs at this time), and 10,000 €/kW (estimated minimum costs for high temperature applications at this time). The calculations also considering a deviation of the efficiency of the TEG from the design point (e.g. due to poor heat transfer), which is reflected in four categories of efficiency on the abscissa (e.g. 0.75 means that the efficiency of the TEG is just 75 % of the maximum efficiency). It is shown that the NPV in scenario 1 is negative in nearly all cases. A considerable positive NPV can be reached only in the case of 3,000 €/kW investment costs. With increasing electricity rate the NPV is getting more and more positive. Even at the currently high investment costs of 10,000 €/kW a good profitability over the lifetime of the plant can be achieved with increasing electricity rates. However, it can be stated that the investment in TEG applications seems not to be profitable for large-scale electricity consumers which are subject to low electricity rates. For smaller companies with higher electricity rates TEG could be interesting. By reaching the target prize of 1,500 – 4,000 €/kW in the future a considerable profitability of such systems could be reached, so that they could be of interest even for large companies.

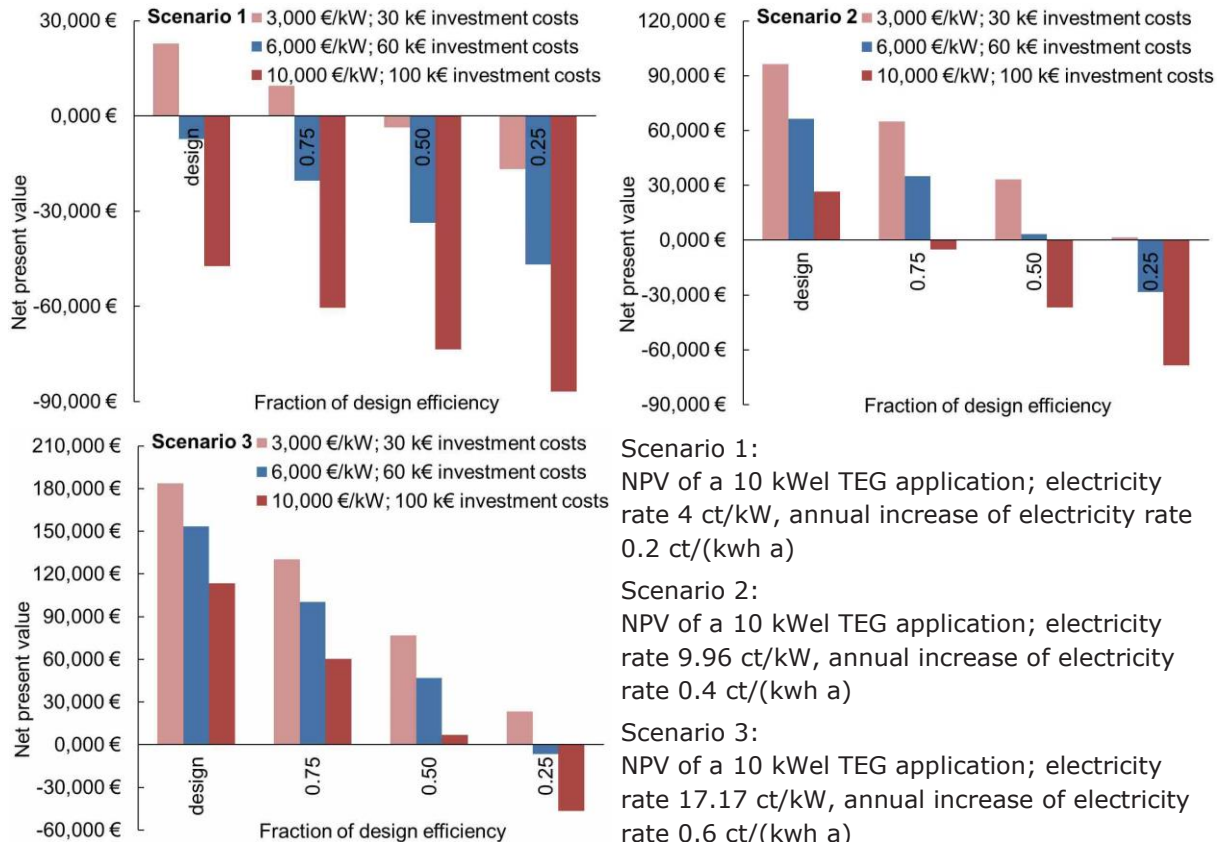


Figure 85: NPV calculations

2.5.8 Task 5.8: Economic and technical comparison with other waste heat power generation systems (BFI, GNTH)

In this task waste heat recovery by means of TEG is compared to other heat to power conversion technologies. **Table 28** summarizes some characteristics of various heat to power conversion techniques: ORC, TEG, steam turbine and steam engine. TEG showing currently the highest specific investment costs. But it should be noted that the additional peripheral costs associated with the other systems may increase the total investment costs significantly. However, this depends on the respective boundary conditions on site and on the size of the plant (the larger the plant, the lower the additional specific investment costs per installed kW through the periphery). Advantages of TEG are certainly on the one hand, the low start-up time and thus the ability to use TEG even in highly discontinuous operation as well as the low maintenance due to the simple peripherals and no moving parts. Furthermore, TEG are built modular and thus can be adapted for a wide range of waste heat sources, e.g. for small applications, and TEG installation is less complex due to a minimum of peripheral devices than for the other techniques. Main disadvantage of TEG is the very low efficiency compared to the other systems.

Table 28: Characteristics of various heat to power conversion systems

	Steam turbine	ORC	TEG	Steam engine
Investment	1,100 – 1,800 €/kW _{el} + peripheral devices	1,500 – 3,000 €/kW _{el} + peripheral devices	1,500 -3,000 €/kW _{el} (target) 6,000 €/kW _{el} (current status) + peripheral devices	1,100 – 1,600 €/kW _{el} + peripheral devices
Necessary peripheral devices	Piping, boiler, desalination plant, water tank, condenser	Piping, heat exchanger	Cooling of the TEG unit, DC converter	Piping, boiler, desalination plant, water tank, condenser
Temperature level	250 – 540 °C	70 – 500°C	150 - 300°C; up to 800°C in development	250 – 540 °C
Efficiency	10 – 42 %	~ 15 %	3 – 6 %	6 – 20 %
Maintenance	Very high	Low	Very low	Medium
Operating behaviour	Continuous operation necessary, start-up time generally > 1 hour	Discontinuous operation possible, start-up time few minutes	Discontinuous operation unproblematic, start-up time several seconds	Discontinuous operation possible, start-up time few minutes

To compare waste heat recovery with the processes listed in Table 28 the payback periods were calculated for two theoretic scenarios: firstly, continuous operation (8,000 operating hours) and, secondly, discontinuous operation (6,500 operating hours, only half of the time at full load). The waste heat flow was supposed with 3 MW. The supposed electricity rate was 10 ct/kWh, which is approx. the average electricity rate of European industry (compare Figure 82). The estimated specific investment costs are inclusive peripheral devices, e.g. cooling and DC converter for the TEG. For TEG two calculations were done: one for the current situation (efficiency 4 %, spec. investment costs just for the TEG 6,000 €/kW_{el}) and one for the target in the future (efficiency 6 %, spec. investment costs just for the TEG 3,000 €/kW_{el}). More boundary conditions and the results of the calculations are shown in **Figure 86**.

Overall, it can be seen that due to the currently high cost of TEG, the payback period of this technology is clearly highest, especially in continuous operating conditions where the other techniques are working well, too. In discontinuous operation, the discrepancy is less, but still present. Taking the target of 3,000 €/kW investment costs for the TEG, which seems to be possible in the future (see also Task 5.7), the use of TEG for waste heat recovery can certainly pay off and could be an alternative to other systems. Under these conditions TE systems may have better chance for producing electric power from

- smaller waste heat sources (lower temperatures or waste heat flows), which are not usable for ORC and SRC,
- discontinuous waste heat or
- waste heat sources, which are not accessible by ORC and SRC, e.g. due to shortage of space.

Furthermore, the comparison shows:

- Which power generation process is most suitable, must be checked for each individual case, a clear general statement cannot be done.
- Following boundary conditions have an impact on the economic viability:

Temperature level of the waste heat, waste heat flow steady/unsteady, capacity of the waste heat, waste gas composition and dust content, on-site boundary conditions (space, accessibility, rebuilding's, ...), qualification of the staff, expected payback period of the company.

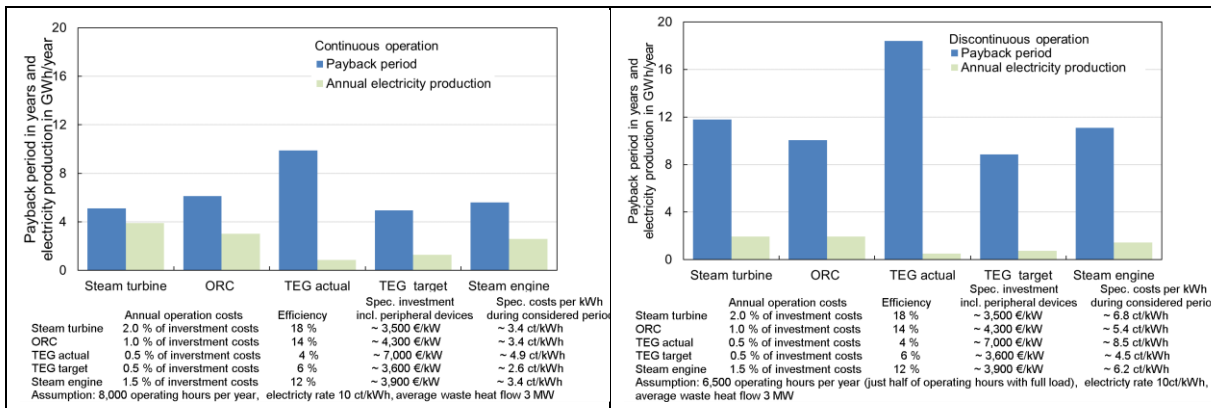


Figure 86: Estimation of payback periods for different waste heat to power generation systems; continuous operation and discontinuous operation

2.5.9 Task 5.9 Development of application concepts for other industries (BFI)

The task was devoted to find concepts for TEG application in other industrial areas.

The results of the project offer a wide perspective for TEG to be used in other sectors and applications. Recovery of waste heat from low or high temperature gas flows is common in many industries. That is why the proposed solution could be in general transferable to other sectors e.g. glass and ceramic industry, cement and non-iron metal industry or smaller companies in the heat treatment sector.

Since waste heat recovery techniques are normally located at the end of process chains a negative impact of them on product quality or single process steps can be excluded. The adaption of the proposed and investigated TE system is nearly independent from the process or industrial area. Essential for its application are the boundary conditions of the gaseous waste heat like temperature, dust load, corrosive or abrasive components, enough space for TEG installation and the availability of the waste heat source.

The direct installation of the TE cartridges requires suitable sizes of the waste gas pipes. This restricts the direct utilization of the cartridges in industrial scale, since gaseous waste heat flows of industrial plants are often in the range of several hundreds of kW up to several MW. Thus, the waste gas pipe diameter is probably bigger than the cartridge diameter in most cases. Direct installation of the cartridges seems only in small applications possible e.g. in the heat treatment industry where smaller plants are common e.g. in hardening shops.

The solution with the bypass system, as investigated in this project, seems not to be feasible since it significantly increases the costs of the recovery system. This solution was preferred in this project, since it offered the possibility to investigate the system under different conditions, but it is not an option for an economic long-term application of this technology.

The heat pipe approach makes an installation of the TE system independent from the waste gas pipe diameter contrary to the direct installation of the cartridges in waste gas pipes. Thus, this approach can be used for a wide range of applications from smaller up to very large waste heat flows independent from process and industry. Crucial in that case will be the waste gas temperature because the kind of TEG and heat pipes has to be adapted to the waste heat temperature. Currently TEG for temperatures up to 300°C are common. Since TEG for temperatures up to 800°C will be available in the near future, a wide range of low and high temperature waste heat sources could be used by this approach. Limiting could be the heat pipe technology, since mainly water filled heat pipes for temperatures up to 300°C are commonly available. High temperature heat pipes are less available and highly expensive.

Furthermore, it is possible to use radiative waste heat, e.g. from slabs or hot strips, with TE systems. But this would mean to significantly change the cartridge concept with the inner hot side heat exchanger. Flat approaches seem to be the best solution to use radiative waste heat. This field of TE application is already under investigation e.g. in [13] - [15].

2.6 WP 6: Coordination and Dissemination

Objectives of WP 6 were:

- Overall project management (coordination and control of project progress).
- WP integration.
- Dissemination of results and reporting.

2.6.1 Task 6.1: Project management (all)

A face to face project meeting with all partners present was held in each semester. Regular telephone conferences of all partners and continuous information exchange via telephone and email were established. The minutes of meetings and telephone conferences were distributed to all partners by the BFI.

The reporting was coordinated by the BFI. Three Annual reports (2015, 2017, 2018) and a Mid-term report were created by the partners.

Due to the high cost of the bypass (WP 2 and 5) tkSE had to place the order of the bypass construction by a tendering process. Despite the long duration of the tendering process (5 months) no company made an offer until September 2018. Result was, that there was not enough time left for the demonstrator construction and test until the end of the project, which was foreseen for 31st of December 2018. Thus, in August 2018 an extension of the project duration to 30th June 2019 was requested by the partners and approved by the Commission on October 25th, 2018. With the extension of the project duration the Technical Annex was adapted.

2.6.2 Task 6.2: Dissemination (all)

A website of the project was created by the BFI (<http://www.bfi-blogs.de/powgeteg/>). The website (**Deliverable 6**, see appendix) includes a project abstract, objectives, the research approach of the project and recent results.

First results of the project were presented by GUN at the 15th European Conference on Thermoelectrics (ECT'17) on 26th September 2017 in Pardova, Italy. Focus of the presentation "MPPT Electronic System for Power Generation from Hot Waste Gases Using a 250 W TEG" was on the results of the experiments at the test-bed.

The entire project was presented by BFI at the Cleantech 4 on 28th/29th December 2018 in Bergamo, Italy and at the 4th ESTAD 2019 on 24th to 28th June 2019 in Düsseldorf, Germany. The presentations "POWER GENERATION FROM HIGH TEMPERATURE WASTE HEAT USING THERMOELECTRIC GENERATORS" (Cleantech) and "Recovery of High Temperature Waste Gas Heat by Thermoelectric Generators" (ESTAD) were about the done work in the project and the current results. Further papers about the project were published in the proceedings of the conferences.

3. Conclusions

A TEG system was developed for the use of high temperature waste gas heat. During the development of the system new solutions for control (Monitoring system), power conversion (Power converter and MPPT algorithm), heat exchange (heat pipe heat exchanger) and TEG protection (antifouling coating and overheating protection by PCM) were designed and investigated. A small-scale demonstrator was investigated in the lab. Test data showed an electrical output of 175 – 260 W at a waste heat temperature of 700 – 800 °C. The newly developed Power converter and MPPT algorithm operated well in combination with the TEG. Based on the small scale tests the entire demonstrator design was adjusted, finished and the demonstrator was constructed.

Operational long-term testing of the whole system at the CSP at tkSE showed:

The bypass design and demonstrator setup proved to be reliable and safe for autonomous operation over weeks. The GEN4 cascading TEG worked as expected, due to the lower flue gas temperature the electrical output was lower than during the lab trials. The heat pipe TEG could not fulfill the expectations, especially the connection between heat pipes and heat exchanger fins is not yet ready for industrial use.

The economic evaluation showed that TEG applications seem not to be profitable for large-scale electricity consumers which are subject to low electricity rates. The expected payback periods cannot be fulfilled (lower than 3 years) at the currently high TEG costs (6,000 – 10,000 €/kW). For smaller companies with higher electricity rates and tolerating higher payback periods (up to 5 years) TEG could be of interest. An NPV calculation (which considers the whole lifetime of the TEG) showed that even at the currently high investment costs of 10,000 €/kW a good profitability over the lifetime of the plant can be achieved with increasing electricity rates.

Compared to other techniques (like ORC and SRC) the payback period of TE technology is currently clearly the highest. In the future the production costs of TEG have to be significantly reduced to the target price of 2,000 €/kW by a couple of measures e.g.:

- Advanced TE materials.
- New concepts for mass production of TE materials as well as economical TEG manufacturing.
- Automated fabrication techniques for mass production of complete TE systems.

Under these conditions TE systems currently may have better chance for producing electric power from smaller waste heat sources (lower temperatures or waste heat flows), which are not usable for ORC and SRC and for smaller applications like power supply of sensors at movable plants/processes.

Overall the project showed, that TEG are sufficient to generate electricity from waste heat. However, at current high costs for TEG, it is not profitable to use TEG for large electricity production at the moment. The approach with directly installed TEG cartridges in the waste gas stream was running unattended in an industrial environment over a longer period and reached the expected power output at the achieved waste gas temperature. Further it was shown that TEG systems have to be operated in the optimum temperature range to achieve a reliable power production. Aberrations from the optimum temperature range can result in a significant loss of power and thus in a decrease of the economic efficiency of such a system. The disadvantage of this approach is that it is not adaptable to a wide range of waste gas sources, since the TEG cartridges cannot be changed in their diameter without great efforts and thus costs. On the other hand, the heat pipe approach, which is adaptable to a wide range of waste sources, since the TEG cartridge is placed outside of the waste gas pipe, was not working due to bad contact between the heat pipes and the fins. A solution has to be found for this problem in the future. Further the cost intensive development of the demonstrator and its components shows that the development of techniques for the mass production of complete TE systems is crucial in the future to reach an economic efficiency of TE power production.

List of figures

Figure 1:	Scheme of N and P type arrays (left), scheme of a TEG consisting of several N and P type arrays (middle) and image of a common Bi ₂ Te ₃ TE module (right)	7
Figure 2:	CSP, exhaust gas system (good accessibility and enough amount of space for demonstrator installation)	8
Figure 3:	Scheme of the proposed cartridge design	8
Figure 4:	Scheme of the final bypass design.....	9
Figure 5:	Scheme of the alternative approach based on a heat pipe heat exchanger	10
Figure 6:	Comparison of data from Gentherm with experimental data: power as a function of waste gas temperature and waste gas flow.....	11
Figure 7:	Finished components of the demonstrator	12
Figure 8:	Drawing of the test facility with extensive measurements.....	13
Figure 9:	Top-view of the industrial testing	13
Figure 10:	Power generation of cascading TEG	14
Figure 11:	Damaged connectors between fins and heat pipe	14
Figure 12:	Scheme of a HDGL [2].....	18
Figure 13:	Scheme of a HRM [2]	18
Figure 14:	Scheme of the CSP at tkSE.....	19
Figure 15:	HDGL 1, recuperator for combustion air preheating (good accessibility and enough amount of space for demonstrator installation)	20
Figure 16:	HDGL 2, recuperator for combustion air preheating (bad accessibility and not enough amount of space for demonstrator installation)	20
Figure 17:	Scheme of the waste gas system of one zone of the CSP	21
Figure 18:	CSP, waste gas temperatures of all 3 zones of the furnace (data from the control system, measuring position No. 3, see Figure 17).....	21
Figure 19:	Installed pressure, temperature and waste gas flow measurement in a stack of the CSP	22
Figure 20:	CSP, waste gas temperatures and pressures of all 3 zones of the furnace	22
Figure 21:	Picture of the exhaust gas sample extraction at a stack of the CSP.....	23
Figure 22:	24 h standard analysis of BOF gas used in the CSP from December 17 th , 2015	23
Figure 23:	CSP, evaluation of the waste gas measurement from December 17 th , 2015	24
Figure 24:	Waste gas pipe of the CSP, connection of the bypass pipe for the demonstrator test	27
Figure 25:	Schemes of bypass options: ladder design 1 (top left), ladder design 2 (top right), revolver design (bottom).....	28
Figure 26:	Example of calculated waste gas streamlines (revolver design)	28
Figure 27:	Scheme of proposed solution for indirect heat-transfer to the TE cartridge via heat pipes	29
Figure 28:	Scheme of the location of necessary measuring points for the tests.....	30
Figure 29:	Flange system for the connection of the cartridge with the bypass pipe.....	31
Figure 30:	Hot gas system.....	31
Figure 31:	Scheme of the air flow in the hot gas system.....	32
Figure 32:	Scheme of the TEG arrangement in the test configuration	33
Figure 33:	Scheme of the overall test configuration	34
Figure 34:	Experimental results from the hot gas system	34
Figure 35:	Comparison of MPPT algorithms: Temperature difference (left) and power output (right).....	35
Figure 36:	Performance of boost converter under test: Electrical Efficiency	35
Figure 37:	Testing results of a GEN4 cartridge at different air temperatures, left: electric output in dependency of the hot air mass flow; right: pressure drop of the air flow through cartridge heat exchanger in dependency of the hot air mass flow	38
Figure 38:	Flow diagram of the safety concept	40
Figure 39:	Axial thermoelectric generator approach and constraints.....	40
Figure 40:	Example of CFD results	41
Figure 41:	Rectangular fins design. The heat pipes will be placed in perforations through the fins.....	42

Figure 42:	Configurations for the heat pipes. Top view of the geometry. Green arrows show gases flow direction. Left) Diamond Centre; Middle) Alternate parallel rows; Right) Triangle.....	42
Figure 43:	Optimal experiment with rectangular heat sink configuration	42
Figure 44:	Left: Contour plot of fins temperature in Kelvin degrees. Only two heat pipes are shown because YZ symmetry has been applied. Right: Thermal contour plot in a cross section of the TEG module with the four heat pipes assembled.....	43
Figure 45:	Heating curve obtained in the DSC/TGA (Thermogravimetric analysis) test.....	45
Figure 46:	Cooling curve obtained in the DSC/TGA test	45
Figure 47:	Second heating curve obtained in the DSC/TGA test	45
Figure 48:	Curves obtained and energy absorption time at several maximum temperatures..	46
Figure 49:	Behaviour of the PCM (50g of Li ₂ CO ₃) in the thermal cycles.....	46
Figure 50:	Isometric view of the physical model with gas inlet (blue), outlet (red) and heat exchanger fins with heat pipes (dark grey)	48
Figure 51:	Sample particle tracks for variant II case 3 colored by particle velocity	49
Figure 52:	Accretion of particles on the heat exchanger versus gas velocity	49
Figure 53:	Isometric view of the accretion rate at the heat exchanger fins for the cases I/3 (top left), II/3 (top right), III/3 (bottom left) and IV/3 (bottom right).....	50
Figure 54:	Top view of the accretion rate at the heat exchanger fins for the cases I/3 (top left), II/3 (top right), III/3 (bottom left) and IV/3 (bottom right)	50
Figure 55:	Main heat transfer mechanisms inside the fins	51
Figure 56:	Picture of the influence of different coatings on the contact angle.....	53
Figure 57:	Silixan T330 additivated samples	55
Figure 58:	X-clean EC2048 additivated samples	55
Figure 59:	Silixan S400 and Thermobarp 800 before and after heating treatment test	55
Figure 60:	Additivated Thermobarp 800 samples before and after heating treatment test	56
Figure 61:	Industrial validation. Location of coated samples in the industrial pipes	56
Figure 62:	Coating after several weeks of demonstrator operation	58
Figure 63:	Construction of the test-bed at the BFI testing facility.....	60
Figure 64:	I-V Tracer test setup	61
Figure 65:	Voltage and power as a function of current at different waste gas temperatures and waste gas flows.....	64
Figure 66:	MPP voltage, current and power as a function of waste gas temperature	64
Figure 67:	Comparison of data from GNTH with experimental data: pressure drop as a function of waste gas temperature and waste gas flow	65
Figure 68:	Left: Connection plate for the bypass before installation, right: after installation ..	67
Figure 69:	Scheme of the cabinet	67
Figure 70:	Location of each connector on the connector panel.....	68
Figure 71:	Interconnection of the Power converters in the cabinet	68
Figure 72:	Typical set of data displayed by the Monitoring system	69
Figure 73:	Images of the Monitoring system during construction at GUN	69
Figure 74:	Bended heat pipes.....	70
Figure 75:	Connection of the heat pipes to the TEG cartridge by a copper block	70
Figure 76:	Final construction of the demonstrator facility at tkSE.....	71
Figure 77:	Long-term evaluation of flue-gas temperature	72
Figure 78:	Temperature and Power at TEG 1.....	73
Figure 79:	Power generation by the heat pipe TEG.....	73
Figure 80:	Left: Lifted heat exchanger with metal chips, Right: View into the channel	74
Figure 81:	Gas temperatures in the cascading TEG pipe	75
Figure 82:	Average electricity rates of the industry in Europe for the year 2017 [1]	76
Figure 83:	Electricity rates of the industry in Germany [3] left: annual consumption of 160,000 – 20 Mio kWh middle: annual consumption of 70 – 150 Mio kWh right: minimum and maximum electricity rate, annual consumption 100 Mio kWh	76
Figure 84:	Maximum permitted specific investment costs of a plant for waste heat recovery by means of TEG as a function of the maximum tolerated payback period.....	78
Figure 85:	NPV calculations.....	79

Figure 86:	Estimation of payback periods for different waste heat to power generation systems; continuous operation and discontinuous operation	81
Figure A.1:	Power converter	100
Figure A.2:	Assembled bench scale unit	101
Figure A.3:	Connection plate between bypass and CSP waste gas pipe	106
Figure A.4:	Studied heat exchanger design	107
Figure A.5:	Accretion rate on the horizontal surfaces of the heat exchanger vs gas velocity..	109
Figure A.6:	Accretion rate on the heat pipes of the heat exchanger vs gas velocity.....	109
Figure A.7:	Accretion rate on the front faces of the fins vs gas velocity	109
Figure A.8:	Accretion rate on the total surface of the heat exchanger vs gas velocity.....	110
Figure A.9:	Convective heat transfer losses over time for selected scenarios	110
Figure A.10:	Scheme of the test bed	113
Figure A.11:	Experimental set-up of the bench scale unit test at the BFI testing facility	113
Figure A.12:	Physical system of the model for TE power production	116
Figure A.13:	Architecture of the combined MATLAB / Simulink model	117
Figure A.14:	Documentation of the heat pipe heat exchanger (CEM)	120
Figure A.15:	Assembly of the heat pipe heat exchanger with the bypass pipe (CEM)	121
Figure A.16:	Assembled demonstrator components	122
Figure A.17:	Top view of the industrial testing	122
Figure A.18:	Maximum permitted specific investment costs of a plant for waste heat recovery by means of TEG as a function of the maximum tolerated payback period.....	126
Figure A.19:	NPV calculations	127
Figure A.20:	Screenshot of the PowGETEG website	127

List of tables

Table 1:	Waste gas composition at the CSP from BOF gas combustion	23
Table 2:	Results of the measurement of additional components in the waste gas	24
Table 3:	Main objectives of planned tests	25
Table 4:	Summary of increased system performance from new MPPT algorithm	35
Table 5:	Expected performance of GEN3 and GEN 4 cartridges	38
Table 6:	Data of the TE cartridges	38
Table 7:	Values rank of each independent variable.....	41
Table 8:	Heat exchanger characteristics	43
Table 9:	Melting points of different possible salts as PCM	44
Table 10:	Comparison of different properties of Li_2CO_3 and $\text{Na}_2\text{CO}_3\text{-K}_2\text{CO}_3$	44
Table 11:	Specification of the dust particles	47
Table 12:	Gas composition	48
Table 13:	Boundary conditions for particle simulations	48
Table 14:	Total accretion of particles on the heat exchanger surface.....	49
Table 15:	Heat transfer characteristics of the heat exchanger fins	51
Table 16:	Selected coatings and their characteristics	53
Table 17:	Additives characteristics.....	54
Table 18:	Substrates heating resistance	54
Table 19:	Validation test results of additized Silixan T330.....	57
Table 20:	Deposition evaluation of the coating test at tkSE.....	57
Table 21:	Calculation of waste gas compositions	59
Table 22:	Average waste gas data during the experiments and at the CSP	61
Table 23:	Average waste gas data during the experiments	62
Table 24:	Steady state periods (greyed out and bold values were changed in comparison to the previous period, see Task 4.2).....	63
Table 25:	Main data of the heat pipe heat exchanger	70
Table 26:	List of measurements at PowGETEG test plant	71
Table 27:	Scenarios for NPV calculations	78
Table 28:	Characteristics of various heat to power conversion systems	80

Table A.1	Necessary data to specify the boundary conditions of the TE system	93
Table A.2	Available and necessary process data of possible waste heat sources	93
Table A.3	Scheme and results of the pre-selection of a suitable waste heat source at tkSE site (Deliverable 1.3, part 1).....	95
Table A.4	Measured components of waste gas dust (Deliverable 1.3, part 2)	96
Table A.5	Results of data evaluation of the CSP as the most promising plant for the demonstrator tests (Deliverable 1.3, part 3)	96
Table A.6	Equipment requirements for the bench-scale unit and the demonstrator (Deliverable 2.1, part 1).....	97
Table A.7	Boundary conditions and limits for the TE application (Deliverable 2.1, part 2)	98
Table A.8	Design concepts of the demonstrator.....	99
Table A.9	Demonstrator design adaptions based on test bed experiments	101
Table A.10	Demonstrator design document	102
Table A.11	Specifications for PCM material selection	106
Table A.12	Gas composition and thermal properties	107
Table A.13	Measured dust composition	107
Table A.14	Elaborated cases for the parametric study	108
Table A.15	Deposition rate of dust particles for the simulated cases	108
Table A.16	Coefficients for the prediction of heat transfer losses for selected scenarios.....	111
Table A.17	Example of a recorded data set during the test bed experiments with the bench scale cartridge	115
Table A.18	Manual for handling of the TEG cartridges (GNTH).....	117
Table A.19	Tables of content of the technical report and manual for the Monitoring system .	119
Table A.20	Commissioning procedure of the demonstrator (BFI, tkSE); Scheme of the bypass design, see Deliverable 2.2	121
Table A.21	Example of a recorded data set during the industrial trial	123
Table A.22	Characteristics of various heat to power conversion systems	124
Table A.23	Scenarios for NPV calculations	126
Table A.24	Publications	128

List of Symbols, Indices, Acronyms and Abbreviations

Abbreviations

AMP	Kind of connector
BF	Blast Furnace
BFI	VDEh-Betriebsforschungsinstitut GmbH
BOF	Blast Oxygen Furnace
CEM	NAITEC. Centro tecnológico en automoción y mecatrónica
CFD	Computational Fluid Dynamics
CO	Coke oven
CSP	Compact Strip Production
D	Deliverable
DAQ	Data acquisition and control
DC	Direct current
DoE	Design of Experiment
DSC	Differential Scanning Calorimetry
EEG	Erneuerbare-Energien-Gesetz (engl.: Renewable Energy Law)
FEM	Finite Element Method
FOC	Fractional open circuit voltage
GEN3, GEN4	Kind of TE cartridges
GNTH	Gentherm GmbH
GUN	University of Glasgow
HDGL	Hot Dip Galvanizing Line
HEX	Heat exchanger
HRM	Hot Rolling Mill
I/O	Input / Output
IP65	Protection class of electrical equipment
KWKG	Kraft-Wärme-Kopplungsgesetz (engl.: Combined Heat and Power Law)
MPPT	Maximum Power Point Tracking
MS	Milestone
NEV	Netzentgeltverordnung (engl.: Grid Fee Edict)
NOF	Non-Oxidizing Furnace
ORC	Organic Rankine Cycle
PCM	Phase Change Material
PHP	Hypertext Preprocessor
P & O	Perturb & Observe
PV	Photovoltaic
PWM	Pulse Width Modulation
RTF	Radiant Tube Furnace
SKW	Heavy hydrocarbons
SRC	Steam Rankine Cycle
SSV	Safety relief valve
TE	Thermoelectric
TEG	Thermoelectric Generator
TGA	Thermogravimetric analysis
TIHS	Temperature measurement with display and control function based on the maximum allowed temperature
tkSE	thyssenkrupp Steel Europe AG
WP	Work Package
XLR	Kind of connector

Indices

CW	Cooling water
e, el	Electrical
OC	Open circuit
th	Thermal
WG	Waste gas

Symbols

b	plant availability	-
F	Volume flow	m^3/h
I	Current	A
NPV	Net present value	€
p	Pressure	Pa
P	Electrical output	W
PP	Tolerated payback period	a
\dot{Q}_H	Heat transfer to the cartridge	W
R	Electricity rate	€/kW
t	Depreciation period	a
T	Temperature	°C
V	Voltage	V
z	Maximum permitted specific investment to meet the tolerated payback period	€/kW
η	Efficiency	%

List of references

- [1] <https://de.statista.com/statistik/daten/studie/151260/umfrage/strompreise-fuer-industriekunden-in-europa/>, 22.01.2019
- [2] Steel Institute VDEH: Steel Manual, Verlag Stahleisen GmbH, Düsseldorf, germany, 2003
- [3] BDEW-Strompreisanalyse Mai 2018, Haushalte und Industrie, Berlin, 18. May 2018, www.bdew.de
- [4] Custom Thermoelectric, <https://customthermoelectric.com/>, 22.01.2019
- [5] Twaha, S.; Zhu, J.; Yan, Y.; Li, B.: A comprehensive review of thermoelectric technology: Materials, applications, modelling and performance improvement, Renewable and Sustainable Energy Reviews 65 (2016), pp. 698 – 726
- [6] Gupta, M.: Review on Heat Recovery Unit with Thermoelectric Generators, International Journal of Engineering and Innovative Technology (IJEIT), Volume 4, Issue 4, October 2014
- [7] Hendricks, T.; Choate, W.: Engineering Scoping Study of Thermoelectric Generator Systems for Industrial Waste Heat Recovery, U.S. Department of Energy, Industrial Technologies Program, November 2006
- [8] Kruszewski, M. J.; et al.: Microstructure and Thermoelectric Properties of Bulk Cobalt Antimonide (CoSb₃) Skutterudites Obtained by Pulse Plasma Sintering, Journal of ELECTRONIC MATERIALS, Published Online 23. September 2015
- [9] Yan, X.; Populoh, S.; Weidenkaff, A.; Rogl, P.; Paschen, S.: Chemical and Thermoelectric Properties of Hot Pressed and Spark Plasma Sintered Type-I Clathrate Ba₈Cu_{4.8}Si_{41.2}, Journal of ELECTRONIC MATERIALS, Published Online 07. December 2015
- [10] Stiewe, C.; Müller, E.: Anwendungspotential thermoelektrischer Generatoren in stationären Systemen – Chancen für NRW, Studie im Auftrag des Ministerium für Innovation, Wissenschaft, Forschung des Landes NRW, January 2015
- [11] den Heijer, M.: A novel thermoelectric module concept based on direct casting of silicide legs; Industrialization and introduction for large volumes, 4th Thermoelectrics Conference, December 10 – 12, 2014, Berlin
- [12] Heuer, J.: Waste heat recovery in stationary systems: Cogeneration power plant and hybrid electric vehicle, 4th Thermoelectrics Conference, December 10 – 12, 2014, Berlin
- [13] Mintus, F.; Stranzinger, B.; Schaper, R.; Küsgen, V.; Spillner, R.: Industrielle Erprobung von thermoelektrischen Generatoren zur Stromerzeugung aus Abwärme, Förderkennzeichen: 03ET1164 A/B/C, Düsseldorf, April 2018
- [14] Kuroki,T.; et al.: Research and Development for Thermoelectric Generation Technology Using Waste Heat from Steelmaking Process, Journal of Electronic Materials, 2015, Volume 44, Issue 6, pp 2151-2156.
- [15] RFSR-CT-2013-00029: Thermoelectric Heat Recovery from Low Temperature Exhausts of Steel Processes (2013-2016) (THERELEXPRO)
- [16] Integrated pollution prevention and control (IPPC): Reference document on best available techniques in the ferrous metals processing industry, December 2001
- [17] Sprecher, M.; Lüngen, H.-B.; Stranzinger, B.; Rosemann, H.; Adler, W.: Abwärmenutzungspotenziale in Anlagen integrierter Hüttenwerke der Stahlindustrie, https://www.umweltbundesamt.de/sites/default/files/medien/1410/publikationen/2019-01-21_texte_07-2019_abwaermenutzungspotenziale-huettenwerke.pdf, 30.03.2020

Appendices

4. Deliverables of WP 1

4.1 Deliverable 1.1: Evaluation document of tkSE processes and their waste heat, qualitative & quantitative (Task 1.1, tkSE)

Table A.1 Necessary data to specify the boundary conditions of the TE system

Process	Process description. Process continuity: annual, weekly and daily operation time. Waste gas pipe: dimensions and geometry, accessibility and amount of space, available media (water, electricity), height above ground, pipe's material.
Combustion gas	Composition
Waste gas	Volume / mass flow (average, value over time: minimum, maximum, discontinuity, duration of discontinuities). Velocity. Temperature (average, value over time: minimum, maximum, discontinuity, duration of discontinuities). Pressure (average, value over time: minimum, maximum, discontinuity). Allowed pressure loss. Allowed temperature drop. Composition (N_2 , CO_2 , O_2 , CO , H_2O , SO_2 , other corrosive components). Dust load. Dust composition. Dew point.
Mechanical measurements: vibrations	In case a dynamic measuring is necessary, it is important to know the space available to monitoring the installation Ambient conditions in the surrounding area
Local supply of cooling water	Temperature. Will it be recirculated, or can it be dumped into the plant infrastructure for further use to the drainage system? Available pressure and flow rate. Grade (is calcification an issue in constant operation of cooling tubes?).
Experience with heat exchanger for each waste heat source	What are the materials typically used or required for the respective media and heat source? Are there issues/recommendations regarding heat exchanger? Which material thickness is recommended (to achieve a 10 year live for example) → to be clarified in WP 2? Which fin geometry is recommended (if any)? → to be clarified in WP 2 and 3.
Surface deposition of dust or other components flowing in the combustion gases	Is there any deposition analysis available (growth rate, influence of particles size, ...)? Materials that better prevent dust deposition, if it's known → to be clarified in WP 3. Possible chemical reactions that could be done on the enclosing surfaces → to be clarified in WP 3.

4.2 Deliverable 1.2: Measurements evaluation document, describing all relevant waste gas properties and their fluctuations (Task 1.2, BFI)

Table A.2 Available and necessary process data of possible waste heat sources

	Unit	Limits	HDGL 1 radiant tubes	HDGL 1 after the recuperato r	HDGL 2	CSP	HRM
Kind of fuel gas	-		Natural gas	Natural gas	Natural gas	BOF gas	CO gas
Fuel gas composition	Vol.- %		$C_3H_8=0.6$ $C_4H_{10}=0.2$ $CH_4=84.2$ $C_2H_6=3.6$ $CO_2=1.4$ $N_2=10.0$	$C_3H_8=0.6$ $C_4H_{10}=0.2$ $CH_4=84.2$ $C_2H_6=3.6$ $CO_2=1.4$ $N_2=10.0$	$C_3H_8=0.6$ $C_4H_{10}=0.2$ $CH_4=84.2$ $C_2H_6=3.6$ $CO_2=1.4$ $N_2=10.0$	$CO=66.0$ $CO_2=15.7$ $N_2=14.3$ $H_2=3.8$ $O_2=0.2$	$CO=6.7$ $CH_4=21.5$ $C_2H_6=0.4$ $CO_2=1.8$ $N_2=5.3$ $SKW= 1.5$ $H_2=62.7$ $O_2=0.1$
Waste gas composition	Vol.- %		Additional measurement necessary	Additional measurement necessary	Additional measurement necessary	Additional measurement necessary	Additional measurement necessary

	Unit	Limits	HDGL 1 radiant tubes	HDGL 1 after the recuperato r	HDGL 2	CSP	HRM
Fuel gas flow	m ³ /h			1,010	368 – 1,840 *****	2,000 – 7,000 per zone	
O ₂ content of waste gas	Vol.- %		3 - 6			4 - 10	5 - 10
Waste gas volume flow	m ³ /h	waste heat min. 40 kW	36 *			18,500 ***	160,000
Waste gas velocity	m/s		0.8 - 0.9			12.4 – 14.9	
Waste gas temperature	°C	> 550°C	450 - 500 **	530-560**	500 - 900 ****	600 - 780	360 - 460
Waste gas pressure	mbar		Additional measure- ment necessary				
Tolerable pressure drop	mbar	Few mbar	Values to be set by tkSE, if plant is selected for demonstrator tests	Values to be set by tkSE, if plant is selected for demonstrator tests	Values to be set by tkSE, if plant is selected for demonstrator tests	Values to be set by tkSE, if plant is selected for demonstrator tests	Values to be set by tkSE, if plant is selected for demonstrator tests
Tolerable waste gas temperature drop	K	Depends on the dew point and the stack effect	Values to be set by tkSE, if plant is selected for demonstrator tests	Values to be set by tkSE, if plant is selected for demonstrator tests	Values to be set by tkSE, if plant is selected for demonstrator tests	Values to be set by tkSE, if plant is selected for demonstrator tests	Values to be set by tkSE, if plant is selected for demonstrator tests
Dust content	mg/m ³		Additional measure- ment necessary	Additional measure- ment necessary	Additional measure- ment necessary	< 5	< 10
Dust composition	%		Additional measure- ment necessary				
Dew point	°C		Max. up to 80°C				
Vibrations	-		Additional measure- ment necessary				
Cooling water and electricity supply	-		Available at the plant				
Cooling water temperature	°C		Depending on time of the year: 10 - 20°C	Depending on time of the year: 10 - 20°C	Depending on time of the year: 10 - 20°C	Depending on time of the year: 10 - 20°C	depending on time of the year: 10 - 20°C
Cooling water pressure	mbar		Normal pressure of water system is adequate				
Cooling water flow	m ³ /h		Adequate	Adequate	Adequate	Adequate	Adequate
Cooling water quality	-		Measure- ment exists				
Accessibilit y and amount of space	-	Space for demonstrator and equipment	Just single TE cartridges can be used	Space for installation and measuring equipment	Little space for installation and measuring equipment	A lot of space for installation and measuring equipment	

	Unit	Limits	HDGL 1 radiant tubes	HDGL 1 after the recuperato r	HDGL 2	CSP	HRM
Waste gas pipe diameter	m		~ 0.2	~ 1.3	~ 1.3	~ 1.3	
* per radiant tube							
** 450 - 500°C at the radiant tubes, 530 - 560°C behind the recuperator							
*** stack 1							
**** max. 900°C in front of the recuperator, max. 600°C after the recuperator							
***** 8 - 40 m³/h per burner, 46 burners --> 368 – 1,840 m³/h							

4.3 *Deliverable 1.3: Summary document for the use of waste heat source selection (summarizing the results of D 1.1, D 1.2 and derived parameters (Task 1.3, BFI))*

Scheme and results of the pre-selection of a suitable waste heat source at tkSE site (Deliverable 1.3, part 1). Main criterions were the waste gas temperature, the accessibility and the amount of space for the demonstrator installation.

Table A.3 Scheme and results of the pre-selection of a suitable waste heat source at tkSE site (Deliverable 1.3, part 1)

	HDGL 1 radiant tubes	HDGL 1 after the recuperator	HDGL 2	CSP	HRM
Waste gas temperature above 550°C?	no (450 - 500°C) → plant is not suitable for the demonstrator test	yes (530 – 560°C, at the lower limit of the required temperature)	yes (500 – 900°C, mostly in the range of the required temperature)	yes (600 – 780°C, well in the range of the required temperature)	no (360 – 460°C) → plant is not suitable for the demonstrator test
good accessibility and enough amount of space?		yes	no → plant is not suitable for the demonstrator test	yes	
Concluding comparison of the residual plants		waste gas temperature is at the lower required limit → just low performance of the TE system expected → plant is less promising for the demonstrator test		waste gas temperature and amount of space optimal → most promising plant for the demonstrator test	

Table A.4 Measured components of waste gas dust (Deliverable 1.3, part 2)

No.	Test point	Unit	Value	No.	Test point	Unit	Value
1	Aluminium	Mass.-%	0.71	14	Manganese	Mass.-%	0.38
2	Arsenic	Mass.-%	< 0.01	15	Molybdenum	Mass.-%	< 0.01
3	Barium	Mass.-%	< 0.01	16	Sodium	Mass.-%	0.33
4	Beryllium	Mass.-%	< 0.01	17	Nickel	Mass.-%	0.06
5	Lead	Mass.-%	0.02	18	Niobium	Mass.-%	< 0.01
6	Cadmium	Mass.-%	< 0.01	19	Phosphor	Mass.-%	0.04
7	Calcium	Mass.-%	0.57	20	Silicon	Mass.-%	1.3
8	Chromium	Mass.-%	0.17	21	Strontium	Mass.-%	< 0.01
9	Cobalt	Mass.-%	< 0.01	22	Titanium	Mass.-%	0.02
10	Iron	Mass.-%	66	23	Vanadium	Mass.-%	< 0.01
11	Potassium	Mass.-%	0.04	24	Zinc	Mass.-%	0.05
12	Copper	Mass.-%	0.10	25	Tin	Mass.-%	0.05
13	Magnesium	Mass.-%	0.05				

Table A.5 Results of data evaluation of the CSP as the most promising plant for the demonstrator tests (Deliverable 1.3, part 3)

	Unit	Heating zone	Setting zone	Store zone
Average waste gas temperature	°C	730	680	600
Minimum waste gas temperature	°C	420	400	380
Maximum waste gas temperature	°C	810	800	670
Average waste heat flow	MW	3.6	2.1	1.7
Possible pressure loss	mbar	Mostly 0	3	4
Waste composition			CO ₂ : 29.19 Vol.-% H ₂ O: 1.36 Vol.-% O ₂ : 3.72 Vol.-% N ₂ : 65.74 Vol.-% Cl: 0.37 mg/m ³ F: 0.30 mg/m ³ SO ₂ : 2.0 mg/m ³	
Dust composition			See table above	

The pre-selection in regards of the main criterions waste gas temperature, accessibility and space for installations resulted in the CSP as the most promising waste heat source for the demonstrator tests. The CSP is divided into 3 zones (Heating zone, Setting zone and Store zone) which are fired differently, so that all three zones had to be evaluated, whether they are suitable for the demonstrator tests. Evaluation of the 3 zones showed that all zones / waste gas systems of the CSP were suitable for the demonstrator tests.

4.4 Milestone 1: Gaseous waste heat source selected (all)

Finally, the Heating zone of furnace 1 of the CSP was selected as the best suitable plant for the demonstrator test. Main criterions were:

- The waste gas temperature is well in the usable range of the TE cartridges (550 -800°C).
- Good accessibility.
- Enough amount of space for demonstrator installation.
- The area is roofed, so that the measuring equipment and data acquisition system are well protected from environmental impacts.

5. Deliverables of WP 2

5.1 *Deliverable 2.1: Requirements to bench scale unit and demonstrator defined (Task 2.1, BFI)*

Table A.6 Equipment requirements for the bench-scale unit and the demonstrator (Deliverable 2.1, part 1)

Bench scale unit	
Waste gas temperature in front and after the bench-scale unit	Deviation of max. 1 % tolerable, to determine the effects of TE application on the waste gas flow also for bigger industrial applications.
Waste gas composition	To determine exactly the waste heat flow, measurement of main waste gas components like CO ₂ , O ₂ and N ₂ is necessary.
Waste gas volume flow	High accuracy even for low volume flows necessary to determine the performance of the bench-scale unit for varying waste heat flows.
Waste gas pressure in front and after the bench-scale unit	Good accuracy necessary (tolerable deviation about 0.5 %), to estimate the pressure drop for bigger industrial applications.
Cooling water temperature in front and after the bench-scale unit	High accuracy necessary (PT 100 necessary, tolerable deviation max. +/- 0.1 K at 100°C), since the difference between the cooling water inlet and outlet will be just a few K. Thus, an error of measurement has a high influence on the accuracy of the calculation of heat removal with the cooling water and on the calculation of the efficiency of the bench-scale unit.
Cooling water flow	Good accuracy necessary (tolerable deviation about +/- 1 %), since an error of measurement has a high influence on the accuracy of the calculation of heat removal with the cooling water and on the calculation of the efficiency of the bench-scale unit.
Voltage, current and power measurement	GUN have both portable and fixed equipment available that is able to measure the I-V curve of the TEG from open- to short-circuit and can operate the TEG at the maximum power point.
Data logging	Data logging every second, to determine exactly the performance of the bench scale unit, even for highly discontinuous conditions.
Demonstrator	
Waste gas temperature in front and after the demonstrator	Deviation of 1 % tolerable, to determine the effects of TE application on the waste gas flow also for bigger industrial applications.
Waste gas composition	Measured waste gas composition from WP 1 will be used to determine the waste heat flow.
Waste gas volume flow	Good accuracy necessary to determine the performance of the demonstrator for varying waste heat flows.
Waste gas pressure in front and after the demonstrator	Good accuracy necessary (tolerable deviation about 0.5 %), to estimate the pressure drop for bigger industrial applications.
Cooling water temperature in front and after the demonstrator	High accuracy necessary (PT 100 necessary, tolerable deviation max. +/- 0.1 K at 100°C), since the difference between the cooling water inlet and outlet will be just a few K. Thus, an error of measurement has a high influence on the accuracy of the calculation of heat removal with the cooling water and on the calculation of the efficiency of the demonstrator.
Cooling water flow	High accuracy necessary (tolerable deviation about +/- 1 %), since an error of measurement has a high influence on the accuracy of the calculation of heat removal with the cooling water and on the calculation of the efficiency of the demonstrator.
Surface temperature of the heat exchanger	Deviation of 1 % tolerable. Connection with the surface of the heat exchanger has to be long-term stable at a temperature of > 550°C (adherence, soldering), since the demonstrator will be installed for several weeks, so that a repair will be difficult.
Voltage, current and power measurement	GUN plan to provide a backplane into which MPPT Power converters can be plugged. These will be connected to the cartridges of the demonstrator and will output 12 V DC to charge a large battery. Full instrumentation of the input and output power will be available also.
Data logging	Data logging every 5 or 10 seconds, since highly discontinuous conditions are not expected
Long-distance data transmission	Daily or online check of measured data by BFI and/or tkSE staff must be possible, to detect errors/failures of the demonstrator or measuring equipment as soon as possible
Further the demonstrator setup and the measuring equipment have to be checked regularly (minimum weekly) by tkSE and/or BFI staff. If necessary, the measuring equipment has to be recalibrated during the long-term testing.	

Table A.7 Boundary conditions and limits for the TE application (Deliverable 2.1, part 2)

Diameter of the waste gas pipe/available space inside the waste gas pipe	Final demonstrator design must be adjusted to the waste gas pipe dimensions. Inner diameter of the CSP waste gas pipe about 1.3 m. If it is not possible to adapt the demonstrator design to the waste gas pipe diameter adequately (e. g. due to available and economic TE cartridge designs) the installation of a bypass system and a fan for the demonstrator tests could be necessary.
Waste gas temperature	The minimum waste gas temperature can be less than 550°C only at the expense of efficiency. The maximum waste gas temperature is 800°C, without changes or addition to the TEG's standard heat exchanger and at a waste gas mass flow below 300 kg/h. If the waste gas mass flow is above 300 kg/h the maximum waste gas temperature is limited to 700°C. The overall allowed maximum temperature is 850°C.
Temperature of the hot side of the TEG	Maximum defined by gas flow and temperature as discussed above.
Tolerable pressure loss of the waste gas	Just a few mbar tolerable, since the pressure in the selected waste gas system is approx. -4 mbar (see chapter 3.2.1.3). To investigate different operation conditions, particularly with regard to TE waste recovery at other plants and industries, the installation of a bypass system and a fan for the demonstrator tests could be necessary.
Tolerable waste gas temperature drop	Depends on stack effect and the dew point of the waste gas. Since the output of the demonstrator is just approx. 800 W _{el} and the waste heat flow of the CSP is in the range of 1.7 to 3.6 MW (with a temperature > 550°C), the decrease of the waste gas temperature will be very low, so that the waste gas temperature should not fall below the dew-point.
Number of necessary cartridges for the bench scale unit (200 W _{el}) and the demonstrator (700 - 800 W _{el})	One cartridge for the 200 W _{el} demonstrator (depending on execution of installation, in case of good to optimal conditions), 3 cartridges for the 800 W _{el} demonstrator (200 - 340 W _{el} for one cartridge at temperatures of 700°C -800°C, depending on execution of installation, in case of good to optimal conditions).
Limits for forces on the TEG flange	444 N axial, 222 N radial.
Limits for water flow and temperature	Nominal flow 11.4 l/min, coolant temperature 60°C.
Time or limits of operation without cooling or with faulty cooling	The cooling must be ensured, no time without cooling allowed, since the TE cartridges would be damaged without cooling.
Method to determine defects in operation or in maintenance	Deviation from nominal resistance (~ 200 mOhm), exact value to be determined.
Potential future use of the electricity generated	Lighting, small valves and control elements, charging batteries.

5.2 Deliverable 2.2 Design concepts finished (Task 2.2, GNTH)

The design concepts of the demonstrator include the design of the TE cartridge, outline of the Power converter design, concepts for the connection of the TE system to the waste gas pipe of the CSP and an alternative concept for the heat exchanger. The summary of design concepts is shown below.

Table A.8 Design concepts of the demonstrator

TE cartridge design	Two cartridge types: GEN3 and GEN4.	
	Inside heat exchanger.	
	Outside coolant water jacket.	
	90 - 150 mm inner diameter.	
	Design point: waste gas flow 130 kg/h, waste gas temperature 800°C, expected power output 180 – 340 W, expected efficiency ~ 6.0 %.	
Outline Power conversion system	Synchronous Boost converter.	
	MPPT algorithm: Modified Fractional Open Circuit Voltage algorithm.	
	Including battery charging management software.	
	Communication to other devices through I2C. This allows the converter to provide measurements of input and output voltage and current.	
Bypass system	Two branches with two GEN4 and one GEN3 cartridge.	
	Integration of a fan into the bypass system to investigate different conditions.	
	Connection between the TE cartridge and the by-pass system by a flange clamp system.	
Alternative heat exchanger design	Indirect approach, transferring the exhaust gas temperature to the thermoelectric module via heat pipes.	
	It is expected to be able to transfer the heat required causing minimum pressure loss in the waste gas pipe.	

5.3 Milestone 2a: System for power conversion complete and ready for WP 4 testing (GUN)

Main components of the power conversion system are the Power converter and the newly developed MPPT algorithm. The function of the developed power converter is to track the maximum power available from the thermoelectric generator(s) connected at its input. The goal of MPPT algorithms is to set the TEG system to operate at its optimum power output according to the temperature conditions.

Main data of the developed Power converter are:

- Maximum power is tracked every 500 ms.

- Electrical energy converted by the converter is stored in a 12 V lead-acid battery.
- Battery charging control algorithm is included in the converter which shuts down if the battery voltage exceeds a pre-defined threshold.
- The converter interfaces TEGs whose voltage can be either lower or higher than the nominal 12 V of the lead acid battery. The converter starts its voltage step-up operation with input voltages as low as 2 V and continues harvesting electrical power provided that the TEG open-circuit voltage does not exceed 30 V.
- The converter can operate in Boost or Buck-Boost mode. The converter can be set to optimize MPPT either for typical energy harvesting applications or for constant temperature systems.
- The converters can communicate to other devices through I2C communications protocol.
- The MPPT capability of the converters is assessed by comparing the operating point set by the converter and the maximum power point obtained during a TEG electrical characterization.
- The electrical efficiency is measured with the KM2 converter powered by a power supply in series with a power resistor to emulate the electrical characteristic of a TEG. A 12 Ah 12 V lead-acid battery with variable load is connected to the output of the KM2 converter. The input and output voltages are measured by high-precision multimeters. The input current measurement is provided by the power analyzer and the output current is measured by a series connected multimeter.

The new developed MPPT algorithm is described as the "Modified FOC" (Fractional Open Circuit Voltage). This algorithm out-performs all other presently available algorithms. The use of this algorithm also results in a reduced heat flux passing through the module to the cold side, reducing system cooling requirements. Tests showed a high efficiency of up to 98 % of the Power converter. Altogether the done work proved that the condition of the Maximum Power Transfer theorem is not sufficient to reach the optimum operating point of a TEG system. Instead, by considering the thermal interactions in the TEG by reducing the Peltier effect the total power generation can be improved. This means that by selecting a different voltage operating point for the MPPT converter the thermal equilibrium of the system can be changed and a greater temperature gradient across the TEG element (and a lower difference across the heat exchangers) provided, which in turn equates to a power increase above that predicted by the Maximum Power Transfer theorem. So far, a +3.7 % increase of the efficiency was achieved.

The images below show the developed and tested power converter.

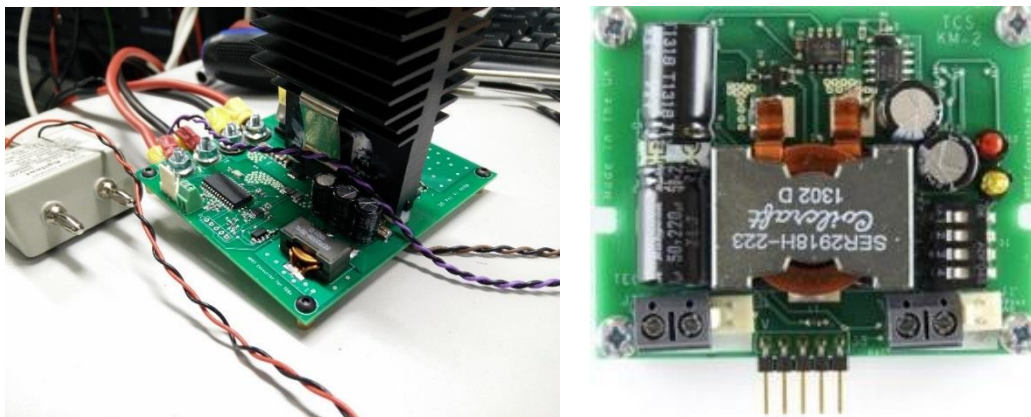


Figure A.1: Power converter

5.4 Milestone 2b: Bench scale unit assembled (GNTH)

For benchmark testing a GEN3 cartridge which is cylindrical, 176 mm in diameter and 164 mm in length (flange to flange) was used. The inner tube has a 90 mm diameter and yields fins for improved heat exchange. The outer tube comprises the coolant water jacket which lets water circulate around the cartridge. The inner tube fins remove heat from the waste gas flowing through the centre opening. Between inner tube and outer tube, several thermoelectric pellets (p and n doted) are placed. The heat flux through the pellets yields a Seebeck-voltage. The pellets are electrically connected to add their individual voltages to the power output. The cartridge can be connected to the waste heat source via flanges. The heat is rejected to the cooling water of the outer tube. For cooling a water flow in the range of 10 - 20 l/min and below 90°C is required. The image below shows the assembled GEN3 bench scale unit, as it was used for the test bed experiments (WP 4).



Figure A.2: Assembled bench scale unit

5.5 Deliverable 2.5: Demonstrator design adaptations defined (Task 2.5, GNTH)

Due to the experimental results from the bench scale tests (WP 4) and during the development of the components of the demonstrator several design adaptions were defined.

Table A.9 Demonstrator design adaptions based on test bed experiments

A GEN3 cartridge was used for the test-bed experiments. Maximum measured power of the tested GEN3 cartridge at 700°C waste gas temperature was approx. 175 W. The expected power output of the GEN4 cartridges is 250 W at 700°C and 340 W at 800°C. Thus, it is planned to use one GEN3 cartridge (in combination with the heat pipe heat exchanger) and two bigger GEN4 cartridges. A power output of the demonstrator in the range of 700 – 800 W _{el} is expected.
One result of the test-bed experiments was that both the Power Converter and the I-V tracer withstand the electrical conditions produced by the GEN3 cartridge. Nevertheless, this must be considered for the further improvements of the Power Converter with a view to maximizing electrical efficiency and hence power generation.
The measured pressure drop of the GEN3 cartridge was higher than 4 mbar. Based on data of GNTH the pressure drop of the GEN4 cartridges is expected to be lower. Nevertheless, a fan is foreseen for the bypass to guarantee an adequate waste gas flow through the bypass.
To get an even waste gas flow to each cartridge diaphragms in the branches of the bypass should be foreseen, so that the waste gas flow can be adapted. Since the cartridges are fixed by flanges with clamps it is possible to integrate the diaphragms between the flanges behind the cartridge.
The cartridges of the demonstrator should be installed at the bypass in that way that the cooling water supply is located at the top of the cartridge to ensure the cooling of the whole circumference of the cartridge with a minimal cooling water flow
To monitor the operational testing of the demonstrator at tkSE it was decided to develop an online monitoring system, which enables all partners to view and download data via a web interface. The proposed system will enable monitoring and logging of the installed TE system at tkSE. The system will be designed for use of up to 5 cartridges. Target power will meet or exceed the putative 1 kW level originally set for the project. Monitoring and logging parameters include temperatures, flow rates, electronic parameters and electrical efficiencies. Further, the monitoring and logging system must operate independently of the CSP plant and require no operator input unless a fault develops. Further, the system must be 'fail-safe' meaning that should any faults develop, they are handled in a safe manner ensuring plant integrity and safety is not compromised. The Monitoring system and tkSE plant safety systems will also be interconnected so that a fault on either triggers protective action in the other. The hardware of the monitoring and logging system will consist of an electrical interface to connect the various sensors from the demonstrator for data collection; MPPT systems developed by GUN; web server to publish the data; database storage; 4G internet connection which will allow access to the Raspberry Pi web interface globally to allow any project partner to view and download data. The monitoring system will handle the following connections and parameters:
<ul style="list-style-type: none"> - External power connections: Mains in (hard-wired 230 V / 1-ph / 16 A), Fan power IN and OUT (5 pin IP67 400 V / 3-ph / 32A), Mains outlet #1 and #2 (British 13 A / IP65). - External PT 100 3-wire probes: Water out temperature (3 pin XLR) for each cartridge. - External Water flow meters: Water flow (All via single 7 pin XLR) for each cartridge. - External Gas flow meters: Gas flow (All via single 6 pin XLR) for each cartridge. - External TEG power connections: Power (40 A 4 pin AMP) for each cartridge. - External thermocouple connections: Gas temperature IN and OUT (2 pin K type) for each cartridge, heat pipe temperature (2 pin K type). - Other external connections: Battery (2 x 16mm² cable via grommet), Earth connection (1x 16mm² via strain relief), waste gas composition (CO, CO₂, O₂), gas pressure IN and OUT, valve state of each valve. - Internal thermistor connections: Load resistor for each cartridge, switchable load, ambient temperature, battery temperature. - Internal relay output connections: Dump resistor for each cartridge, RO3 / MPP relay select for each cartridge, waste gas circulation fan.

- Other internal connections: Battery voltage, fan current transformer, voltage of each cartridge, power supply to the fan.

The test-bed experiments provided satisfactory results in terms of general functionality of the second prototype of Power converter and the I-V tracer necessary to evaluate its electrical and MPPT performance. Further work is required to improve electrical power conversion efficiency and to optimise the MPPT algorithm for constant heat application, e.g. at tkSE.

More work is required to interface the Power converter and the I-V tracer to operate seamlessly with the Monitoring system to ensure reliable communication of data and operational parameters through I2C. It is also necessary to improve the electronics system to ensure safe and reliable operation for a prolonged operation time, unattended.

5.6 Milestone 4: Demonstrator design is reviewed and adjusted (Task 2.5, all)

The demonstrator design adaptions (see Deliverable 2.5) were implemented into the final layout of the different demonstrator components (see also Deliverable 2.6). The demonstrator is ready for assembling.

5.7 Deliverable 2.6: Demonstrator design document (Task 2.6, GNTH)

Table A.10 Demonstrator design document

The entire demonstrator will consist of following main components:

Bypass system, one GEN3 cartridge, two GEN4 cartridges, heat pipe heat exchanger, Monitoring system, Power Converter and MPPT algorithm, and cooling of the TEG.

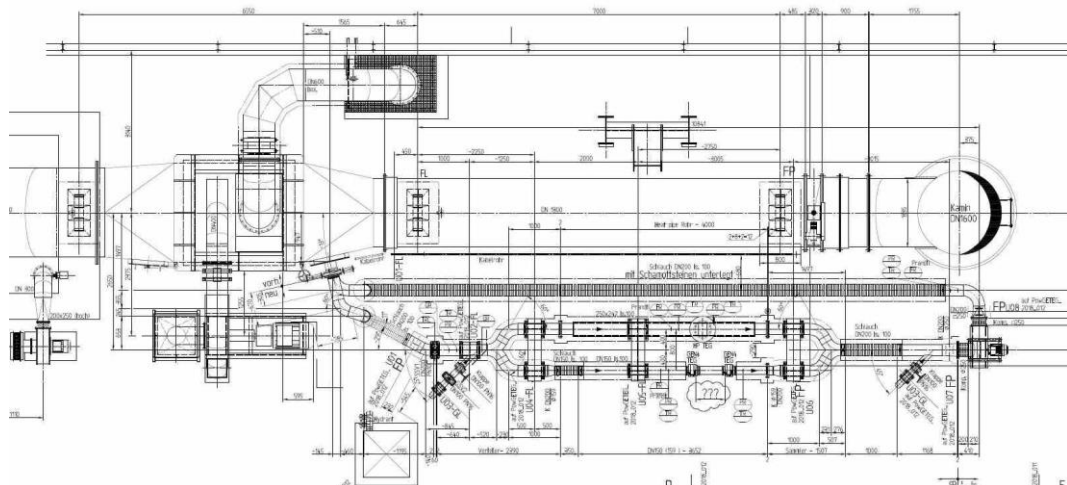
A couple of measuring instruments will be installed to gather information about the performance of the demonstrator. The Online Monitoring system will allow access to any project partner to view and download live data. Further a safety concept was developed to prevent the demonstrator from damages.

Main data of the demonstrator are:

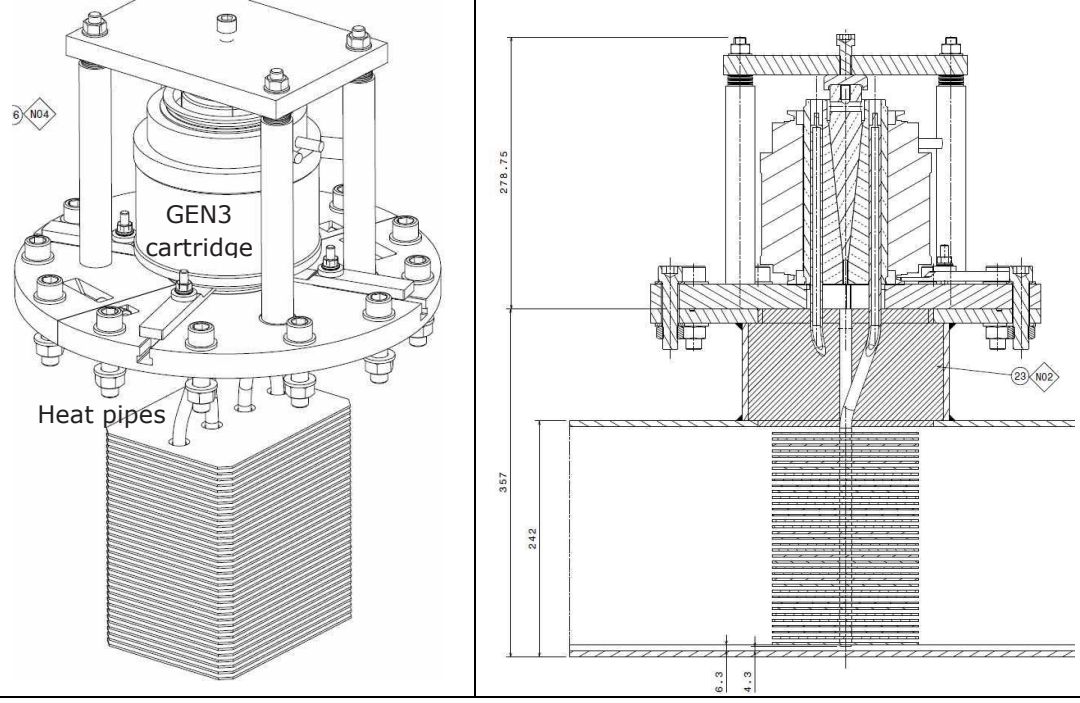
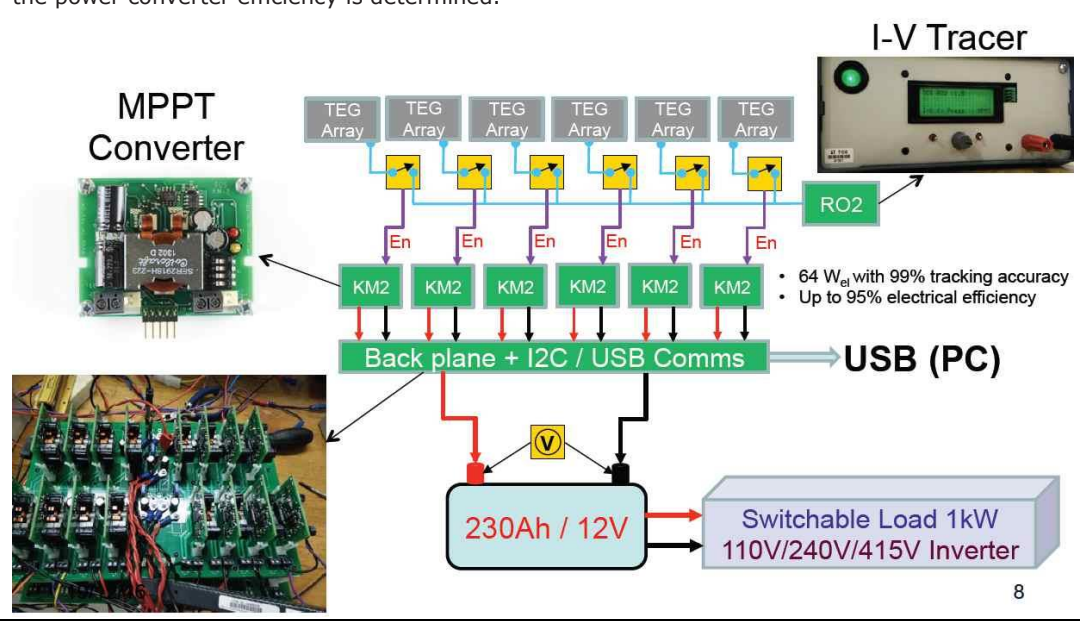
Expected power output at 800°C waste gas temperature: 700 - 800 W

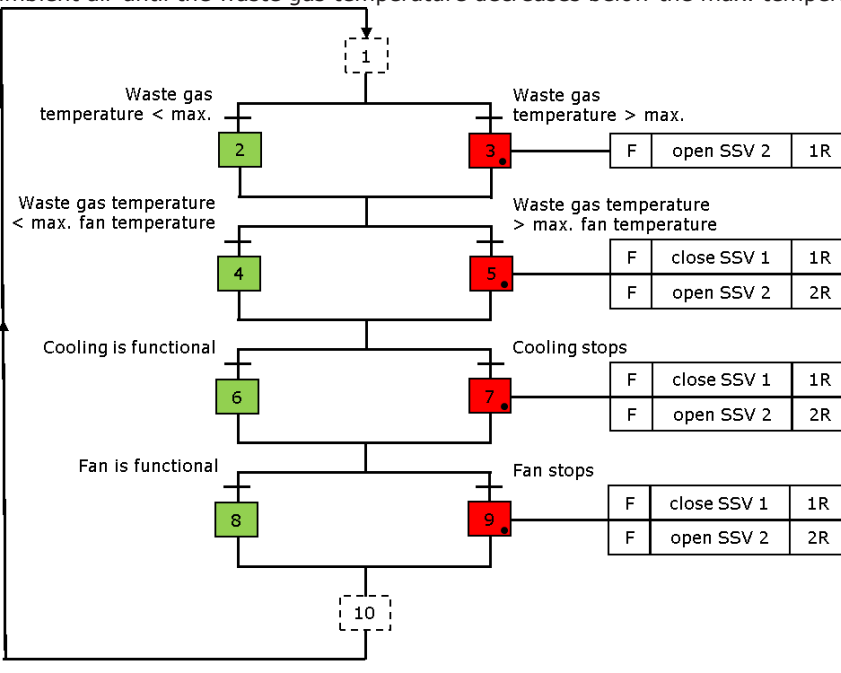
Required waste gas flow: approx. 800 kg/h (130 kg/h for GEN4 cartridges and 630 kg/h for the heat pipe HEX)

Bypass	The waste gas is removed from the CSP waste gas pipe after the main heat exchanger. A special connection plate at an inspection chamber of the heat exchanger is used to link the bypass system to the CSP waste gas pipe. The waste gas is removed and refeed can be closed by valves, so that it is possible to work at the demonstrator during the normal operation of the CSP. Two safety valves (SSV1 and SSV2) will be installed to protect the demonstrator from damages e. g. through overheating. It is foreseen to investigate 3 cartridges in two branches: one branch with two GEN4 cartridges placed in series and one branch for the heat pipe approach with the adapted GEN3 cartridge. The branches have different diameters: DN 150 for the GEN4 cartridges and a rectangular shape with lengths of approx. 0.24 m for the heat pipe approach. To ensure the waste gas flow through the bypass a fan will be installed after the cartridges. This allowed the investigation of the cartridges at different waste gas flows.
--------	--



	<p>Schnittdiagramm B-B aus PowGETEG_2018_010</p> <p>Detaillierte technische Zeichnung eines industriellen Anlagenbaus mit diversen Komponenten wie Rohrleitungen, Ventilen und einem Generator.</p>
GEN3 cartridge	<p>The cartridge is connected to the heat pipe heat exchanger. For that reason, the fin heat exchanger was omitted, and the generator now offers a cylindrical inner tube to interface with the heat pipe setup.</p> <p>Expected power output at 800°C waste gas temperature and 630 kg/h waste gas flow to the heat pipe HEX: 200 W</p> <p>Expected pressure drop at 800°C waste gas temperature and 630 kg/h waste gas flow: 1 mbar</p> <p>POWER CONNECTION Ø 2.4mm 2 PLCS COOLANT CONNECTION FOR 16mm ID HOSE 2 PLCS EXHAUST FLOW → Ø 176 Ø 90 140 164 265 30</p>
GEN4 cartridge	<p>Two GEN4 cartridges will be connected via flanges to a branch of the bypass. The cartridges will be placed in series.</p> <p>Expected power output at 800°C waste gas temperature and 130 kg/h waste gas flow: 340 W</p> <p>Expected power output at 700°C waste gas temperature (due to the temperature decrease by the first cartridge) and 130 kg/h waste gas flow: 250 W</p> <p>Expected pressure drop at 700 - 800°C waste gas temperature and 130 kg/h waste gas flow: 4 mbar</p> <p>COOLANT CONNECTION FOR 16mm ID HOSE 2 PLCS JIC-10 37° CONNECTION EXHAUST FLOW → POWER CONNECTION Ø 2.4mm 2 PLCS Ø 237 Ø 149 ID 161 238 6IN FLANGE CONNECTION 2 PLCS SEE NOTE 1. Ø 90 140 164 265 30 65</p>

Heat pipe heat exchanger for GEN3 cartridge	<p>A heat pipe heat exchanger will be used for heat transfer to the GEN3 cartridge.</p> <p>Heat exchanger characteristics:</p> <ul style="list-style-type: none"> No. of fins: 35 Fin thickness: 2 mm No. of high temperature heat pipes: 4 Pressure drop: 1 mbar Gap between fins: 4 mm HEX dimensions: 200 x 200 x 150 mm 
Power converter and MPPT	<p>The I-V Tracer and at-load Tester device is an independent electronic load specifically designed to test TEGs and to operate them at load. The tracer can instantaneously inspect the electrical performance of the device connected to its input terminals or continuously operate it at-load. The power obtained from the TEG is dissipated internally to the tracer unit. The tracer is rated for 150 W continuous power dissipation and 250 W during I-V trace measurements.</p> <p>The converter developed is a MPPT converter designed specifically for TE power generating modules. One is used for each TE cartridge and it operates the TEG at its optimal operating point and efficiently transfers electrical power to the connected output battery. The converter also includes battery charging management software to ensure the battery is not over-charged.</p> <p>The converter uses a special MPPT algorithm (a modified FOC algorithm) that tracks fast thermal transients and recognises steady states to increase the thermal-to-electrical efficiency of the system.</p> <p>The Power converter can communicate to other devices through I2C. This allows the converter to provide measurements of input and output voltage and current (4 measurements) and from these the power converter efficiency is determined.</p> 
Cooling system	<p>The final choice for the cooling system is to use the water supply available at the tkSE plant. A tube from the water supply of the roll cooling to the demonstrator must be installed. The water supply should be quite safe, since the cooling of the rolls in the CSP is fundamental for the operation of the whole plant and is safeguarded by several measures.</p>

Measuring technique	The bypass/demonstrator will be equipped with following measuring technique: Waste gas temperature in front and after each cartridge and the heat pipe heat exchanger, waste gas composition at the waste gas inlet, waste gas volume flow in front of each cartridge and the heat pipe heat exchanger, cooling water temperature at the overall inlet and at the outlet of each cartridge, overall cooling water volume flow, current of the fan, state / position of the safety valves, current and voltage of each cartridge.
Online monitoring system	Monitoring and logging parameters include temperatures, flow rates, electronic parameters and electrical efficiencies. The hardware of the monitoring and logging system consists of an electrical interface to connect the various sensors from the tkSE 'revolver'; a data processing unit for data collection; MPPT systems developed by GUN; web server to publish the data; database storage; 4G internet connection for access to data produced by the system over-the-air. The data processing unit consists of a Raspberry Pi running Linux-based operating system. The operating system is responsible for automation of the data collection from the electrical interfaces using a scripting language, Python. The Raspberry Pi also integrates the database function based on the SQLite framework and webserver. The website for online access will be built in PHP following the Model-View-Controller concept. This allows for maximum flexibility cross platform while ensuring data integrity. The data generated by the system will be stored locally on the Raspberry Pi before being uploaded to Cloud Storage at weekly intervals. Further, the website will include a calendar function that will enable the user to view and download any dataset from the system start. A 4G internet connection is included with the Raspberry Pi. This allowed access to the Raspberry Pi web interface globally to allow any project partner to view and download data.
Safety concept	To protect the cartridges from damages the following safety concept will be integrated. Three malfunctions could cause a damage of the cartridges – “Cooling of the TEG stops”, “Waste gas temperature > max. allowed temperature”, “Fan stops” - and one malfunction could damage the fan – “Waste gas temperature > max. allowed fan temperature”. In all four cases safety valve SSV 2 will open to cool the waste gas stream. In the cases “Waste gas temperature > max. fan temperature”, “Cooling stops” and “Fan stops” SSV 1 closes additionally, so that no more waste gas will flow through the bypass. In these cases, the cooling or fan have to be checked and repaired if necessary, before the demonstrator test can continue. In the case of “waste gas temperature > max.” it is sufficient to cool the waste gas stream with ambient air until the waste gas temperature decreases below the max. temperature. 

6. Deliverables of WP 3

- 6.1 *Deliverable 3.1: Design document of TE safe-guarding system (Task 3.1, CEM)*

Specifications the PCM material must fulfil to be used for the safeguarding system are as follows.

Table A.11 Specifications for PCM material selection

The demanded melting temperature must be in the desirable interval of working temperatures (700°C).
High specific thermal capacity, heat of fusion and density to reduce the size of the heat storage unit.
High heat conductivity providing the minimum temperature gradients, demanded for charging and discharging.
Reliable convertibility at repeated phase transformations.
Minimum volume change during phase change process. It allows to use simple forms of containers and heat.
Insignificant overcooling during hardening.
Compatibility and resistance to oxidation with constructional materials (steel).
Nontoxic.
Good availability and cheapness.

- Lithium carbonate (Li_2CO_3) has been selected as the material which meets the main requirements for the application: a proper melting point (723°C) and high enthalpy (487 J/g). These values have been confirmed with a DSC/TGA analysis.
- The PCM is capable of absorbing thermal peaks (in this case of 800°C) for different times depending on the weight of the material.
- If a temperature absorber is required, the salt should be confined inside a stainless-steel container highly resistant to corrosion. On the other hand, this salt is stable at 700°C temperature, being its degradation temperature, weight loss, 1,300°C, far away from the 700°C operating temperature. Although a light degradation was observed by DSC/TGA analysis at a temperature slightly higher, it was not observed if salt was inside the container. Therefore, there is no risk once confined to the container.

- 6.2 *Deliverable 3.2: Construction requirements (considering the assembly and its connection to the gas duct) sheet finished (Task 3.2, CEM)*

To minimize the influence of vibrations caused by the fan and the CSP waste gas pipe on the components of the demonstrator two compensators are integrated into the bypass pipe. Due to their construction the compensators prevent the TE system from thermal induced stresses and from damages due to the vibrations/frequency of the fan.

The connection of the directly into the bypass pipe integrated cartridges (GEN4) will be done by flanges which are not screwed but braced with clamps. The 3rd cartridge (GEN3) will be connected to the heat pipe heat exchanger. The heat pipe heat exchanger was fixed to the bypass via a screwed flange.

The entire bypass will be connected to the CSP waste gas pipe by a connection plate. Further the bypass is stabilized by pillars to prevent damages caused by its own weight. The following image shows the connection plate between bypass and CSP waste gas pipe.



Figure A.3: Connection plate between bypass and CSP waste gas pipe

6.3 Deliverable 3.3: Build-up quantified (Task 3.3, BFI)

Due to the lack of operational data, the Build-up of particle depositions has been studied within Task 3.4 and the results are therefore presented in Deliverable 3.4.

6.4 Deliverable 3.4: Evaluation document about the deposition phenomenon and its effect on the heat transfer (Task 3.4, BFI)

A parametric CFD-study has been conducted to evaluate the deposition of dust particles on the heat exchanger surfaces. The studied heat exchanger design was derived from the current tested module and is shown below.

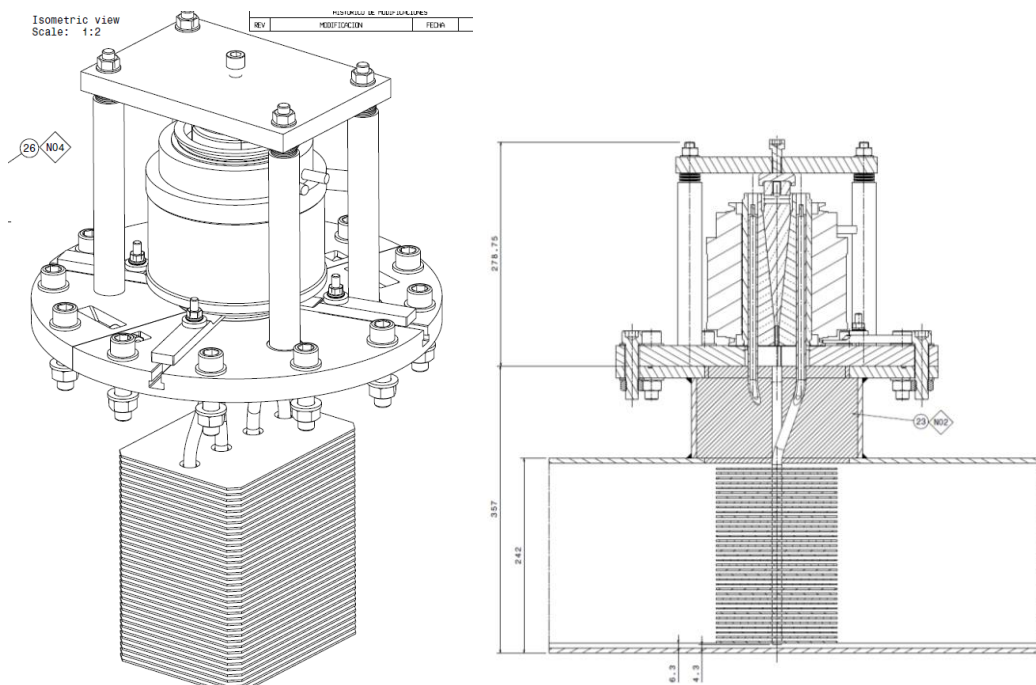


Figure A.4: Studied heat exchanger design

The gas composition and thermal properties have been determined within operational measurements.

Table A.12 Gas composition and thermal properties

Waste gas from BOF gas combustion		
CO ₂	29.19	Vol.-%
H ₂ O	1.36	Vol.-%
O ₂	3.72	Vol.-%
N ₂	65.74	Vol.-%
Temperature	800	°C
Operational density	0.37	kg/m ³

The dust composition is derived from a dust sample analysis.

Table A.13 Measured dust composition

iron	66	wt.-%		magnesium	0.05	wt.-%
silicium	1.3	wt.-%		zinc	0.05	wt.-%
aluminium	0.71	wt.-%		tin	0.05	wt.-%
calcium	0.57	wt.-%		potassium	0.04	wt.-%
manganese	0.38	wt.-%		phosphor	0.04	wt.-%
sodium	0.33	wt.-%		lead	0.02	wt.-%
chromium	0.17	wt.-%		titane	0.02	wt.-%
copper	0.1	wt.-%		bulk density	6.021	kg/m ³
nickel	0.06	wt.-%				

The selected cases for the simulations have been elaborated based on current measurements and possible scenarios for other applications. Variants I – IV represent different waste gas mass flows: While variant IV is related to the necessary waste gas flow of 630 kg/h for the heat pipe heat exchanger the other variants represent a partial load of the heat exchanger with a minimum value of 315 kg/h (50 % of the necessary waste gas flow). Cases 1 – 4 are representing different dust loads of the waste gas. While the actual measurement showed a dust load of 1,48 mg/m³ (Case 4), typical dust loads (e. g. for hot rolling mills) up to 50 mg/m³ (Case 3) must be expected [16].

Table A.14 Elaborated cases for the parametric study

Variant	Mass flow Off-gas	Dust load Case 1	Dust load Case 2	Dust load Case 3	Dust load Case 4**
	in kg/s	in mg/s	in mg/s	in mg/s	in mg/s
I	0.083	0.569*	1.708*	2.846	0.008
II	0.111	0.759*	2.277*	3.795	0.112
III	0.139	0.948	2.846	4.744	0.140
IV	0.175	1.196	3.587	5.978	0.177

*Simulations omitted due to linear proportional behaviour

**measured dust load

Results of the simulation were evaluated regarding particle deposition (accretion) on the heat exchanger surfaces.

Table A.15 Deposition rate of dust particles for the simulated cases

Variant	Case	Horizontal faces in kg/s	Back faces in kg/s	Heatpipes in kg/s	Front faces in kg/s	Side faces in kg/s	Sum in kg/s
IV	1	3.40E-07	0	4.74E-08	3.76E-07	0	7.64E-07
IV	2	4.43E-07	0	7.94E-08	5.35E-07	0	1.06E-06
IV	3	7.39E-07	0	1.32E-07	8.92E-07	0	1.76E-06
IV	4	2.19E-08	0	3.93E-09	2.65E-08	0	5.23E-08
III	1	1.23E-07	0	1.88E-08	1.46E-07	0	2.87E-07
III	2	3.68E-07	0	5.64E-08	4.34E-07	0	8.60E-07
III	3	6.15E-07	0	9.40E-08	7.24E-07	0	1.43E-06
III	4	1.82E-08	0	2.79E-09	2.14E-08	0	4.24E-08
II	3	4.20E-07	0	7.95E-08	5.04E-07	0	1.01E-06
II	4	1.24E-08	0	2.36E-09	1.50E-08	0	2.97E-08
I	3	2.79E-07	0	5.98E-08	3.75E-07	0	7.12E-07
I	4	8.25E-09	0	1.77E-09	1.11E-08	0	2.11E-08

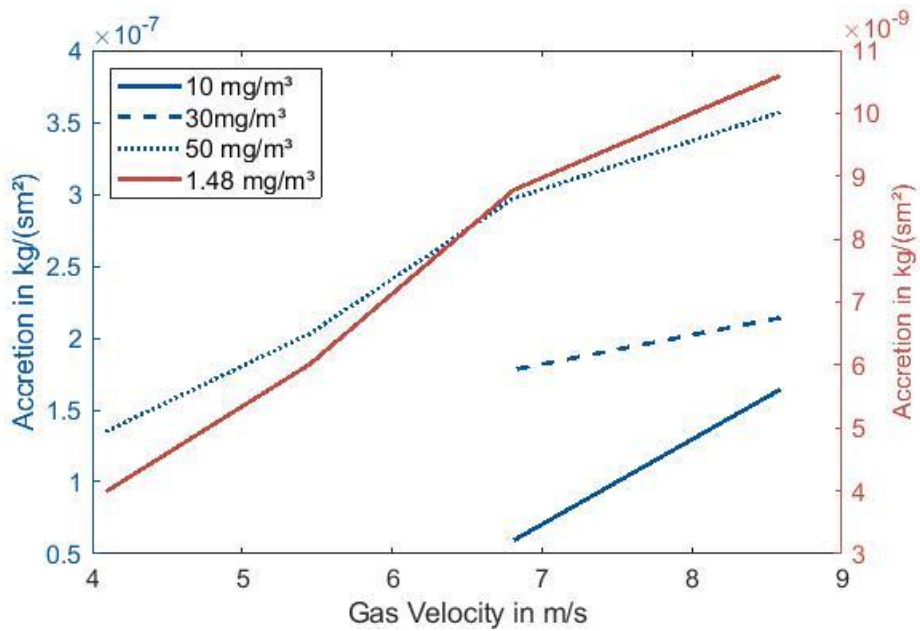


Figure A.5: Accretion rate on the horizontal surfaces of the heat exchanger vs gas velocity

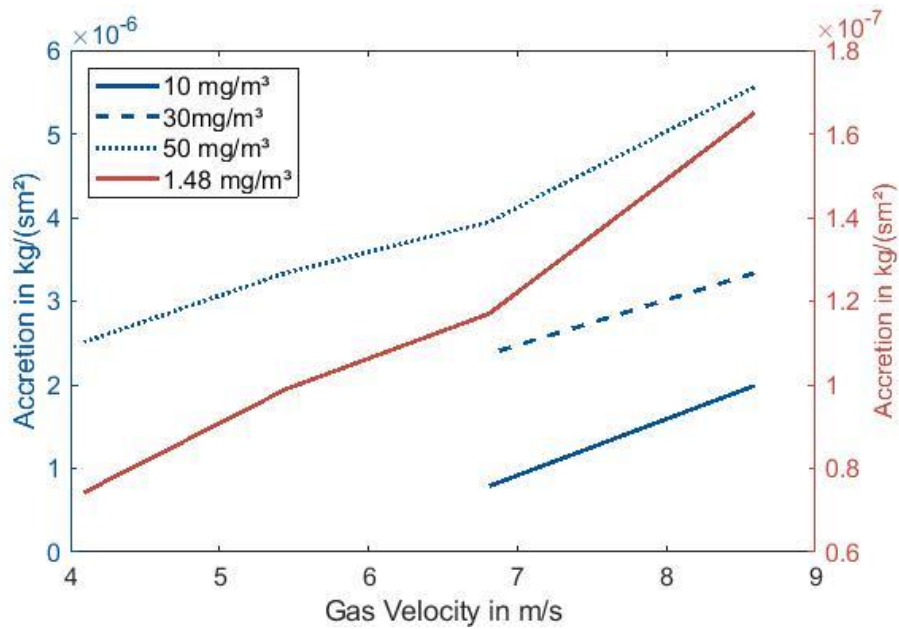


Figure A.6: Accretion rate on the heat pipes of the heat exchanger vs gas velocity

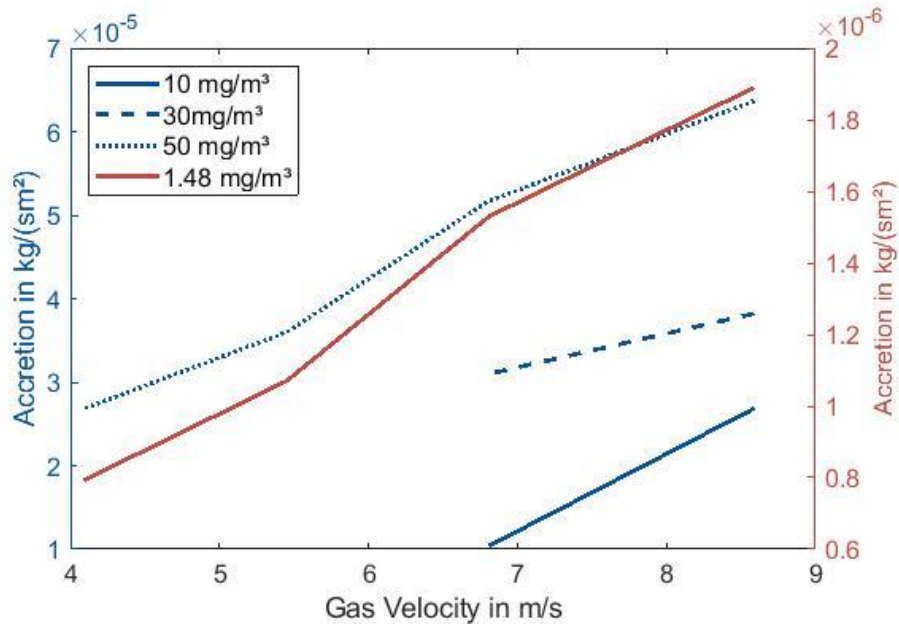


Figure A.7: Accretion rate on the front faces of the fins vs gas velocity

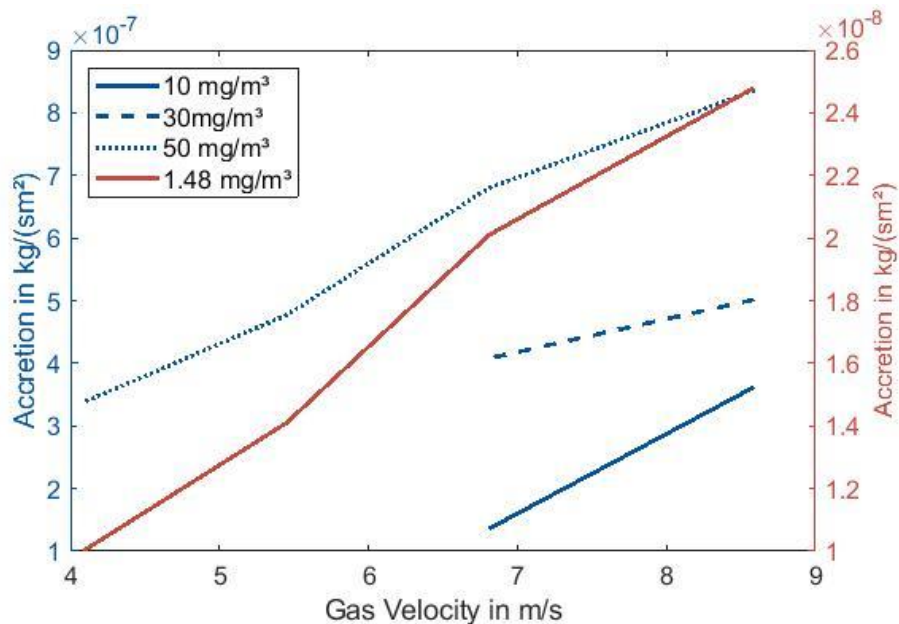


Figure A.8: Accretion rate on the total surface of the heat exchanger vs gas velocity

The heat transfer losses caused by particle deposition were evaluated under the following assumptions:

- Main driving heat transfer mechanism is convective heat transfer
- Heat transfer losses occur due to decreasing channel height between the fins, thus increasing pressure drop across the heat exchanger
- Flow displacement due to increased pressure drop is neglected
- Pressure drop between inlet and outlet of the by-pass is constant
- The calculated accretion rates are extrapolated assuming homogeneous distribution across the surfaces
- Changes in accretion rates due to decreasing flow rates are neglected

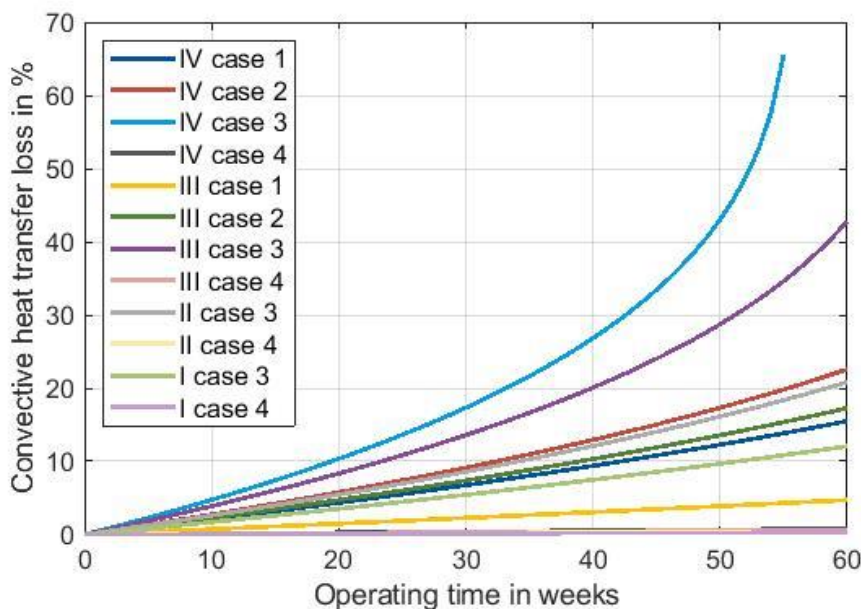


Figure A.9: Convective heat transfer losses over time for selected scenarios

The heat transfer loss has been approximated as a function of time (t in weeks) using quadratic regression with the general model for the heat transfer losses (α_{loss} in %):

$$\alpha_{loss} = c_0 + c_1 t + c_2 t^2$$

The coefficients for the simulated cases and the respective adjusted r^2 values are shown below.

Table A.16 Coefficients for the prediction of heat transfer losses for selected scenarios

	C_0	C_1	C_2	r^2 adjusted
IV case 1	6.60E-02	1.90E-01	1.10E-03	1.000E+00
IV case 2	2.00E-01	2.26E-01	2.36E-03	9.998E-01
IV case 3	2.98E+00	-8.67E-02	1.84E-02	9.762E-01
IV case 4	8.88E-06	1.30E-02	2.77E-06	1.000E+00
III case 1	1.88E-03	7.26E-02	9.95E-05	1.000E+00
III case 2	9.09E-02	2.02E-01	1.37E-03	9.999E-01
III case 3	1.19E+00	1.62E-01	8.13E-03	9.960E-01
III case 4	5.01E-06	1.08E-02	1.89E-06	1.000E+00
II case 3	1.58E-01	2.20E-01	2.01E-03	9.998E-01
II case 4	1.59E-06	7.40E-03	8.79E-07	1.000E+00
I case 3	3.13E-02	1.60E-01	6.64E-04	1.000E+00
I case 4	4.61E-07	4.91E-03	3.84E-07	1.000E+00

6.5 Deliverable 3.5: Developed concept for preservation of high heat transfer and performance results (Task 3.5, CEM)

Aim was the identification of high temperature resistant coatings that prevent the formation of deposits in the heat exchanger system, in order to maintain its efficiency. The coatings consist of industrial high temperature resistant coatings modified with anti-adherent additives in order to increase anti-adherent properties. A theoretical study of coating and additive characteristics narrowed the selection of coatings and additives. Coatings and additives were applied on substrates made of the type of materials that can be used for the construction of heat exchangers. In a first step the selected materials were investigated under high temperature conditions (750°C) in a lab scale oven for 8 h:

1. Five industrial high temperature resistant coatings have been investigated: Cerastil E-1001, Silixan T330-40/IPA, X-clean EC 2048, Silixan S400-35/PE and Thermobarp 800.
2. Four additives have been used to improve the anti-adherence properties of the industrial high temperature resistant coatings and to avoid or reduce the formation of deposits on their surface: Molybdenum Disilicide, Boron Nitride, Alpha-Silicon Nitride, and Aluminum Nitride.
3. Three substrates have been selected to apply the coatings: copper, rusting steel and stainless steel in two grades (AISI 304 and 310S). Copper samples and rusting steel did not show resistance to heating treatment (750°C for 8h). Stainless steel, AISI 304, apparently resisted to heat, although a darkening of the sample and a detaching of small particles were observed. AISI 310 showed the best behavior in high temperature application.
4. In the first approach, Cerastil E-1001, X-Clean EC 2048 and Silixan T330 were considered. Cerastil E-1001 was discarded due to its hydrophilic behavior. Then, X-Clean EC 2048 and Silixan T330 were modified with the four additives. Silixan T330 showed better adherence to the substrates than X-Clean, therefore Silixan T330 was selected to be tested in industrial conditions.
5. In the second approach, Silixan S400-35/PE and Thermobarp 800 were considered and additivated with the four anti-adherent additives. Both presented good adherence and no detachment was observed. Therefore, they were selected as samples to be evaluated in industrial environment, too.

In a next step, best performance materials (Silixan T330, Silixan S400-35/PE and Thermobarp 800) were tested under industrial conditions in the waste gas pipe of the CSP at tkSE. The probes were installed in the waste gas stream for several weeks. Results were:

- Silixan T330: most of the samples showed a weight loss. This means that a degradation of the substrate or the coating may have occurred. Thus, other coatings had to be investigated, too. Silixan S400-35/PE and Thermobarp 800 were selected.
- The industrial test of Silixan S400-35/PE and Thermobarp 800 showed:
 - No deposition was observed.
 - The thermal behaviour was good.
 - No degradation of the coating due to the high temperature.

Furthermore, the results show, that the waste gas of the CSP contains just a minor dust load and that no deposits are expected for the long-term demonstrator test. Nevertheless, some of the heat

pipe heat exchanger fins were treated with the Thermobarp coating to test them over a longer period during the demonstrator test at tkSE.

6.6 Milestone 3: Solutions for sustained performance tested (CEM)

Due to the design of the TE cartridges the firstly supposed overheating protection of the TEG by a PCM material cannot be integrated into the demonstrator. Nevertheless, different PCM materials for overheating protection have been investigated for their use in other TEG applications. A proper PCM material was identified and investigated in the lab:

- Lithium carbonate (Li_2CO_3) has a proper melting point (723°C) and high enthalpy (487 J/g).
- In order to simulate real working conditions of the material, a study of thermal stability has been carried out. Variations in the melting point or the enthalpy of the material have not been observed after performing several cycles. The melting curves are identical in all the cases. So, these results indicate no degradation of the PCM.
- The PCM is capable of absorbing thermal peaks (in this case of 800°C) for different times depending on the weight of the material.

For overheating protection of the demonstrator in the current case another safety concept was developed which is described in detail under Deliverable 2.6.

For prevention of build-up formation suitable coatings and additives have been identified. Best suitable coating identified was Silixan T330. High temperature lab scale tests of this coating were highly promising. However, the investigation in industrial environment of Silixan T330 showed a degradation of the substrate or the coating. Thus, other coatings were investigated, too. Silixan S400-35/PE and Thermobarp 800 were selected. Both showed good behavior during the long-term tests. Thermobarp was selected for coating of some fins of the heat pipe heat exchanger. However, due to the minimum measured dust content in the waste gas (in WP 1) build up formation was not expected to be a major issue.

7. Deliverables of WP 4

7.1 Deliverable 4.1: Test-bed design document (Task 4.1, BFI)

The waste gas, produced in the combustion chamber by a BF gas burner, is sucked into the DN 150 waste gas pipe by the fan at the end of the waste gas system. The waste gas can be cooled in a double wall pipe section, if necessary. The following safety relief valve is controlled by the waste gas temperature measurement in front of the valve (TIHS), to protect the TE cartridge from overheating. The inlet path between the safety relief valve and the TE cartridge shows a length of tenfold of the inner pipe diameter to get a non-disturbed flow in front of the cartridge. The allowed max. temperature of the flow measuring device after the cartridge is 200°C . Thus, to cool down the waste gas to the allowed temperature, two cooling coils are installed between the TEG cartridge and the volume flow measurement. The bypass to the volume flow measurement is installed for safety reasons, to protect the flow measurement from overheating and from water condensation during the start-up process of the test-bed. The test-bed is connected to the main waste gas pipe of the combustion chamber which is located beneath of the combustion chamber. An additional air supply in the waste gas pipe is used for control reasons of the fan. Behind the fan the waste gas pipe is connected to the chimney of the combustion chamber.

Measurements: Waste gas composition (WG composition), waste gas temperature in front and after the TE cartridge (T_{WG}), waste gas pressure in front and after the cartridge (p_{WG}), waste gas volume flow (F_{WG}), cooling water temperature in front and after the cartridge (T_{CW}) and cooling water flow (F_{CW}). The scheme of the test bed is shown below.

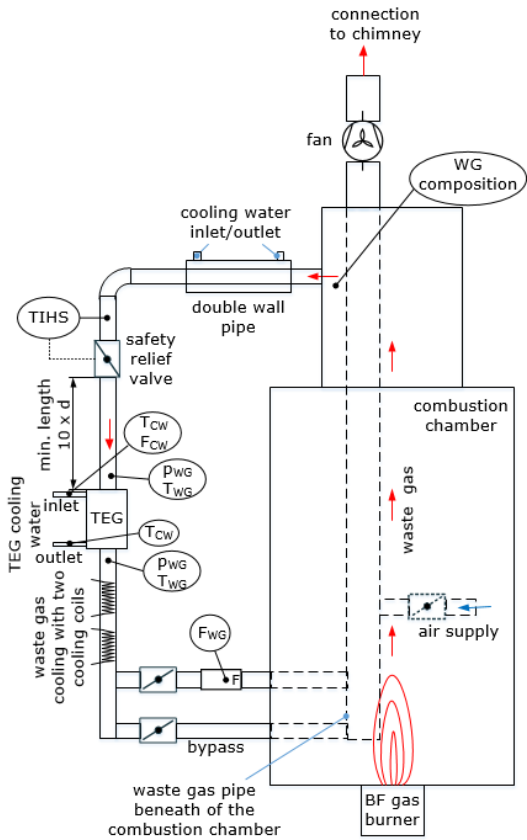


Figure A.10: Scheme of the test bed

7.2 Milestone 4.1: Bench scale unit & power conversion system integrated in test-bed (BFI)

The experimental set-up of the bench scale unit test at the BFI testing facility is shown in the images below:

Left: Waste gas pipe, benchmark cartridge connected to the cooling water supply, I-V Tracer and Power Converter; Right: Electronics enclosure (I-V tracer, MPPT converter and Relay)

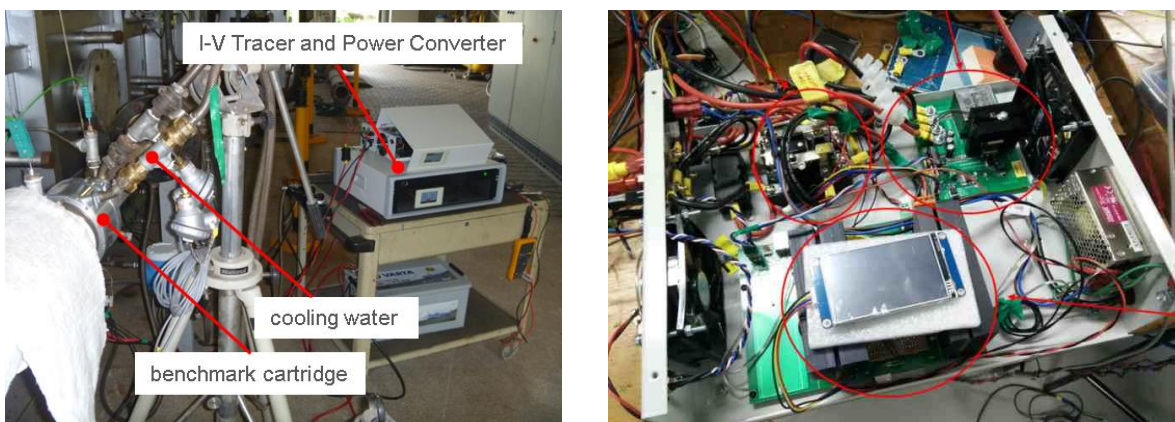


Figure A.11: Experimental set-up of the bench scale unit test at the BFI testing facility

7.3 Deliverable 4.2: Data set ready for analysis (Task 4.2, BFI)

During the experiments data of waste gas flow, waste gas temperature at different positions, waste gas composition, pressure drop, cooling water flow and cooling water temperature in front and after the TEG cartridge were recorded every second. Performance data of the TE cartridge (power, current and voltage) were recorded by the I-V Tracer and Power Converter. The recording of these data was initialized by personnel of GUN if a steady state of waste gas temperature, waste gas flow and cooling water flow was reached. Thus, data sets including several thousands of measuring values were recorded.

In a first step periods of steady state were identified in the different data sets. Since the recording density of several values was 1 s (see above) average values for the steady state periods were

calculated. Based on time and date the performance data of the TE cartridge (which were recorded selective, see above) were assigned to the steady state periods. After that the data were analysed and the result evaluation was done. The next table shows an example of collected measuring data, which were used for the described procedure of data evaluation.

Table A.17 Example of a recorded data set during the test bed experiments with the bench scale cartridge

L6	Uhrzeit	T1_AG [°C]	T2_AG [°C]	T3_AG [°C]	T6_AG [°C]	delta_T_TEG [°C]	V_AG_ [Nm3/h]	p_AG [mbar]	T_H2O_Vor kläuf_TEG [°C]	T_H2O_Rück kläuf_TEG [°C]	delta_T_H2O [°C]	V_H2O_TE G [l/h]	delta_p_T EG [mbar]	O2_TEG [Vol.-%]	CO2_TEG [Vol.-%]	(assumption) [Vol.-%]	N2 (calculate d) [Vol.-%]	CH4_BG [Vol.-%]	CO_BG [Vol.-%]	CO2_BG [Vol.-%]	H2_BG [Vol.-%]	V_GG [Nm3/h]	V_BL [Nm3/h]	c_p O2 [kJ/(kg K)]	c_p CO2 [kJ/(kg K)]	c_p H2O [kJ/(kg K)]	c_p N2 [kJ/(kg K)]	c_p waste gas [kJ/(kg K)]
L7	10:15:23	356,83	310,73	240,57	82,81	70,16	24,08	-30,63	21,43	22,13	0,70	580,34	6,23	3,11	26,17	2,65	68,07	0,09	24,34	20,46	4,36	266,65	280,79	0,998	1,067	2,021	1,085	1,10
L8	10:15:24	362,37	316,93	240,57	82,93	76,36	24,8	-33,33	21,44	22,13	0,69	579,82	5,86	3,11	26,18	2,65	68,06	0,09	24,35	20,46	4,36	265,6	279,73	0,999	1,069	2,024	1,086	1,10
L9	10:15:25	367,82	316,93	243,09	83,06	73,84	25,27	-33,33	21,44	22,13	0,69	580,56	7,31	3,11	26,23	2,65	68,01	0,09	24,34	20,46	4,36	264,97	279,39	0,999	1,069	2,024	1,086	1,10
L0	10:15:26	367,82	323,21	245,55	83,25	77,66	25,52	-32,68	21,43	22,13	0,70	580,32	5,75	3,11	26,25	2,65	67,99	0,08	24,34	20,46	4,37	263,83	278,5	1,000	1,072	2,028	1,087	1,10
L1	10:15:27	373,14	329,56	247,82	83,49	81,74	24,33	-34,33	21,43	22,13	0,70	579,78	5,75	3,09	26,23	2,65	68,03	0,09	24,34	20,46	4,36	263,12	278,38	1,001	1,074	2,032	1,088	1,10
L2	10:15:28	377,75	335,11	249,72	83,71	85,39	24,33	-33,42	21,42	22,15	0,73	580,3	7,37	3,09	26,23	2,65	68,03	0,09	24,34	20,46	4,36	262,39	278,63	1,002	1,076	2,035	1,089	1,10
L3	10:15:29	362,08	359,68	251,65	83,96	88,03	23,87	-33,95	21,43	22,15	0,72	581,09	6,93	3,07	26,19	2,65	68,09	0,09	24,33	20,46	4,36	262,22	277,74	1,003	1,078	2,036	1,089	1,10
L4	10:15:30	386,16	343,91	253,61	84,18	90,3	24,57	-34,36	21,43	22,15	0,72	579,64	6,29	3,09	26,14	2,65	68,12	0,09	24,33	20,45	4,36	262,31	279,05	1,004	1,080	2,040	1,090	1,11
L5	10:15:31	390,14	347,93	255,63	84,18	92,3	24,8	-33,23	21,43	22,13	0,70	578,84	6,05	3,1	26,08	2,65	68,17	0,09	24,33	20,46	4,36	263,44	279,91	1,004	1,081	2,042	1,091	1,11
L6	10:15:32	393,44	351,17	257,5	84,4	93,67	24,33	-30,87	21,43	22,12	0,69	578,84	6,53	3,13	26,05	2,65	68,17	0,09	24,34	20,45	4,36	264,1	277,66	1,005	1,082	2,044	1,091	1,11
L7	10:15:33	396,55	354,31	257,5	84,61	96,81	24,33	-26,9	21,44	22,17	0,73	579,46	6,63	3,13	26,05	2,65	68,17	0,09	24,34	20,46	4,36	264,43	279,34	1,006	1,084	2,046	1,092	1,11
L8	10:15:34	398,86	354,31	259,12	84,86	95,19	23,65	-28,97	21,43	22,16	0,73	580,3	6,38	3,16	26,05	2,65	68,14	0,09	24,34	20,46	4,36	265,75	279,23	1,006	1,084	2,046	1,092	1,11
L9	10:15:35	398,86	356,65	260,55	85,11	96,1	23,64	-30,97	21,43	22,16	0,73	579,46	6,07	3,19	26,05	2,65	68,11	0,09	24,34	20,46	4,36	264,83	278,88	1,006	1,084	2,047	1,092	1,11
L10	10:15:36	400,82	358,79	261,98	85,27	96,81	23,88	-30,97	21,43	22,16	0,73	579,33	7,27	3,2	26,06	2,65	68,09	0,09	24,34	20,46	4,36	264,81	278,86	1,006	1,085	2,049	1,092	1,11
L11	10:15:37	402,96	361,07	263,42	85,46	97,65	24,09	-33,04	21,43	22,18	0,75	580,23	6,04	3,2	26,06	2,65	68,09	0,09	24,34	20,46	4,36	265,85	277,48	1,007	1,086	2,050	1,093	1,11
L12	10:15:38	405,64	363,15	264,75	85,64	98,4	23,64	-33,16	21,44	22,18	0,74	579,36	7,34	3,21	26,09	2,65	68,05	0,09	24,33	20,46	4,36	266,86	277,43	1,007	1,087	2,051	1,093	1,11
L13	10:15:39	408,38	365,02	266,12	85,64	98,9	23,64	-34,69	21,45	22,19	0,74	579,95	7,34	3,21	26,09	2,65	68,05	0,09	24,33	20,46	4,35	267,14	278,58	1,007	1,087	2,052	1,093	1,11
L14	10:15:40	410,93	366,48	267,4	85,86	99,08	23,64	-31,5	21,45	22,18	0,73	579,95	6,13	3,21	26,09	2,65	68,05	0,09	24,33	20,46	4,35	267,42	278,05	1,008	1,088	2,053	1,093	1,11
L15	10:15:41	413,33	367,82	268,68	86,05	99,14	22,94	-36,23	21,45	22,18	0,73	579,33	7,36	3,2	26,09	2,65	68,06	0,09	24,33	20,46	4,35	266,18	277,93	1,008	1,088	2,054	1,094	1,11
L16	10:15:42	415,63	369,78	268,68	86,2	101,1	24,32	-31,82	21,46	22,21	0,75	579,33	7,14	3,2	26,09	2,65	68,12	0,09	24,32	20,47	4,35	266,23	278,58	1,008	1,089	2,055	1,094	1,11
L17	10:15:43	417,81	369,78	270,17	86,39	99,61	24,33	-33,16	21,45	22,21	0,76	579,74	6,87	3,21	25,95	2,65	68,19	0,09	24,32	20,47	4,35	269,16	279,43	1,008	1,089	2,055	1,094	1,11
L18	10:15:44	417,81	371,99	271,48	86,51	100,51	24,33	-33,55	21,47	22,19	0,72	579,58	6,94	3,21	25,95	2,65	68,19	0,09	24,32	20,47	4,35	270,32	278,73	1,009	1,090	2,056	1,094	1,11
L19	10:15:45	419,46	373,61	272,66	86,7	100,95	23,89	-32,5	21,46	22,23	0,77	579,46	6,04	3,24	25,9	2,65	68,21	0,09	24,32	20,47	4,34	271,02	278,58	1,009	1,090	2,057	1,095	1,11
L20	10:15:46	421,08	374,82	274	86,82	100,82	24,57	-34,95	21,46	22,23	0,77	580,54	6,15	3,29	25,89	2,65	68,17	0,09	24,32	20,47	4,34	270,49	278,57	1,009	1,091	2,058	1,095	1,11
L21	10:15:47	422,79	376,23	275,4	86,98	100,83	25,05	-34,05	21,45	22,23	0,78	580,03	7,21	3,3	25,89	2,65	68,16	0,09	24,32	20,47	4,35	270,82	279,09	1,009	1,091	2,059	1,095	1,11
L22	10:15:48	424,51	377,97	276,77	86,98	101,2	25,27	-34,05	21,46	22,23	0,77	579,05	7,22	3,32	25,88	2,65	68,15	0,08	24,32	20,47	4,34	271,56	278,12	1,010	1,092	2,060	1,095	1,11
L23	10:15:49	426,22	379,31	278,08	87,14	101,23	24,33	-32,3	21,48	22,21	0,73	578,91	7,22	3,32	25,86	2,65	68,17	0,08	24,32	20,47	4,34	270,49	278,42	1,010	1,092	2,061	1,095	1,11
L24	10:15:50	427,53	380,43	279,23	87,29	101,2	24,33	-35,05	21,48	22,23	0,75	578,86	6,42	3,33	25,86	2,65	68,16	0,08	24,32	20,47	4,34	270,66	277,92	1,010	1,093	2,061	1,096	1,11
L25	10:15:51	428,24	380,93	279,23	87,45	101,7	24,33	-35,02	21,48	22,23	0,75	579,7	6,13	3,34	25,89	2,65	68,12	0,08	24,31	20,48	4,35	271,03	277,65	1,010	1,093	2,062	1,096	1,11
L26	10:15:52	428,46	380,93	280,1	87,63	100,83	22,45	-32,8	21,46	22,24	0,78	578,72	6,61	3,34	25,92	2,65	68,09	0,08	24,32	20,48	4,35	270,96	277,93	1,010	1,093	2,062	1,096	1,11
L27	10:15:53	428,46	381,21	280,66	87,73	100,55	21,53	-30,22	21,5	22,24	0,74	579,83	6,04	3,34	25,92	2,65	68,09	0,08	24,31	20,47	4,34	270,91	278,25	1,010	1,093	2,062	1,096	1,11
L28	10:15:54	428,83	380,74	281,13	87,85	99,61	21,52	-32,68	21,47	22,26	0,79	579,83	6,45	3,33	25,93	2,65	68,09	0,08	24,32	20,47	4,35	271,66	278,2	1,010	1,093	2,061	1,096	1,11
L29	10:15:55	429,74	380,71	281,78	87,98	98,93	21,52	-32,56	21,48	22,24	0,76	579,72	7,05	3,35	25,99	2,65	68,09	0,08	24,32	20,47	4,35	270,14	277,59	1,010	1,093	2,061	1,096	1,11
L30	10:15:56	430,82	381,05	282,72	88,07	98,33	22,93	-30,61	21,48	22,27	0,79	580,19	7,83	3,31	25,92	2,65	68,12	0,08	24,32	20,47	4,34	269,8	278,38	1,010	1,093	2,062	1,096	1,11
L31	10:15:57	431,88	382,02	283,71	88,16	98,31	23,61	-32,62	21,48	22,27	0,79	580,05	6,96	3,31	25,9	2,65	68,14	0,08	24,32	20,47	4,35	269,83	277,8	1,010	1,093</			

7.4 Deliverable 4.3: Model for TE power production available (Task 4.3, BFI)

There are many models that aim to predict the behaviour of a thermoelectric module but none that attempt to assess the module's performance if embedded in a complete thermoelectric system. The aim of this Simulink model is to develop a computer tool to accurately simulate the thermal and electrical dynamics of a real thermoelectric power generating system. The model takes into account the complex and non-linear interactions of the thermoelectric effects (Seebeck, Peltier), electrical (Joule heating) and heat transfer through the module and heat exchanger materials (1-D Fourier). The way in which the coupling between these parameters is modified during changes in the operating conditions, e.g. temperature or electrical load variations, can also be analysed. The physical system can be represented as in the diagram below.

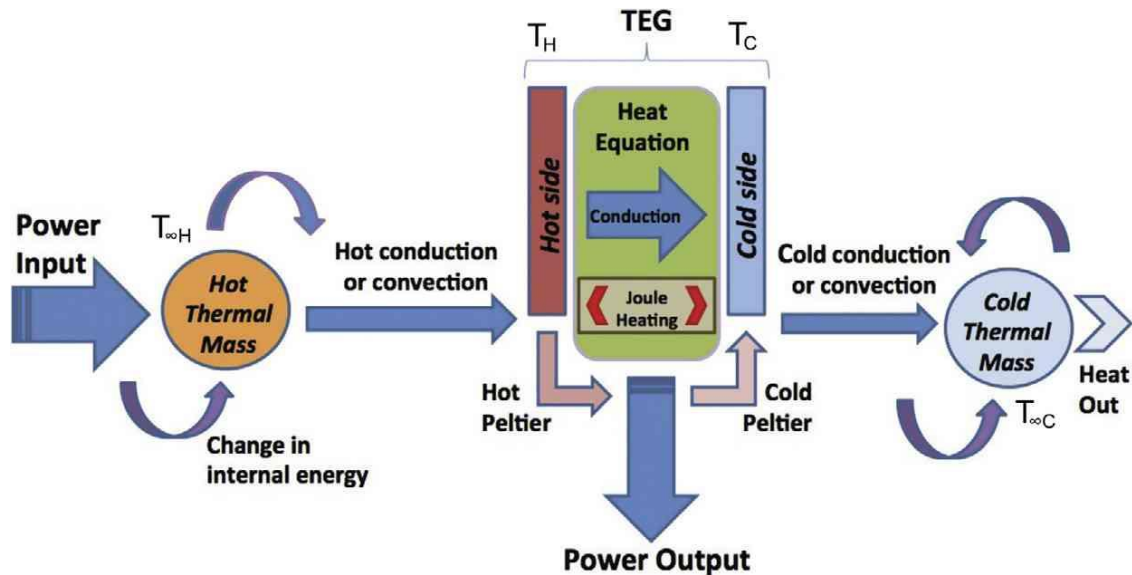


Figure A.12: Physical system of the model for TE power production

This physical model is used as the basis of a computer model created in Simulink and Matlab.

There are three main parts:

1. The heat equation block

The input variables to the block are:

- a. TEG geometrical parameters: surface area and thickness.
- b. Conduction and convection coefficients: open-circuit thermal conductivity and thermal diffusivity coefficient, thermal conductivity, volumetric heat capacity of the TEG; thermal transfer coefficients through the hot and cold mediums.
- c. Electrical parameters of the TEG: internal resistance and load current load.
- d. Temperatures at the beginning of each iteration.
- e. Time step duration.

2. The thermal block:

The most important tasks executed by the hot side block are the update of the temperature of the hot thermal mass and the update of the TEG hot side temperature accounting for the Peltier effect. For the cold part of the system similar considerations hold true: the power flowing to the cold thermal mass is the sum of the thermal power flowing through the TEG and the thermal power pumped to the cold junction by the Peltier effect. The block also takes into account the electrical power removed from the TEG, the thermal power removed from the cold thermal mass and any thermal power lost to ambient on the cold side.

3. The electrical block

A TEG can be modelled as a voltage source (derived from the Seebeck effect and the properties of the materials in use) in series with its internal resistance, even during transients, because the electrical dynamic response is in order of nanoseconds. The electrical block also deals with series and parallel connection of TEG modules. It is assumed that all the modules are identical, and all are subjected to equal thermal conditions.

The electrical part of the Simulink model computes the values of the internal resistance and load voltage depending on the current temperature gradient DT and on the electrical load current. The Peltier term is calculated as single equivalent current passing through a single equivalent module to account for the series / parallel array of modules.

The load current (or voltage) in a real TE system is set either by a constant load resistance connected to the TEG, or by interfacing it to a power electronic converter with MPPT. For flexibility of simulation, the desired load is passed to the model as an input, but the model also provides the maximum theoretical power as described by the Maximum Power Transfer Theorem.

The figure below shows the architecture of the combined MATLAB / Simulink model developed. The computer model has been experimentally verified and found to predict system performance with good accuracy in both transient and steady-state conditions.

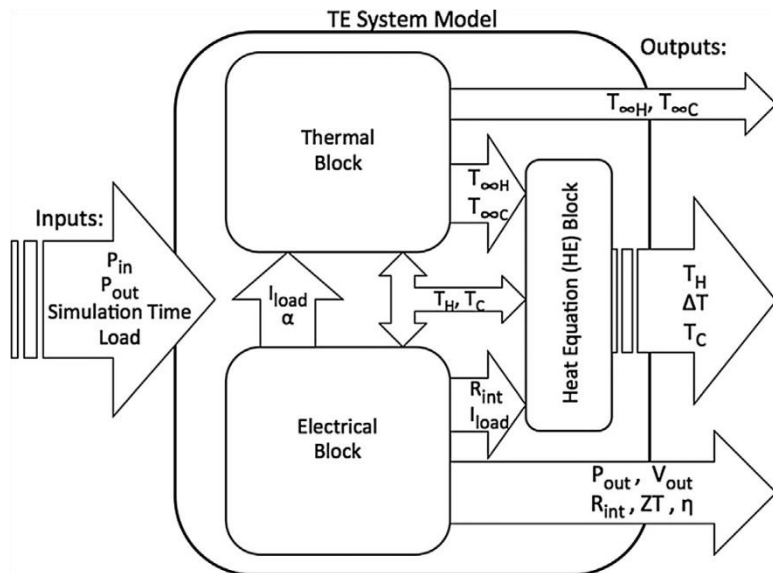


Figure A.13: Architecture of the combined MATLAB / Simulink model

8. Deliverables of WP 5

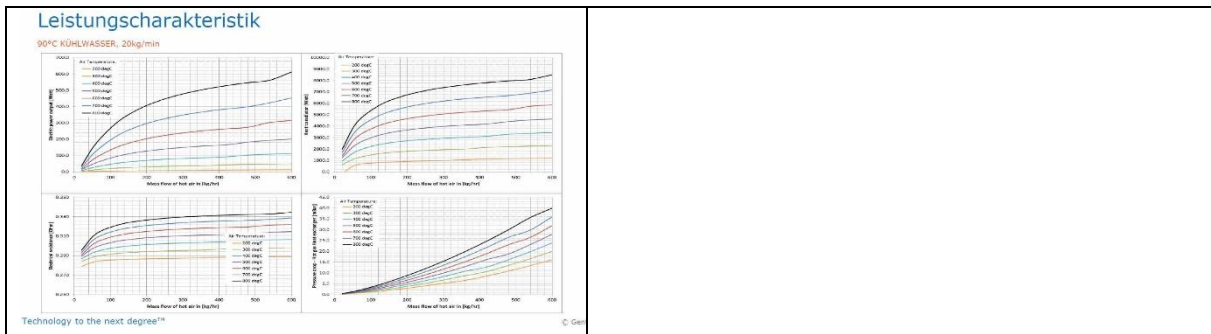
8.1 Deliverable 5.1: Demonstrator documentation including manual ready (Task 5.1, GNTH)

Manuals and documentations of demonstrator components were created.

Table A.18 Manual for handling of the TEG cartridges (GNTH)

Funktion und Einsatzbereich	Funktion und Einsatzbereich
ALLGEMEINE BESCHREIBUNG Einsatzzweck Der thermoelektrische Generator dient zur Erzeugung elektrischer Leistung aus Abwärme. Funktionsweise Basis der Funktion ist der Seebeck-Effekt: Bei einem Temperaturunterschied in einem Leiterkreis aus zwei unterschiedlichen Metallen entsteht eine Spannung (Thermospannung). Dieser Effekt hängt von der Höhe des Temperaturunterschiedes sowie den verwendeten Materialkombinationen ab (Seebeck-Koeffizient). Um die verhältnismäßig kleine Thermospannung technisch nutzbar zu machen, werden in dem Generator eine Vielzahl an speziellen Leiterbausteinen (Pellets) aus dichten Halbleitermaterialien elektrisch zusammenge schaltet. Die Pellets sind zwischen einer inneren und äußeren Röhre angeordnet. Diese Röhre wird durch einen gasdichten, die äußere durch einen wasser dichten Dichtungsring abgedichtet. Die dadurch entstehende Thermospannung der Pellets wird durch einen Leiter nach außen geführt. Der Behälter ist gasdicht verschlossen um die Pellets vor einer Oxidation zu schützen. Technology to the next degree™	ALLGEMEINE BESCHREIBUNG Skizze Wasser-Wärmetauscher Thermoelektrik Heißgas-Wärmetauscher Heißgas Einlass Heißgas Auslass Wasser Zu- und Ablauf Strom-Abnahme Technology to the next degree™
Bauteil-Ansichten Technology to the next degree™	 COPING CONNECTION FOR 16mm ID HOSE 2 PCS JC-10.3/4" CONNECTION EXHAUST FLOW POWER CONNECTION 0.24mm 2 Pcs Ø 149 ID Ø 237 161 238 AIR FLANGE CONNECTION SEE NOTE 1. ITEM NO. PART NUMBER DESCRIPTION 1 TEG12-09107 TEG CORE 2 TEG12-11304 WATER JACK ASSY WITH O-RING Technology to the next degree™

<p>Sicherheitshinweise</p> <p>MONTAGE / DEMONTAGE</p> <p>VORSICHT Bauteilgewicht ca 15kg Sicherheitsschuhe tragen!</p> <p>ACHTUNG Oberflächen können heiß sein! (bis 850°C) Schwere Verbrennung möglich! Vor Demontage abkühlen lassen!</p> <p>ACHTUNG Kann heiße Flüssigkeiten und Gase enthalten! Verbrennung und Verbrühung möglich! Gaszufuhr und Wasserzufuhr vor Montage/Demontage trennen! Abkühlen lassen!</p> <p>Technology to the next degree™</p> <p>© Gentherm 2018</p>	<p>Sicherheitshinweise</p> <p>MONTAGE / DEMONTAGE</p> <p>VORSICHT Handschuhe!</p> <p>Abgasrückstände unbekannter Toxizität können am Rohr verbleiben und in Kontakt kommen. Bei Hautkontakt gründlich waschen. (P280, P303)</p> <p>ACHTUNG Behälter nicht durchstechen! (P251)</p> <p>Technology to the next degree™</p> <p>© Gentherm 2018</p>
<p>Sicherheitshinweise</p> <p>BETRIEB</p> <p>ACHTUNG Oberflächen sind heiß! (bis 850°C) Schwere Verbrennung möglich! Nicht Berühren!</p> <p>HINWEIS Der einzelne Generator liefert < 60VDC (Kleinspannung nach IEC 60449).</p> <p>HINWEIS Die Generatoren haben keine nennenswerte elektrische Kapazität.</p> <p>Technology to the next degree™</p> <p>© Gentherm 2018</p>	<p>Sicherheitshinweise</p> <p>BRAND/TOXIZITÄT/ENTSORGUNG</p> <p>BRENNBARKEIT Unbekannt</p> <p>Außere Bestandteile: Edelstahl, Kupfer, Aluminium. Innere Bestandteile (unter Schutzgas): Edelstahl, Kupfer, Aluminium, Keramik, Polyamid (entzündbarer Feststoff H228), geringe Mengen Bismuth-Tellurid, Skutterudit (entzündbarer Feststoff H228), geringe Mengen sonstiger Stoffe.</p> <p>LÖSCHMITTEL/TOXIZITÄT Unbekannt</p> <p>Außere Bestandteile: Edelstahl, Kupfer, Aluminium. Innere Bestandteile (Exposition nur nach Beschädigung möglich): Edelstahl, Kupfer, Aluminium, Keramik, Polyamid, geringe Mengen Bismuth-Tellurid, Skutterudit, geringe Mengen sonstiger Stoffe.</p> <p>ENTSORGUNG Rücküberstellung an die Gentherm GmbH, Rudolf-Diesel-Str. 12, 85235 Odelzhausen, Deutschland</p> <p>Technology to the next degree™</p> <p>© Gentherm 2018</p>
<p>Hinweise zu Montage und Betrieb</p> <p>WICHTIG</p> <p>Generator NIEMALS ohne Kühlung betreiben!</p> <p>Kühlung immer vor Zufuhr heißer Gase einschalten und frühestens nach Trennen der Gaszufuhr ausschalten! Kühlwasser möglichst erst nach Abkühlen des Generators abstellen (<100°C oder 5-10 min Nachlauf). Kühlwasserzufuhr gegen unbeabsichtigtes Ausschalten oder Trennen sichern!</p> <p>Sonst: Überhitz und irreparable Schädigung des Generators! Leistungsverlust, Schmelzen von Teilen im Generator oder in der Wassermanschette. Undichtigkeit oder Verstopfung der Kühlwasserleitungen möglich!</p> <p>Unterhalb 850°C Gaszufuhr keine weiteren gefährdenden oder kritischen Auswirkungen bekannt.</p> <p>Höhere Gefährdung erst zu erwarten, wenn Überhitzung bzw. Gastemperatur ausreicht um Edelstahlteile der Röhre oder Manschette zu schmelzen.</p> <p>Nach einer Überhitzung: Gaszufuhr abstellen, Abkühlen lassen, Wasserkühlung abstellen, Demontieren und gegebenenfalls austauschen.</p> <p>Technology to the next degree™</p> <p>© Gentherm 2018</p>	<p>Hinweise zu Montage und Betrieb</p> <p>WICHTIG</p> <p>MECHANIK</p> <p>Grenze für auf Flansch wirkende Kräfte: 444N axial 222N radial</p> <p>KÜHLUNG</p> <p>Grenze für Kühlwasserdruk: 275kPa (40psig) Nominaler Kühlwasserdurchfluss: 11l/min bei 60°C Eingangstemperatur Grenze für Kühlwassertemperatur: 90°C bei 20l/min (Bei geringerer Durchfluss gilt eine geringere Grenztemperatur!) Maximaltemperatur: 850°C Flansch, Innenrohr-Wärmetauscher</p> <p>Technology to the next degree™</p> <p>© Gentherm 2018</p>
<p>Hinweise zu Montage und Betrieb</p> <p>WICHTIG</p> <p>ELEKTRIK</p> <p>Die abgehenden 3mm Kupferleitungen können bei Bedarf gebogen werden. Eine Kraftübertragung auf die Basis der Kupfer-Leitungen ist stets zu vermeiden!</p> <p>Beim Biegen ist eine Abstützung der Basis vorzunehmen, derart, dass die auf den ersten 5mm ab Abgang keine Biegung auftritt.</p> <p>Vor dem Anchluss ist auf eine hinreichende Zugentlastung der Leitungen bzw. Kabel zu achten.</p> <p>Der Generator ist passiv verschlossen, wobei an der Basis der ausgewendigen Kupferleiter jeweils eine Dichtung eingebracht ist. Eine mechanische Überlastung an dieser Stelle kann zur Undichtigkeit oder in der Folge zur Schädigung des Generators führen.</p> <p>Bei einer offensichtlichen Schädigung der Versiegelung (Risse o.ä.) darf der Generator nicht mehr betrieben werden.</p> <p>Technology to the next degree™</p> <p>© Gentherm 2018</p>	<p>Anschluss</p> <p>KÜHLWASSER</p> <p>Das Kühlwasser kann verbunden werden über:</p> <ol style="list-style-type: none"> 1) Geviindeschluss passend zu JIC-10 37° (5/8") 2) Schlauch mit Schlauchschelle, 16mm ID <p>Die Kühlwasseranschlüsse sollten bevorzugt oben liegen um eine Entlüftung zu ermöglichen. Der Kühlwasserablauf ist dabei bevorzugt vorn, L bzw. an der gasangeströmten Seite zu wählen.</p> <p>Erfahrungswert: Bei höheren Wasser- oder Umgebungstemperaturen neigen manche mit Schellen befestigten Schläuche zur Nachgiebigkeit und folgend zu Undichtigkeit. Es sollten keine zu weichen oder temperaturempfindlichen Schläuche eingesetzt oder statt Schellen der Schraubanschluss verwendet werden.</p> <p>Hinweise zum Betrieb berücksichtigen (Maximaldruck)!</p> <p>Technology to the next degree™</p> <p>© Gentherm 2018</p>
<p>Anschluss</p> <p>ROHR</p> <p>Die Montage kann über die mitgelieferten Schraubklammern erfolgen. Hierzu können die ebenfalls mitgelieferten Flansche an Zu- und Ablauf verschweißt werden. Zu beachten sind dabei die unterschiedlichen Überstände des Rohrs bzw. des Flansches bei Zu- und Ablauf, sowie die bevorzugte Durchflussrichtung des Generators (siehe Abbildungen). Auch die Lage der Wasser- und Stromabgänge sollte berücksichtigt werden. Alternative Montagevarianten sind grundsätzlich zulässig.</p> <p>Flansch und Schraub-klamme</p> <p>Zulaufseite</p> <p>Durchflussrichtung</p> <p>Rohr—</p> <p>Generator</p> <p>Rohr—</p> <p>Ablaufseite</p> <p>Empfohlener Überstand am Flansch +/- 1mm</p> <p>Detektion</p> <p>Technology to the next degree™</p> <p>© Gentherm 2018</p>	<p>Anschluss</p> <p>ELEKTRIK</p> <p>Der Innenwiderstand der Generatoren liegt zwischen 250 und 300 mOhm. Für eine gute Leistungsausbeute sind Übergangs- und Leitungswiderstände möglichst klein zu halten (deutlich unter 100 mOhm).</p> <p>Die vom Generator ausgehenden Kupferleiter sind möglichst niedrigerohmig mit den Leitungen zu verbinden. Hierzu eignen sich z.B. Kupfer- oder Messing-Freileitungsklemmen (Übergangswiderstand möglichst im einstelligen Milli-Ohm-Bereich oder darunter).</p> <p>Bei längeren Leitungen sind höhere Leitungssquerschnitte oder parallele Leitungen zu empfehlen.</p> <p>Die Polarität der Kupferleiter ist am Mantel gekennzeichnet (+/-). Eine Beschriftung der Kabel wird empfohlen (Generator+, Pol).</p> <p>Auf die Basis der Kupferleiter dürfen keine hohen Kräfte wirken, sonst kann der Generator beschädigt werden. Zugentlastung! Bei freistehenden Anlagen wird ein Nässe- bzw. Witterungsschutz empfohlen.</p> <p>Freileitungsklemme</p> <p>Polarung der Kupferleiter</p> <p>Technology to the next degree™</p> <p>© Gentherm 2018</p>
<p>Nominalwiderstand</p> <p>ELEKTRIK</p> <p>Eine größere Abweichung vom Nominalwiderstand weist in der Regel auf eine Schädigung des Generators hin. Bei Verdacht auf Schäden sollte eine Vergleichsmessung im abgekühlten und elektrisch getrennten Zustand vorgenommen werden. Änderungen über 15% vom Ursprungswert sind als bedenklich einzustufen.</p> <p>Innenwiderstand bei Auslieferung</p> <ul style="list-style-type: none"> Generator #1 281mOhm Generator #2 277mOhm Generator #3 262mOhm <p>Messbedingungen: Vierleitermessung, Wechselspannung (Delta-Mode) 24 Hz, Umgebung 25°C</p> <p>Technology to the next degree™</p> <p>© Gentherm 2018</p>	<p>Leistungscharakteristik</p> <p>60°C KÜHLWASSER, 20kg/min</p> <p>Technology to the next degree™</p> <p>© Gentherm 2018</p>



Manual for handling of the Monitoring system (GUN)

Table A.19 Tables of content of the technical report and manual for the Monitoring system

Technical report	
PowGeTEG Monitoring System	
Contents	
1	General Description of the PowGeTEG Monitoring System 1
1.1	RO3 3
1.1.1	Technical Description of the RO3 device 3
1.1.2	Specifications of the RO3 device 5
1.1.3	Connections to the RO3 device 6
1.1.4	Operation of the RO3 device 6
1.1.5	Circuit Diagram of the RO3 device 8
1.1.6	Thermal Performance of the RO3 device 9
1.2	Switchable Electronic Load for Battery Management 11
1.2.1	Description of the Switchable Electronic Load 11
1.2.2	Specifications of the switchable load: 11
1.2.3	Connections to the switchable load unit are: 11
1.2.4	Operation of the switchable load: 11
1.2.5	Circuit diagrams for the switchable load: 13
1.2.6	Thermal performance of the switchable load: 15
1.2.7	Connection of the equipment 16
1.3	Electronic Load for TEG Protection 17
1.3.1	Description of the Electronic Load for TEG Protection 17
1.3.2	Thermal performance of the switchable load: 18
1.3.3	Connection of the equipment 19
Manual	

Table of Contents

System Overview	1
Liabilities and System Support	3
Supporting Hardware Requirements	4
TEG devices - Device(s) under test	4
Absolute Maximum rating (per device)	4
Energy Storage Battery	4
Battery Capacity	4
Main System Overview	6
Data Acquisition and Power Management Cabinet	6
Physical Dimensions	6
Fan Inlet Vents and Outlet Vents	6
Mains Input	6
Mains Supply Isolator Switch	7
Power Interlock	7
4G Antenna	7
Battery Isolator Switch	7
Input and Output Connections	7
Connector Panel	8
Thermocouple Inputs	8
Gas Sampling Input	9
16 Relay External Controller	9
TEG Power Inputs	10
Battery Terminals	10
PT-100 Temperature Probes	10
Fluid Flow Connector	11
Gas Flow Connector	12
Fan Contactor	12
Power Input System	13
Internal Measurements	13
User Interface	14
Administrative Access Credentials:	16
Mobile Connectivity	16
Local Access	16
Local Administrative Access Credentials:	16
Appendix of Database IDs	18

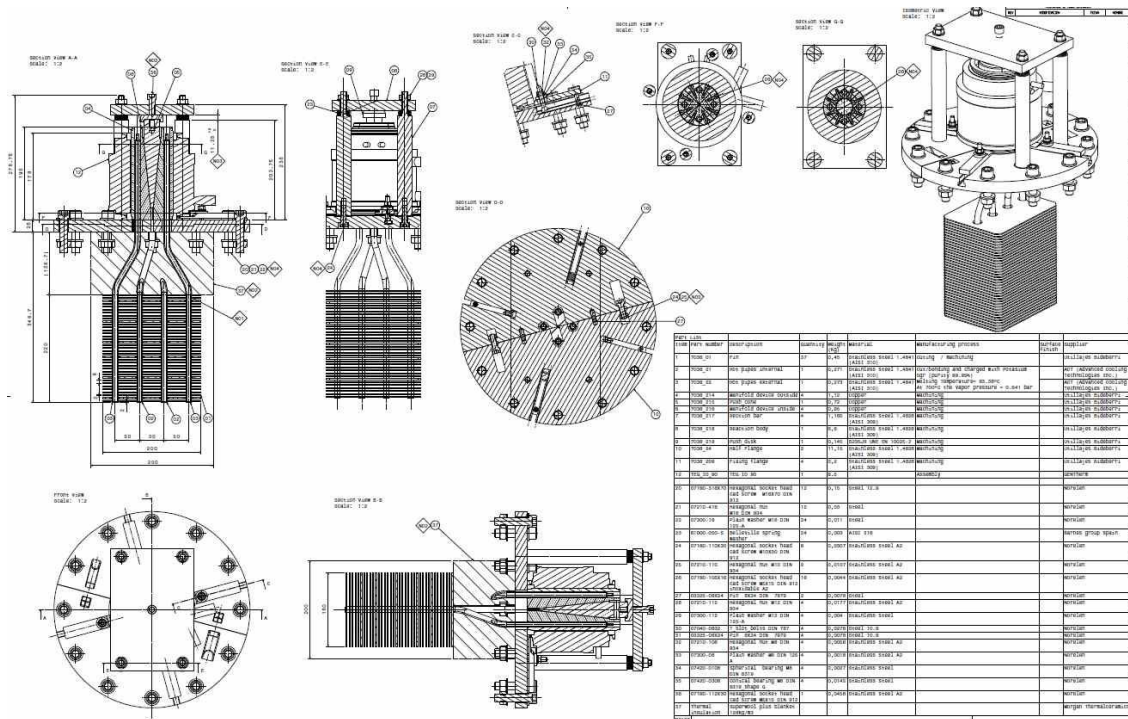


Figure A.14: Documentation of the heat pipe heat exchanger (CEM)

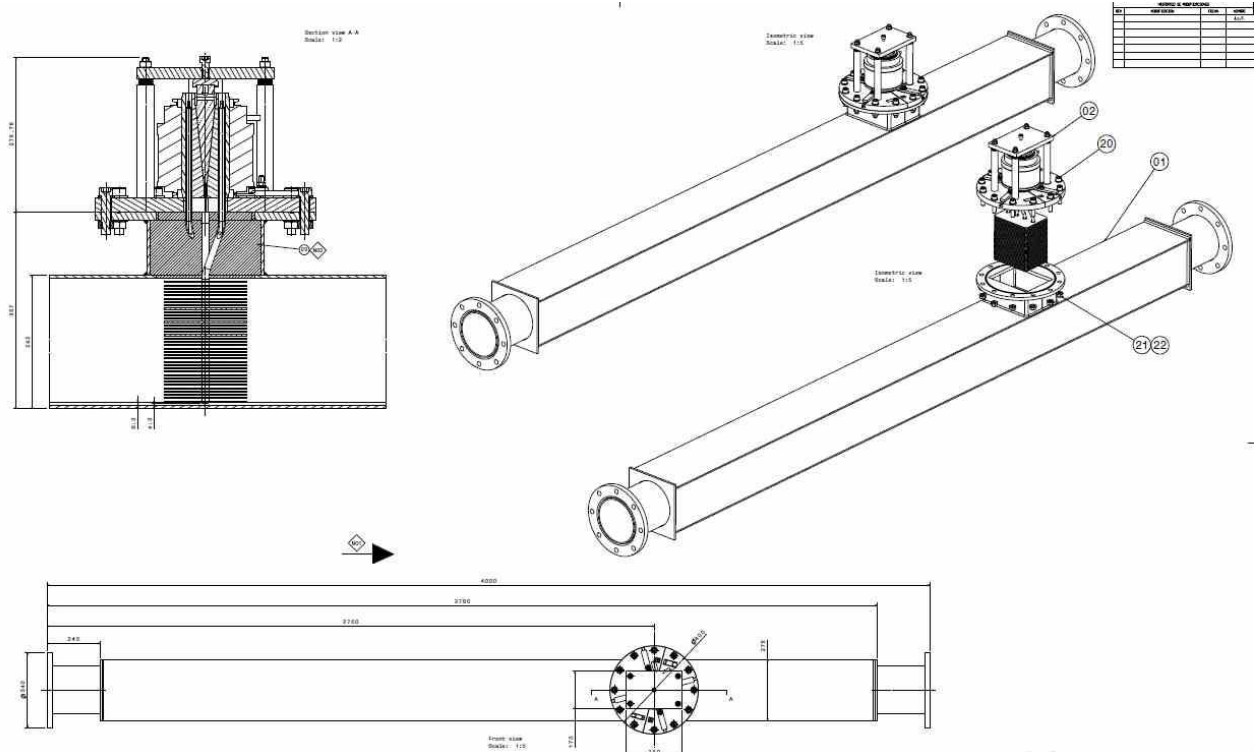


Figure A.15: Assembly of the heat pipe heat exchanger with the bypass pipe (CEM)

Table A.20 Commissioning procedure of the demonstrator (BFI, tkSE); Scheme of the bypass design, see Deliverable 2.2

8.2 Deliverable 5.2: Demonstrator constructed (Task 5.2, GNTH)

Construction of main components of the demonstrator is finished:



GEN4 cartridge (GNTH)

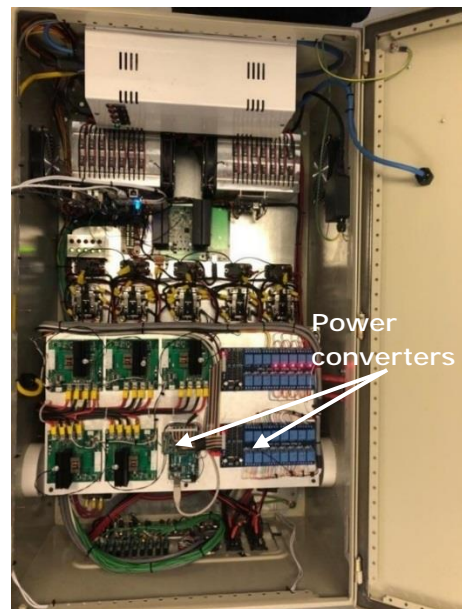


Left: the adapted GEN3 cartridge, refit for conductive heat transfer with a heat pipe-core.

Right (just for comparison): a GEN3 cartridge with fins and nozzle for convective heat transfer (GNTH)



Heat pipe heat exchanger (CEM), already connected to the adapted GEN3



Monitoring system inclusive Power converter (GUN)

Figure A.16: Assembled demonstrator components

All the components of the demonstrator were integrated into the test-bed with the complex measuring equipment. A photo of the test-bed is shown below.

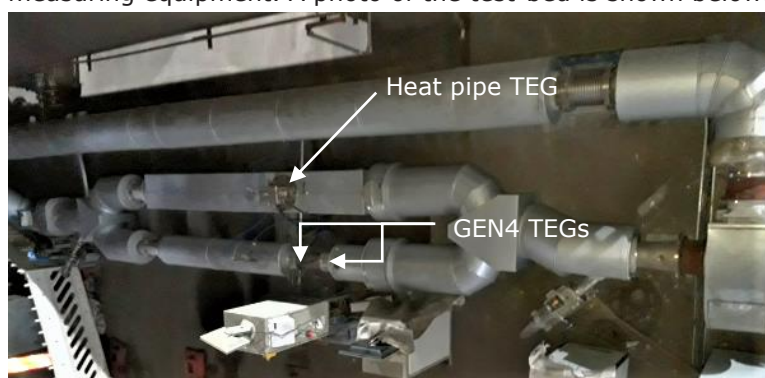


Figure A.17: Top view of the industrial testing

8.3 Milestone 5: Demonstrator tests have started (BFI)

The commissioning of the demonstrator was successfully completed. The main challenges concerned the safety requirements for autonomous operation and continuous reliable measurement data acquisition with online connection. The demonstrator proved to be reliable and the test were carried out over several weeks.

8.4 Deliverable 5.4: Data set of demonstrator tests available (Task 5.4, BFI)

Measured data contained waste gas temperature at different positions, waste gas composition, pressure drop, cooling water flow and cooling water temperature in front and after the TEG cartridges. Performance data of the TE cartridge (power, current and voltage) were recorded too. The recording of these data took place during autonomous operation and covered process situations at the CSP plant over several weeks. The next table shows an example of collected measuring data regarding waste gas composition, temperature, pressure drop and TEG performance.

Table A.21 Example of a recorded data set during the industrial trial

Time	Content in Vol.-%		Waste gas temperature in °C						Pressure drop in mbar					TEG performance								
	O2	CO2	TypK_1	TypK_2	TypK_3	TypK_4	TypK_5	TypK_6	p1	p2	p3	p4	p5	HP_U	HP_I	HP_P	TEG1_U	TEG1_I	TEG1_P	TEG2_U	TEG2_I	TEG2_P
11:07:00	4,43	27,10	530,97	527,35	486,38	361,85	334,76	288,70	-3,05	-3,96	-8,14	-2,97	-13,59	1,69	0,06	0,00	14,44	1,41	20,39	4,59	10,26	47,07
11:08:00	4,55	26,51	529,61	526,03	485,07	361,07	333,95	288,18	-2,90	-3,79	-7,98	-2,85	-13,41	1,93	0,05	0,00	14,74	1,41	20,85	4,71	10,25	48,29
11:09:00	4,25	27,02	528,34	524,84	484,31	360,62	333,55	287,82	-2,78	-3,66	-7,89	-2,69	-13,35	1,56	0,04	-0,02	14,46	1,45	20,94	4,98	10,24	50,98
11:10:00	4,26	27,03	527,69	523,85	483,47	359,72	333,00	287,31	-2,67	-3,56	-7,71	-2,62	-13,21	1,48	0,06	0,00	13,83	2,86	39,62	4,68	10,25	47,96
11:11:00	4,51	26,61	527,34	523,15	483,50	359,21	332,49	286,75	-2,61	-3,48	-7,80	-2,65	-13,23	1,83	0,06	0,00	13,96	3,36	46,85	4,55	10,27	46,77
11:12:00	4,65	26,78	526,09	522,07	482,55	358,76	331,89	286,39	-2,51	-3,40	-7,52	-2,43	-13,04	1,68	0,06	0,00	13,98	4,04	56,50	4,43	10,30	45,65
11:13:00	4,75	26,69	526,07	521,55	482,95	358,93	331,80	286,28	-2,44	-3,31	-7,52	-2,38	-13,05	1,96	0,07	-0,01	11,61	7,80	90,56	4,50	10,30	46,35
11:14:00	4,39	27,28	525,98	521,28	482,96	359,27	331,87	286,49	-2,41	-3,30	-7,44	-2,38	-13,04	1,90	0,09	0,00	11,01	9,33	102,81	4,53	10,32	46,75
11:15:00	4,29	27,22	524,86	520,64	482,37	359,26	332,02	286,64	-2,40	-3,28	-7,49	-2,42	-13,01	1,43	0,09	-0,02	9,76	13,91	135,70	4,62	10,33	47,77
11:16:00	4,32	27,17	522,58	519,16	480,40	358,61	331,75	286,51	-2,47	-3,38	-7,49	-2,52	-13,06	1,68	0,06	0,00	8,02	15,86	127,18	4,43	10,39	46,04
11:17:00	4,54	26,65	521,24	517,77	478,98	357,84	331,12	286,29	-2,47	-3,44	-7,53	-2,48	-13,04	2,26	0,07	-0,01	7,39	17,85	131,86	4,56	10,42	47,49
11:18:00	4,31	26,85	519,91	516,55	478,23	357,21	330,64	286,00	-2,55	-3,40	-7,60	-2,58	-13,15	1,79	0,08	0,00	7,50	17,74	133,14	4,65	10,39	48,27
11:19:00	3,96	27,38	519,14	515,39	477,12	356,40	329,88	285,22	-2,63	-3,51	-7,76	-2,62	-13,15	1,51	0,08	0,00	7,87	17,73	139,44	4,79	10,41	49,90
11:20:00	4,41	26,84	518,53	514,65	476,68	355,72	329,21	284,66	-2,66	-3,54	-7,70	-2,55	-13,19	1,78	0,09	0,01	7,49	17,77	133,18	5,10	10,39	52,98
11:21:00	4,61	26,73	518,08	513,99	476,18	354,98	328,44	284,06	-2,57	-3,54	-7,67	-2,63	-13,15	2,04	0,10	0,00	8,10	17,78	144,06	5,07	10,39	52,62
11:22:00	4,35	27,26	519,96	514,42	477,79	355,65	328,59	284,29	-2,61	-3,50	-7,67	-2,63	-13,20	2,11	0,07	-0,01	7,72	17,79	137,41	4,48	10,41	46,66
11:23:00	3,88	28,10	523,53	516,45	480,14	357,51	329,78	285,24	-2,64	-3,51	-7,68	-2,65	-13,22	1,74	0,04	0,00	7,60	17,77	135,07	4,58	10,45	47,86
11:24:00	4,60	26,85	524,87	517,72	480,75	358,06	330,20	285,95	-2,65	-3,53	-7,63	-2,61	-13,12	1,36	0,04	0,00	7,69	17,74	136,37	5,07	10,50	53,23
11:25:00	4,77	26,23	522,82	517,45	479,64	357,74	330,02	286,00	-2,20	-3,13	-7,22	-2,23	-12,85	1,87	0,04	0,00	7,44	17,75	132,08	4,61	10,54	48,62
11:26:00	4,82	26,07	519,83	516,08	477,49	357,07	329,64	285,88	-1,91	-2,83	-7,03	-1,94	-12,58	1,92	0,05	0,00	7,53	17,74	133,59	4,72	10,56	49,87
11:27:00	4,92	25,84	519,19	515,23	476,99	356,77	329,44	285,98	-1,85	-2,83	-6,91	-1,86	-12,57	1,86	0,10	0,00	7,45	17,74	132,13	4,67	10,59	49,50
11:28:00	5,01	25,59	519,49	514,88	476,80	356,25	328,89	285,56	-1,95	-2,88	-7,03	-1,95	-12,57	1,39	0,35	0,00	7,92	17,80	140,95	4,72	10,60	50,04
11:29:00	4,84	25,82	520,03	515,12	476,87	355,68	328,39	284,56	-2,22	-3,14	-7,28	-2,19	-12,86	1,71	0,62	0,00	7,65	17,82	136,37	5,08	10,64	54,05
11:30:00	4,91	25,91	519,68	514,83	476,71	355,26	327,74	283,93	-2,25	-3,15	-7,33	-2,21	-12,85	1,61	0,69	-0,01	7,54	17,79	134,10	4,82	10,70	51,60
11:31:00	4,91	25,98	520,21	515,03	477,07	355,24	327,80	283,85	-2,03	-2,97	-7,06	-2,05	-12,65	1,72	0,67	0,01	7,77	17,80	138,36	5,05	10,72	54,18
11:32:00	5,31	25,72	520,84	515,38	477,06	355,83	328,09	284,12	-1,92	-2,90	-7,07	-1,93	-12,62	1,89	0,69	-0,01	7,51	17,83	133,98	4,60	10,70	49,22
11:33:00	4,95	26,24	521,20	515,71	477,30	356,04	328,34	284,65	-2,18	-3,08	-7,23	-2,12	-12,76	1,38	0,69	0,00	8,00	17,79	142,36	4,70	10,67	50,18
11:34:00	4,61	26,83	520,57	515,62	476,58	355,78	328,11	284,39	-2,30	-3,25	-7,37	-2,31	-12,90	1,67	0,68	-0,01	7,26	17,82	129,40	4,71	10,66	50,20
11:35:00	4,53	26,80	519,38	515,09	475,90	355,74	328,06	284,40	-2,39	-3,23	-7,40	-2,38	-12,93	1,73	0,73	0,00	7,59	17,85	135,55	4,79	10,66	51,09
11:36:00	5,00	26,10	519,41	514,82	475,95	356,09	328,67	284,95	-2,28	-3,20	-7,28	-2,24	-12,83	1,13	0,90	-0,01	7,78	17,80	138,50	5,16	10,68	55,07
11:37:00	5,12	25,64	521,78	515,86	476,98	356,62	328,89	285,32	-2,28	-3,19	-7,39	-2,31	-12,88	1,44	0,89	0,00	7,75	17,83	138,23	4,60	10,72	49,36

8.5 *Deliverable 5.6.1: Recommendations for TEG optimizing ready (Task 5.6, GUN)*

The recommendations for further optimization of the TEG essentially cover the following areas: technology and peripherals. The TEG face competition with other heat to power technologies.

Table A.22 Characteristics of various heat to power conversion systems

	Steam turbine	ORC	TEG	Steam engine
Investment	1,100 – 1,800 €/kW _{el} + peripheral devices	1,500 – 3,000 €/kW _{el} + peripheral devices	1,500 -3,000 €/kW _{el} (target) 6,000 €/kW _{el} (current status) + peripheral devices	1,100 – 1,600 €/kW _{el} + peripheral devices
Necessary peripheral devices	Piping, boiler, desalination plant, water tank, condenser	Piping, heat exchanger	Cooling of the TEG unit, DC converter	Piping, boiler, desalination plant, water tank, condenser
Temperature level	250 – 540 °C	70 – 500°C	150 – 300°C; up to 800°C in development	250 – 540 °C
Efficiency	10 – 42 %	~ 15 %	3 – 6 %	6 – 20 %
Maintenance	Very high	Low	Very low	Medium
Operating behaviour	Continuous operation necessary, start-up time generally > 1 hour	Discontinuous operation possible, start-up time few minutes	Discontinuous operation unproblematic, start-up time several seconds	Discontinuous operation possible, start-up time few minutes

Currently the main disadvantage is the low efficiency compared to other technologies.

Consequently, this leads to the highest specific investment costs. Although there are several possible applications where TEG have advantages, developments are necessary, especially in industrial scale.

In the area of technology the TEG should be optimized in terms of:

- Advanced TE materials with higher efficiency and for higher temperatures.
- New concepts for mass production of TE materials, e.g. via induction melting, vibration ball milling, spark and pulse plasma sintering gas phase atomization or rapid thermal synthesis methods.
- Economical TEG manufacturing and automated fabrication techniques for mass production of TEG and complete TE systems including necessary devices.
- Optimization of TEG structure e.g. by segmentation of different TE materials for the TEG.

The required peripherals of the TEG show demand for improvements especially in:

- High performance heat exchangers for convective and radiative heat transfer and high performing connection to the TEG.
- High temperature and corrosion resistant antifouling coatings to extend lifetime of the heat exchangers and to ensure their performance during lifetime.

Application advices:

- Which power generation process is most suitable, must be checked for each individual case, a clear general statement cannot be made.
- Following boundary conditions have an impact on the economic viability:

Temperature level of the waste heat, waste heat flow steady/unsteady, capacity of the waste heat, waste gas composition and dust content, on-site boundary conditions (space, accessibility, rebuilding's, ...), qualification of the staff, expected payback period of the company.

8.6 *Deliverable 5.6.2: Models ready for techno-economical evaluation (Task 5.6, CEM)*

The techno-economical evaluation of the use of TEG to generate power from hot waste gases must consider the available amount of waste heat and the temperature level. As referenced in [17],

avoidance of waste heat by process optimization or the use of the waste heat in the process or the plant are in general more economic than power generation by TEG. The economic viability of power generation systems is significantly influenced by the electricity rate and the production costs of the heat recovery system.

Based on the price for common available BiTe-TEG, which is in the range of 3 – 5 €/W_{el} [4], and that necessary devices like heat exchanger, wiring, DC converter, cooling etc. can double these costs, it can be estimated that the costs of systems for utilisation of low temperature waste heat (up to 300°C) are in the range of 6,000 – 10,000 €/kW_{el}. It is expected that the production costs can be significantly reduced by a couple of measures in the near future [5] - [7]. Due to these measures it is expected that TE systems can be commercially available at a price ranging from 1,500 - 4,000 €/kW_{el} in the near future [10] - [12].

Based on the above explained boundary conditions the following evaluation of economic viability of TE waste heat recovery was carried out.

Initially a general economic analysis of TE power generation takes place. Cases considered:

- a. Annual electricity consumption 160,000 kWh to 20 Mio kWh, average electricity price 17.17 ct/kWh.
- b. Annual electricity consumption 70 to 150 Mio kWh, average electricity price 9.96 ct/kWh.
- c. Annual electricity consumption 100 Mio kWh, average electricity price 4.0 ct/kWh.

For the three cases, the permitted specific investment costs of a plant for waste heat recovery by means of TEG were calculated as a function of the maximum tolerated payback period. In large companies, a payback period of 3 years maximum is usually tolerated, while in smaller companies 5 years are often accepted. Further boundary conditions of the calculation were:

- Plant availability 90 %
- Depreciation period 19 years

The calculations are based on the following equations:

$$\text{Payback period} = \frac{\text{Investment}}{\text{Saved costs} + \frac{\text{Investment}}{\text{depreciation period}}}$$

$$PP = \frac{z \cdot P_{el}}{R \cdot P_{el} \cdot 8.760 \text{ hours/year} \cdot b + \frac{z \cdot P_{el}}{t}}$$

with

PP: tolerated payback period

z: maximum permitted specific investment to meet the tolerated payback period in €/kW

P_{el}: TEG performance in kW

R: electricity rate in €/kWh

b: plant availability (-)

t: depreciation period in years

The figure below shows the maximum permitted specific investment costs depending on the maximum tolerated payback period and the electricity rate. It is observed that the permissible investment costs for industrial bulk consumers amount to a maximum of approx. 2.000 €/kW, even at an assumed tolerated payback period of 5 years. As explained above the specific investment costs for industrial applications of TEG can be estimated currently with 6,000 €/kW minimum, even for commercial TEG with a maximum operating temperature of approx. 300°C. With this background it follows that only at relatively high electricity rates of at least 17 ct/kWh the required payback periods can be met.

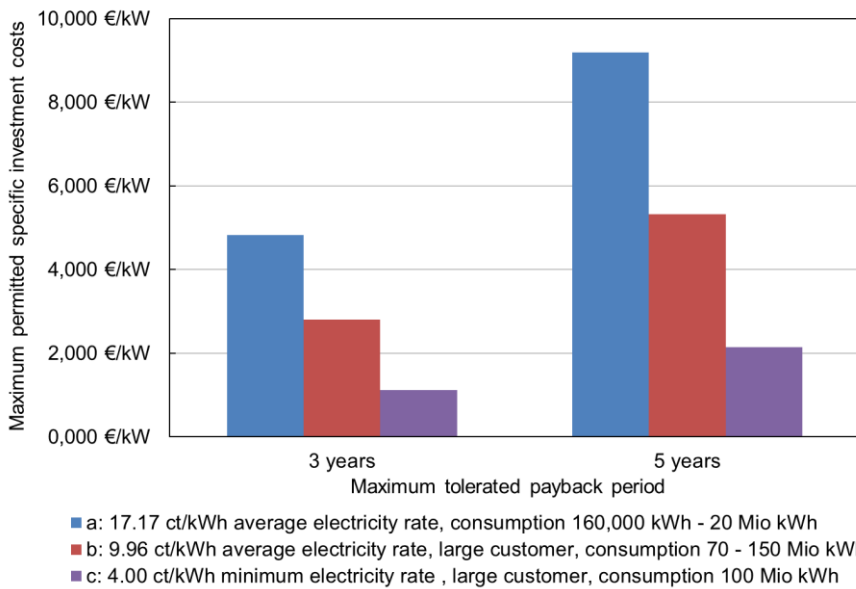


Figure A.18: Maximum permitted specific investment costs of a plant for waste heat recovery by means of TEG as a function of the maximum tolerated payback period

Disadvantage of evaluation of feasibility using the payback period is that savings after the payback period are not considered. This is not the case if the net present value (NPV) is used for evaluation, since this method considers the entire lifetime of the plant:

$$NPV = \text{Investment} + \sum_{t=1}^{t=25} \frac{\text{saved costs}}{(1 + \text{rate of interest})^t}$$

If the NPV is positive within the lifetime of the plant, the investment can be considered as economic. If comparing the payback period calculation with the NPV method, it is possible that investments that exceed the maximum tolerable payback period still have an $NPV > 0$ and thus are profitable over their entire lifetime. Investment decisions based on the NPV method are often taken by companies in terms of long-term investment. In the following, three scenarios for a 10 kW_{el} TEG application were calculated with the NPV method.

Table A.23 Scenarios for NPV calculations

	Scenario 1	Scenario 2	Scenario 3
Electrical power	10 kW	10 kW	10 kW
Plant availability	90 %	90 %	90 %
Electricity rate	4.00 ct/kWh	9.96 ct/kWh	17.17 ct/kWh
Annual increase of electricity rate	0.1 ct/(kWh a)	0.2 ct/(kWh a)	0.3 ct/(kWh a)
Rate of interest	4 %	4 %	4 %
Plant lifetime	20 years	20 years	20 years

The results of the NPV calculations are summarized below. In all scenarios different investment costs were assumed. According to the above explained costs for TEG, following values were assumed: 3,000 €/kW (possible costs in the future), 6,000 €/kW (estimated minimum costs at this time), and 10,000 €/kW (estimated minimum costs for high temperature applications at this time). The calculations also considering a deviation of the efficiency of the TEG from the design point (e.g. due to poor heat transfer), which is reflected in four categories of efficiency on the abscissa (e.g. 0.75 means that the efficiency of the TEG is just 75 % of the maximum efficiency). It is shown that the NPV in scenario 1 is negative in nearly all cases. A considerable positive NPV can be reached only in the case of 3,000 €/kW investment costs. With increasing electricity rate the NPV is getting more and more positive. Even at the currently high investment costs of 10,000 €/kW a good profitability over the lifetime of the plant can be achieved with increasing electricity rates. However, it can be stated that the investment in TEG applications seems not to be profitable for large-scale electricity consumers which are subject to low electricity rates. For smaller companies with higher electricity rates TEG could be interesting. By reaching the target prize of 1,500 – 4,000 €/kW in the future a considerable profitability of such systems could be reached, so that they could be of interest even for large companies.

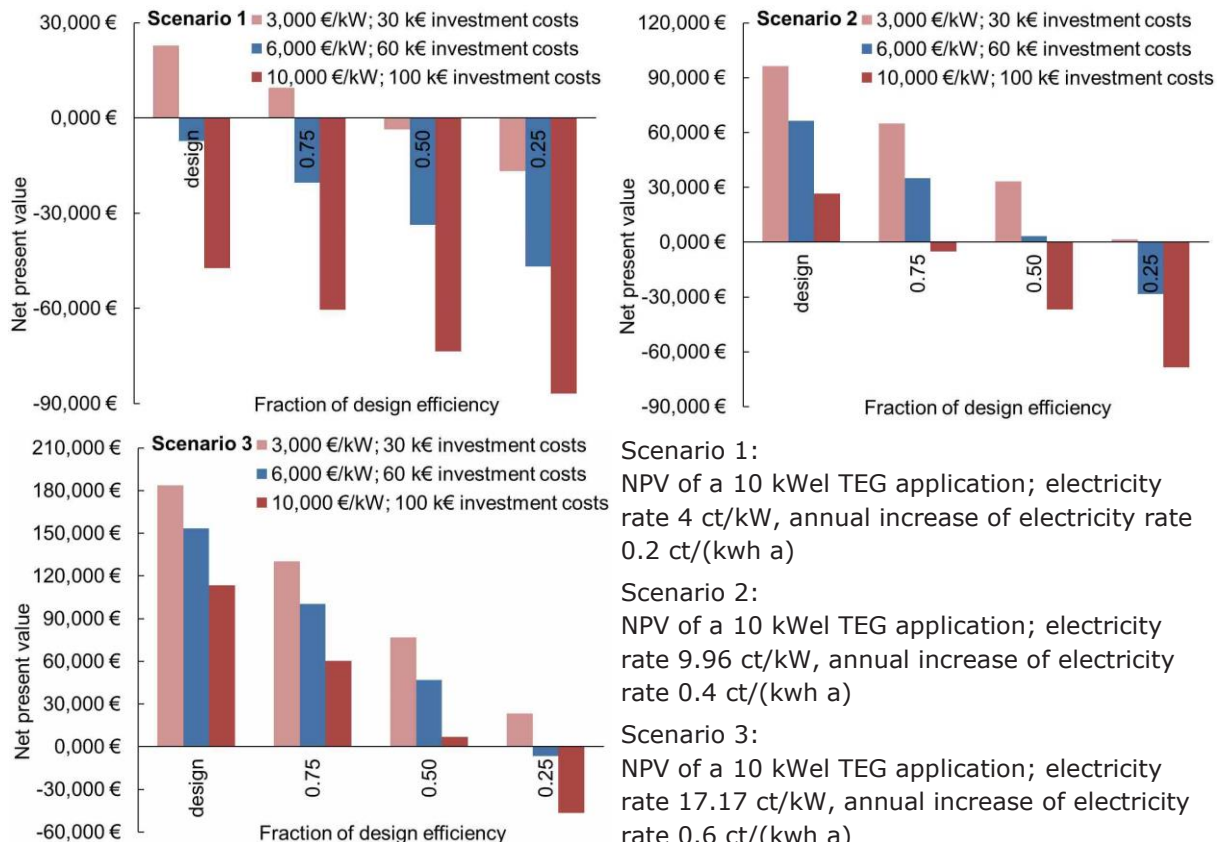


Figure A.19: NPV calculations

9. Deliverables of WP 6

9.1 Deliverable 6: PowGETEG website online (Task 6.1, BFI)

A website of the project was created by the BFI (<http://www.bfi-blogs.de/powgeteg/>). The website includes a project abstract, objectives, the research approach of the project and recent results. The website will be continuously updated by the BFI. A screenshot of the PowGETEG website is shown below.



PowGETEG

PowGETEG

Recent results of the RFSR research project PowGETEG (Power generation from hot waste gases using thermoelectrics)

PowGETEG project abstract

Industries involve a huge amount of energy consumption. A considerable amount of this energy is lost and escapes to ambient as waste heat. Energy recovery from industrial waste-heat streams attracts interest for commercial and strategic reasons. Main drivers are international competition and technological opportunities, combined with geopolitical issues such as security of energy supply, energy consumption and greenhouse gas emission. In recent years, numerous ideas have been suggested either for better process integration, reuse in other settings, or for power generation. For an efficient use of waste heat generally following order is essential:

Figure A.20: Screenshot of the PowGETEG website

9.2 *Milestone 6: Publishable results from bench scale testing*

Table A.24 Publications

Date & place, publisher	Congress, conference, meeting, workshop, journal	Type of dissemination	Dissemination title	Authors
26.09. 2017	15 th European Conference on Thermoelectrics (ECT'17), Pardova, Italy	Slides and oral presentation	MPPT Electronic System for Power Generation from Hot Waste Gases Using a 250 W TEG	Montecucco, A.; Siviter, J.; Knox, A
28.11. 2018	Cleantech 4, Bergamo, Italy	Slides and oral presentation	Power Generation from High Temperature Waste Heat Using Thermoelectric Generators	Mintus, F.; Knox, A.; Spillner, R.; Domels, H. P.; Esarte, J.
26.06. 2019	4 th ESTAD 2019	Slides and oral presentation	Recovery of High Temperature Waste Gas Heat by Thermoelectric Generators	Mintus, F.; Knox, A.; Spillner, R.; Domels, H. P.; Esarte, J.

Getting in touch with the EU

In person

All over the European Union there are hundreds of Europe Direct information centres. You can find the address of the centre nearest you at:
https://europa.eu/european-union/contact_en

On the phone or by email

Europe Direct is a service that answers your questions about the European Union. You can contact this service:

- by freephone: 00 800 6 7 8 9 10 11 (certain operators may charge for these calls),
- at the following standard number: +32 22999696 or
- by email via: https://europa.eu/european-union/contact_en

Finding information about the EU

Online

Information about the European Union in all the official languages of the EU is available on the Europa website at: https://europa.eu/european-union/index_en

EU publications

You can download or order free and priced EU publications at: <https://publications.europa.eu/en/publications>. Multiple copies of free publications may be obtained by contacting Europe Direct or your local information centre (see https://europa.eu/european-union/contact_en).

EU law and related documents

For access to legal information from the EU, including all EU law since 1952 in all the official language versions, go to EUR-Lex at: <https://eur-lex.europa.eu>

Open data from the EU

The EU Open Data Portal (<https://data.europa.eu/euodp/en/home>) provides access to datasets from the EU. Data can be downloaded and reused for free, for both commercial and non-commercial purposes.

The project was dedicated to the determination of possibilities of thermoelectric power generation using industrial gaseous waste heat at temperatures above 550°C. To reach the target new solutions for control, power conversion, heat exchange as well as for overheating and fouling protection of thermoelectric generators were developed and investigated. A demonstrator consisting of 3 TEG cartridges, a heat pipe heat exchanger, a Power converter and an Online monitoring system was designed. A bench scale unit (200 Wei) was tested in the laboratory. Based on the bench scale unit results the demonstrator design was adjusted and an entire demonstrator with an electrical output of 800 Wei constructed. The demonstrator was tested under industrial conditions at a selected waste source of tkSE steel plant. Furthermore, technoeconomical possibilities of thermoelectric power production were determined and evaluated. Payback periods and net present values were calculated for different scenarios and thermoelectric technology was compared with other competing heat to power conversion technologies.

